



**HAL**  
open science

**Huiles vegetales epoxydees, durcisseur dynamique,  
resine biosourcee, recyclabilite, reparabilite,  
reprocessabilite (3R), memoire de forme, fibres  
naturelles, bio-composites**

Chiara Domenica Di Mauro

► **To cite this version:**

Chiara Domenica Di Mauro. Huiles vegetales epoxydees, durcisseur dynamique, resine biosourcee, recyclabilite, reparabilite, reprocessabilite (3R), memoire de forme, fibres naturelles, bio-composites. Material chemistry. Université Côte d'Azur, 2020. English. NNT : 2020COAZ4076 . tel-03475596

**HAL Id: tel-03475596**

**<https://theses.hal.science/tel-03475596v1>**

Submitted on 11 Dec 2021

**HAL** is a multi-disciplinary open access archive for the deposit and dissemination of scientific research documents, whether they are published or not. The documents may come from teaching and research institutions in France or abroad, or from public or private research centers.

L'archive ouverte pluridisciplinaire **HAL**, est destinée au dépôt et à la diffusion de documents scientifiques de niveau recherche, publiés ou non, émanant des établissements d'enseignement et de recherche français ou étrangers, des laboratoires publics ou privés.



$$\rho \left( \frac{\partial v}{\partial t} + v \cdot \nabla v \right) = -\nabla p + \nabla \cdot T + f$$

$$e^{i\pi} + 1 = 0$$

# THÈSE DE DOCTORAT

## Développement durable des résines & composites biosourcées, recyclables, réparables et reprocessables (3R) à base d'huiles végétales époxydées

Epoxidized vegetable oils as sustainable monomers for recyclable, reshapable and repairable (3R) bio-based thermosets and composites

**Chiara DI MAURO**

Institut de Chimie de Nice

Présentée en vue de l'obtention du  
grade de Docteur en Chimie  
de l'Université Côte d'Azur

Thèse dirigée par: Prof. Alice MIJA

Soutenance le : 10 Décembre 2020

Jury

Rapporteurs

Dr. Iuliana SPIRIDON, "P. Poni" Institute of  
Macromolecular Chemistry, Iasi (Romania)  
Prof. Ignazio BLANCO, Univ. Catania (Italy)

Examineurs

Dr. Aratz GENUA, CIDETEC, San-Sebastian,  
(Spain)  
Prof. Véronique MICHELET, Univ. Côte d'Azur  
Prof. Alice MIJA, Univ. Côte d'Azur





# **Développement durable des résines & composites biosourcées, recyclables, réparables et reprocessables (3R) à base d'huiles végétales époxydées**

Epoxidized vegetable oils as sustainable monomers for recyclable, reshapable and repairable (3R) bio-based thermosets and composites

## **Jury :**

### **Président du jury\***

Prof. Véronique MICHELET, Univ. Côte d'Azur

### **Rapporteurs**

Dr. Iuliana SPIRIDON, "P. Poni" Institute of Macromolecular Chemistry, Iasi (Romania)

Prof. Ignazio BLANCO, Univ. Catania (Italy)

### **Examineurs**

Dr. Aratz GENUA, CIDETEC, San-Sebastian, (Spain)

Prof. Alice MIJA, Univ. Côte d'Azur

## Abstract

The use of renewable biomass is a sustainable solution to replace petroleum resource. The vegetable oils (VO) have a wide availability, biodegradability and low toxicity. Their functionalization, by epoxidation, can produce crosslinkable monomers. The incorporation of dynamic covalent bonds, by dynamic hardeners, into crosslinked polymer networks is a powerful way to convert thermosets into reprocessable materials. The main purpose of this thesis is the synthesis and characterization of EVOs-based thermosets and bio-composites with recyclability properties. The copolymerization reactions of a series of 12 new EVOs with an aromatic diacid hardener were investigated through a series of studies starting with the nature of initiator influence, the epoxide/hardener ratio, the EVOs content in epoxy groups and finalizing with recyclability analysis. The influence of the initiator and the epoxy / hardener ratio were investigated as parameters affecting not only the copolymerization reactions but also the networks mechanical and chemical recycling. The twelve new EVOs homopolymers or copolymers showed a large variety of properties, from soft to brittle, in strong correlation with the epoxy content of the starting monomers. The synthesized thermosets displayed properties of recyclability, repairability, reshapability (3R) and shape memory. Finally, a selection of EVOs-based resins were reinforced with flax fibers and PLA woven for the production of reprocessable bio-composites. The synthesized biocomposites showed also recyclability properties, the flax fibers being recuperated after chemical recycling and reused for the production of a second generation composite.

**Keywords:** epoxidized vegetable oils, dynamic disulfide hardener, bio-based thermosets, recyclability, repairability, reshapability (3R), shape memory, natural fibres, bio-composites.

## Résumé

L'utilisation de la biomasse renouvelable est une solution durable pour remplacer les ressources pétrolières. Les huiles végétales (VO) ont une grande disponibilité, biodégradabilité et une faible toxicité. Leurs fonctionnalisation, par époxydation, peut conduire à des monomères réticulables. L'incorporation de liaisons covalentes dynamiques, via de durcisseurs, dans des réseaux de polymères réticulés est un moyen de conférer aux matériaux thermodurs un caractère recyclable. L'objectif principal de cette thèse est la synthèse et la caractérisation de résines et bio-composites à base d'EVO, avec des propriétés de recyclabilité. Les réactions de copolymérisation d'une série de 12 nouveaux EVO avec un durcisseur diacide aromatique ont été étudiées à travers une série d'études commençant par l'influence de la nature de l'initiateur, le rapport époxyde / durcisseur, la teneur en EVO en fonctions époxydes et finissant par une analyse de recyclabilité. L'influence de l'initiateur et le rapport époxy / durcisseur ont été étudiés comme paramètres affectant non seulement les réactions de copolymérisation mais également le recyclage mécanique et chimique. Les douze nouveaux homopolymères ou copolymères EVO ont montré une grande variété de propriétés, en forte corrélation avec la teneur en époxydes des monomères de départ. Les matériaux synthétisés ont présenté des propriétés de recyclabilité, réparabilité, remodelage (3R) et de mémoire de forme. Enfin, une sélection de ces résines a été renforcée avec des fibres de lin et du PLA pour la production de bio-composites. Les bio-composites synthétisés ont également montré des propriétés de recyclabilité, les fibres de lin récupérées après recyclage chimique ayant été réutilisées pour la production d'un composite de deuxième génération.

**Mots-clés:** huiles végétales époxydées, durcisseur dynamique, résine biosourcée, recyclabilité, réparabilité, reprocessabilité (3R), mémoire de forme, fibres naturelles, bio-composites.

## Acknowledgments

I would like to express my sincere gratitude to my supervisor, Prof. Alice Mija, for her continued efforts in mentoring me. Without her support, guidance and encouragement to improve, I would never have overcome many difficulties and to complete my Ph.D. In the last three years, she led me towards exciting research fields and showed me how to be a successful and independent scientist. It has been my honour and privilege to work with her, as well as for providing me the chance of attending and presenting at several international conferences.

I would like to thank to my thesis committee members, Dr. Aratz Genua and Prof. Véronique Michelet, and my thesis rapporteurs, Dr. Iuliana Spiridon and Prof. Ignazio Blanco, for agreeing to be part of this jury.

Many thanks to the European Commission and the ECOxy project and to all the consortium partners, for the collaborations and for including and accepting me in their family.

I would like to be grateful to Institute of Chemistry (ICN) and its director Prof. Uwe Meierhenrich for “hosting” me. Certainly, my stay here would not have been the same without all the smiles I received from all the staff, employees and secretaries included.

Particular thanks to my all colleagues, for their extreme availability and friendship towards me. Special thanks to Roxana and Luna my first colleagues, for confessions, comparisons and much more.

Thanks to my long-time friends, Manuela and Serena, for their support, always attentive, for their desire to always be part of my world, sharing joys and sorrows.

Moreover, I would like to thank the people I owe them everything, my parents, my brother and Gabriele. Maybe I wouldn't have survived a single day here without their unwavering support to urge me to move forward and believe in my abilities. Thanks to my mom, for always being there and always putting my needs in front of hers, resisting the inevitable needs of sons without ever say. Thanks to my dad, for never letting me break down, claiming to be resilient and that at the end of the race I would be successful.

Finally, thanks to the one I admire and love, Gabriele, I would not be here without him and without his loving support. Thank you for taking the time to help me correct, reread and calculate everything (including activation energies). Thank you for never giving up and never making me weigh the distance or the sacrifices made to see us. But most of all thanks for making me the person I am.



## Index of Abbreviations

### Chemicals

1-MI	1-Methylimidazole
1-MP	1-Methylpiperazine
1,2-DMI	1,2 Dimethylimidazole
2E4MI	2-Ethyl 4-Methylimidazole
2-MI	2- Methylimidazole
4-AFD	4-Aminophenyl disulfide
DCAs	Dicarboxylic acids
DGEBA	Diglycidyl ether of bisphenol A
DMAP	Dimethylaminopyridine
DMBA	N,N-Dimethylbenzylamine
DMC	Dichloromethane
DMF	N,N'-Dimethylformamide
DMP30	2,4,6 Tris (dimethylaminomethyl)phenol
DMSO	Dimethyl sulfoxide
DTBA	2,2'-Dithiodibenzoic acid
DTDA	3,3'- Dithiodipropionic acid
ECMO	Epoxidized Camelina Oil
ECO	Epoxidized Castor Oil
EGRO	Epoxidized Grapeseed Oil
EHO	Epoxidized Hemp Oil
EKRNO	Epoxidized Karanja Oil
ELO	Epoxidized Linseed Oil
EPLO	Epoxidized Perilla Oil
EPO	Epoxidized Peanut Oil
ERPO	Epoxidized Rapeseed Oil
ESFO	Epoxidized Safflower Oil
ESJWO	Epoxidized St John's Wort Oil
ESO	Epoxidized Soybean Oil
EtOH	Ethanol
EVOs	Epoxidized Vegetable Oils
FF	Flax Fibres
HCl	Hydrochloric acid
IM	Imidazole
NaOH	Sodium hydroxide
PLA	Poly (lactic acid)
TBD	1,5,7-Triazabicyclo[4.4.0]dec-5-ene
THF	Tetrahydrofuran



## Characterization techniques

ATR-FTIR	Attenuated total reflection Fourier transform infrared spectroscopy
DMA	Dynamic mechanical analysis
DSC	Differential scanning calorimetry
DTG	Derivative thermogravimetric analysis
FTIR	Fourier transform infrared spectroscopy
SEM	Scanning electron microscopy
TGA	Thermogravimetric analysis

## Other abbreviations

$E'$	Storage modulus
$E''$	Loss modulus
ESI	Electronic Supplementary Information
GC %	Gel Content %
LCA	Life-Cycle Assessment
$M_c$	Average molecular weight between crosslinks
$R$	Universal gas constant
$T_{5\%}$	Temperature at which the material loses 5 wt.%
$\tan \delta$	Damping factor
$T$	Temperature
$T_g$	Glass transition temperature
$T_s$	Statistic heat-resistant index temperature
wt.%	Weight percentage
$\alpha$	Degree of conversion
$\Delta H$	Reaction enthalpy
$\nu$	Crosslink density
$\rho$	Density
vs.	versus
WA	Water Absorption

## Table of Content

<b>1. Introduction and objectives</b>	1
<b>1.1 Epoxy resins</b>	2
1.1.1 Cross-linking process	4
1.1.2 Problem of BPA-based resins	6
<b>1.2 Bio-based epoxy resins from renewable resources</b>	7
1.2.1 Epoxy monomers from plant oils	7
1.2.2 Epoxy monomers from other renewable sources	10
1.2.2.1 Saccharide-based epoxy resins	10
1.2.2.2 Lignin-based epoxy resins	12
1.2.2.3 Phenolic and polyphenolic epoxies	12
1.2.3 Bio-based curing agents	13
<b>1.3 Recyclable bio-based epoxy resins</b>	14
1.3.1 Networks with dynamic covalent bonds	15
1.3.2 Vitrimers	15
1.3.2.1 CANs based on carboxylate transesterification reaction	16
1.3.2.2 CANs based on disulfide exchange reactions	18
1.3.2.3 CANs based on imine exchange reaction	21
1.3.2.4 CANs based on Diels-Alder reactions	22
1.3.2.5 Other CANs with reversible covalent bonds	23
<b>1.4 Reinforced epoxy composites</b>	23
1.4.1 Natural fibres	24
1.4.1.1 Composition of plant fibres	24
1.4.2 PLA as matrix or reinforcement	25
1.4.3 Properties of bio-based reinforced composites	26
<b>1.5 Recyclables composites</b>	28
<b>1.6 Scope of the thesis</b>	29
References	30
<b>2. Enhancing the recyclability of a vegetable oil-based epoxy thermoset through initiator influence</b>	37
Abstract	38
<b>2.1 Introduction</b>	39
<b>2.2 Results and discussion</b>	41
2.2.1 Structural investigation of ELO/DTBA copolymerization by FT-IR	41
2.2.2 Thermomechanical analyses of ELO/DTBA thermosets: comparison of virgin and recycled materials.	43
2.2.2.1 Dynamic mechanical analysis	45

2.2.2.2 Thermal stability	46
2.2.3 Study on the multiple reprocessing effect on materials performance	48
2.2.4 Swelling tests	50
<b>2.3 Conclusions</b>	51
<b>References</b>	52
<b>Electronic Supplementary Information (ESI)</b>	55
<b>3 Building thermally and chemically reversible covalent bonds in vegetable oils-based epoxy thermosets. Influence of epoxy-hardener ratio to promote recyclability</b>	64
<b>Abstract</b>	65
<b>3.1 Introduction</b>	66
<b>3.2 Results and discussion</b>	67
3.2.1 Influence of the EVO/DTBA ratio on the crosslinking by DSC investigation	67
3.2.2 Influence of the epoxy/acid ratio analyzed by FT-IR studies	69
3.2.3 Thermo-mechanical analysis of virgin and recycled thermosets	70
3.2.3.1 Glass transition study	71
3.2.3.2 DMA analysis	72
3.2.3.3 Thermal stability analysis	74
3.2.3.4 Chemical recycling and characterization of recycled materials	74
<b>3.3 Conclusions</b>	78
<b>References</b>	79
<b>Electronic Supplementary Information (ESI)</b>	81
<b>4 Sustainable access to bio-based epoxidized vegetable oil thermoset materials: from homopolymers to copolymers</b>	88
<b>Abstract</b>	89
<b>4.1 Introduction</b>	90
<b>4.2 Results and discussion</b>	93
4.2.1 Study of EVOs homopolymerization	93
4.2.1.1 Thermal stability of EVOs	93
4.2.1.2 EVOs reactivity analysed by DSC and FT-IR	94
4.2.1.3 Properties of thermo-cured EVOs homopolymers	95
4.2.2 Study of EVOs copolymerization with DTBA	96
4.2.2.1 Copolymerization reactions followed by DSC and FT-IR studies	97

4.2.2.2 Thermomechanical properties of EVOs/DTBA/IM thermosets	100
4.2.2.3 Solvent and chemical stabilities	106
4.2.2.4 Bio-based content	109
<b>4.3 Conclusions</b>	109
<b>References</b>	110
<b>Electronic Supplementary Information (ESI)</b>	113
<b>5 Recyclable, repairable and reshapable (3R) thermoset materials with shape memory properties from bio-based epoxidized vegetable oils</b>	121
<b>Abstract</b>	122
<b>5.1 Introduction</b>	123
<b>5.2 Results and discussions</b>	124
5.2.1 Mechanical recycling	126
5.2.1.1 Investigation of the recycled thermosets	126
5.2.1.2 Repairability and reshapability	130
5.2.1.3 Shape memory	131
5.2.2 Chemical stability	133
<b>5.3 Conclusions</b>	135
<b>References</b>	135
<b>Electronic Supplementary Information (ESI)</b>	138
<b>6 Chemical and mechanical reprocessed resins and bio-composites based on five epoxidized vegetable oils thermosets reinforced with flax fibers or PLA woven</b>	147
<b>Abstract</b>	148
<b>6.1 Introduction</b>	149
<b>6.2. Results and discussion</b>	150
6.2.1 Reactivity study of the EVOs-based resins in presence of FF or PLA fillers	150
6.2.2 Thermo-mechanical characterization of bio-composites	152
6.2.2.1 Glass transition analysis	152
6.2.2.2 Dynamic mechanical analysis	153
6.2.2.3 Thermal Stability	155
6.2.2.4 Fibre-resin interaction: SEM investigation	156
6.2.3 Water absorption analysis	157
6.2.4 Recycling and repairing	158
6.2.4.1 Mechanical reprocessing	158

6.2.4.2 Chemical	159
<b>6.3 Conclusions</b>	160
<b>References</b>	160
<b>Electronic Supplementary Information (ESI)</b>	163
<b>Conclusions and perspectives</b>	172
<b>Scientific contributions</b>	175

# Chapter 1

*Introduction and objectives*

## Chapter 1

### Context

In an era in which petroleum resources are in decline and the environmental concerns associated to the use of polymers are growing, the bio-based polymers or those derived from bio-renewable raw materials, represent an important solution for the sustainable global development. The dynamic polymers emerged over the last decades with the aim of minimizing the accumulation in landfills of materials that cannot be recycled or repaired. The main purpose of this chapter is the bibliographical investigation on epoxy resins and composites obtained from renewable sources, used for the production of potential recyclable, self-repairing or shape memory materials.

### 1.1 Epoxy resins

The epoxy resins are thermosetting polymers characterized by the presence in their structure of oxiranes or epoxy groups.<sup>1</sup> The epoxy monomers have the ability of forming cross-linked high molecular weight polymers. The three membered epoxy ring is highly strained and is reactive to many substances acting as curing agents. Through the ring opening reaction, their properties depend strongly on the specific combination of the type of epoxy monomers and the used curing agents that generally contain hydroxyl, carboxylic, amino and anhydride groups. Due to the variety of potential hardeners, a large scale of properties and applications can be obtained.

The epoxy resins are known for their general excellent mechanical properties, high adhesiveness to different substrates, and good thermal and chemical resistances,<sup>2</sup> high-performance coatings, excellent dimensional stability and high corrosion resistance and encapsulating materials.<sup>3</sup> They have found applications in numerous industrial fields since their commercialization in 1946 by Devoe-Reynolds Company,<sup>4</sup> whose production increased over the years; in particular, the most important application fields are:

- Adhesives, especially in aircraft, automobiles, bicycles, boats, golf clubs, skis, snowboards, and other applications. In this case the epoxy resins are cured at elevated temperatures to increase their strength and activate the chemical bonding at the substrate / adhesive interface;<sup>5-7</sup>
- Aerospace industry, usually to obtain reinforced composites with high strength glass, carbon, Kevlar, or boron fibres for the manufacture of structural parts of airplanes and wind turbines;<sup>8-9</sup>

- Industrial tooling, replacing metal, wood and other traditional materials improving the efficiency of the process and reducing the cost and delivery time of the many industrial processes;<sup>10</sup>
- Electronic devices materials, *i.e.* as encapsulation to protect integrated circuits from moisture and environmental conditions such as temperature, radiation, humidity, and mechanical and physical damage;<sup>11-12</sup>
- Flame retardants, most notably in electronics;<sup>13-14</sup>
- Biomedical applications for dental or orthopaedic uses as adhesives and cements.<sup>15-16</sup>

In 2016, the global value of epoxy-based thermosets reached a market value of US \$ 21.5 billion and it's estimated that it may reach US \$27.5 billion by the end of 2020 and increase to US \$ 37.3 billion by 2025 in the forecast. Strong demand for epoxy composites market and epoxy adhesives market is expected.<sup>17</sup>

Historically, the first epoxy resins were synthesized concurrently by two independent researchers: Pierre Castan and Sylvan Greenlee in 1981.<sup>18-19</sup> The first one discovered the epoxy resin by reacting the diglycidyl ether of bisphenol A, DGEBA (obtained by the reaction of bisphenol- A-2,2'-bis(4-hydroxyphenyl) propane or 4,4'-isopropylidene diphenol with epichlorohydrin) with cyclic dicarboxylic anhydride. The second one, Sylvan Greenlee investigated the synthesis of epichlorohydrin and bisphenol A for the production of resins that can be used as coatings.

Some of the most typical epoxy resins structures are collected in Figure 1:

they are characterized by having the core of the molecule with aliphatic, cycloaliphatic or

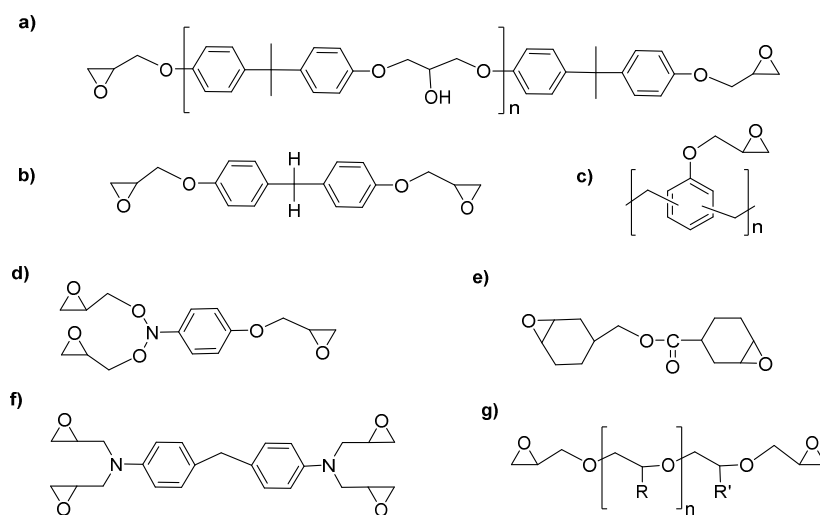


Figure 1 . Structure of different epoxy resins

aromatic structure, and consequently different characteristics. The Novolac epoxy resins and tetrafunctional epoxies (Figure 1 c and 1 f) are characterized by a high epoxy functionality generating high cross-linking densities. They are often used in applications where high temperatures and chemical resistance are required. Nowadays, the most important epoxy



## Chapter 1

resins are prepared from bisphenol A (BPA) and epichlorohydrin. The obtained resin is called diglycidyl ether of bisphenol A (DGEBA) (Figure 1 a), constituting approximately 85% of commercial epoxies.

### 1.1.1 Cross-linking process

The epoxy monomers should be reacted with a hardener or homopolymerized, through an anionic or cationic homopolymerization, to obtain thermosetting materials. The choice of one hardener over another depends on the required final properties of the resin and / or on the expected conditions, stoichiometry and the processing method.

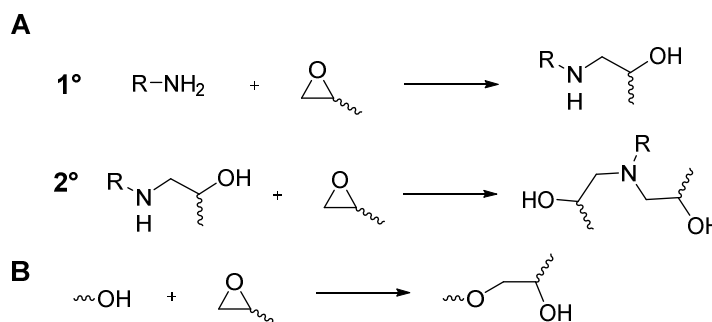
The process takes place by heating (thermo-curing) or stimulation by external irradiation and the mechanisms to generate an epoxy network are the following:<sup>20</sup>

- Step growth polymerization (polyaddition, polycondensation): as the reactions of epoxy groups with amines, alcohols or carboxylic acids. For instance, the reaction mechanism

between epoxy monomer and primary amines is shown in Scheme 1 A: initially the reaction produces an alcohol and a secondary amine that reacts with another epoxy group, producing a tertiary amine and two secondary hydroxyl groups. If the epoxy functionality of the reaction exceeds, a second reaction, called etherification (Scheme 1 B), can occur by the addition of the hydroxyl group to the oxirane in excess. In the case of condensation reactions, the two reagents are reacting and eliminate a small molecule (usually an alcohol, a water molecule or an acid);

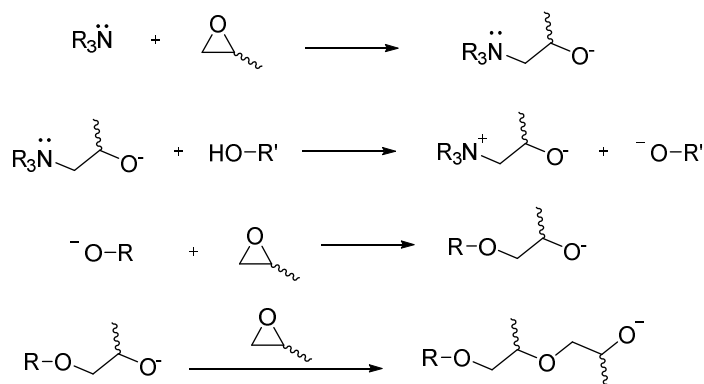
- Chain-growth polymerization is basically a three-stage process, involving initiation, propagation and termination of the active chain ends. The reaction requires, usually, the presence of an initiator to react with the monomer and to form a reactive species.

For the synthesis of thermosetting resins, two types of curing agents are widely used: stoichiometric agents and catalytic ones.<sup>21</sup> Catalytic agents can be divided in anionic and cationic initiators. Lewis bases contain unshared electron pairs that can attack as low electron density nucleophilic sites. Tertiary amines are used to initiate the anionic polymerization of



*Scheme 1. Mechanism of reactions of epoxy groups with a primary amine*

epoxies and the reaction involves a zwitterion, which consists on an ammonium and alkoxide groups. A new epoxy group is opened by the alkoxide with the generation of another anion which reacts with a further epoxy group (Scheme 2).



**Scheme 2.** Mechanisms of reaction of epoxy groups with tertiary amines

The most used anionic curing

agents are imidazoles, substituted pyridine and other tertiary amines. The stoichiometric agents react as co-monomers during the copolymerizations, while the second one acts as initiator for the process of homopolymerization of the resin. In the first class can be included anhydrides, acids, amines, polyamides, etc.

The reactivity of the curing agent depends on its nucleophilic behavior. Some strong nucleophiles such as thiols and amines are very reactive and can even react at room temperature. Carboxylic acids or acid anhydrides, on the other hand, are among weak nucleophiles and usually require high reaction temperatures with the advantage to be lower toxic than the amines, as reported by Xiao and Wong.<sup>22</sup> The lower reactivity between these curing agents and the epoxy groups can be remedied by adding a percentage of catalyst / initiator, as tertiary amines or imidazoles (between 0.5 and 10%).

The formation of the network, by the chemical connectivity between the hardener and epoxy resin, occurs accompanied by physical processes of gelation and vitrification. The cure of thermosetting polymers involves a series of complex chemo-rheological variations. The mixture of monomers or low molecular weight oligomers in the liquid state turns into a solid network densely crosslinked. In this process the two states of aggregation are separated by the gelation point. The growth and branching of the polymer chains start in the liquid phase where the system is still soluble and fusible. The cross-linked network is formed only after the gelling point when the polymer chains become an insoluble and infusible solid macromolecular where the final reactions take place by diffusion in the solid state. The transformation from a viscous liquid to an elastic gel, called *gelification*, is sudden and irreversible, and involves the formation of the three-dimensional network. Before gelation, in the absence of a cross-linking agent, the resin particles are separated from each other or interact only through weak reversible intermolecular forces, called Van der Waals forces. As

## Chapter 1

the crosslinking progresses, intermolecular covalent bonds are formed, forming a hardened 3D network.

Another physical phenomenon that can occur during the curing reaction is the *vitrification*, that is the transformation of a viscous liquid or an elastic gel into a glassy solid.

The thermally hardened polymer, if properly formulated and processed, is densely cross-linked forming a dimensionally infinite three-dimensional network which gives it a good dimensional and thermal stability, good chemical resistance, etc.

### 1.1.2 Problem of BPA-based resins

The most used epoxy resin so far, DGEBA, is considered actually as a molecule to be replaced, due to the BPA toxicity. Its synthesis occurs by the reaction of epichlorohydrin and bisphenol-A. The epichlorohydrin is obtained from glycerine via glycerol chlorination and it is considered environmentally friendly,<sup>23</sup> but the BPA is strongly non-renewable because of its fossil sources of phenol and acetone.<sup>24</sup> BPA has been widely used in the industries of polycarbonate, baby plastic bottles, dental sealants and epoxy coating of beverage and canned food packaging.<sup>25</sup> When included in a polymer structure obviously the BPA is non-toxic, but when exposed to heat, UV light or a change in pH conditions, it converts to monomeric form and it's released into food and water, causing health risk for humans. Vandenberg *et al.*<sup>25</sup> demonstrated that BPA is absorbed from the intestinal tract and metabolized in the liver to form BPA glucuronide which is chemically inert, and it's accumulated. The researchers also shown that BPA is an endocrine disruptor even at low doses (below 50 mg.kg<sup>-1</sup> body weight /day) producing reproductive cancers , fertility problems and other endocrine related endpoints and to affect glucose metabolism through insulin resistance.<sup>26</sup>

Considering these harmful effects, the European government, decided to limit the exposure of their citizens to this substance. In 2004 the Commission of Implementing Regulation (EU) with the opinion of the Risk Assessment Committee (RAC) classified BPA as hazard class reproductive toxicity category 1B with potential toxicity for fertility.<sup>27</sup> European legislation severely limited BPA-based products in applications such as baby bottles and medical supplies, authorizing it only as additive or monomer in the production of plastics and articles in contact with food and water,<sup>28</sup> but a specific migration limit value of 0.6 mg.kg<sup>-1</sup> has been set.<sup>29</sup> France approved the restriction of BPA-based products since 6 July 2016, under the REACH regulation.<sup>30</sup> Following the various bans on the use of BPA, the industry developed various alternatives to BPA for its many applications. Unfortunately, these substances are not

always better than the original compound. Some “BPA-free” bottles continue, for example, to release substances that imitate the action of oestrogens and a substance very similar to BPA, bisphenol S (BPS), is present in cash receipts. Recent studies<sup>31</sup> have confirmed that this bisphenol is also an endocrine disruptor, therefore the wording "BPA-free" is not synonymous with the absence of toxic risk. There are also other alternatives that seem less harmful, but it will take some years and numerous studies to be sure of the harmlessness of these substances currently little known.

## 1.2 Bio-based epoxy resins from renewable resources

Due to the above mentioned issues, the interest has constantly increased on renewable sources and on natural polymers to be used in the production of materials to substitute the traditional plastics, or in the development and engineering of the new generation of bio-based plastic materials. The bio-plastics have shown technological properties and applications interest that make them competitive on the market, compared to traditional plastics. Bio-based epoxy resin components are currently produced from different bio-resources,<sup>32</sup> such as vegetable oils, lignin, tannin, cardanol, rosin, eugenol, carbohydrate, etc.

### 1.2.1 Epoxy monomers from plant oils

US Department of Agriculture estimated that the world production of vegetable oils was around 203 million metric tons in 2018 / 2019 (Figure 2)<sup>33</sup> with around 75% of global plant oil

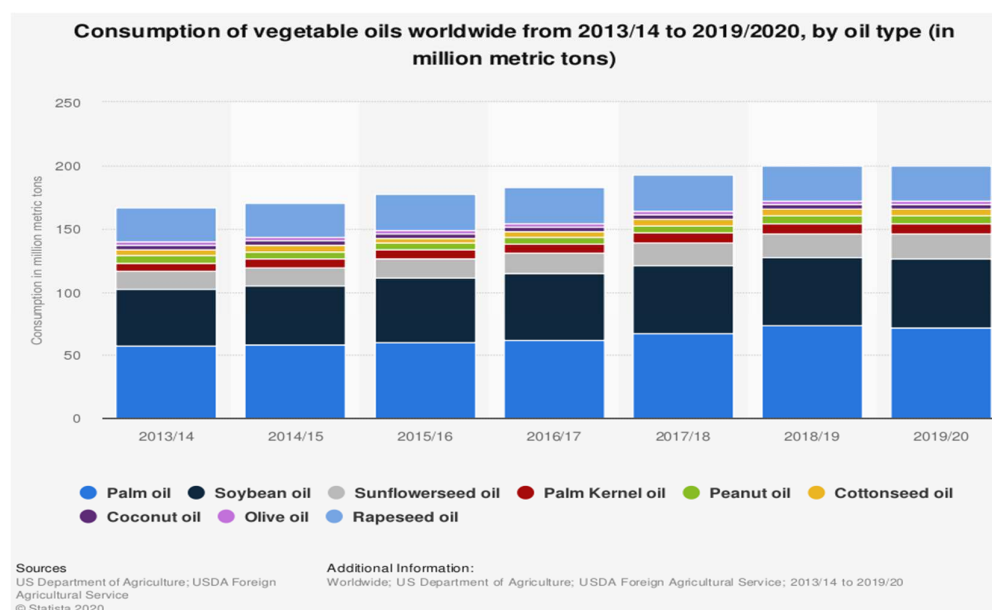


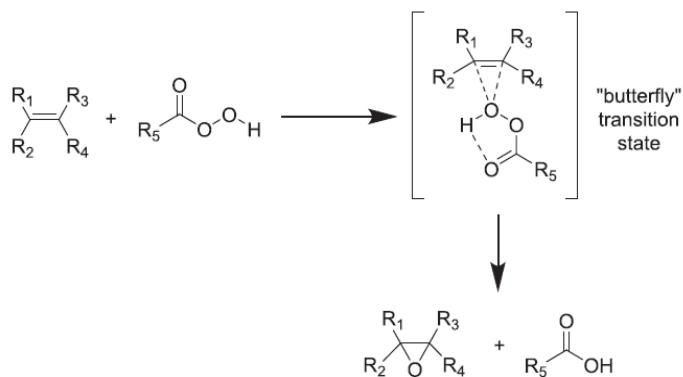
**Figure 2.** World production of vegetable oil from 2013 to 2020<sup>33</sup>

## Chapter 1

production used for food and the remaining 25% used for industrial applications, such as coatings, adhesives, cosmetics, inks, and plasticizers.

The abundance of carbon-carbon double bonds makes the vegetable oils a choice for the formation of resin. The C=C bonds of fatty acids are useful sites where the polymerization reaction can occur. Double bonds can undergo various modifications; it can be oxidised, halogenated, reduced or epoxidated. The epoxidation is a commercially important reaction in organic synthesis since the high reactivity of the oxirane rings makes them readily transformed into the desired products. Therefore, numerous researches on the epoxidation of vegetal oils were conducted in order to optimize the conversion rate and increase the epoxy yield. The epoxidation methods are:

- through peracids in presence of inorganic catalyst with H<sub>2</sub>SO<sub>4</sub> (bi-phasic system) or acidic ion exchange resin (AIER) (tri-phasic system), called Prileshajev epoxidation (Scheme 3)<sup>34</sup>;
- through organic or inorganic peroxides using transition metals or enzymatic species as catalysts;
- Epoxidation with molecular oxygen.



Although the latter is the most cheaper and greener method, the epoxidation

**Scheme 3.** Mechanism of epoxide formation mediated by peracids<sup>34</sup>

process is not efficient in the case of vegetable oils since there is a risk of the cleavage and degradation up to aldehydes and ketones, as well as chains of short dicarboxylic acids.<sup>35-36</sup>

In general nowadays, the epoxidized vegetable oils (EVOs) find applications as plasticizers or stabilizers for PVC synthesis, toughening agents for petroleum-based epoxy systems, or as epoxy pre-polymers for the production of thermosetting resins. Among the main industrial producers of epoxidized vegetable oils there are Akcros Chemicals<sup>37</sup> and Arkema Co.<sup>38</sup> for the production of and Lankroflex L (epoxidized linseed oil - ELO) and VIKOFLEX® (epoxidized soybean oil - ESO), respectively. Unfortunately, due to long aliphatic and flexible chains in which there is a relatively low amount of epoxy rings many of them being internal, EVOs have a low reactivity. Also, some EVOs based resins have poor rigidity, strength, thermal and mechanical properties compared with DGEBA-based ones. Among the most advantageous, the use of aromatic hardeners allows to obtain thermosets with good performances. For

example, Earls *et al.*<sup>39</sup> cured ELO with two anhydride acids: phthalic (PA) and 4,4'-methylenedianiline (MDA) anhydrides obtaining materials with a  $T_g$  between 54 and 133 °C, compared to ~ 190 °C that of DGEBA resin.

Ding *et al.*<sup>40</sup> evaluated how the chain length of a series of  $\alpha, \omega$ -DCAs (with the number of carbon atoms from C<sub>6</sub> to C<sub>18</sub> and a diacid C<sub>36</sub>, Pripol 1009F, obtained by biological derivation) produce variations on the physical and mechanical properties of the resulting cross-linked systems based on ELO. The authors observed that increasing the DCAs chain length, the  $T_g$  decreased from 7 °C, for C<sub>6</sub>, to -15 °C of C<sub>36</sub>, due to the decrease in crosslink density. Also, the network density was higher for the thermosets with shorter chain length. A similar trend was observed by Shimbo *et al.*<sup>41</sup> that cured DGEBA with aliphatic  $\alpha, \omega$ -diamines (C<sub>2</sub>, C<sub>4</sub>, C<sub>6</sub>, C<sub>12</sub>) ranging  $T_g$  from 75 °C, for C<sub>12</sub>, to 135 °C for C<sub>2</sub>. A similar study was conducted by Gobin *et al.*<sup>42</sup> by copolymerizing the synthesized epoxidized broccoli oil with several aliphatic carboxylic diacids (C<sub>5</sub>, C<sub>6</sub>, C<sub>8</sub>, C<sub>10</sub>, C<sub>12</sub>, C<sub>14</sub>, C<sub>16</sub>) and one aromatic diacid (o-phenylene diacetic acid) demonstrating that the  $T_g$  depends on the nature and length of the diacid used in the crosslinking reaction. Despite the low  $T_g$  (from -1.4 to 16 °C), the authors propose to mix these green polymers with other polymers to increase the  $T_g$  by "permanent" plasticization.

In order to improve the properties of EVOs-based epoxy resins, petroleum-based epoxies like DGEBA are used in mixture with EVOs. Altuna *et al.*<sup>43</sup> increased the storage modulus in the glassy state and the  $T_g$  by adding variable percentages of DGEBA to ESO and curing the system with methyltetrahydrophthalic anhydride (MTHPA) and 1-methyl imidazole (1-MI), as catalyst. The same strategy has been used by Abu Bakar *et al.*<sup>44</sup> by preparing DGEBA / ESO blends crosslinked with methylhexahydrophthalic anhydride (MHHPA) in presence of 2-ethyl-4-methylimidazole (EMI). By increasing the percentage of ESO in the mixture, the authors observed a decrease of the tensile, flexural and thermal stability properties due to the reduced crosslink density of the network. However, a significant enhancement on impact strength proves that ESO acts as a plasticizer in the blends as well as improving the toughness of ESO / DGEBA thermoset blend. Park *et al.*<sup>45-46</sup> investigated the effect of different ECO and ESO contents on the properties of DGEBA mixed systems cured by N-benzylpyrazinium hexafluoroantimonate (BPH), observing an increasing of impact strength in the resins by adding the EVOs.

However, excellent mechanical properties can be obtained by copolymerizing EVOs with appropriate and selected hardeners. Pin *et al.*<sup>47</sup> realized an epoxy resin with a high crosslink density by copolymerizing ELO with methylhexahydrophthalic anhydride (MHHPA) and benzophenone-3,3',4,4'-tetracarboxylic dianhydride (BTDA) with  $T_g$  from 68 to 134 °C in

## Chapter 1

function of the epoxy / anhydride ratio, obtaining high thermal degradation ( $\sim 337$  °C). The authors<sup>48</sup> synthesized a completely bio-based resin by combining ELO with polyfurfuryl alcohol (PFA), in the presence of boron trifluoride ethylamine complex, as catalyst, obtaining ductile resins as consequence of ELO flexible chains introduced into the PFA network.

Kadam *et al.*<sup>49</sup> synthesized bio-based epoxy resins from karanja oil. The epoxidized oil was reacted with two bio-based acids: citric acid (CA) and tartaric acid (TAR). The obtained thermosets showed thermal stability comparable to DGEBA based resins. As a further advantage, from the analysis of biodegradability it was obtained that TAR/epoxy resin was 95% degraded in 259 days compared to the CA / epoxy resin that degraded by 82 % in 69 days. A recent cationic photo-polymerization study<sup>50</sup> was carried out on epoxy functionalized bio-renewable monomers for coating applications: epoxidized castor oil (ECO), phloroglucinol trisepoxy (PHTE) and diglycidylether of vanillyl alcohol (DGEVA) with triarylsulfonium hexafluoroantimonate, as cationic photoinitiator. The ECO-based coatings achieved high conversion of the epoxy groups but low  $T_g$  ( $\sim 20$  °C) compared with the rigid aromatic structure of DGEVA and PHTE, with  $T_g$  values of 82 and 75 °C, respectively. Huang *et al.*<sup>51</sup> synthesized bio-based thermosetting epoxy foams through a reaction between ESO with fumaropimaric acid (FPA) using N,N'-dimethylbenzylamine (DMBA), as catalyst, and sodium bicarbonate as foaming agent. The thermosetting epoxy-foams showed excellent thermal stability with a density between 361 to 231 kg.m<sup>-3</sup> and variable compressive strength depending on the ESO / FPA ratio. Bio-based structural foams were obtained from Mazzon *et al.*<sup>52</sup> mixing of two epoxidized plant oil-derivates (ELO and glycerol triglycidyl ether) with different cyclic anhydrides and a non-toxic foaming agent (KHCO<sub>3</sub>) using a short production time (lower than 3 minutes). The foams were characterized by a glass transition higher than 80 °C with potential applications as lightweight structural materials.

Parada Hernandez *et al.*<sup>53</sup> synthesized and characterized copolyester derived from epoxidized castor oil and citric acid with a toxicity-free copolymerization process with comonomers that can be metabolized by the human body and that can be used in the biomedical area.

### 1.2.2 Epoxy monomers from other renewable sources

#### 1.2.2.1 Saccharide-based epoxy resins

Carbohydrates are interesting renewable resources, some of them have long been studied such as monosaccharide (sorbitol), disaccharides (sucrose and isosorbide) and derived acid compounds. The great availability and the great variety of chemical structures, with great

stereo-chemical diversity, made the carbohydrates an important natural source, easily renewable, for building blocks for the synthesis of biodegradable polymers.

Isosorbide is obtained from starch and found several applications in epoxy resins field. Łukaszczuk *et al.*<sup>2</sup> synthesized isosorbide-based epoxy resin (IS-EPO) from 1,4:3,6-dianhydro-D-glucitol (isosorbide) and epichlorohydrin in the presence of concentrated aqueous solutions of NaOH. The epoxy monomer was cured with phthalic anhydride and tetrahydrophthalic anhydride, and with triethylenetetramine and isophoronediamine, showing low hydrophilicity for the compositions done with acid anhydride hardeners. Hong *et al.*<sup>54</sup> prepared a resin from diglycidyl ethers of isosorbide and isosorbide diamine (ISODA). The obtained resin exhibited water solubility and excellent mechanical properties.

The combination of sucrose and vegetable oil fatty acids yielded to sucrose esters of fatty acids (SEFA) as coatings, firstly explored in the 1960s. Webster *et al.*<sup>55</sup> synthesized high functionalized epoxy resins by the epoxidation of sucrose ester resins of fatty acids. Compared to the epoxidized vegetable oils, the epoxidized sucrose esters showed high stiffness (due to rigid sucrose core) and crosslinking densities. The authors<sup>56</sup> synthesized thermosets from epoxidized sucrose soyate (ESS), synthesized by the epoxidation of sucrose ester resins of soybean oil fatty acids. These epoxies were cured with citric or malic acids (found naturally in juices) in presence of different solvents (water, ethanol, 1-propanol, 2-propanol, and 1,4-dioxane). The authors investigated the effect of the used solvent on the curing reaction and on properties of the final resins. They found that the alcohols increased the curing reactivity, compared to the systems using water or 1,4-dioxane, but the thermo-mechanical properties were slightly lower. The authors explained this result to the possible reactions between hydroxyl groups from alcohols with carboxylic acid group from hardeners and / or with the epoxy group in the networks.

Among carbohydrate derivatives, furanic compounds are attracting a growing interest as valuable alternatives to petroleum-based molecules. They derive from cellulose and hemicellulose and contain a heteroaromatic five-member ring that mimics the rigid structure and properties of DGEBA resins. Miao *et al.*<sup>57</sup> prepared bio-based resins (EUFU-EP) synthesized from two bio-based green and low toxic compounds (2,5-furandicarboxylic acid and eugenol) curing them with methyl hexahydrophthalic anhydride (MHHPA). The authors compared the properties of the bio-based epoxy resins with DGEBA resin. The EUFU-EP / MHHPA exhibited higher  $\tan \delta$  and crosslinking density (153 °C / 1.25 g.cm<sup>-3</sup>) than DGEBA / MHHPA resin (114.1 °C / 1.18 g.cm<sup>-3</sup>). Marotta *et al.*<sup>58</sup> synthesised and characterized a furan-derived epoxy resins based on 2,5-bis[(oxiran-2-ylmethoxy) methyl]furan and cured it with



## Chapter 1

methyl nadic anhydride (MNA) in presence of with different initiators. The authors obtained large range of properties modulating the ratio between epoxy / anhydride, with  $\tan \delta$  from 29 to 70 °C, and comparable thermal stability as DGEBA / MNA thermoset (256 °C for the bio-based thermosets and 271 °C for the fossil derivatives resin).

### 1.2.2.2 Lignin-based epoxy resins

Lignin is one of the three main constituents of wood together with cellulose and hemicellulose, considered the second most abundant biopolymer and it represents the most abundant natural aromatic compound.<sup>59</sup> Some scientific research on polymers based on lignin derivatives focused on its epoxidation. Ferdosian *et al.*<sup>60</sup> synthesized lignin-based epoxy resins in a preliminary study in 2012, using de-polymerized organosolv lignin in alkali medium treated with epichlorohydrin. Wang *et al.*<sup>61</sup> synthesized two novel bio-based epoxy monomers not directly by lignin but from its derivatives: vanillin-based epoxies with  $T_g$  of 214 °C, tensile strength of 80.3 MPa, and tensile modulus of 2709 MPa, much higher than the cured DGEBA reference sample, showing in addition excellent flame retardancy ability. Lignin-based epoxy resin were obtained by Zhu *et al.*<sup>62</sup> from pulping black liquor at different pH values. The mechanical and thermal properties of cured lignin-based epoxy resins with ethylenediamine were compared in function of reaction temperatures. Sasaki *et al.*<sup>63</sup> used the lignin extracted from steam-exploded bamboo, as raw material for the synthesis of epoxy resins cured thereafter with a bamboo lignin (BL-BL) or with 1-(2-cyanoethyl)-2-ethyl-4-methylimidazole. The first one exhibited good thermal and mechanical properties but lower compared with the DGEBA resin.

### 1.2.2.3 Phenolic and polyphenolic epoxies

Phenolic compounds have the advantages of very good chemical and temperature resistance as well as structural stability. For example, the tannins are natural polyphenolic structures generally obtained from plants. Catechin is one of the main components of tannins and one of the most studied natural polyphenols for the generation of new epoxy resins. In 2015, Basnet *et al.*<sup>64</sup> extracted catechin from green tea, epoxidized it and cured with a lignin extracted from eucalyptus, soluble in methanol, as a natural curing agent. A  $T_g \sim 179$  °C was obtained with thermal stability were similar or higher than those of DGEBA based resins.

The gallic acid (GA) or its derivatives are present in grapes, tea, gallnuts, oak bark, some fruits, vegetables, honey and can also be found in plant tissues also considered as a potential source for bio-based thermosetting epoxy resins.<sup>65</sup> Tomita *et al.*<sup>66</sup> patented the epoxidation of gallic acid or tannic acid with epichlorohydrin then their curing with 3,6-endomethylene /

2,3,6-tetrahydromethylphthalic anhydride (methylhimic anhydride) at different proportions. The comparison with DGEBA derivative epoxy resin showed high values of heat deflection temperatures for the bio-based systems. Recently, Karaseva *et al.*<sup>67</sup> investigated the ability of GA to act as flame retardant for the epoxy resins by treating the GA with boric acid, obtaining gallic acid derivatives to introduce borate ester moieties. Through the grafting of borates groups the thermal stability was increased from 269 to 528 °C.

Cardanol is another phenolic molecule obtained from cashew nut shell liquid extracts; it finds wide applications in the form of brake linings, surface coatings, paints, and varnishes. The cardanol has the advantage of having both, aliphatic and aromatic structures. Jaillet *et al.*<sup>68</sup> used a commercial epoxidated cardanol NC-514 from Cardolite cured with IPDA and Jeffamine D400. The  $T_g$  value of the obtained thermoset films was 50 °C, with the first hardener, and 15 °C with second ones. These materials exhibited thermal stability > 300 °C but the crosslinking density of 0.07 mol.m<sup>-3</sup> was four times lower than those of the thermoset based on epoxidized soybean oil cured with a cycloaliphatic anhydride. Recently, Noé *et al.*<sup>69</sup> synthesized 3 epoxy cardanol-based products: epoxidized cardolite ECO 84, 85 and 86 with 3.88, 3.89 and 2.82 meq.g<sup>-1</sup> epoxy content, respectively. The synthesis was done in molar ratio conditions C=C / Acetic Acid / H<sub>2</sub>O<sub>2</sub> (35% w/w) in 1 / 0.5 / 1.5 eq. with amberlite® IR-120. These epoxy monomers were photocured with triarylsulfonium hexafluoroantimonate salts, as photoinitiator. The  $T_g$  values ranged from 38 to 65 °C for the network obtained by the monomer with low epoxy content. Higher  $T_g$  and crosslink density values were obtained for ECO 86.

### 1.2.3 Bio-based curing agents

In 2014, Ding and Matharu<sup>70</sup> reported the developments regarding hardeners from renewable materials. For example, from vegetable oils it's possible to obtain polyols through hydroxylation of double bonds, by opening the epoxy ring of epoxidized vegetable oils (EPO) or dimerization of fatty acids. Liu *et al.*<sup>71</sup> used the hydroxyl group in castor oil to produce hardeners, combining it with phosphoryl chloride to create phosphorylated castor oil and subsequently, crosslinked it with ELO and ESO. The synthesized elastomer was biodegradable and biocompatible with potential applications in biotechnology and bioengineering.

In 2004, the U.S. Department of Energy (DOE) identified 12 sugar-derived building blocks, the so-called "platform molecules",<sup>72</sup> including the glutaric, itaconic, aspartic, succinic acids and the glycerol. Ma *et al.*<sup>73</sup> prepared 100% bio-based polymers based on natural acids (citric, DL-malic, L-tartaric, malonic, oxalic, and glutaric acid) reacted with epoxidized sucrose soyate

## Chapter 1

(ESS) and soybean oil, in presence of water. The obtained materials displayed excellent thermal and mechanical properties and their fully dissolution in NaOH aqueous solutions. Supanchaiyamat *et al.*<sup>74</sup> synthesized a 99.5% bio-thermosetting resin based on ELO reacted with a bio-derived diacid crosslinker (Pripol 1009 - a dimerised fatty acid derived from natural oils and fats) demonstrating that the thermo-mechanical properties are strongly influenced by the different amine catalysts used. The Pripol 1040 (mixture of tricarboxylic and dicarboxylic fatty acids) has been used by Leibler *et al.*<sup>75-76</sup> to cure DGEBA in the presence of different transesterification catalysts, the obtained materials, "vitrimers", being strong organic glass covalent formers able to change their topology through thermoactivated bond exchange reactions.

### 1.3 Recyclable bio-based epoxy resins

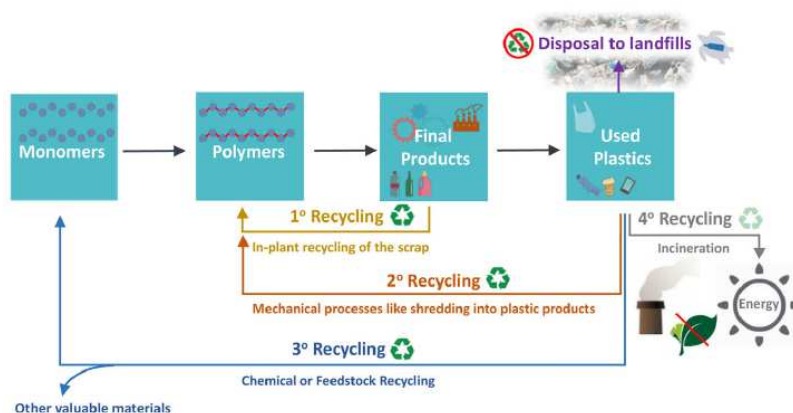


Figure 3. Types of plastic waste recycling<sup>77</sup>

The plastic recycling market was evaluated at US\$ 41.73 Bn in 2018 and is forecasted to grow with 6.6% from 2019 to 2027.<sup>77</sup>

Today, around 50% of plastics are made for single-use applications, such as

disposable consumer items and packaging, leading to ecological and consequently social problems. According to American Society for Testing and Materials ASTM D5033,<sup>78</sup> the recycling processes can be classified as following<sup>79-80</sup> (Figure 3):

- Primary recycling: is “the processing of scrap plastic product into a product with characteristic similar to those of the original ones”.
- Secondary recycling: is “the processing of scrap plastic product into a product that has characteristics different from those of the original ones”.
- Tertiary recycling: is “the production of basic chemicals or fuels from segregated plastic scrap or plastic material that is part of a municipal waste stream of other source”.
- Quaternary recycling: is “the useful retrieval of the energy content of scrap plastic by its use as a fuel to produce products such as steam, electricity and so forth”.

Due to the highly cross-linked structure after complete curing, thermosetting plastics cannot be recycled while thermoplastic materials are recyclable. Making the thermosets reprocessable is therefore of great importance from a practical point of view. The most efficient strategy to confer reprocessability to a thermoset is to introduce exchangeable chemical bonds into the polymer network, which leads to dynamic crosslinks.

### 1.3.1 Networks with dynamic covalent bonds

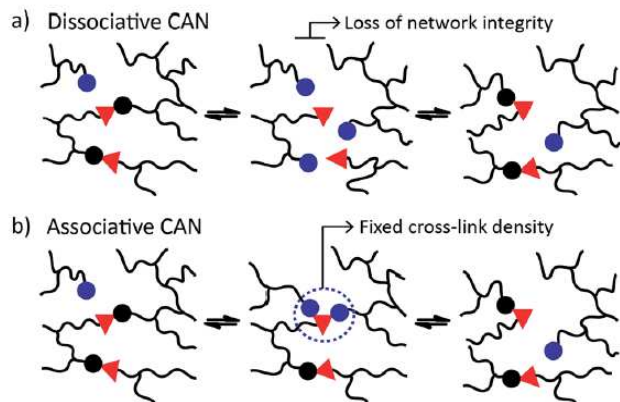


**Figure 4.** Schematic representation of CANs: (A) dissociative, and (B) associative<sup>83</sup>

In 2010, Bowman *et al.*<sup>81</sup> defined covalent adaptable networks (CANs) as “networks which contain a sufficient number and topology of reversible covalent bonds, enabling the crosslinked network structure to respond chemically to an applied stimulus, changing in the physical structure, state, and / or shape of the network”. These materials

show excellent thermo-mechanical properties and chemical stability as traditional thermosetting materials and are reworkable and recyclable like the thermoplastics. There are a variety of dynamic covalent reactions that can be used in CANs and can be classified in two classes:<sup>82-83</sup>

- *Dissociative* mechanism, in which the chemical bonds are firstly broken and then formed again at another point (Figure 4 A). Finally the material maintains almost a constant level of crosslink density. Examples of these CANs are the networks obtained through the development of thermally triggered transesterification catalyst for epoxy / anhydride and epoxy / acid polyester-based network or the metathesis of the olefin;
- *Associative* bonds between polymer chains, in which the original crosslink is broken only when a new covalent bond is formed in another position (e.g. condensation of imines, esters formation ) (Figure 4 B).

### 1.3.2 Vitrimers

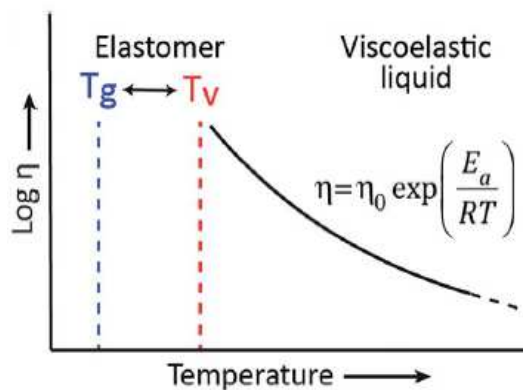
In 2011, some CANs were discovered, these materials showing a gradual change in viscosity following the Arrhenian dependence with the temperature. At a certain temperature range

## Chapter 1

above  $T_g$ , they behave similar to strong glass formers, for example vitreous silica.

Leibler *et al.*<sup>75, 84</sup> called this group of CANs "vitrimers" which are typically based on thermally responsive exchange reactions. The viscoelastic behavior of vitrimers can be described using

two transition temperatures<sup>83</sup> (Figure 5): *i/* the conventional  $T_g$ , glassy to rubbery (during heating) state transition, related to the coordinated long-range molecular chains movement and *ii/* the freezing transition temperature ( $T_v$ ) on which the reversibility of the dynamic bonds is activated and the change of the topology begins to occur.



When the network is in  $T > T_v > T_g$ , the viscosity of the vitrimers is

Figure 5. Viscoelastic behavior of vitrimers<sup>83</sup>

governed by the kinetics of the split and reform of the reversible bonds; so, it follows the Arrhenian dependence on temperature. This transition, situated between the phase transition of viscoelastic solids to viscoelastic liquids, it's conventionally chosen at the point where a viscosity of 1012 Pa.s is reached.<sup>75</sup>

For the design of vitrimer materials, the two temperatures should be considered: the  $T_g$  is correlated to the density of crosslinking or rigidity of the monomeric structures, while the  $T_v$  can be manipulated according to the nature of dynamic bonds, the type of catalysts and its concentration etc. In vitrimers, the viscosity is controlled by chemical exchange reactions and thanks to this, these class of materials can be reprocessed in a wide temperature range without losing the integrity of the network. The thermoplastic materials and dissociative CANs show a significant drop in viscosity and of crosslinking density when the temperature increases.<sup>85</sup>

Vitrimers materials can be synthesized through many chemicals including an efficient covalent exchange mechanism, in some cases in the presence of a catalyst, to modulate the exchange process, other times without, finding applications in the aviation, automotive, electronics and sports industries.

### 1.3.2.1 CANs based on carboxylate transesterification reaction

Transesterification is a process of interchanging where an ester and an alcohol are in equilibrium with a different ester and alcohol<sup>86</sup> (Figure 6).

The first vitrimer was developed by Leibler *et al.*<sup>75</sup> with a simple transesterification reaction of the carboxylates by preparing an elastomeric epoxy resin based on DGEBA and Pripol 1040

(a mixture of fatty acids containing triacids and diacids in an approximately 7:3 ratio) and controlling the reaction with zinc acetate  $[\text{Zn}(\text{Ac})_2]$  as catalyst.

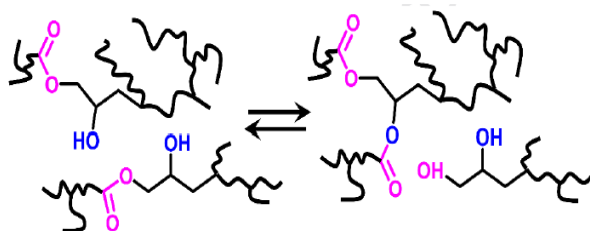


**Figure 6.** Rearrangement of crosslinked network via dynamic transesterification reactions<sup>86</sup>

The presence of a catalyst favours the transesterification reactions at high temperatures, as a cross-exchange way to allow the polymer to rearrange the topology and flow. The authors observed a complete relaxation at elevated temperatures with an Arrhenius-type dependence of the

viscosity. Similar resins were prepared with DGEBA / glutaric anhydride in molar ratio 1:1 and in the presence of 5 or - 10% of zinc acetylacetonate ( $\text{Zn}(\text{acac})_2$ ). By grinding this polymer was obtained a powder that was further remoulded for a complete recycling. The obtained material registered only a moderate loss of elastic modulus while maintaining the same tensile strength as the virgin material.

The possibility of breaking and reforming some covalent bonds has been used by Altuna *et al.*<sup>87</sup> to prepare catalyst-free “green” epoxy-acid vitrimers, completely derived from plant-based monomers, from ESO and citric acid in the presence of water. The networks were capable of stress relaxation and self-healing with moldability and weldability at 160 °C. The authors reported that the system was recyclable. Recently, the same authors<sup>88</sup> reported the synthesis of epoxy resins based on DGEBA crosslinked with tricarboxylic acid (citric, CA) and sebacic (SA) and glutaric (GA) dicarboxylic acids, in presence of 1-methyl imidazole, obtaining vitrimers with  $T_g$  values between 51 °C and 62 °C and a high rate of stress relaxation (less than 1 hour at 160 °C to reach 63% of relaxation). The comparison of the uncatalyzed DGEBA / CA-SA network with the vitrimer obtained without initiator shows the strong effect of the 1-MI catalyst, that enhances the transesterification rate by around three orders of magnitude speeding up the re-shuffling and enabling the permanent re-shaping of the vitrimer in about 1 hour. A high shape recovery ratio, > 99% was obtained, indicating overall a good performance of the shape memory guaranteeing to create new permanent or temporary frames of the thermosetting polymer.

Liu *et al.*<sup>89</sup> synthesized an eugenol epoxide (Eu-EP) cured with succinic anhydride (SA) at different ratios, in presence of zinc acetylacetonate ( $\text{Zn}(\text{acac})_2$ ), as catalyst. The materials presented a fast relaxation time of  $\sim 128$  seconds when  $R_{e/a} = 1:0.5$  compared to 2080s for the thermosets formulated at R 1:0.75. The authors attributed the fast relaxation time to the

## Chapter 1

high content on hydroxyl or carbonyl groups that could trigger the transesterification reaction; in contrast, the Eu-EP / SA at R = 1:0.7, with fewer hydroxyl groups, exhibited a slowest stress relaxation. In addition, the authors displayed the dissolution of the polymer in ethanol at 160 °C after 7 hours; the authors showed that the solvent provided extra hydroxyl groups to induce the exchange reactions in the resins producing the network dissolution.

Yu *et al.*<sup>90</sup> reported a series of epoxy vitrimers prepared from DGEBA reacted with a mixture of curing agents based on carboxylic acid (Pripol 1040-mixture of dimer and trimer acid) / glutaric anhydride in the presence of zinc acetate ( $Zn(Ac)_2$ ). The rate of relaxation and crosslink density decreased with the quantity of glutaric anhydride, useful for promoting dynamic transesterification reaction. The same authors<sup>91</sup> investigated the physical recycling of the BPA cured with Pripol 1040 (23 wt.% of diacid and 77 wt.% of triacid) with 5 mol.% of zinc catalyst. Recyclable resins were obtained applying 180 °C with a pressure of 45 kPa for 30 minutes. The reprocessed materials exhibited a tensile stress value of 2.9 MPa which was ~ 76.7% of that of the original sample. The authors highlighted that without applying pressure, the material cannot be efficiently recycled because the vitrimer, even in the powdered form, remains crosslinked and cannot flow like thermoplastics at elevated temperatures, while under pressure, the particles closely contact with each other, so the dynamic transesterification exchange can effectively occur.

A fully bio-based epoxy vitrimer was synthesized by Yang *et al.*<sup>92</sup> based on ESO and a rosin derivative-fumaropimaric acid (FPA) in presence of zinc acetylacetonate ( $Zn(acac)_2$ ). The obtained network underwent structural rearrangements through transesterifications as directly confirmed by stress relaxation tests, with a relaxation at 200 °C of 1349 seconds. Above the  $T_v$ , the material showed good self-healing and excellent shape memory properties. Moreover, the authors demonstrated the possible chemical recycling in ethanol at 140 °C and reprocessing into new vitrimers at 180 °C.

Recently, Yue *et al.*<sup>93</sup> proposed an economic, ecological and efficient method, called “*vitrimization*” to manufacture vitrimer-type polymers: a DGEBA / glutaric anhydride resin was cured in presence of imidazole; subsequently grinded into small particles and then ball milled with zinc acetate for 1 hour yielded to “*vitrimized*” resins in form of a fine powder and cured at 120 °C for 8 hours and at 160 °C for another 8 hours. The final material exhibited recyclable and reprocessable ability for multiple cycles, applying heat and pressure (250 °C and 5 MPa pressure for 1 hour).

### 1.3.2.2 CANs based on disulfide exchange reactions

In 1964 Tobolsky *et al.*<sup>94</sup> introduced for the first-time the stress relaxation term in the case

of disulfide and tetrasulfide polymers. The polysulfide polymers were prepared by interfacial polycondensation of mixtures of ethylene dichloride, 1,2,3-trichloropropane, and sodium polysulfide. The authors observed that these polymers undergo stress decay by the reversible interchange of polysulfide bonds. However, only several years later were reported the research studies on recyclable thermosetting resins cured with agents

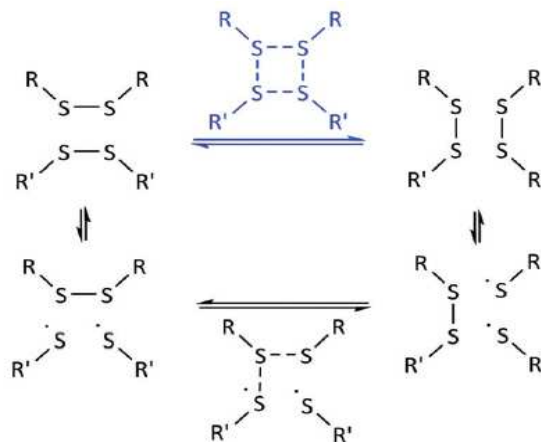


**Figure 7.** Schematic representation of the [2+2] metathesis and [2+1] radical mediated reaction mechanisms<sup>97</sup>

containing disulfide links.<sup>95</sup> Several authors<sup>96-97</sup> proposed a mechanism through a transition state implying a [2+2] metathesis reaction and a [2+1] radical mediated mechanism (Figure 7). In one mechanism the disulfide bonds break and form simultaneously (blue schematized in Figure 7), while in another (represented in black), by a radical mechanism, the breaking of one disulfide bond lead to the formation of radicals that would eventually attack other disulfide bonds (Figure 7). As model, Rekondo *et al.*<sup>98</sup> studied the metathesis reaction of equimolar amounts of aromatic disulfide mixtures (bis (4-aminophenyl) disulfide and bis (4-methoxyphenyl) disulfide) by <sup>1</sup>H-NMR at room temperature. In absence of any catalyst the metathesis started in less than 1 hour, achieving the equilibrium after 22 hours. But, when the reaction occurred in the presence of 0.1 equivalents of NEt<sub>3</sub>, the equilibrium was reached in shorter time. However, to demonstrate that the reaction did not occurred by a self-catalysis effect of primary aromatic amines presented in starting monomers, the same experiment was performed using bis(p-tolyl) disulfide and bis(4-methoxyphenyl) disulfide, without NEt<sub>3</sub> and the equilibration was achieved after 24 hours, demonstrating that the exchange reaction occurs without any catalyst. Nevejans *et al.*<sup>97</sup> repeated the experiment by kinetic studies in <sup>13</sup>C NMR to analyse the exchange reaction modifying parameters such as initiator, inhibitor, catalyst, UV radiation and following the reaction (for 12 hours at 35 °C) of 4-aminophenyl disulfide (4-AFD) and diphenyl disulfide. The authors confirmed that the exchange reaction between the two disulfide compounds occurred via a radical-mediated mechanism and that the catalysts enhanced the disulfide exchange reactions through the formation of S- based anions in addition to the radical-mediated mechanism.



## Chapter 1

Several studies were dedicated to compare the materials obtained from monomers with and without disulfide bonds to highlight how S-S can be employed to obtain recyclable/reprocessable networks. Takahashi *et al.*<sup>99</sup> reported comparable mechanical properties for the epoxy resins obtained with and without disulfide bonds (with  $T_g \sim 150$  °C) demonstrating that the disulfide bonds influence more the degradation of the network than if the bonds are in the curing agent. Ruiz de Luzuriaga *et al.*<sup>100</sup> fabricated an epoxy fiber-reinforced composite using DGEBA. The material was cured with 4-aminophenyl disulfide (4-AFD) and diethyltoluenediamine (DETDA), crosslinkers with comparable thermal and mechanical properties. The main difference was found regarding the recyclability and the stress relaxation behaviour of the two matrix: the epoxy resin based on 4-aminophenyl disulfide (4-AFD) exhibited very short relaxation times (20 second at 200 °C), an excellent reprocessability, and repairability in hot press at 200 °C and 100 bar for 5 minutes, while, DETDA-based resin showed no significant relaxation time at 160 °C and no recyclability. Imbernon *et al.*<sup>101</sup> compared dodecanedioic acid (DA) with dithiodibutyric acid (DTDB) highlighting the importance of the S-S bonds in the stress relaxation process, adhesion and recyclability behaviour for the epoxidized natural rubber resins.

Chen *et al.*<sup>102</sup> synthesized epoxy vitrimers with simultaneous disulfide metathesis and carboxylate transesterification, in presence of triazobicyclodecene (TBD). Excellent recycling and recovery was obtained for the dual dynamic vitrimer after 1 hour at 100 °C, while the vitrimers based on single COO<sup>-</sup> and S-S exchange reactions failed the reprocessing tests.

Moreover, the S-S bonds are also responsible of the self-healing in several applications. Li *et al.*<sup>103</sup> fabricated polyurethane elastomers manufactured by 3D printing with great potential applications in electronics, soft robotics, and sensors. The materials exhibited recyclability and self-healing after 12 hours at 80 °C. Recently, degradable self-healing hydrogels were obtained by Tron *et al.*<sup>104</sup> with features for biomedical and engineering applications: the hydrogels exhibited extremely fast (within  $\sim 5$  seconds) self-healing both in air and underwater with complete and rapid degradation in glutathione (GSH), a biological reducing agent after 5 hours at 60 °C.

The challenge of obtaining materials that recover multiple shapes and sizes can be an additional advantage for some specific applications. In literature, several publications concern polymeric materials with disulfide bonds that exhibited shape-memory abilities. Ji *et al.*<sup>105</sup> produced an epoxy-vitrimer based on dynamic aromatic disulfide bonds (dithioaniline) reacted Epoxy (E51) / polycaprolactone (PCL). The resin exhibited recycling property, obtained at 150 °C applying 5 MPa, and also reprocessability to permanent helix shapes at

130 °C within 0.5 hours. The multi-shape-memory effect was proved through a “welding” method and constructing a multi layered system. A polyurethane network, with tuneable shape-memory, self-healing and shape recovery was obtained by Deng *et al.*<sup>106</sup> The network is based on poly (tetramethylene ether) glycol, isophorone diisocyanate, different content of 2,2-hydroxy ethyl disulfide and triethanolamine as cross-linker. The authors observed that the best healing efficiency (~ 94 °C) was obtained for the specimen with the highest disulfide bond content at 55 °C for 12 hours, while the networks with relatively high degree of crosslink presented multi-shape (until quadruple) memory effect.

### 1.3.2.3 CANs based on imine exchange reaction

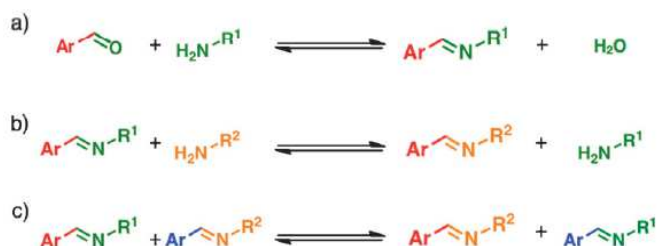


**Figure 8.** Imine reactions : (a) condensation, (b) exchange and (c) metathesis<sup>107</sup>

The imines, known as “Schiff’s bases”, derive from the reversible condensation reaction between an amine and an aldehyde or ketone. Imines can participate in three types of equilibrium controlled reactions<sup>107</sup> (Figure 8):

- hydrolysis, where the imine can be recovery in the starting monomers with the H<sub>2</sub>O addition;
- exchange, introducing a second amine while the original imine can undergo transimination, resulting in the R groups exchanging; and
- metathesis, introducing a second imine while the two imines can undergo a reaction in which the two R groups are exchanged.

The imine-linked polymers are attractive for the development of dynamic covalent networks due to the simply requires monomers. Taynton *et al.*<sup>108</sup> synthesized a catalyst-free network based on commercial monomers. The obtained material was recycled completely for several times. The authors also demonstrated that the material can be reworked at room temperature using water, obtaining a soft and flexible polymer from a hard-glassy material that swells and remains constant after 12 hours.

However, many green monomers were also used to obtain recyclable materials by exploiting the exchange reactions. Dhers *et al.*<sup>109</sup> synthesized the first fully bio-based vitrimer containing 100% renewable carbon based on 2,5-furandicarboxaldehyde obtained from fructose with bio-based diamine and triamine prepared from fatty acids. The materials showed a fast stress relaxation, close to room temperature, attributed to the reversibility of the covalent imine

## Chapter 1

bonds. Thereafter, the recyclability was tested via compression molding for 10 minutes at 120 °C, without any significant loss of mechanical properties after recycling. Recently, Guo *et al.*<sup>110</sup> obtained a vitrimer containing multiple reversible covalent bonds (imine exchange reaction and disulfide bonds) from vanillin-derived dialdehyde and amine monomers (tris(2-aminoethyl) amine and 4,4-disulfanediyldianiline). The material showed degradability and chemical recyclability in acid conditions, hydrochloric acid aqueous solution at pH 2 at 50 °C for 24 hours, and excellent self-healing and recycling properties by adding a catalytic amount of ethylenediamine. To reach high performance and versatile recyclability, Memon *et al.*<sup>111</sup> synthesized two imine-containing hardeners, IH-VAN from vanillin and isophorone diamine and a similar, IH-HB, containing from the petroleum-based counterpart. The two vitrimers showed comparable thermal and mechanical properties with degradability in isophorone diamine solution at 60 °C. The degradation products were used to prepare new epoxy resins, leading to a closed-loop recycling process.

### 1.3.2.4 CANs based on Diels-Alder reactions

The Diels-Alder (DA) reaction is a reaction between a conjugated diene and an activated alkene, referred to as dienophile, to give a cyclic product called adduct (Figure 9).

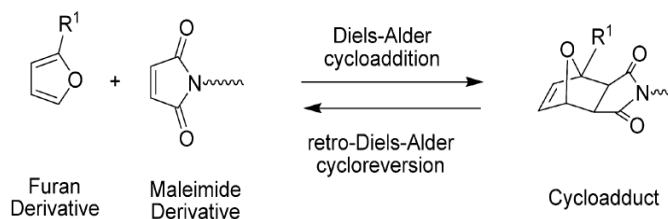


Figure 9. Diels–Alder/retro Diels–Alder reaction<sup>112</sup>

This reversible reaction, called

*retro* Diels-Alder, is favored by heating to temperatures > 90 °C.

The most popular pair of monomers to obtain recycled thermosets by DA reaction is the furan / maleimide reaction.<sup>112</sup> Trovatti *et al.*<sup>113</sup> applied this reaction to functionalize the polybutadiene with furan groups. The crosslinking was obtained incorporating furan heterocycles (Fu) as side groups to poly(butadiene) (PBD) using the thiol-ene reactions of furfuryl thiol (FT) with some of the PBD unsaturations and the subsequent DA crosslinking of the ensuing PBD-Fu with an aromatic bismaleimide. The synthesized elastomers were recycled, applying thermal stimuli due to the *rDA* reactions, finding possible applications in the production of recyclable tires. Bai *et al.*<sup>114</sup> combined the polybutadiene with furan via thiol-ene reactions, and the crosslinked network was built via DA reaction between the bismaleimide and the attached furan groups from polybutadiene. The elastomer was thermally recycled similar to thermoplastic materials. The authors showed that a crack on the

polymer film starts to decrease at about 90 °C, and disappears completely at 150 °C. A self-healing material was also synthesized by Oehlenschlaeger *et al.*<sup>115</sup> based on cyanodithioester (CDTE) compound and cyclopentadiene ( $C_p$ ). The healed sample was achieved in a very short timeframe at relatively low temperatures (120 °C) with identical mechanical properties as the original one. Tanasi *et al.*<sup>116</sup> obtained a fully and reversibly resin with self-repair capacity (healed at 150 °C) from natural rubber. The healed fracture was studied by SEM analysis, achieving almost a complete recovery after temperature treatment.

### 1.3.2.5 Other CANs with reversible covalent bonds

Other examples of covalent exchange dynamic chemical reactions are including transalkylation reactions of ammonium halide salts, siloxane–silanol exchange, olefin metathesis, and imine–amine exchange reactions, etc.

Siloxane-silanol exchange reaction is based on the addition and elimination of a silanolate anion. Zheng et McCarthy<sup>117</sup> demonstrated quantitative healing and stress-relaxation in polydimethylsiloxane networks.

Regarding the olefinic metathesis exchange reaction, Tang *et al.*<sup>118</sup> combined alkaline stability of bulky imidazolium groups with a Grubb's second-generation initiator catalyzed crosslinkable olefin metathesis reaction to produce a reticulated and anion-conductive poly(2,6-dimethyl-1,4-phenylene oxide).

Concerning the vitrimers based on the transalkylation reaction, Drockenmuller *et al.*<sup>119</sup> obtained a series of poly(1,2,3-triazolium ionic liquids) by solvent and catalyst-free polyaddition of an  $\alpha$ -azide-alkyne monomer and simultaneous alkylation of the resulting poly(1,2,3-triazoles) with a series of difunctional cross-linking agents. Temperature promotes the transalkylation exchange reactions of C-N, guaranteeing the reprocessability and recycling. Depolymerization was achieved through halogenated hydrocarbons as 1-bromopentane within 24 and 96 hours at 110 °C.

## 1.4 Reinforced epoxy composites

Nowadays, there is an increasing trend in the application of composite materials in numerous domains ranging from aerospace, automotive, construction and large-scale civil engineering projects, etc. This is due to their excellent mechanical properties combined with a low weight and great fatigue behaviour. The main constituents of composites are essentially two, the fibre or reinforcement (as glass, carbon or natural fibres) and the continuous phase (the matrix). The first component, the reinforcement, has the purpose of increasing the

## Chapter 1

strength of the composite, therefore it determines the mechanical stresses. To obtain a composite with high mechanical strength, it is essential to ensure a good adhesion between the matrix and the reinforcement.

The fibre composites have predominantly been produced from non-renewable, petro-chemical based materials. The introduction of biodegradable and eco-friendly vegetable matrix and reinforcements represent solution to make "green" composite materials. Moreover, the worldwide availability of low-cost plant-based fibers increased their use in recent years.

### 1.4.1 Natural fibres

The Global Natural Fibers Market Industry<sup>120</sup> estimated that it should be achieved to reach \$ 64020 million by the end of 2026, growing with 1.3% in 2021 - 2025. The world production of vegetable fibres in 2018 reached 29% of the total and 45% for the synthetic staple 20% (polyester, about 90% of the world production of filaments).

Natural fibers are divided according to their origin, i.e. vegetable, animal or mineral.<sup>121</sup> Among the main advantages of natural fibers compared to synthetic ones there are the ease of processing, low-density, cellular structure with acoustic and thermal insulation properties, as well as a reduction of the carbon footprint resulting from the growth of plants and greater energy recovery at end of their life cycle.<sup>122</sup> However, they often have a low resistance to moisture absorption with consequent a poor compatibility matrix-fiber. The use of chemical treatments, such as an alkaline treatment, allows to overcome this problem by changing the structure and surface properties of the fibers, thus allowing greater fiber-matrix compatibility. Another disadvantage of vegetable fibers is the low heat resistance. In fact the thermal stability values ( $\sim 200$  °C) restrict strongly the choice of the matrix and the application of natural composites in specific conditions.<sup>123</sup>

#### 1.4.1.1 Composition of plant fibres

Natural fibers represent environmentally friendly alternatives to conventional reinforcing fibers (glass, carbon, Kevlar), being low cost, with high toughness, low density and good biodegradability. Moreover, thanks to their hollow and cellular nature, they can find applications as acoustic and thermal insulators, and exhibit reduced bulk density.

The mechanical properties, as tensile strength and Young's modulus of fibers, which increase with cellulose content, are strongly dependent of the geometry of the elementary cell. The hydrogen bonds are linking together the cellulosic macromolecular interchains, arranging it

in parallel. The resulting supramolecular structure through linkages with amorphous hemicelluloses and lignins confer stiffness to fibres, called microfibrils (Figure 10).

The flax fibers are made mainly of pure cellulose (about 70 - 75%), the remaining part is hemicellulose (15%), lignins and pectic materials (proteins or minerals, tannins, dyes and a small amount of waxes and fat) (Table 1). The cell walls are responsible for the structural and mechanical support, as well as the mechanical strength of the fiber.<sup>122,</sup>

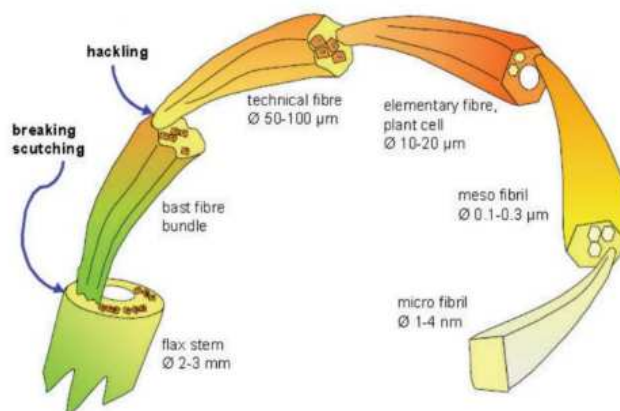


Figure 4. Structure of a plant fibre<sup>122</sup>

<sup>124-125</sup> Ahmad *et al.*<sup>126</sup> summarized

the chemical composition of several natural fibers. The presence of hydroxyl groups can be involved in the hydrogen bonding within the cellulose molecules, thus reducing the activity towards the matrix. Several treatments (acrylation, acetylation etc.) are used as chemical interlock with the matrix.<sup>122</sup>

Table 1. Composition of some common plant fibres<sup>124</sup>

Fibre	Cellulose (%)	Hemi-Cellulose (%)	Lignin (%)	Pectin (%)	Other (%)
Jute	61-71	13.6-20.4	12-13	0.2	0.5
Flax	71-78	18.6-20.6	2.2	2.2	5.5
Hemp	70.2-74.4	17.9-22.4	3.7-5.7	0.9	7
Kenaf	53-57	15-19	5.9-9.3	-	7.9
Sisal	67-78	10-14.2	8-11	10	3
Cotton	82.7	5.7	-	-	0.6

The removal of non-lignocellulosic materials, such as lignin and hemicellulose, are carried out by applying alkaline treatment (called *mercerization*) using NaOH. Saha *et al.*<sup>127</sup>, analysed jute fibers, reporting that the mechanical properties increased by treating the fibers with a 4% alkaline solution for 30 minutes, but overcoming these conditions a diminution of the properties were observed.

### 1.4.2 PLA as matrix or reinforcement

Poly (lactic acid) (PLA) is a crystalline biodegradable thermoplastic polymer with relatively high melting point (150 - 175 °C) and excellent mechanical properties, synthesized by the polymerization of *D* or *L*-lactic acid or ring-opening polymerization of the corresponding

## Chapter 1

lactide.<sup>128</sup> PLA has long been known as a biomaterial but only recently it was used as a polymer matrix in composites. Only in 2002, Cargill-Dow LLC started a commercial PLA plant, with the aim of produce PLA fibers for fabrics and nonwovens, as well as PLA films for packaging applications and rigid containers.<sup>129</sup> By combining a biodegradable matrix with bio-fibres reinforcement, PLA found application in bio-composites fully biodegradable.<sup>130</sup>

Several kinds of natural fibres were used to reinforce PLA. Oksman *et al.*<sup>131</sup> studied the strength of PLA / flax fibres composites obtaining comparable results to similar PP / flax fibre composites, showing no difficulties in extrusion or compression moulding processes for application in automotive panels. Recently, Shih *et al.*<sup>132</sup> prepared several green compounds with PLA bamboo fiber with flame retardancy ability. The loss and storage moduli were increased due to the addition of natural fibers, demonstrating how these fibers improved the stiffness of PLA, as well as the thermal resistance. Jia *et al.*<sup>133</sup> developed two PLA polymers achieved using highly oriented PLA fibres (semi-crystalline) as reinforcement, and an amorphous PLA as matrix, using as reference a PBS matrix reinforced with PLA fibre composite. The authors compared these materials with the PLA self-reinforced composite (SRC). PLA-SRC had higher tensile strength and Young's modulus than PLA–PBS composite, due to the fact that the PLA has better tensile properties compared to PBS and also a better interfacial adhesion between PLA yarn and PLA matrix. Goutianos *et al.*<sup>134</sup> prepared a bio-based self-reinforced composites (PLA-SRC), based a high stiffness PLA fibres (with high melting temperature) and low melting PLA matrix. The PLA-SRC showed enhanced stiffness compared to the commercially available self-reinforced polypropylene composites.

### 1.4.3 Properties of bio-based reinforced composites

In the recent years, the natural fibers were combined with bio-based polymers to produce bio-based composites. In 2017 Bachmann *et al.*<sup>135</sup> compared the physico-mechanical properties of synthetic and biological fibers for the preparation of composites with potential use in the aviation sector. Most of reported life cycle assessment (LCA) studies confirmed that the use of natural fibers by replacing the synthetic materials in composites can reduce the overall environmental impacts of these materials. La Rosa *et al.*<sup>136</sup> examined the production of an eco-sandwich panel containing bio-based epoxy resin and fibers compared with a traditional composite made of glass fibers and petroleum-based epoxy resin. The authors found good results in terms of LCA and environmental impact and energy consumption. Shibata *et al.*<sup>137</sup> reported bio-composites produced from ESO, tannic acid (TA) and microfibrillated cellulose (MFC), by compression molding. The addition of MFC produced an improvement in terms of thermal and mechanical properties: the tensile modulus and

tensile strength increase of 2.9 times and 72%, respectively, compared to the neat epoxy resins.

Liu *et al.*<sup>138</sup> prepared four resins including *i*/ acrylated epoxidized soybean oil (AESO), *ii*/ AESO with methacrylated isosorbide (MI) as comonomer (MI-AESO), *iii*/ methacrylated AESO with MI (MIMAESO), and *iv*/MI resins. The authors reported comparable or superior  $T_g$  and storage modulus in the rubbery plateau. The water absorption test, performed at room temperature or at 100 °C, for 24 hours, confirmed high absorption % for the composites, due to the incorporation of highly hydrophilic units, obtaining high values especially for bamboo fibre. The authors correlate these results with the nature of bamboo fibers, constituted of filaments bonded together by non-cellulosic substances, leading to the presence of microgaps between the filaments that can cause the water absorption. High water absorption values and fire resistance were observed by Di Landro and Janszen<sup>139</sup> for a composite made by bio-epoxy resin, partly based on natural components (01 S and 01 F – provided by ALPAS srl, Italy), and hemp for a reinforced laminates.

Ozkur *et al.*<sup>140</sup> obtained bio-composites containing acrylated epoxidized soybean oil (AESO) with a commercial epoxy resin (F-1564, Fibermak) and hardener (F-3486, Fibermak) reinforced with four-ply jute woven fabrics, by vacuum infusion method. The authors showed that the percentage of AESO was decisive for the tensile and flexural strength of bio-materials. The composites with AESO content > 50 wt.% showed a high impact resistance with potential applications in automotive industry, construction etc.

Bio-based flax-epoxy composites were prepared by Musa *et al.*<sup>141</sup> from diglycidyl ether of isosorbide cured with isophorone diamine reinforced with flax fibres. The tensile strength of composite showed values comparable to reported values of unidirectional composites made with petroleum-based epoxy resins. Moreover, a good interfacial adhesion between the bio-based resin and the flax fibres was reported. These fibres have been used for the production of a green composite as early as 2006 by Liu *et al.*<sup>142</sup> as reinforcement for a composite based on ESO, 1,1,1-tris (*p*-hydroxyphenyl) ethane triglycidyl ether (THPEGE). The obtained bio-composite was produced by compression molding method. The nature of the hardener and the length of the flax fibers were found to be key parameters. Triethylenetetramine (TETA) and diethylenetriamine (DETA) were used as crosslinkers, providing increased physical properties compared to those obtained when using Jeffamine, D-230 and EDR-148, with a significant increase in the modulus of flexion and traction.



## Chapter 1

Bledzki *et al.*<sup>143</sup> used EVOs-based epoxy (different formulations based on epoxidized plant oil / DGEBA and petrochemical anhydrides or bio-hardeners) reinforced with jute fibers to produce bio-based composites by resin transfer molding. The impact strength increased with the amount of EVOs in the composites. The bio-composites exhibited comparable properties to those based on petrochemical epoxides and high impact resistance due to the presence of natural fibers.

### 1.5 Recyclables composites

The composites are used in a wide range of applications but usually cannot be properly recycled, due to their inherent nature of heterogeneity, in particular for the thermoset-based polymer composites. Oliveux *et al.*<sup>144</sup> summarized the recycling techniques of reinforced fibers composites including mechanical, thermal (pyrolysis) and chemical. The recycling is an interesting alternative approach guaranteeing to obtain clean fibers and valuable monomers from the matrix. Kuang *et al.*<sup>145</sup> prepared epoxy composites based on Epon 828, Epikure 3253 and hexahydro-4-methylphthalic anhydride reinforced with carbon fibers (CF). The authors recycled the composites, using 2-ethyl-hexanol/N-methyl-2-pyrrolidone) (10/90, v/v) with 0.30 mol/L of triazobicyclodecene (TBD), as catalyst, at 170 °C. A full recover of the CF was obtained and in addition epoxy resin was depolymerized, opening to its possible reuse for the preparation of new epoxy resins.

In 2016, Ruiz de Luzuriaga *et al.*<sup>100</sup> displayed the thermoforming (or reshability) of the composites based on DGEBA and 4-aminophenyl disulfide (4-AFD) using a zig-zag mold. The composite's repairability was obtained, applying 200 °C, 100 bar for 5 minutes in a hot press. Moreover, the authors applied chemical and mechanical recycling. For the chemical recycling the authors immersed the samples in a solution of 2-mercaptoethanol in dimetilformamide (DMF), at room temperature for 24 hours. The CF were recovered due to the thiol-disulfides exchanges. The mechanical recycling was achieved by grinding the composite in fine powder submitted thereafter to compression molding.

La Rosa *et al.*<sup>146-147</sup> recycled chemically a commercial epoxy resin (based on SuperSap300 and diethanolamine) reinforced with CFs. The composite was treated with 25 vol.% of acetic acid at 80 °C for 1,5 hours and, when the CFs were separated from the composite, the solution was neutralised with NaOH. The solid was filtered, washed and dissolved again with NaOH solution. A white solid precipitation was obtained, allowing to recover a thermoplastic resin. Finally, Pietroluongo *et al.*<sup>148</sup> applied mechanical recycling to radiator parts coming from an end-of-life vehicle reinforced with 35.7% of short glass fibers. The material was pelletized,

and injection moulded three times. The results were compared with the composite material currently used to produce the same component, showing no thermal degradation after the recycling. However, by increasing the recycling cycles, a change in viscosity was observed, caused by the breaking of the fibers.

## 1.6 Scope of the thesis

The main aim of this Ph.D. thesis was the development of new bio-based epoxy resins and composite materials with recyclability properties starting from epoxidized vegetable oils and dynamic disulfides crosslinkers, as monomers.

This manuscript is organized as follows:

**Chapter 1** introduces the thesis context, the bibliographic study on bio-based epoxy monomers, on recyclability mechanism involved in the preparation of bio-based epoxy resins, and on their composites.

**Chapter 2** focus on the nature of the initiator as key parameter in the crosslinking and recycling process. A reference epoxy monomer was selected for the thermoset's preparation and the chemical nature of the prepared network was correlated with the materials ability for mechanical reprocessing or chemical recycling.

In **Chapter 3** the effect of the ratio epoxy / hardener was studied as another important parameter affecting the crosslinking reaction, the crosslinking density and the properties of the thermosets. Moreover, this parameter was considered for its impact on the networks' recycling, thermal and chemical, considering two references epoxidized vegetable oils.

In **Chapter 4** a series of thermoset materials with chemical recycling ability were synthesized starting from twelve new epoxidized vegetable oils. The investigation of crosslinked copolymers and homopolymers (hardeners-free) was done in correlation with the epoxy content of the starting monomers, as a third parameter to modulate the final properties of the thermosets that vary from soft to hard.

In **Chapter 5** the thermo-mechanical properties of the previously developed bio-based copolymers were compared. Their recycling, repairing and reshaping (3R) ability combined with the shape memory capability were studied.

In **Chapter 6** the EVOs-based resins developed in Chapter 4 were studied as matrices for the design of green composites, using two reinforcements, flax fibre and PLA woven. In the first part, the influence of the nature of fibers and its percentage on the physico-chemical and mechanical properties of composites were investigated. Then, the reprocessing abilities of the matrices and composites were evaluated.

## Chapter 1

Finally, some general conclusions and future perspectives are proposed.

## References

1. Park, S. J.; Jin, F. L., Epoxy resins: fluorine systems. *Wiley Encyclopedia of Composites*, John Wiley & Sons **2011**.
2. Łukaszczyk, J.; Janicki, B.; Kaczmarek, M., Synthesis and properties of isosorbide based epoxy resin. *European Polymer Journal* **2011**, *47* (8), 1601-1606.
3. Yuan, L.; Liang, G.; Xie, J.; Li, L.; Guo, J., Preparation and characterization of poly(urea-formaldehyde) microcapsules filled with epoxy resins. *Polymer* **2006**, *47* (15), 5338-5349.
4. Pham, H. A. Q., Maurice and Marks, J., "Encyclopedia of Polymer Science and Technology". John Wiley and sons, New York: 1986; Vol. 9.
5. Nguyen, H.-V.; Andreassen, E.; Kristiansen, H.; Johannessen, R.; Hoivik, N.; Aasmundtveit, K. E., Rheological characterization of a novel isotropic conductive adhesive-epoxy filled with metal-coated polymer spheres. *Materials & Design* **2013**, *46*, 784-793.
6. Jin, H.; Miller, G. M.; Pety, S. J.; Griffin, A. S.; Stradley, D. S.; Roach, D.; Sottos, N. R.; White, S. R., Fracture behavior of a self-healing, toughened epoxy adhesive. *Int. J. Adhes. Adhes.* **2013**, *44*, 157-165.
7. Kaboorani, A.; Riedl, B., Nano-aluminum oxide as a reinforcing material for thermoplastic adhesives. *J. Ind. Eng. Chem.* **2012**, *18* (3), 1076-1081.
8. Toldy, A.; Szolnoki, B.; Marosi, G., Flame retardancy of fibre-reinforced epoxy resin composites for aerospace applications. *Polymer Degradation and Stability* **2011**, *96* (3), 371-376.
9. Kaiser, A. L.; Albelo, I. V.; Wardle, B. L. In *Fabrication of Aerospace-grade Epoxy and Bismaleimide Matrix Nanocomposites with High Density Aligned Carbon Nanotube Reinforcement*, AIAA Scitech 2020 Forum, 2020; p 2256.
10. Capricho, J. C.; Fox, B.; Hameed, N., Multifunctionality in Epoxy Resins. *Polymer Reviews* **2020**, *60* (1), 1-41.
11. Huang, X.; Li, R.; Zeng, L.; Li, X.; Xi, Z.; Wang, K.; Li, Y., A multifunctional carbon nanotube reinforced nanocomposite modified via soy protein isolate: A study on dispersion, electrical and mechanical properties. *Carbon* **2020**, *161*, 350-358.
12. Saiki, N.; Yamazaki, O.; Ebe, K., UV/heat dual-curable adhesive tapes for fabricating stacked packages of semiconductors. *Journal of applied polymer science* **2008**, *108* (2), 1178-1183.
13. Zhou, L.; Zhang, G.; Li, J.; Jing, Z.; Qin, J.; Feng, Y., The flame retardancy and thermal stability properties of flame-retarded epoxy resins based on  $\alpha$ -hydroxyphosphonate cyclotriphosphazene. *Journal of Thermal Analysis and Calorimetry* **2017**, *129* (3), 1667-1678.
14. Levchik, S.; Piotrowski, A.; Weil, E.; Yao, Q., New developments in flame retardancy of epoxy resins. *Polymer Degradation and Stability* **2005**, *88* (1), 57-62.
15. Hadjinikolaou, I. N.; Bell, J. P.; Spangberg, L., Fast Curing Epoxy and Episulfide Resins for Biomedical Applications. *MRS Online Proceedings Library Archive* **1987**, *110*.
16. Garcia, F. G.; Elena Leyva, M.; Alencar de Queiroz, A. A.; Zazuco Higa, O., Epoxy networks for medicine applications: Mechanical properties and in vitro biological properties. *Journal of Applied Polymer Science* **2009**, *112* (3), 1215-1225.
17. Market Report Global Epoxy Resin Market 3rd Edition Latest Update: June,2017. Publisher: Acmite Market Intelligence.
18. Hamerton, I., *Recent developments in epoxy resins*. iSmithers Rapra Publishing: 1996; Vol. 91.
19. Lee, H.; Neville, K., *Handbook of epoxy resins*. McGraw-Hill Inc., New York, 1967.
20. Ravve, A., *Principles of polymer chemistry*. Springer Science & Business Media: 2013.
21. Park, S.-J.; Jin, F.-L.; Lee, J.-R.; Shin, J.-S., Cationic polymerization and physicochemical properties of a biobased epoxy resin initiated by thermally latent catalysts. *European Polymer Journal* **2005**, *41* (2), 231-237.
22. Li, Y.; Xiao, F.; Wong, C. P., Novel, environmentally friendly crosslinking system of an epoxy using an amino acid: Tryptophan-cured diglycidyl ether of bisphenol A epoxy. *Journal of Polymer Science Part A: Polymer Chemistry* **2007**, *45* (2), 181-190.

23. Cespi, D.; Cucciniello, R.; Ricciardi, M.; Capacchione, C.; Vassura, I.; Passarini, F.; Proto, A., A simplified early stage assessment of process intensification: glycidol as a value-added product from epichlorohydrin industry wastes. *Green Chemistry* **2016**, *18* (16), 4559-4570.
24. Reinicker, R.; Gates, B., Bisphenol a synthesis: Kinetics of the phenol-acetone condensation reaction catalyzed by sulfonic acid resin. *AIChE J.* **1974**, *20* (5), 933-940.
25. Vandenberg, L. N.; Maffini, M. V.; Sonnenschein, C.; Rubin, B. S.; Soto, A. M., Bisphenol-A and the great divide: a review of controversies in the field of endocrine disruption. *Endocr Rev* **2009**, *30* (1), 75-95.
26. Vandenberg, L. N.; Hauser, R.; Marcus, M.; Olea, N.; Welshons, W. V., Human exposure to bisphenol A (BPA). *Reproductive toxicology* **2007**, *24* (2), 139-177.
27. REGULATIONS COMMISSION IMPLEMENTING REGULATION (EU) No 321/2011 of 1 April 2011 amending Regulation (EU) No 10/2011 as regards the restriction of use of Bisphenol A in plastic infant feeding bottles. 2011.
28. COMMISSION DIRECTIVE 2014/81/EU of 23 June 2014 amending Appendix C of Annex II to Directive 2009/48/EC of the European Parliament and of the Council on the safety of toys, as regards bisphenol A (Text with EEA relevance).
29. COMMISSION REGULATION (EU) No 10/2011 of 14 January 2011 on plastic materials and articles intended to come into contact with food (Text with EEA relevance). 2011.
30. Registry of SVHC intentions - ECHA. <https://echa.europa.eu/registry-of-svhcintentions>.
31. Zoller, O.; Brüschweiler, B. J.; Magnin, R.; Reinhard, H.; Rhyn, P.; Rupp, H.; Zeltner, S.; Felleisen, R., Natural occurrence of bisphenol F in mustard. *Food additives & contaminants. Part A, Chemistry, analysis, control, exposure & risk assessment* **2016**, *33* (1), 137-46.
32. Kumar, S.; Samal, S. K.; Mohanty, S.; Nayak, S. K., Recent Development of Biobased Epoxy Resins: A Review. *Polymer-Plastics Technology and Engineering* **2018**, *57* (3), 133-155.
33. U.S. Vegetable Oils and Fats - Statistics & Facts, S. R. D., Mar 19, 2018.
34. Armylisas, A. N.; Hazirah, M. S.; Yeong, S.; Hazimah, A., Modification of olefinic double bonds of unsaturated fatty acids and other vegetable oil derivatives via epoxidation: A review. *Grasas y Aceites* **2017**, *68* (1), 174.
35. Sheldon, R. A.; Dakka, J., Heterogeneous catalytic oxidations in the manufacture of fine chemicals. *Catal. Today* **1994**, *19* (2), 215-245.
36. Dinda, S.; Patwardhan, A. V.; Goud, V. V.; Pradhan, N. C., Epoxidation of cottonseed oil by aqueous hydrogen peroxide catalysed by liquid inorganic acids. *Bioresource Technology* **2008**, *99* (9), 3737-3744.
37. Ackros Chemicals, <http://akcros-22681.dev.iasprojects.com/>.
38. Arkema. <https://www.arkema.com/en/>.
39. Earls, J. D.; White, J. E.; López, L. C.; Lysenko, Z.; Dettloff, M. L.; Null, M. J., Amine-cured  $\omega$ -epoxy fatty acid triglycerides: Fundamental structure–property relationships. *Polymer* **2007**, *48* (3), 712-719.
40. Ding, C.; Shuttleworth, P. S.; Makin, S.; Clark, J. H.; Matharu, A. S., New insights into the curing of epoxidized linseed oil with dicarboxylic acids. *Green Chemistry* **2015**, *17* (7), 4000-4008.
41. Shimbo, M.; Ochi, M.; Shigeta, Y., Shrinkage and internal stress during curing of epoxide resins. *Journal of Applied Polymer Science* **1981**, *26* (7), 2265-2277.
42. Gobin, M.; Loulergue, P.; Audic, J.-L.; Lemiègre, L., Synthesis and characterisation of bio-based polyester materials from vegetable oil and short to long chain dicarboxylic acids. *Industrial Crops and Products* **2015**, *70*, 213-220.
43. Altuna, F. I.; Espósito, L. H.; Ruseckaite, R. A.; Stefani, P. M., Thermal and mechanical properties of anhydride-cured epoxy resins with different contents of biobased epoxidized soybean oil. *Journal of Applied Polymer Science* **2011**, *120* (2), 789-798.
44. Bakar, M. B. A.; Masri, M. N.; Amini, M. H. M.; Thirmizir, M. Z. M.; Salim, M. S., Mechanical, thermal and morphological properties of epoxy resin toughened with epoxidized soybean oil. *AIP Conference Proceedings* **2018**, *2030* (1), 020277.
45. Park, S.-J.; Jin, F.-L.; Lee, J.-R., Effect of Biodegradable Epoxidized Castor Oil on Physicochemical and Mechanical Properties of Epoxy Resins. *Macromolecular Chemistry and Physics* **2004**, *205* (15), 2048-2054.
46. Jin, F.-L.; Park, S.-J., Impact-strength improvement of epoxy resins reinforced with a biodegradable polymer. *Materials Science and Engineering: A* **2008**, *478* (1), 402-405.
47. Pin, J. M.; Sbirrazzuoli, N.; Mija, A., *From Epoxidized Linseed Oil to Bioresin: An Overall Approach of Epoxy/Anhydride Cross-Linking*. 2015; Vol. 8.

## Chapter 1

48. Pin, J.-M.; Guigo, N.; Vincent, L.; Sbirrazzuoli, N.; Mija, A., Copolymerization as a Strategy to Combine Epoxidized Linseed Oil and Furfuryl Alcohol: The Design of a Fully Bio-Based Thermoset. *ChemSusChem* **2015**, *8* (24), 4149-4161.
49. Kadam, A.; Pawar, M.; Yemul, O.; Thamke, V.; Kodam, K., Biodegradable biobased epoxy resin from karanja oil. *Polymer* **2015**, *72*, 82-92.
50. Noè, C.; Malburet, S.; Bouvet-Marchand, A.; Graillot, A.; Loubat, C.; Sangermano, M., Cationic photopolymerization of bio-renewable epoxidized monomers. *Progress in Organic Coatings* **2019**, *133*, 131-138.
51. Huang, X.; Yang, X.; Liu, H.; Shang, S.; Cai, Z.; Wu, K., Bio-based thermosetting epoxy foams from epoxidized soybean oil and rosin with enhanced properties. *Industrial Crops and Products* **2019**, *139*, 111540.
52. Mazzon, E.; Guigues, P.; Habas, J.-P., Biobased structural epoxy foams derived from plant-oil: Formulation, manufacturing and characterization. *Industrial Crops and Products* **2020**, *144*, 111994.
53. Parada Hernandez, N. L.; Bahú, J. O.; Schiavon, M. I. R. B.; Bonon, A. J.; Benites, C. I.; Jardini, A. L.; Maciel Filho, R.; Wolf Maciel, M. R., (Epoxidized castor oil – citric acid) copolyester as a candidate polymer for biomedical applications. *Journal of Polymer Research* **2019**, *26* (6), 149.
54. Hong, J.; Radojčić, D.; Ionescu, M.; Petrović, Z. S.; Eastwood, E., Advanced materials from corn: isosorbide-based epoxy resins. *Polymer Chemistry* **2014**, *5* (18), 5360-5368.
55. Pan, X.; Sengupta, P.; Webster, D., Novel biobased epoxy compounds: Epoxidized sucrose esters of fatty acids. *Green Chem.* **2011**, *13*, 965-975.
56. Ma, S.; Kovash, C. S.; Webster, D. C., Effect of solvents on the curing and properties of fully bio-based thermosets for coatings. *Journal of Coatings Technology and Research* **2017**, *14* (2), 367-375.
57. Miao, J.-T.; Yuan, L.; Guan, Q.; Liang, G.; Gu, A., Biobased heat resistant epoxy resin with extremely high biomass content from 2, 5-furandicarboxylic acid and eugenol. *ACS Sustainable Chemistry & Engineering* **2017**, *5* (8), 7003-7011.
58. Marotta, A.; Faggio, N.; Ambrogio, V.; Cerruti, P.; Gentile, G.; Mija, A., Curing Behavior and Properties of Sustainable Furan-Based Epoxy/Anhydride Resins. *Biomacromolecules* **2019**, *20* (10), 3831-3841.
59. McCarthy, J. L.; Islam, A., Lignin chemistry, technology, and utilization: a brief history. ACS Publications: 2000.
60. Ferdosian, F.; Yuan, Z.; Anderson, M.; Xu, C., Chemically Modified Lignin through Epoxidation and its Thermal Properties. *Journal of Science & Technology for Forest Products and Processes* **2012**, *2*, 11-15.
61. Wang, S.; Ma, S.; Xu, C.; Liu, Y.; Dai, J.; Wang, Z.; Liu, X.; Chen, J.; Shen, X.; Wei, J.; Zhu, J., Vanillin-Derived High-Performance Flame Retardant Epoxy Resins: Facile Synthesis and Properties. *Macromolecules* **2017**, *50* (5), 1892-1901.
62. Zhu, Y.; Li, Z.; Wang, X.; Ding, N.; Tian, Y., Preparation and Application of Lignin-Based Epoxy Resin from Pulping Black Liquor. *ChemistrySelect* **2020**, *5* (12), 3494-3502.
63. Sasaki, C.; Wanaka, M.; Takagi, H.; Tamura, S.; Asada, C.; Nakamura, Y., Evaluation of epoxy resins synthesized from steam-exploded bamboo lignin. *Industrial Crops and Products* **2013**, *43*, 757-761.
64. Basnet, S.; Otsuka, M.; Sasaki, C.; Asada, C.; Nakamura, Y., Functionalization of the active ingredients of Japanese green tea (*Camellia sinensis*) for the synthesis of bio-based epoxy resin. *Industrial Crops and Products* **2015**, *73*, 63-72.
65. Badhani, B.; Sharma, N.; Kakkar, R., Gallic acid: a versatile antioxidant with promising therapeutic and industrial applications. *Rsc Advances* **2015**, *5* (35), 27540-27557.
66. Tomita, H. Y., K. Epoxy Resin and Process for Preparing the Same. U.S. Patent No. 4,540,802, 10 September 1985
67. Karaseva, V.; Bergeret, A.; Lacoste, C.; Fulcrand, H.; Ferry, L., New Biosourced Flame Retardant Agents Based on Gallic and Ellagic Acids for Epoxy Resins. *Molecules* **2019**, *24* (23), 4305.
68. Jailliet, F.; Desroches, M.; Auvergne, R.; Boutevin, B.; Caillol, S., New biobased carboxylic acid hardeners for epoxy resins. *European Journal of Lipid Science and Technology* **2013**, *115* (6), 698-708.
69. Noè, C.; Malburet, S.; Milani, E.; Bouvet-Marchand, A.; Graillot, A.; Sangermano, M., Cationic UV-Curing of Epoxidized Cardanol Derivatives. *Polymer International n/a* (n/a).
70. Ding, C.; Matharu, A. S., Recent Developments on Biobased Curing Agents: A Review of Their Preparation and Use. *ACS Sustainable Chemistry & Engineering* **2014**, *2* (10), 2217-2236.

71. Liu, Z.; Xu, Y.; Cao, L.; Bao, C.; Sun, H.; Wang, L.; Dai, K.; Zhu, L., Phosphoester cross-linked vegetable oil to construct a biodegradable and biocompatible elastomer. *Soft Matter* **2012**, *8* (21), 5888-5895.
72. Top Value Added Chemicals from Biomass. Volume I: Results of Screening for Potential Candidates from Sugars and Synthesis Gas. U.S. Department of Energy: Washington, DC, 2013.
73. Ma, S.; Webster, D. C., Naturally Occurring Acids as Cross-Linkers To Yield VOC-Free, High-Performance, Fully Bio-Based, Degradable Thermosets. *Macromolecules* **2015**, *48* (19), 7127-7137.
74. Supanchaiyamat, N.; Shuttleworth, P. S.; Hunt, A. J.; Clark, J. H.; Matharu, A. S., Thermosetting resin based on epoxidised linseed oil and bio-derived crosslinker. *Green. Chem.* **2012**, *14* (6), 1759.
75. Montarnal, D.; Capelot, M.; Tournilhac, F.; Leibler, L., Silica-like malleable materials from permanent organic networks. *Science* **2011**, *334* (6058), 965.
76. Capelot, M.; Unterlass, M. M.; Tournilhac, F.; Leibler, L., Catalytic Control of the Vitrimer Glass Transition. *ACS Macro Letters* **2012**, *1* (7), 789-792.
77. Global Plastic Recycling Market Trends Report 2020, <http://www.researchandmarkets.com>.
78. ASTM D5033-00 Standard Guide for Development of ASTM Standards Relating to Recycling and Use of Recycled Plastics (Withdrawn 2007).
79. Okan, M.; Aydin, H. M.; Barsbay, M., Current approaches to waste polymer utilization and minimization: a review. *Journal of Chemical Technology & Biotechnology* **2019**, *94* (1), 8-21.
80. Ignatyev, I. A.; Thielemans, W.; Vander Beke, B., Recycling of Polymers: A Review. *ChemSusChem* **2014**, *7* (6), 1579-1593.
81. Kloxin, C. J.; Scott, T. F.; Adzima, B. J.; Bowman, C. N., Covalent Adaptable Networks (CANs): A Unique Paradigm in Crosslinked Polymers. *Macromolecules* **2010**, *43* (6), 2643-2653.
82. Koshima, H., *Mechanically Responsive Materials for Soft Robotics*. John Wiley & Sons: 2019.
83. Denissen, W.; Winne, J. M.; Du Prez, F. E., Vitrimers: permanent organic networks with glass-like fluidity. *Chemical Science* **2016**, *7* (1), 30-38.
84. Capelot, M.; Montarnal, D.; Tournilhac, F.; Leibler, L., Metal-Catalyzed Transesterification for Healing and Assembling of Thermosets. *Journal of the American Chemical Society* **2012**, *134* (18), 7664-7667.
85. Denissen, W.; Droesbeke, M.; Nicolaÿ, R.; Leibler, L.; Winne, J. M.; Du Prez, F. E., Chemical control of the viscoelastic properties of vinylogous urethane vitrimers. *Nature communications* **2017**, *8* (1), 1-7.
86. Liu, T.; Zhao, B.; Zhang, J., Recent development of repairable, malleable and recyclable thermosetting polymers through dynamic transesterification. *Polymer* **2020**, *194*, 122392.
87. Altuna, F. I.; Pettarin, V.; Williams, R. J. J., Self-healable polymer networks based on the cross-linking of epoxidised soybean oil by an aqueous citric acid solution. *Green Chemistry* **2013**, *15* (12), 3360-3366.
88. Altuna, F. I.; Hoppe, C. E.; Williams, R. J. J., Shape memory epoxy vitrimers based on DGEBA crosslinked with dicarboxylic acids and their blends with citric acid. *RSC Advances* **2016**, *6* (91), 88647-88655.
89. Liu, T.; Hao, C.; Wang, L.; Li, Y.; Liu, W.; Xin, J.; Zhang, J., Eugenol-Derived Biobased Epoxy: Shape Memory, Repairing, and Recyclability. *Macromolecules* **2017**, *50* (21), 8588-8597.
90. Yu, K.; Taynton, P.; Zhang, W.; Dunn, M. L.; Qi, H. J., Influence of stoichiometry on the glass transition and bond exchange reactions in epoxy thermoset polymers. *RSC Advances* **2014**, *4* (89), 48682-48690.
91. Yu, K.; Taynton, P.; Zhang, W.; Dunn, M. L.; Qi, H. J., Reprocessing and recycling of thermosetting polymers based on bond exchange reactions. *RSC Advances* **2014**, *4* (20), 10108-10117.
92. Yang, X.; Guo, L.; Xu, X.; Shang, S.; Liu, H., A fully bio-based epoxy vitrimer: Self-healing, triple-shape memory and reprocessing triggered by dynamic covalent bond exchange. *Materials & Design* **2020**, *186*, 108248.
93. Yue, L.; Guo, H.; Kennedy, A.; Patel, A.; Gong, X.; Ju, T.; Gray, T.; Manas-Zloczower, I., Vitrimerization: Converting Thermoset Polymers into Vitrimers. *ACS Macro Letters* **2020**, 836-842.
94. Tobolsky, A.; MacKnight, W.; Takahashi, M., Relaxation of disulfide and tetrasulfide polymers. *The Journal of Physical Chemistry* **1964**, *68* (4), 787-790.
95. Tesoro, G. C.; Sastri, V., Reversible crosslinking in epoxy resins. I. Feasibility studies. *Journal of Applied Polymer Science* **1990**, *39* (7), 1425-1437.

## Chapter 1

96. Matxain, J. M.; Asua, J. M.; Ruipérez, F., Design of new disulfide-based organic compounds for the improvement of self-healing materials. *Physical Chemistry Chemical Physics* **2016**, *18* (3), 1758-1770.
97. Nevejans, S.; Ballard, N.; Miranda, J. I.; Reck, B.; Asua, J. M., The underlying mechanisms for self-healing of poly(disulfide)s. *Physical Chemistry Chemical Physics* **2016**, *18* (39), 27577-27583.
98. Rekondo, A.; Martin, R.; Ruiz de Luzuriaga, A.; Cabañero, G.; Grande, H. J.; Odriozola, I., Catalyst-free room-temperature self-healing elastomers based on aromatic disulfide metathesis. *Materials Horizons* **2014**, *1* (2), 237-240.
99. Takahashi, A.; Ohishi, T.; Goseki, R.; Otsuka, H., Degradable epoxy resins prepared from diepoxide monomer with dynamic covalent disulfide linkage. *Polymer* **2016**, *82*, 319-326.
100. Ruiz de Luzuriaga, A.; Martin, R.; Markaide, N.; Rekondo, A.; Cabañero, G.; Rodríguez, J.; Odriozola, I., Epoxy resin with exchangeable disulfide crosslinks to obtain reprocessable, repairable and recyclable fiber-reinforced thermoset composites. *Materials Horizons* **2016**, *3* (3), 241-247.
101. Imbernon, L.; Oikonomou, E. K.; Norvez, S.; Leibler, L., Chemically crosslinked yet reprocessable epoxidized natural rubber via thermo-activated disulfide rearrangements. *Polymer Chemistry* **2015**, *6* (23), 4271-4278.
102. Chen, M.; Zhou, L.; Wu, Y.; Zhao, X.; Zhang, Y., Rapid Stress Relaxation and Moderate Temperature of Malleability Enabled by the Synergy of Disulfide Metathesis and Carboxylate Transesterification in Epoxy Vitrimers. *ACS Macro Letters* **2019**, *8* (3), 255-260.
103. Li, X.; Yu, R.; He, Y.; Zhang, Y.; Yang, X.; Zhao, X.; Huang, W., Self-Healing Polyurethane Elastomers Based on a Disulfide Bond by Digital Light Processing 3D Printing. *ACS Macro Letters* **2019**, *8* (11), 1511-1516.
104. Tran, V. T.; Mredha, M. T. I.; Na, J. Y.; Seon, J.-K.; Cui, J.; Jeon, I., Multifunctional poly(disulfide) hydrogels with extremely fast self-healing ability and degradability. *Chemical Engineering Journal* **2020**, *394*, 124941.
105. Ji, F.; Liu, X.; Sheng, D.; Yang, Y., Epoxy-vitrimer composites based on exchangeable aromatic disulfide bonds: Reprocessibility, adhesive, multi-shape memory effect. *Polymer* **2020**, *197*, 122514.
106. Deng, X.-Y.; Xie, H.; Du, L.; Fan, C.-J.; Cheng, C.-Y.; Yang, K.-K.; Wang, Y.-Z., Polyurethane networks based on disulfide bonds: from tunable multi-shape memory effects to simultaneous self-healing. *Science China Materials* **2019**, *62* (3), 437-447.
107. Belowich, M. E.; Stoddart, J. F., Dynamic imine chemistry. *Chemical Society Reviews* **2012**, *41* (6), 2003-2024.
108. Taynton, P.; Yu, K.; Shoemaker, R. K.; Jin, Y.; Qi, H. J.; Zhang, W., Heat- or Water-Driven Malleability in a Highly Recyclable Covalent Network Polymer. *Adv. Mater.* **2014**, *26* (23), 3938-3942.
109. Dhers, S.; Vantomme, G.; Avérous, L., A fully bio-based polyimine vitrimer derived from fructose. *Green Chemistry* **2019**, *21* (7), 1596-1601.
110. Guo, Z.; Liu, B.; Zhou, L.; Wang, L.; Majeed, K.; Zhang, B.; Zhou, F.; Zhang, Q., Preparation of environmentally friendly bio-based vitrimers from vanillin derivatives by introducing two types of dynamic covalent CN and S-S bonds. *Polymer* **2020**, *197*, 122483.
111. Memon, H.; Liu, H.; Rashid, M. A.; Chen, L.; Jiang, Q.; Zhang, L.; Wei, Y.; Liu, W.; Qiu, Y., Vanillin-Based Epoxy Vitrimer with High Performance and Closed-Loop Recyclability. *Macromolecules* **2020**, *53* (2), 621-630.
112. Sanyal, A., Diels-Alder Cycloaddition-Cycloreversion: A Powerful Combo in Materials Design. *Macromolecular Chemistry and Physics* **2010**, *211* (13), 1417-1425.
113. Trovatti, E.; Lacerda, T. M.; Carvalho, A. J. F.; Gandini, A., Recycling Tires? Reversible Crosslinking of Poly(butadiene). *Adv. Mater.* **2015**, *27* (13), 2242-2245.
114. Bai, J.; Li, H.; Shi, Z.; Yin, J., An Eco-Friendly Scheme for the Cross-Linked Polybutadiene Elastomer via Thiol-Ene and Diels-Alder Click Chemistry. *Macromolecules* **2015**, *48* (11), 3539-3546.
115. Oehlenschlaeger, K. K.; Mueller, J. O.; Brandt, J.; Hilf, S.; Lederer, A.; Wilhelm, M.; Graf, R.; Coote, M. L.; Schmidt, F. G.; Barner-Kowollik, C., Adaptable Hetero Diels-Alder Networks for Fast Self-Healing under Mild Conditions. *Adv. Mater.* **2014**, *26* (21), 3561-3566.
116. Tanasi, P.; Hernández Santana, M.; Carretero-González, J.; Verdejo, R.; López-Manchado, M. A., Thermo-reversible crosslinked natural rubber: A Diels-Alder route for reuse and self-healing properties in elastomers. *Polymer* **2019**, *175*, 15-24.
117. Zheng, P.; McCarthy, T. J., A Surprise from 1954: Siloxane Equilibration Is a Simple, Robust, and Obvious Polymer Self-Healing Mechanism. *Journal of the American Chemical Society* **2012**, *134* (4), 2024-2027.

118. Zhang, X.; Cao, Y.; Zhang, M.; Wang, Y.; Tang, H.; Li, N., Olefin metathesis-crosslinked, bulky imidazolium-based anion exchange membranes with excellent base stability and mechanical properties. *Journal of Membrane Science* **2020**, *598*, 117793.
119. Obadia, M. M.; Mudraboyina, B. P.; Serghei, A.; Montarnal, D.; Drockenmuller, E., Reprocessing and Recycling of Highly Cross-Linked Ion-Conducting Networks through Transalkylation Exchanges of C–N Bonds. *Journal of the American Chemical Society* **2015**, *137* (18), 6078-6083.
120. Global Natural Fibers Market Status and Future Forecast 2015-2025, 17 March **2020**.
121. Bunsell AR & Renard J 2005, Fundamentals of fibre reinforced composite materials, CRC Press, USA.
122. Cristaldi, G.; Latteri, A.; Recca, G.; Cicala, G., Composites based on natural fibre fabrics. *Woven fabric engineering* **2010**, *17*, 317-342.
123. Sgriccia, N.; Hawley, M. C.; Misra, M., Characterization of natural fiber surfaces and natural fiber composites. *Composites Part A: Applied Science and Manufacturing* **2008**, *39* (10), 1632-1637.
124. Bogoeva-Gaceva, G.; Avella, M.; Malinconico, M.; Buzarovska, A.; Grozdanov, A.; Gentile, G.; Errico, M. E., Natural fiber eco-composites. *Polymer Composites* **2007**, *28* (1), 98-107.
125. N.W. Manthey, F. C., T. Aravinthan, H. Wang & T. Cooney In *Natural Fibre Composites with Epoxidized Vegetable Oil (EVO) Resins: A Review*, Southern Region Engineering Conference Toowoomba, Australia Toowoomba, Australia 2010.
126. Ahmad, F.; Choi, H. S.; Park, M. K., A Review: Natural Fiber Composites Selection in View of Mechanical, Light Weight, and Economic Properties. *Macromolecular Materials and Engineering* **2015**, *300* (1), 10-24.
127. Saha, P.; Manna, S.; Chowdhury, S. R.; Sen, R.; Roy, D.; Adhikari, B., Enhancement of tensile strength of lignocellulosic jute fibers by alkali-steam treatment. *Bioresour. Technol.* **2010**, *101* (9), 3182-7.
128. Garlotta, D., A literature review of poly (lactic acid). *Journal of Polymers and the Environment* **2001**, *9* (2), 63-84.
129. Galimzyanova, R. Y.; Mevliyanova, M.; Hisamieva, D.; Pesternnikova, N.; Musin, I. N.; Lisanevich, M. In *The Use of Polylactic Acid to Obtain Biodegradable Medical Devices*, Key Eng. Mater., Trans Tech Publ: 2019; pp 285-289.
130. Sudamrao Getme, A.; Patel, B., A Review: Bio-fiber's as reinforcement in composites of polylactic acid (PLA). *Materials Today: Proceedings* **2020**, *26*, 2116-2122.
131. Oksman, K.; Skrifvars, M.; Selin, J. F., Natural fibres as reinforcement in polylactic acid (PLA) composites. *Composites Science and Technology* **2003**, *63* (9), 1317-1324.
132. Shih, Y.-F.; Lai, Z.-Z., Green Composites Based on Poly (Lactic Acid) and Bamboo Fiber: Flame Retardancy, Thermal, and Mechanical Properties. In *NAC 2019*, Springer: 2020; pp 61-69.
133. Jia, W.; Gong, R. H.; Hogg, P. J., Poly (lactic acid) fibre reinforced biodegradable composites. *Composites Part B: Engineering* **2014**, *62*, 104-112.
134. Goutianos, S.; Van der Schueren, L.; Beauson, J., Failure mechanisms in unidirectional self-reinforced biobased composites based on high stiffness PLA fibres. *Composites Part A: Applied Science and Manufacturing* **2019**, *117*, 169-179.
135. Bachmann, J.; Hidalgo, C.; Bricout, S., Environmental analysis of innovative sustainable composites with potential use in aviation sector—A life cycle assessment review. *Science China Technological Sciences* **2017**, *60* (9), 1301-1317.
136. La Rosa, A. D.; Recca, G.; Summerscales, J.; Latteri, A.; Cozzo, G.; Cicala, G., Bio-based versus traditional polymer composites. A life cycle assessment perspective. *Journal of Cleaner Production* **2014**, *74*, 135-144.
137. Shibata, M.; Teramoto, N.; Makino, K., Preparation and properties of biocomposites composed of epoxidized soybean oil, tannic acid, and microfibrillated cellulose. *Journal of Applied Polymer Science* **2011**, *120* (1), 273-278.
138. Liu, W.; Chen, T.; Fei, M.-e.; Qiu, R.; Yu, D.; Fu, T.; Qiu, J., Properties of natural fiber-reinforced biobased thermoset biocomposites: Effects of fiber type and resin composition. *Composites Part B: Engineering* **2019**, *171*, 87-95.
139. Di Landro, L.; Janszen, G., Composites with hemp reinforcement and bio-based epoxy matrix. *Composites Part B: Engineering* **2014**, *67*, 220-226.
140. Ozkur, S.; Sezgin, H.; Akay, E.; Yalcin-Enis, I., Hybrid bio-based composites from blends of epoxy and soybean oil resins reinforced with jute woven fabrics. *Materials Research Express* **2020**, *7* (1), 015335.

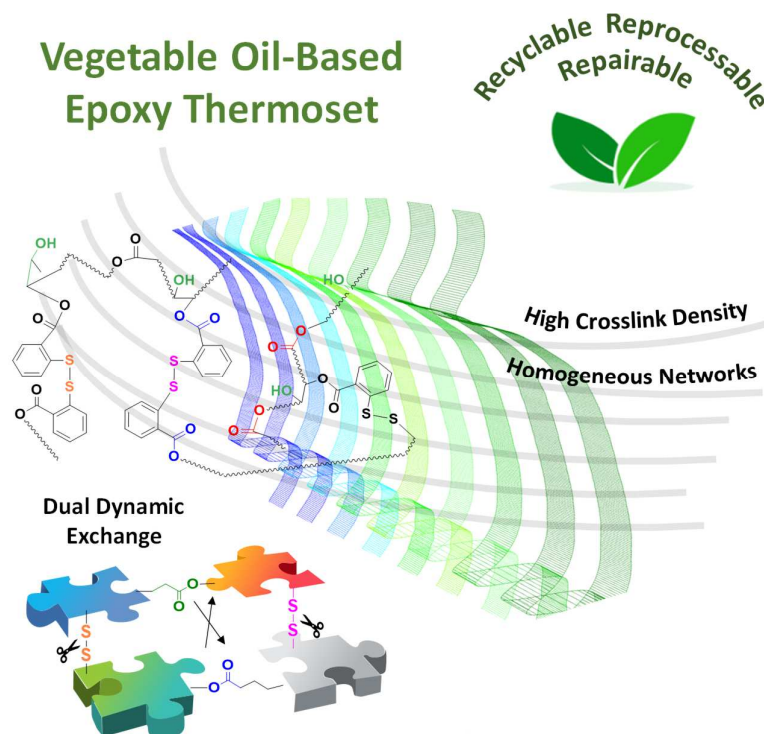


## Chapter 1

141. Musa, C.; Kervoëlen, A.; Danjou, P.-E.; Bourmaud, A.; Delattre, F., Bio-based unidirectional composite made of flax fibre and isosorbide-based epoxy resin. *Materials Letters* **2020**, *258*, 126818.
142. Liu, Z.; Erhan, S. Z.; Akin, D. E.; Barton, F. E., "Green" Composites from Renewable Resources: Preparation of Epoxidized Soybean Oil and Flax Fiber Composites. *Journal of Agricultural and Food Chemistry* **2006**, *54* (6), 2134-2137.
143. Bledzki, A.; Urbaniak, M.; Boettcher, A.; Berger, C.; Pilawka, R., Bio-Based Epoxies and Composites for Technical Applications. *Key Eng. Mater.* **2013**, *559*, 1-6.
144. Oliveux, G.; Dandy, L. O.; Leeke, G. A., Current status of recycling of fibre reinforced polymers: Review of technologies, reuse and resulting properties. *Prog. Mater Sci.* **2015**, *72*, 61-99.
145. Kuang, X.; Zhou, Y.; Shi, Q.; Wang, T.; Qi, H. J., Recycling of Epoxy Thermoset and Composites via Good Solvent Assisted and Small Molecules Participated Exchange Reactions. *ACS Sustainable Chemistry & Engineering* **2018**, *6* (7), 9189-9197.
146. La Rosa, A. D.; Banatao, D. R.; Pastine, S. J.; Latteri, A.; Cicala, G., Recycling treatment of carbon fibre/epoxy composites: Materials recovery and characterization and environmental impacts through life cycle assessment. *Composites Part B: Engineering* **2016**, *104*, 17-25.
147. La Rosa, A. D.; Blanco, I.; Banatao, D. R.; Pastine, S. J.; Björklund, A.; Cicala, G., Innovative Chemical Process for Recycling Thermosets Cured with Recyclamines<sup>®</sup> by Converting Bio-Epoxy Composites in Reusable Thermoplastic—An LCA Study. *Materials* **2018**, *11* (3), 353.
148. Pietrolungo, M.; Padovano, E.; Frache, A.; Badini, C., Mechanical recycling of an end-of-life automotive composite component. *Sustainable Materials and Technologies* **2020**, *23*, e00143.

# Chapter 2

Enhancing the recyclability of a vegetable oil-based epoxy thermoset through initiator influence



## Chapter 2

This chapter is based on Chiara Di Mauro, Thi-Nguyet Tran, Alain Graillot, Alice Mija, Enhancing the Recyclability of a Vegetable Oil-Based Epoxy Thermoset through Initiator Influence. *ACS Sustainable Chemistry & Engineering* 2020, 8 (20), 7690-7700.

DOI: 10.1021/acssuschemeng.0c01419 (invited cover page).

### Abstract

Bisphenol A-based epoxy thermosets involve both environmental and health risks. By reacting a vegetal oil-based epoxide with an aromatic diacid containing S–S bonds a thermoset is produced. Herein, reprocessable thermosets were synthesized, the recyclability being designed through a dual mechanism: that of disulfide metathesis and of transesterifications. To assess the feasibility of the reprocessing, a series of 10 initiators was tested to probe their effect not only on the cross-linking reaction but also on the recyclability. This study introduces for the first time the key role of the initiator on the material performance and on their reprocessing. A very good reprocessability was obtained for thermosets prepared using as initiator the imidazole. Moreover, the thermosets exhibit complete chemical recyclability in 1 N NaOH at 80 °C, after 3 days, without needing additional chemicals. The reprocessed materials have similar performance with the virgin ones, even after 10 cycles of reprocessing.

## 2.1 Introduction

The polymeric materials are mainly classified into two groups, as thermoplastic and thermosetting, in relation to their own properties when subjected to heating. The first group is formed by linear or slightly branched chains, and after increasing the temperature, they melt and can be reprocessed. Some of these materials are recyclable. The thermosetting materials include 3D networks like epoxy resins with excellent thermal and chemical stability; moreover, being constituted by cross-links and strong covalent bonds, the whole mobility of the macromolecule is limited. After cross-linking, the material becomes infusible and insoluble and its reprocessing impossible. Therefore, once damaged or at the end of life, the materials of the second group are treated as waste and disposed in landfills, leading to an increase of product costs and causing as well serious environmental and social consequences. For this reason, in recent years interest in recyclable and reprocessable plastics has grown increasingly, especially for thermosets<sup>1-9</sup> and fiber-reinforced epoxy composites. To overcome the conventional problems of these polymers, a solution was found by introduction of dynamic interconnections in the thermoset network<sup>10-13</sup> based on associative exchangeable covalent bonds in which the chemical linkages can be broken and reformed. Consequently, the dynamic character of the network is shown by changing its topology; otherwise, the number of cross-links established between inter- and intramolecular polymer chains remains constant. Leibler *et al.*<sup>14</sup> pioneered a malleable and recyclable thermoset, called “vitriimer”, by an epoxy–acid curing system. The underlying concept that allowed us to achieve this intrinsic property is based on a transesterification reaction. The authors demonstrated that the exchange reaction could be accelerated by catalysts such as 1,5,7-triazabicyclo[4.4.0]dec-5-ene (TBD),<sup>15</sup> 1,2-dimethylimidazole (1,2-DMI),<sup>16</sup> or zinc acetate (Zn(OAc)<sub>2</sub>).<sup>14</sup> Qi *et al.*<sup>2</sup> proved for diglycidyl ether of bisphenol A (DGEBA) and a mixture of fatty acids (Pripol 1040) system in the presence of 5 mol % of Zn(OAc)<sub>2</sub> that the reprocessing and recycling can be achieved. Along with transesterification, Odriozola *et al.*<sup>5,7</sup> designed reshapable and recyclable thermosets by introducing disulfide dynamic chemical cross-links on DGEBA networks. The authors showed that the dynamic character of S-S metathesis is also attractive because of its multiple responsive characteristics. For example, instead of a two-step process as in Diels–Alder exchange reactions, the self-healing of polymers containing S-S bonds can occur only in one step.<sup>17</sup> By taking these advantages, we can design new epoxy thermosets with a dual intrinsic exchange mechanism. However, most of the above examples use bisphenol A (BPA) and epichlorohydrin.<sup>18-21</sup> The harmful risk of BPA on the environment

DGEBA as epoxide monomer, which is prepared by the condensation reaction between and especially on human health as an endocrine disruptor has been proved and published.<sup>22-24</sup> Global ecological issues are requiring sustainable development of the polymer industry. For this reason, our attention focused on epoxidized vegetable oils,<sup>1,25-27</sup> in particular, on epoxidized linseed oil (ELO), as starting materials due to their relatively low cost and high epoxy content. In this work, we report the preparation and characterization of new biobased recyclable and reprocessable epoxy thermosets using a disulfide containing dicarboxylic acid (DTBA) as curing agent in the presence of several imidazole derivatives, N-heterocyclic or amines, as initiators. To our knowledge, this study introduces for the first time the influence of the initiator on the reprocessing ability and on the thermoset's performance.

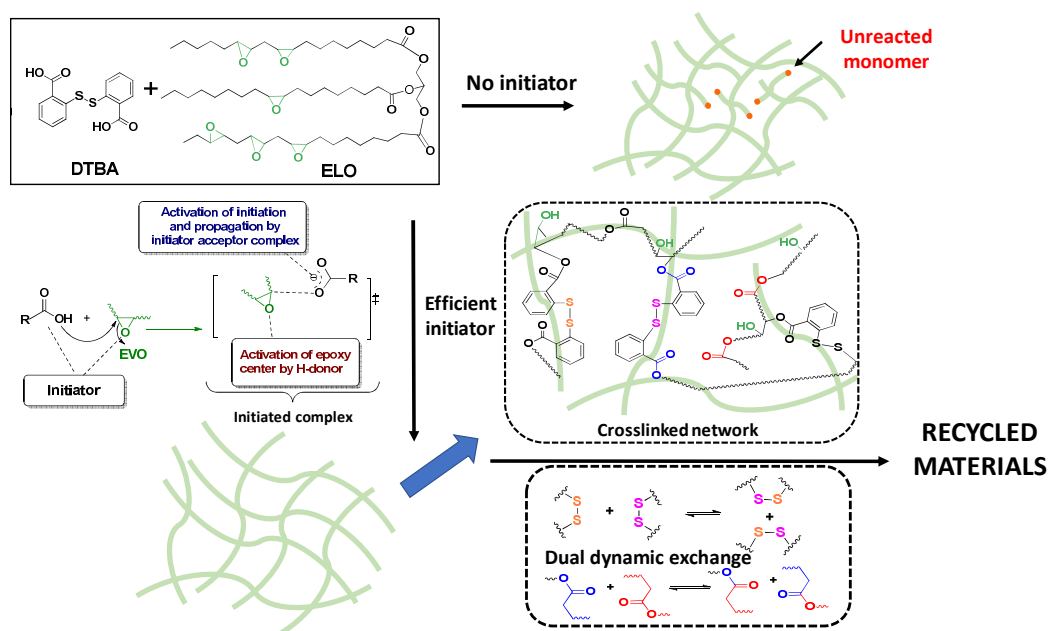


**Figure 1.** Synthesis of epoxidized linseed oil (ELO)/2,2'-dithiodibenzoic acid (DTBA) crosslinked structures and network rearrangement by simultaneous exchange reactions: disulfide metathesis and carboxylate transesterification

The objective of this study is to emphasize that the initiators not only play a key role on the epoxy–diacid copolymerization reaction but have a more extended impact. Therefore, their influence on the thermosets thermomechanical performance and recyclability is studied in this work. Three groups of nitrogen Lewis base initiators were selected. The first group includes two tertiary amines N,N-dimethylbenzylamine (DMBA) and 2,4,6-tris(dimethylaminomethyl) phenol (DMP30); this kind of initiator is currently used for the epoxy ring opening. The second group comprises the heterocyclic nitrogen initiators including Dimethylaminopyridine (DMAP), imidazole (IM), 1-methylpiperazine (1-MP), and 1,5,7-

triazabicyclo[4.4.0]dec-5-ene (TBD). Finally, the last group focuses on the imidazole and its derivatives. Imidazole was initially selected as the reference initiator due to its high reactivity and relatively low cost.<sup>28–32</sup> IM is an amphoteric molecule behaving both as a donor and as an acceptor center with two nitrogen atoms. To comprehend how the substituent groups on the imidazole ring have an influence on the reaction and network behavior, 1-N- and 2-N-substituted imidazoles were studied. The prepared networks, containing S–S dynamic bonds via the hardener structure, are therefore able to rearrange by dual-simultaneous exchange reactions: disulfide metathesis and carboxylate transesterification. The thermoset synthesis, the role of the initiators, and the network reprocessing are illustrated in Figure 1.

The reactivity study of the novel formulations was realized by in situ Fourier transform infrared spectroscopy (FTIR) and differential scanning calorimetry (DSC). The physical and thermomechanical properties of the virgin thermosets and of the reprocessed materials were analyzed by DSC, thermogravimetric analysis (TGA), and dynamic mechanical analysis (DMA).

## 2.2 Results and discussion

The protocol of the curing and post-curing processes was determined for each formulation by differential scanning calorimetry DSC studies (Figure ESI 1 and Table ESI 2). An equimolar ratio between acid and epoxide functional groups was used for preparing the formulations. Ten initiators were selected to study their effect on the curing reaction. An initiator percentage of 1wt.% of mixture mass was found as optimal, as studied and deduced in a previous study.<sup>33</sup> As highlighted in Table ESI 2, the ELO–DTBA cross-linking study illustrates the initiator efficiency by lowering the activation energy of the reaction and accelerating the curing rate. Due to a very low reactivity, the noninitiated system was discarded.

### 2.2.1 Structural investigation of ELO/DTBA copolymerization by FTIR

To highlight the structural evolutions between the initial ELO/DTBA reactive mixtures and those of the final thermosets a series of FTIR analyses was performed. To these studies was added the comparison with the systems (mixtures or thermosets) prepared with or without the selected initiators. The obtained results are presented in Figure 2. Considering that only 1.0 wt.% of initiator is present in the reactive mixture, Figure 2 A shows that all ELO/DTBA systems, with and without initiators, have similar spectra. Therefore, the initiator signals are negligible compared to that of ELO and DTBA. In the spectra of reactive mixtures, the characteristic peaks of the epoxy groups appear at 823 and 847  $\text{cm}^{-1}$ <sup>32,34,35</sup> while those of the carboxylic groups, with very broad vibration bands, are in the region of 3300–2300 and at 895

$\text{cm}^{-1}$  assigned, respectively, to the O–H stretching and O–H bending of the –COOH groups. Other characteristic peaks are observed including the –C=O stretching of triglycerides' ester of ELO at 1740 and 1673  $\text{cm}^{-1}$  attributed to –C=O stretching of DTBA. Compared with these reference peaks, we notice in the FTIR spectra of all ELO/DTBA thermosets complete disappearance of the oxirane peaks (823 and 847  $\text{cm}^{-1}$ ) along with the appearance of the –OH band at 3550  $\text{cm}^{-1}$ . This result demonstrates a complete epoxide ring opening via nucleophilic addition.

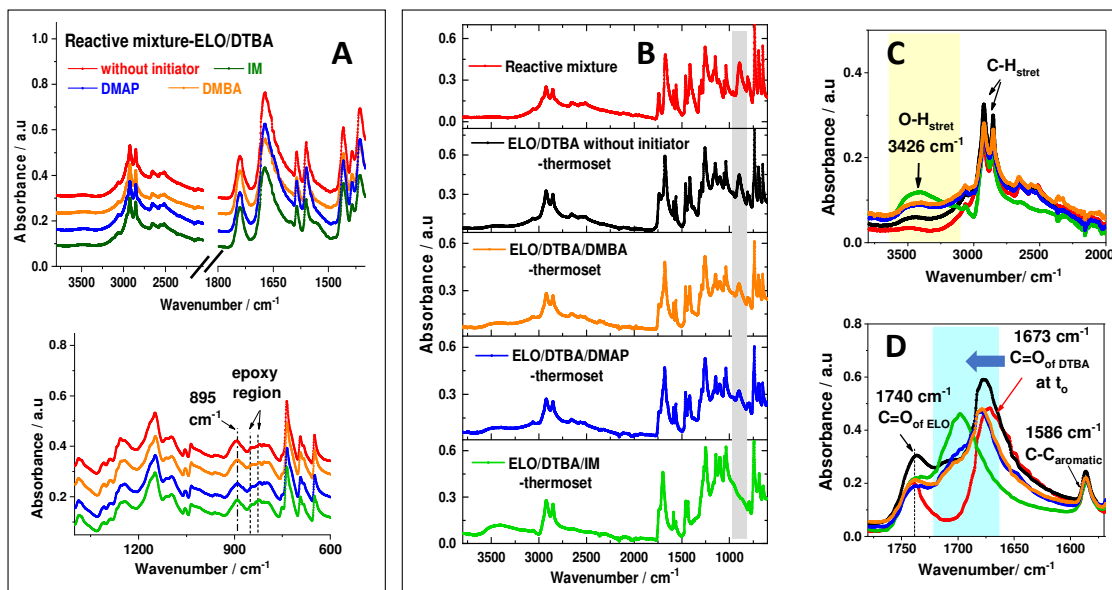


**Figure 2.** (A): Comparison between the FTIR spectra of ELO/DTBA reactive mixture without initiator and that of ELO / DTBA reactive mixture with DMBA, DMAP and IM; (B, C, D) FTIR spectra of ELO / DTBA final thermosets in comparison to reactive mixture: (B): whole spectrum; (C), zoom in the region 3800 - 2000  $\text{cm}^{-1}$ ; (D): zoom in the region 1780 - 1570  $\text{cm}^{-1}$

By introduction of DTBA acid as a hardener in the ELO network, the carbonyl stretching band (C=O) is shifted from 1673  $\text{cm}^{-1}$  in DTBA to higher frequency at about 1700  $\text{cm}^{-1}$  for the newly created ester (Figure 2 D). This peak is proof of ester bond formation by ELO/DTBA thermocuring copolymerization. However, at the same time, other side reactions could involve the residual epoxy functions via homopolymerization or etherifications.<sup>36–39</sup> Depending strongly on the initiator efficiency, these secondary reactions can be dismissed. As shown in Figure 2 B, in the presence of 1wt.% of IM, complete copolymerization was achieved as confirmed by the complete disappearance of the epoxide and of the -OH from -COOH. In the FTIR spectra of ELO/DTBA/No initiator thermoset or that with inefficient initiators, like DMBA or 1-MP, we can observe that the epoxide absorptions at 847 and 823  $\text{cm}^{-1}$  disappear completely while the O–H band of the carboxylic acid at 895  $\text{cm}^{-1}$  is still present. For example, ~ 50% of -COOH

remains unreacted in the ELO/DTBA/No initiator or ELO/DTBA/DMBA thermoset system. This result indicates extra consumption of epoxy groups in comparison to that of the -COOH groups, meaning secondary reactions like etherifications occur.<sup>39</sup> On the basis of this observation, copolymerization conversion was quantified by the peak area of the -OH absorption of the carboxylic functions at about  $895\text{ cm}^{-1}$  with reference to the aromatic peak at about  $1586\text{ cm}^{-1}$  corresponding to C=C stretching of the aromatic ring. The obtained results are presented in Figure 3 and discussed in detail in the next section.

## 2.2.2 Thermomechanical analyses of ELO/DTBA thermosets: comparison of virgin and recycled materials

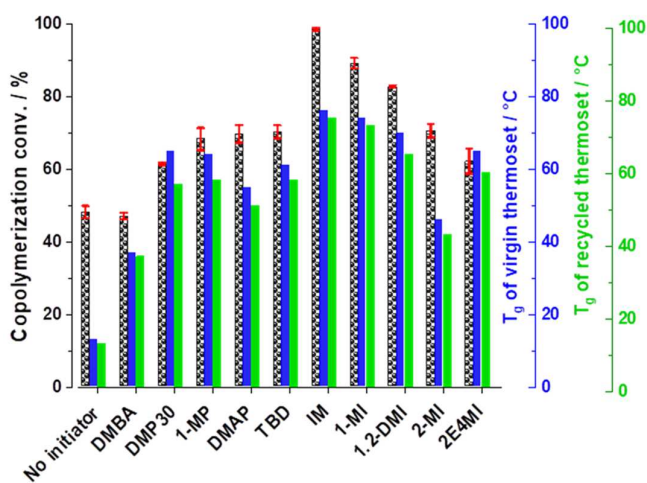


**Figure 3.** Comparison between virgin and reprocessed ELO/DTBA/Initiators thermosets:  $T_g$  values of virgin (blue) and reprocessed (green) thermosets determined by DSC analysis correlated with the copolymerization conversion (black) as calculated by FTIR analysis. In abscissa are indicated the initiators used for each ELO/DTBA/Initiator system

The present work studies the ability of synthesized thermosets to be reprocessable and recyclable and to analyze how the materials properties are affected by the reprocessing. Table ESI 5 summarizes the reprocessing parameters applied for each system to obtain a completely reprocessed sample. As illustrated in Table ESI 7, the prepared thermosets have good reprocessability that can be attributed to the combination of two mechanisms: dynamic disulfide bonds and

transesterification exchange as schematized in Figure 1. The temperature, pressure, and time needed for recycling the ELO/DTBA thermosets are lower compared with those reported for DGEBA/4-aminophenyl disulfide (AFD) thermosets that require a hot pressing at  $200\text{ °C}$  and  $100\text{ bar}$  for  $5\text{ min}$ .<sup>7</sup> It is well known that the polymer architecture topology is deeply affected by the side reactions that can occur during network building. For example, the etherification reactions can introduce some branching points, therefore changing the network cross-link density and thus impacting the final properties. To evaluate the initiator influence on the network properties, the  $T_g$  transitions were evaluated by DSC. The obtained results are given



in Figure 3, where we compare the glass transitions of ELO/DTBA thermosets synthesized with and without initiator. In the same figure we report also the conversion of copolymerization, determined by FTIR. Figure 3 illustrates very well the strong impact of the initiator nature on the properties of the synthesized thermosets. The efficiency of the initiator not only controls the copolymerization mechanism but impacts the network building, architecture, and so overall performance. It can be observed in Figure 3 that the virgin thermosets present a large variety of  $T_g$  from 13 to 76 °C for the thermoset prepared without or with IM, respectively. Use of epoxidized vegetable oil, with an aliphatic structure, formed materials with lower  $T_g$  compared to those of DGEBA-based thermosets. Considering the reprocessable systems, values of  $T_g = 130$  °C were reported for a DGEBA / 4-aminophenyl disulfide (AFD) thermoset.<sup>5</sup> Zhang *et al.*<sup>15</sup> produced vitrimers based on DGEBA / 4,4'-dithiodibutyric acid (DTDA) with  $T_g = 30$  °C. The impact of the aliphatic epoxide on the material properties was studied by Altuna *et al.*<sup>41</sup> for DGEBA mixed with different amounts of epoxidized soybean oil (ESO). This epoxide mixture was cured with methyltetrahydrophthalic anhydride (MTHPA) in the presence of 1-MI initiator. The authors show that the  $\tan \delta$  values decrease with ESO content from 108 to 57 °C for the fully ESO thermoset. Compared to these results, we report in this work that by initiator influence we can modulate the  $T_g$  from 13 °C for ELO/DTBA/without initiator to  $\sim 76$  °C for ELO/DTBA/IM thermoset.

The obtained thermomechanical properties were compared with that of the recycled materials. After reprocessing, similar values were measured with a small decrease of  $T_g$  for all of the studied systems (difference  $\Delta T_g \leq 9$  °C). In the same trend as ELO/DTBA uncatalyzed virgin thermoset, its reprocessed material also exhibits the lowest  $T_g$  ( $\sim 12$  °C) combined with the lowest copolymerization conversion; only  $\sim 50\%$  of  $-\text{COOH}$  was converted. This result suggests a heterogeneous thermoset network characterized by pending unbonded chains of triglyceride and dicarboxylic acid. In contrast, the systems with 1 wt.% initiator show higher  $T_g$  values before or after reprocessing. In the imidazole series, the synthesized thermosets have comparable  $T_g$  values, except the system with 2-MI that presents a low  $T_g$ . A similar behavior was reported by Such *et al.*<sup>42</sup> for the curing of the diglycidyl ether of bisphenol A initiated by different imidazoles. According to this study, the lower  $T_g$  of the network obtained in the presence of 2-MI was attributed to a plasticizing effect of the initiator. Figure 3 shows that the 2E4MI system displays a lower copolymerization conversion in the imidazole series. In the case of thermosets systems with 1-MP and DMP30, reprocessing was more difficult, requiring a longer time and a higher temperature. Among the 10 catalyzed thermosets, ELO/DTBA/DMBA exhibits a lower  $T_g = 37$  °C for the virgin and  $T_g = 36$  °C for the recycled

material. This result could be first related to the copolymerization conversion with only ~ 50 % of carboxylic functions converted in ester bonding with the ELO network (Figure 3). Therefore, it can be also correlated to a low cross-linking density that allows a certain chain mobility and consequently a low  $T_g$  value. Hu *et al.*<sup>43</sup> report that the glass transition decreases during the reprocessing by decreasing the network crosslinking.

To evaluate if structural modifications occur in the thermoset network during the reprocessing, FTIR analyses were performed before and after mechanical recycling. The obtained results show that no changes occur after reprocessing; similar spectra for virgin and recycled thermoset are obtained. This observation was confirmed by complementary experiments, as illustrated in Figure ESI 2, by an isothermal FTIR study at 170 °C (reprocessing temperature) at which no difference was detected even after 90 min.

### 2.2.2.1 Dynamic mechanical analysis

To analyze the viscoelastic properties, the following thermoset systems were selected: ELO/DTBA/IM, ELO/DTBA/DMBA, and ELO/DTBA/DMAP. The storage modulus ( $E'$ ) values and loss factor ( $\tan \delta$ ) curves of these systems are presented as a function of temperature in Figure 4. The  $\tan \delta$ -correlated to the  $\alpha$  relaxations and associated with the macroscopic glass transition ( $T_g$ ) were determined, ranging from 15 to 89 °C. A similar range of  $T_g$  was reported by Gobin *et al.*<sup>44</sup> with a  $T_g = 16$  °C for epoxidized broccoli oil cross-linked with ophenylene diacetic acid in the absence of initiator. In comparison with ELO/aliphatic diacid thermosets,<sup>32</sup> the  $\tan \delta$  values are higher for ELO/DTBA networks due to the presence of the aromatic structure of DTBA cross-linker introducing rigid segments. The  $\tan \delta$  of the noncatalyzed system exhibits the lowest value; meanwhile, the system has the highest storage modulus (Figure 4). The associated  $T_g$  values obtained by DSC for the virgin and recycled thermosets are in the same trend with that measured by DMA. These results indicate that the initiated systems exhibit higher  $\tan \delta$  and  $T_g$ . After mechanical recycling, the ELO/DTBA/IM thermoset displays the highest  $\tan \delta = 97$  °C while DMBA is confirmed again as a less efficient catalyst with produced thermosets having  $\tan \delta = 58$  °C combined with the higher decrease in the storage modulus through the rubbery plateau. The thermosets cross-link density was calculated using the  $E'$  value in the rubbery plateau according to Eq. ESI 2. As illustrated in Tables 1 and ESI 6, depending on the initiator nature, the cross-link densities vary from 1.91 to 0.82 mmol.cm<sup>-3</sup>. Among the 10 initiators (Figures ESI 4 and ESI 5), DMP30 and 2E4MI allow us to produce thermosets with the highest cross-link density; nevertheless, these values decrease drastically after reprocessing: 1.97 mmol.cm<sup>-3</sup> for virgin vs. 0.58 mmol.cm<sup>-3</sup> for

## Chapter 2

reprocessed ELO/DTBA/DMP30 and 1.84 vs. 0.38 mmol.cm<sup>-3</sup> for ELO/DTBA/2E4MI, respectively. This result can be attributed to formation of supplementary cross-links with some pending chains. The ELO/DTBA/IM thermosets have the highest values of tan  $\delta$  and cross-linking density before and after reprocessing.

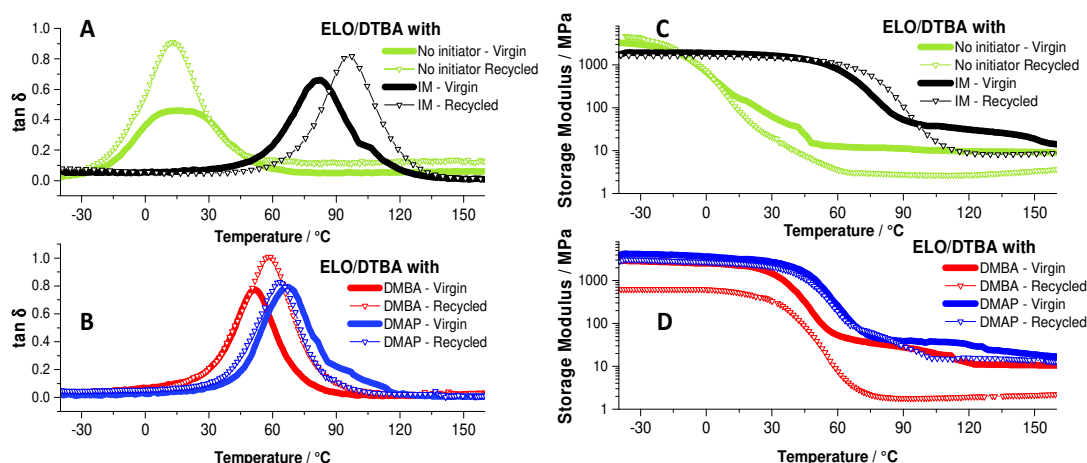


**Figure 4.** DMA results:  $\tan \delta$  and storage modulus vs. temperature of thermosets and reprocessed samples in function of the initiators: (A) and (C) uncatalyzed thermosets and ELO/DTBA/IM; (B) and (D) uncatalyzed thermosets and ELO/DTBA/DMBA and ELO/DTBA/DMAP

**Table 1.** Mechanical properties of virgin and reprocessed ELO/DTBA thermosets

	No Initiator		IM		DMBA		DMAP	
	Virgin	Recycled	Virgin	Recycled	Virgin	Recycled	Virgin	Recycled
$\tan \delta^a$ (°C)	15	13	83	97	52	58	66	63
$(\tan \delta)^a_{\max}$	0.45	0.91	0.66	0.82	0.77	1.0	0.79	0.83
$E'^a$ at -50 °C (MPa)	3390	4730	1560	2550	2660	700	2380	2600
$E'^a$ at 160 °C (MPa)	9	3	16	9	8	2	7	4
Crosslinking density <sup>a</sup> (mmol/cm <sup>3</sup> )	0.82	0.30	1.25	0.81	0.98	0.21	1.18	0.79
Density <sup>b</sup> (g/cm <sup>3</sup> )	0.905	/	1.025	/	0.896	/	0.913	/
$M_c^a$ (g/mol)	1104	/	820	/	914	/	774	/

<sup>a</sup>: Determined by DMA. <sup>b</sup>: Determined by ratio of mass/volume

### 2.2.2.2 Thermal stability

The thermal stabilities of virgin and recycled resins were investigated by thermogravimetric analysis (TGA) under air atmosphere (thermal oxidation). The TGA curves as recorded during continuous heating at 10 °C.min<sup>-1</sup> are shown in Figure 5. The degradation process involves a two stages process (Figure ESI 6). For quantitative analysis of the investigated samples, the degradation onset temperature ( $T_{\text{onset}}$ ) and the temperature at 5% weight-loss ( $T_{5\%}$ ) were determined. The main data are summarized in Tables 2 and ESI 6. No degradation occurs before 200 °C except for noncatalyzed thermoset. In systems with 1 wt % initiator, the  $T_{\text{onset}}$

temperature increases  $\sim 50$  °C ( $\sim 200$  vs.  $150$  °C, Figure 5) and the  $T_{5\%}$  values were shifted to higher temperature from  $230$  to  $275$  °C in the following order: uncatalyzed < DMP30 = DMAP

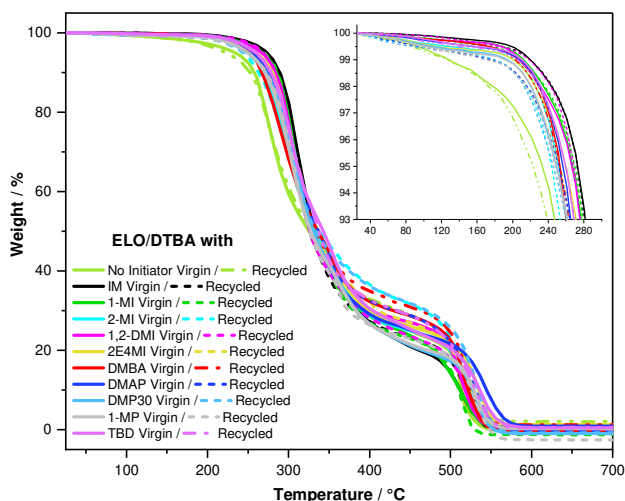


**Figure 5.** TGA comparison between the virgin and the recycled resins with and without initiators

< 2-MI = 1-MP < DMBA < 2E4MI = TBD < 1,2-DMI = 1-MI < IM. Very interestingly, as illustrated in Table 2, the  $T_{5\%}$  values were not affected by reprocessing. The only significant decrease of the  $T_{5\%}$  value could be observed for the uncatalyzed and recycled ELO/DTBA thermoset ( $T_{5\%} \approx 220$  °C compared to  $230$  °C for virgin thermoset). All virgin and recycled resins were degraded almost completely before  $650$  °C.

**Table 2.** TGA  $T_{5\%}$  values of virgin and recycled resins

ELO/DTBA systems	$T_{5\%}$ (°C)		
	Virgin	Recycled	$\Delta T_{5\%}$
No initiator	230	220	-10
IM	275	275	0
1-MI	265	267	2
2-MI	250	250	0
1.2-DMI	264	264	0
2E4MI	260	252	-8
DMBA	255	252	-3
DMAP	245	245	0
DMP30	245	245	0
1-MP	250	245	-5
TBD	260	260	0

$$\Delta T = T_{5\%, \text{ recycled}} - T_{5\%, \text{ virgin}}, T_{5\%} = \text{Temperature for 5\% weight loss determined by TGA}$$

Two degradation steps are observed in the TGA and DTG curves (Figure ESI 6). A similar thermal decomposition behavior was reported by Ding *et al.*<sup>32</sup> for ELO / aliphatic dicarboxylic acids / DMAP thermoset. The authors<sup>32,46</sup> suggest that the first degradation stage involves the breakdown of the ester–methylene linkages and of hydroxyls, while at higher temperatures aromatic products are formed. The first degradation step for the virgin and recycled ELO/DTBA catalyzed thermosets occurs around  $\sim 305$  °C, except for the ELO/DTBA/DMBA thermoset that starts to degrade at  $290$  °C. This result can be correlated to the lower cross-link degree of this network, as demonstrated previously by DMA analysis.

## 2.2.3 Study on the multiple reprocessing effect on materials performance

The dual dynamic character of the S–S exchanges and of the transesterification reactions improves the ability of materials to be reprocessed. As presented in the previous sections, all of the studied thermosets can be recycled. To evaluate how many times the thermoset can be reprocessed without losing its thermomechanical properties, the ELO/DTBA/IM thermoset was selected to perform this study because the IM allows the highest conversion rates. Thus, the reprocessing process was performed using the same parameters and repeated 10 times (Figure 6 and Table ESI 6). After several cycles, we observe a slightly dark coloration of the sample, probably due to a partial oxidation and aging.<sup>47</sup> The properties of recycled materials were investigated by DSC, FTIR, TGA, and DMA analyses.

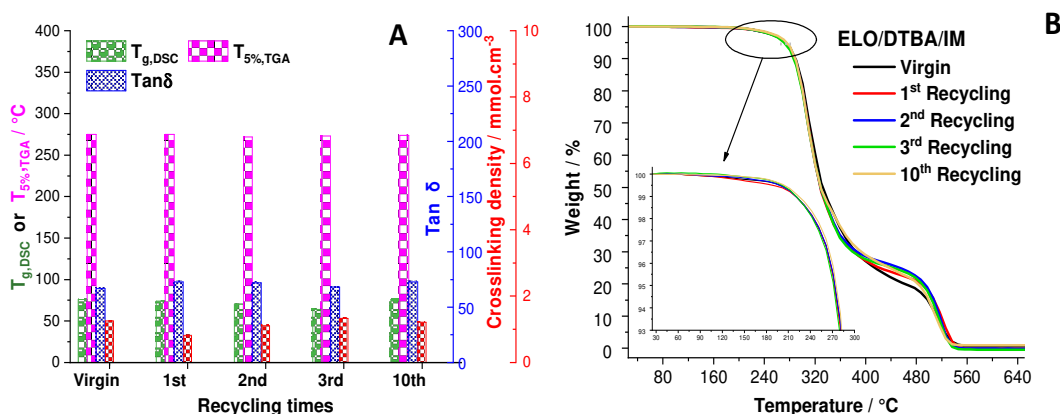


**Figure 6.** (A) Characteristic values in comparison after different reprocessing cycles:  $T_g$  (DSC);  $T_{5\%}$  (TGA);  $\tan \delta$  (DMA) and crosslinking density calculated by DMA; (B): TGA curves of the virgin and reprocessed ELO/DTBA/IM thermoset

Table 3 summarizes the results of the investigated properties. It was found, by scanning DSC, that the glass transition decreases progressively during the reprocessing cycles, from 76 °C in the virgin resin to 64 °C at the end of the third cycle. This result can be attributed to the continuous S–S exchange during the reprocessing and therefore to network modification. An unexpected result is that at the 10<sup>th</sup> cycle the resin presents the same  $T_g$  value as the virgin resin (Figure 6 A). It seems that during the recycling procedure the mechanical properties of the sample decrease, but at certain point there is a reversal of the properties. The dual mechanism of recycling that operates during reprocessing contributes to the increasing cross-linking density and finally regaining the material properties.

The thermal stability of the samples after several recycling stages remains approximately constant, showing very close values of  $T_{5\%}$  even at the end of the 10<sup>th</sup> reprocessing cycle (Figure 6 B). As shown in the DTG thermograms presented in Figure ESI 7, all of the curves are

very similar. The  $\tan \delta$  values increase until the third cycle; thereafter, a slight decrease was measured. After the 10<sup>th</sup> cycle the material has, once again, a similar value to the virgin sample (Figure 6 A). According with the obtained results after the first reprocessing, the  $E'$  values in glassy state and the  $E''$  moduli increase by  $\sim 4$  or 5 times while the cross-link density remains more or less constant except for its values after the second cycle. These results can be explained as resulting from the dynamic covalent bonds recreating linkages during material recycling.

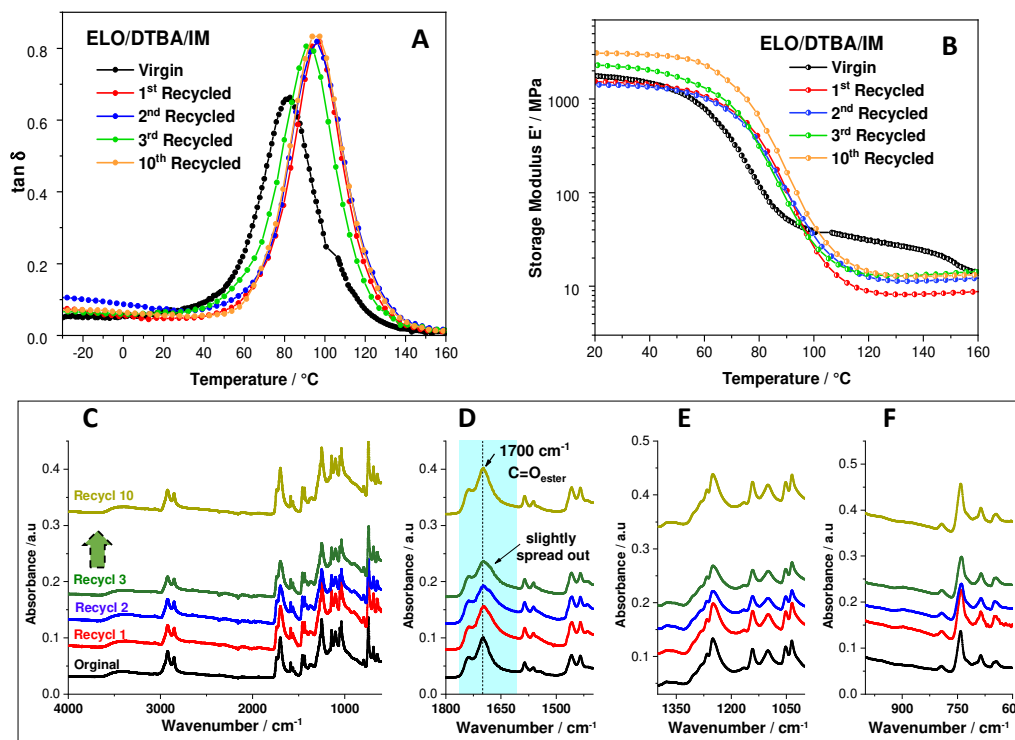


**Figure 7.**  $\tan \delta$  (A) and Storage Modulus (B) vs. temperature; FTIR spectra (C; D, E, F) for the virgin and recycled ELO/DTBA/IM

**Table 3.** Thermal and mechanical properties of ELO/DTBA/IM thermosets after several reprocessing

Characteristic values	Virgin	1 <sup>st</sup> Recycling	2 <sup>nd</sup> Recycling	3 <sup>rd</sup> Recycling	10 <sup>th</sup> Recycling
$T_g^a$ , (°C)	76	74	70	64	76
$T_{5\%}^b$ (°C)	275	275	272	273	274
$\tan \delta^c$	89	97	96	91	97
( $\tan \delta$ )max <sup>c</sup>	0.68	0.82	0.82	0.79	0.83
$E'^c$ (MPa) at -50 °C	1560	1720	2500	4400	6200
$E'^c$ (MPa) at 150 °C	8.6	8.9	12	13.8	13
$E''^c$ (MPa)max	70	200	200	350	370
Crosslink density <sup>c</sup> (mmol/cm <sup>3</sup> )	1.25	0.81	1.11	1.33	1.21

<sup>a</sup>Determined by DSC, <sup>b</sup>Determined by TGA, <sup>c</sup>Determined by DMA

## Chapter 2

The initial reduction of the cross-linking density after the first reprocessing cycle is restored at the end of the 10<sup>th</sup> cycle. In fact, after the third cycle, the cross-link density increases again until it reaches the initial value at the end of the 10<sup>th</sup> recycling. This behavior could be attributed to an internal rearrangement of the thermoset network. Very few changes were observed through the ATR-FTIR spectra in the carbonyl region at 1700 cm<sup>-1</sup> (Figure 7 D). This ester peak seems slightly spread out after the first reprocessing. It suggests the occurrence of transesterification reactions. The 10 times recycled sample has almost an identical structure compared to the virgin one. As the characteristic absorption of the S–S bonds is in the region from 540 to 500 cm<sup>-1</sup> (very low frequency), their change during reprocessing is difficult to follow by FTIR.

### 2.2.4 Swelling tests

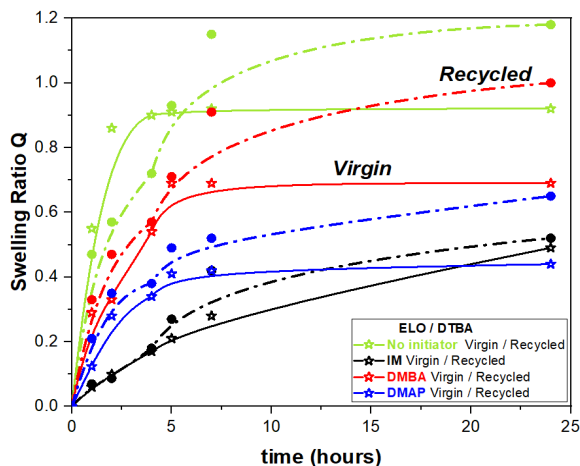


**Figure 8.** Swelling test in toluene of virgin and reprocessed thermoset resins

The swelling and solvent stability were tested in several solvents: toluene, acetone, methanol, THF, DMSO, 1 N NaOH, 1 N HCl (Figure ESI 9). The time-dependent swelling ratio evolution of the prepared thermosets in different solvents reflects the solvent diffusion inside the polymer network. After 8 h of immersion in toluene, all samples including virgin and recycled thermosets reached the maximum of the swelling asymptotic curves. Figure 8

shows clearly that the swelling ratio increases in the order IM < DMAP < DMBA < No initiator. The swelling ratio is inversely proportional to the cross-link densities reported in Table 1. We observed also that after 3 weeks of immersion in toluene at room temperature, all of the materials remained unaffected (Figure 9 A) without any detected degradation or dissolution. A similar behavior was observed for the test stability in 1 N HCl. Concerning the chemical recycling in 1 N NaOH, very interestingly, all of the ELO/DTBA thermosets start to lose their integrity after 24 h at room temperature without the aid of an external compound (Figure 9) and were completely dissolved at 80 °C after 3 days (Figure 9 B) in contrast with the results reported by Ruiz *et al.*<sup>7</sup> for an epoxy/disulfide amine thermoset.

The authors showed that the obtained thermosets were not degraded in 1 N NaOH solution. To completely dissolve the epoxy thermoset, 2-mercaptoethanol as catalyst in DMF organic solvent needed to be added. This observation reflects that the degradation of epoxy resin depends not only on the dissociative nature of the disulfide bonds in alkaline conditions<sup>17,43</sup> but also on the stability of ester linkages from ELO triglycerides<sup>47,48</sup> and that of new ester

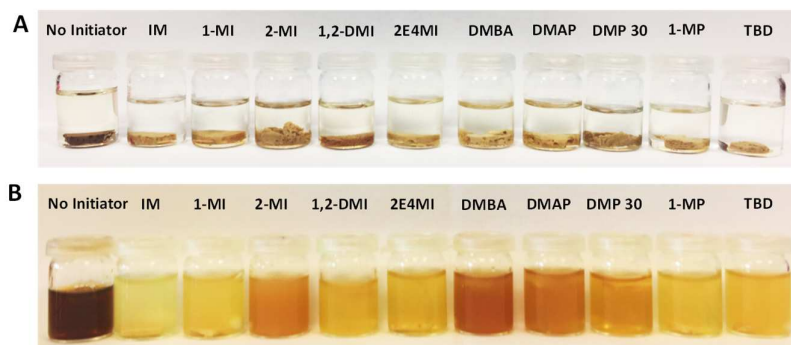


**Figure 9.** (A): Solvent stability of the ELO/DTBA thermosets in toluene after 3 weeks. (B): Auto-degradation in 1N NaOH solution at 80 °C after 3 days

linkages formed during copolymerization. It should be noticed that the decrease in the cross-link density can facilitate complete degradation of thermosets. By lowering the distance between cross-links within the networks, the solvent permeation increases and thus facilitates the polymer–solvent interactions.

## 2.3 Conclusions

In this study, the ELO/DTBA copolymerization reaction was studied in the presence of a series of 10 initiators. Their effects on the copolymerization reaction, network properties, and reprocessing were analyzed. The initiator nature impact on the curing mechanism is further reflected in the final properties. The thermosets obtained without initiator have low crosslinking density, low  $T_g$ , and thermal stability as consequence of a lower functional group conversion. Some initiators failed, such as 1-MP or DMBA, since they produce low copolymerization conversions. For the imidazole series, 2-MI is the least performing on the conversion percentage, producing thermosets that after reprocessing had decreased properties. In the series of heterocyclic initiators, the DMAP allows obtaining materials with excellent properties: one of the highest crosslink densities at the end of the recycling. Analysis of the materials performance confirms that IM conducts to thermosets with the highest values of conversion percentage, cross-link density, solvent resistance, and thermal stability. These results demonstrate that imidazole is the best initiator for the ELO/DTBA system. The thermal stability and mechanical properties underlined that all of the thermosets



## Chapter 2

can be reprocessed. The materials' properties were kept until the 10<sup>th</sup> cycle, which is very important considering a further application of these materials. Another important result is the ability of the prepared thermosets to be easily chemically recycled, in suitable solvents, without the need of supplementary chemicals. The biobased thermosets developed in this manuscript can have sustainable applications as matrices in reprocessable composites.

## Acknowledgments

This work was supported by the ECOXY project. ECOXY is a project funded by the European Commission. This project received funding from the Bio Based Industries Joint Undertaking under the European Union's Horizon 2020 research and innovation program (Grant agreement no. 744311).

## References

1. Liu, T.; Hao, C.; Wang, L.; Li, Y.; Liu, W.; Xin, J.; Zhang, J. Eugenol-Derived Biobased Epoxy: Shape Memory, Repairing, and Recyclability. *Macromolecules* **2017**, *50* (21), 8588–8597.
2. Yu, K.; Taynton, P.; Zhang, W.; Dunn, M. L.; Qi, H. J. Reprocessing and recycling of thermosetting polymers based on bond exchange reactions. *RSC Adv.* **2014**, *4* (20), 10108–10117.
3. Baruah, R.; Kumar, A.; Ujjwal, R. R.; Kedia, S.; Ranjan, A.; Ojha, U. Recyclable Thermosets Based on Dynamic Amidation and Aza-Michael Addition Chemistry. *Macromolecules* **2016**, *49* (20), 7814–7824.
4. Lu, L.; Pan, J.; Li, G. Recyclable high-performance epoxy based on transesterification reaction. *J. Mater. Chem. A* **2017**, *5* (40), 21505–21513.
5. Azcune, I.; Odriozola, I. Aromatic disulfide crosslinks in polymer systems: Self-healing, reprocessability, recyclability and more. *Eur. Polym. J.* **2016**, *84*, 147–160.
6. Cicala, G.; Pergolizzi, E.; Piscopo, F.; Carbone, D.; Recca, G. Hybrid composites manufactured by resin infusion with a fully recyclable bioepoxy resin. *Composites, Part B* **2018**, *132*, 69–76.
7. Ruiz de Luzuriaga, A.; Martin, R.; Markaide, N.; Rekondo, A.; Cabañero, G.; Rodríguez, J.; Odriozola, I. Epoxy resin with exchangeable disulfide crosslinks to obtain reprocessable, repairable and recyclable fiber-reinforced thermoset composites. *Mater. Horiz.* **2016**, *3* (3), 241–247.
8. Cicala, G.; Mannino, S.; La Rosa, A. D.; Banatao, D. R.; Pastine, S. J.; Kosinski, S. T.; Scarpa, F. Hybrid biobased recyclable epoxy composites for mass production. *Polym. Compos.* **2018**, *39* (S4), E2217–E2225.
9. La Rosa, A. D.; Blanco, I.; Banatao, D. R.; Pastine, S. J.; Björklund, A.; Cicala, G. Innovative Chemical Process for Recycling Thermosets Cured with Recyclamines® by Converting Bio-Epoxy Composites in Reusable Thermoplastic-An LCA Study. *Materials* **2018**, *11* (3), 353.
10. Rowan, S. J.; Cantrill, S. J.; Cousins, G. R. L.; Sanders, J. K. M.; Stoddart, J. F. Dynamic Covalent Chemistry. *Angew. Chem., Int. Ed.* **2002**, *41* (6), 898–952.
11. Fan, M.; Liu, J.; Li, X.; Zhang, J.; Cheng, J. Recyclable Diels-Alder Furan/Maleimide Polymer Networks with Shape Memory Effect. *Ind. Eng. Chem. Res.* **2014**, *53* (42), 16156–16163.
12. Roy, N.; Bruchmann, B.; Lehn, J.-M. DYNAMERS: dynamic polymers as self-healing materials. *Chem. Soc. Rev.* **2015**, *44* (11), 3786–3807.
13. Bowman, C. N.; Kloxin, C. J. Covalent Adaptable Networks: Reversible Bond Structures Incorporated in Polymer Networks. *Angew. Chem., Int. Ed.* **2012**, *51* (18), 4272–4274.
14. Capelot, M.; Unterlass, M. M.; Tournilhac, F.; Leibler, L. Catalytic Control of the Vitrimers Glass Transition. *ACS Macro Lett.* **2012**, *1* (7), 789–792.
15. Chen, M.; Zhou, L.; Wu, Y.; Zhao, X.; Zhang, Y. Rapid Stress Relaxation and Moderate Temperature of Malleability Enabled by the Synergy of Disulfide Metathesis and Carboxylate Transesterification in Epoxy Vitrimers. *ACS Macro Lett.* **2019**, *8* (3), 255–260.

16. Imbernon, L.; Oikonomou, E. K.; Norvez, S.; Leibler, L. Chemically crosslinked yet reprocessable epoxidized natural rubber via thermo-activated disulfide rearrangements. *Polym. Chem.* **2015**, 6 (23), 4271–4278.
17. Lei, Z. Q.; Xiang, H. P.; Yuan, Y. J.; Rong, M. Z.; Zhang, M. Q. Room-Temperature Self-Healable and Remoldable Cross-linked Polymer Based on the Dynamic Exchange of Disulfide Bonds. *Chem. Mater.* **2014**, 26 (6), 2038–2046.
18. Kumar, S.; Samal, S. K.; Mohanty, S.; Nayak, S. K. Recent Development of Biobased Epoxy Resins: A Review. *Polym.-Plast. Technol. Eng.* **2018**, 57 (3), 133–155.
19. Nouailhas, H.; Aouf, C.; Le Guerneve, C.; Caillol, S.; Boutevin, B.; Fulcrand, H. Synthesis and Properties of Biobased Epoxy Resins. Part 1. Glycidylation of Flavonoids by Epichlorohydrin. *J. Polym. Sci., Part A: Polym. Chem.* **2011**, 49, 2261–2270.
20. Ramon, E.; Sguazzo, C.; Moreira, P. M. G. P. A Review of Recent Research on Bio-Based Epoxy Systems for Engineering Applications and Potentialities in the Aviation Sector. *Aerospace.* **2018**, 5 (4), 110.
21. Mustapha, R.; Rahmat, A. R.; Abdul Majid, R.; Mustapha, S. N. H. Vegetable oil-based epoxy resins and their composites with biobased hardener: a short review. *Polym. Plast. Technol. Mater.* **2019**, 58 (12), 1311–1326.
22. Rubin, B. S. Bisphenol A: An endocrine disruptor with widespread exposure and multiple effects. *J. Steroid Biochem. Mol. Biol.* **2011**, 127 (1), 27–34.
23. U.S. Environmental Protection Agency; <https://www.epa.gov/assessing-and-managing-chemicals-under-tsca/bisphenol-bpsummary>, **2010**.
24. Almeida, S.; Raposo, A.; Almeida-González, M.; Carrascosa, C. Bisphenol A: Food Exposure and Impact on Human Health. *Compr. Rev. Food Sci. Food Saf.* **2018**, 17 (6), 1503–1517.
25. Andjelkovic, D.; Valverde, M.; Henna, P.; Li, F. C.; Larock, R. Novel thermosets prepared by cationic copolymerization of various vegetable oils - Synthesis and their structure-property relationships. *Polymer* **2005**, 46, 9674–9685.
26. Hondred, P. R.; Salat, L.; Mangler, J.; Kessler, M. R. Tung oilbased thermosetting polymers for self-healing applications. *J. Appl. Polym. Sci.* **2014**, 131 (12), 40406–40415.
27. Pin, J.-M.; Sbirrazzuoli, N.; Mija, A. From Epoxidized Linseed Oil to Bioresin: An Overall Approach of Epoxy/Anhydride Cross-Linking. *ChemSusChem* **2015**, 8 (7), 1232–1243.
28. Ricciardi, F.; Romanchick, W. A.; Joullié, M. M. Mechanism of imidazole catalysis in the curing of epoxy resins. *J. Polym. Sci., Polym. Chem. Ed.* **1983**, 21 (5), 1475–1490.
29. Heise, M. S.; Martin, G. C. Curing mechanism and thermal properties of epoxy-imidazole systems. *Macromolecules* **1989**, 22, 99–104.
30. Yang, S.; Zhang, Q.; Hu, Y.; Ding, G.; Wang, J. Synthesis of maleimide modified imidazole derivatives and their application in one-component epoxy resin systems. *Mater. Lett.* **2019**, 234, 379–383.
31. Liu, L.; Li, M. Curing mechanisms and kinetic analysis of DGEBA cured with a novel imidazole derivative curing agent using DSC techniques. *J. Appl. Polym. Sci.* **2010**, 117 (6), 3220–3227.
32. Ding, C.; Shuttleworth, P. S.; Makin, S.; Clark, J. H.; Matharu, A. S. New insights into the curing of epoxidized linseed oil with dicarboxylic acids. *Green Chem.* **2015**, 17 (7), 4000–4008.
33. Tran, T.-N.; Di Mauro, C.; Graillot, A.; Mija, A. Chemical reactivity and the influence of initiators on the epoxidized vegetable oil-dicarboxylic acid system. *Macromolecules* **2020**, 53 (7), 2526–2538.
34. Liu, Z.; Erhan, S. Ring-Opening Polymerization of Epoxidized Soybean Oil. *J. Am. Oil Chem. Soc.* **2010**, 87 (4), 437–444.
35. Mahendran, A. R.; Aust, N.; Wuzella, G.; Kandelbauer, A. Synthesis and Characterization of a Bio-Based Resin from Linseed Oil. *Macromol. Symp.* **2012**, 311 (1), 18–27.
36. Blank, W. J.; He, Z. A.; Picci, M. Catalysis of the epoxy-carboxyl reaction. *J. Coat. Technol.* **2002**, 74 (926), 33–41.
37. Jang, K.-S.; Eom, Y.-S.; Choi, K.-S.; Bae, H.-C. Crosslinkable Deoxidizing Hybrid Adhesive of Epoxy-Diacid for Electrical Interconnections in Semiconductor Packaging. *Polym. Int.* **2018**, 67 (9), 1241–1247.
38. Supanchaiyamat, N.; Shuttleworth, P. S.; Hunt, A. J.; Clark, J. H.; Matharu, A. S. Thermosetting resin based on epoxidised linseed oil and bio-derived crosslinker. *Green Chem.* **2012**, 14 (6), 1759–1765.
39. Schuchardt, U.; Sercheli, R.; Rogério Matheus, V. Transesterification of vegetable oils: A review. *J. Braz. Chem. Soc.* **1998**, 9 (3), 199–210.
40. Falco, G.; Sbirrazzuoli, N.; Mija, A. Biomass derived epoxy systems: From reactivity to final properties. *Mater. Today Commun.* **2019**, 21, 100683.

## Chapter 2

41. Altuna, F. I.; Espósito, L. H.; Ruseckaite, R. A.; Stefani, P. M. Thermal and mechanical properties of anhydride-cured epoxy resins with different contents of biobased epoxidized soybean oil. *J. Appl. Polym. Sci.* **2011**, 120 (2), 789–798.
42. Ooi, S. K.; Cook, W. D.; Simon, G. P.; Such, C. H. DSC studies of the curing mechanisms and kinetics of DGEBA using imidazole curing agents. *Polymer* **2000**, 41 (10), 3639–3649.
43. Ma, Z.; Wang, Y.; Zhu, J.; Yu, J.; Hu, Z. Bio-based epoxy vitrimers: Reprocessability, controllable shape memory, and degradability. *J. Polym. Sci., Part A: Polym. Chem.* **2017**, 55 (10), 1790–1799.
44. Gobin, M.; Loulergue, P.; Audic, J.-L.; Lemiègre, L. Synthesis and characterisation of bio-based polyester materials from vegetable oil and short to long chain dicarboxylic acids. *Ind. Crops Prod.* **2015**, 70, 213–220.
45. Mustata, F.; Tudorachi, N. Thermal behavior of epoxy resin cured with aromatic dicarboxylic acids. *J. Therm. Anal. Calorim.* **2016**, 125 (1), 97–110.
46. Zhang, H.; Cai, C.; Liu, W.; Li, D.; Zhang, J.; Zhao, N.; Xu, J. Recyclable Polydimethylsiloxane Network Crosslinked by Dynamic Transesterification Reaction. *Sci. Rep.* **2017**, 7 (1), 11833–11842.
47. Yang, G.; Rohde, B. J.; Robertson, M. L. Hydrolytic degradation and thermal properties of epoxy resins derived from soybean oil. *Green Mater.* **2013**, 1 (2), 125–134.
48. Shen, M.; Almallahi, R.; Rizvi, Z.; Gonzalez-Martinez, E.; Yang, G.; Robertson, M. L. Accelerated hydrolytic degradation of ester containing biobased epoxy resins. *Polym. Chem.* **2019**, 10 (23), 3217–3229.

## Electronic Supplementary Information (ESI)

### Experimental

#### Materials

The reagents structure and their physicochemical characteristics are summarized in Table ESI 1. The epoxidized linseed oil (ELO) was obtained by *Valtris Specialty Chemicals*. The hardener and all of the initiators were purchased from Sigma-Aldrich and used as received without further purification: DTBA (2,2'-dithiodibenzoic acid, 95%), IM (imidazole, 99%), 1-MI (1-methylimidazole, 99%), 2-MI (2-methylimidazole, 99%), 1,2-DMI (1,2-dimethylimidazole, 97%), 2E4MI (2-ethyl 4-methylimidazole, 95%), DMBA (N,N-dimethylbenzylamine, 99%), DMAP (dimethylaminopyridine, 99%), DMP30 (2,4,6-tris(dimethylaminomethyl) phenol, 95%), 1-MP (1-methylpiperazine, 99%), and TBD (1,5,7-triazabicyclo[4.4.0]dec-5-ene, 98%).

#### Samples Preparation

The curing formulations were prepared at a 1:1 ratio between epoxy and acid groups, according with Dusek *et al.*<sup>1</sup> First, the epoxy monomer was heated to around 80 °C to decrease the viscosity. Thereafter, the selected initiator was added at 1 wt.% and mixed until homogenization. At this point the mixture was introduced to the hardener. Each formulation was stirred at 80 °C for 10 min, placed into a silicone mold, and cured in an oven. The curing and post-curing protocols for preparation of the thermosets were determined based on a DSC study of the reactivity (Figure ESI 1), the protocol being displayed in Table ESI 2. According to this procedure, the samples for DMA analysis were prepared in special rectangular molds.

### Analytical Methods

#### Differential Scanning Calorimetry (DSC)

DSC measurements were carried out on a Mettler-Toledo DSC 3 apparatus controlled by STAR<sup>®</sup> Software developed by Mettler-Toledo. The instrument heat flow and temperature were calibrated in 3 points using water, indium, and zinc standards. Samples of 8–12 mg were placed into 40 µL aluminum crucibles. The DSC was used for study of the copolymerization reactivity and the glass transition of the obtained resins using a heating rate  $\beta$  of 10 °C·min<sup>-1</sup> over a temperature range from 0 to 220 °C for the copolymerizations and from – 80 to 180 °C for the  $T_g$  studies.

#### Fourier Transform Infrared Spectroscopy (FTIR)

The FT-IR spectra of the samples were recorded using a Thermo Scientific Nicolet iS50 FT-IR spectrometer with a deuterated L-alanine-doped triglycine sulfate (DLaTGS) detector in attenuated total reflectance (ATR) mode. The absorption bands were recorded in the range of 4000–525 cm<sup>-1</sup> with 32 scans and a resolution of 4 cm<sup>-1</sup>. The data were analyzed using OMNIC software. Conversion of functional groups at time (t) is denoted as percent and defined by Equation ESI 1:

$$\% = \frac{\left(\frac{A_{1586}}{\text{functional groups}}\right)_0 - \left(\frac{A_{1586}}{\text{functional groups}}\right)_t}{\left(\frac{A_{1586}}{\text{functional groups}}\right)_0} * 100 \quad (\text{ESI 1})$$

## Chapter 2

The area absorbance peaks were calculated and reported at the initial time ( $A_0$ ) and at different times ( $A_t$ ). The selected peak at about  $823\text{ cm}^{-1}$  corresponds to the oxirane C–O groups, that at  $895\text{ cm}^{-1}$  corresponds to carboxylic groups, while the peak at  $1586\text{ cm}^{-1}$  is the reference band belonging to the  $\delta_{\text{C=C}}$  of the aromatic signal.

### Thermogravimetric Analysis (TGA)

TGA measurements were carried out on a Mettler-Toledo TGA 2. The microbalance has a precision of  $\pm 0.1\text{ }\mu\text{g}$ . Samples of about  $10\text{ mg}$  were placed into  $70\text{ }\mu\text{L}$  alumina pans. To characterize the thermal stability of the thermosets, the samples were heated at  $10\text{ }^\circ\text{C}\cdot\text{min}^{-1}$  from  $25$  to  $1000\text{ }^\circ\text{C}$  under  $50\text{ mL}\cdot\text{min}^{-1}$  air flow.

### Dynamic Mechanical Analysis (DMA)

DMA analyses were performed using a Mettler-Toledo DMA 1 instrument equipped with STAR software. The analyzed samples had rectangular dimensions of  $30 \times 7 \times 2\text{ mm}^3$  (length  $\times$  width  $\times$  thickness). Each thermoset system was analyzed 3 times, and the values were averaged. The DMA was operated in the temperature-scanning mode with a constant displacement amplitude and frequency using the tension method for analysis of virgin and recycled materials. Elastic modulus values ( $E'$ ) and damping factor ( $\tan \delta$ ) were collected at a  $3\text{ }^\circ\text{C}\cdot\text{min}^{-1}$  heating rate from  $-80$  to  $170\text{ }^\circ\text{C}$  and  $1.0\text{ Hz}$  frequency. The glass transition value was assigned at the maximum of damping factor ( $\tan \delta = E''/E'$ ).

Cross-linking density was calculated by Equation ESI 2:

$$\nu = \frac{E'}{3RT} \quad (\text{ESI 2})$$

where  $E'$  is the storage modulus of the thermoset in the rubbery plateau region at  $T_g + 50\text{ }^\circ\text{C}$ ,  $R$  is the gas constant, and  $T$  is the absolute temperature in Kelvin. The obtained value was used to calculate the molecular weight ( $M_c$ ) of the segment chains between the crosslinks:

$$M_c = \frac{\delta}{\nu} \quad (\text{ESI 3})$$

where  $\delta$  is the density of the thermoset resin.

### Density Calculation

The sample densities were determined by measuring the volume of each sample and its weight obtained using a Mettler Toledo ML 3002T precision balance ( $\pm 0.0001\text{ g}$ ).

### Solvent Stability

The resin swelling test was performed in different solvents: methanol, acetone, and toluene. A piece of each material (virgin and reprocessed) was left in the selected solvents for 24 hours, and the weight was followed over the time. The swelling factor was calculated according to Equation ESI 4:

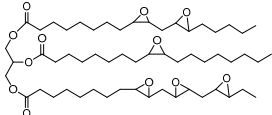
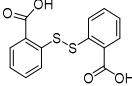
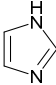
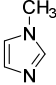
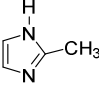
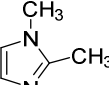
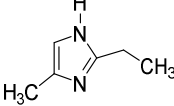
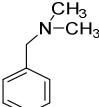
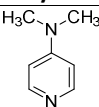
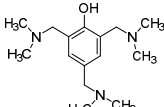
$$Q = \frac{m_s - m_u}{m_u} \quad (\text{ESI 4})$$

where  $m_s$  and  $m_u$  are the swollen and unswollen sample mass. The same procedure was applied for virgin and reprocessed materials. The materials solvent stability was also studied in stronger solvents as tetrahydrofuran, dimethyl sulfoxide,  $1\text{ N NaOH}$ , and  $1\text{ N HCl}$  for 3 days at  $80\text{ }^\circ\text{C}$ .

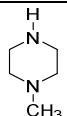
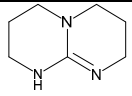
## Reprocessing Procedure

To test the mechanical reprocessing, the cross-linked thermosets were reduced in small pieces. Thereafter, the obtained grinded material was compressed between two Kapton films and reprocessed with the help of a CARVER manual heating press at temperatures in the range 150 – 170 °C under a pressure of ~ 60 bar.

**Table ESI 1.** Chemical structures and physico-chemical characteristics of selected reagents

Acronym	Structure and name	Molar mass [g/mol]	Melting temp. [°C]	pKa	Functionality
ELO	 <b>Epoxidized Linseed Oil</b>	980	-	-	Matrix 5,5 (5,6 meq/g)
DTBA	 <b>2,2'-Dithiobenzic acid</b>	306.35	287-290	-	Hardener 2
IM	 <b>Imidazole</b>	68.07	89-91	6.95	Initiator
1-MI	 <b>1-Methylimidazole</b>	82.10	-60	7.21	Initiator
2-MI	 <b>2-Methylimidazole</b>	82.10	145	7.85	Initiator
1,2-DMI	 <b>1,2 Dimethylimidazole</b>	96.13	37 - 39	8.21	Initiator
2E4MI	 <b>2-Ethyl 4-Methylimidazole</b>	110.16	47 - 54	8.68	Initiator
DMBA	 <b>N,N-Dimethylbenzylamine</b>	149.19	43 - 45	8.97	Initiator
DMAP	 <b>Dimethylaminopyridine</b>	122.17	108 - 110	9.2	Initiator
DMP30	 <b>2,4,6 Tris (dimethylaminomethyl)phenol</b>	265.39	< -20	8.41 9.12 9.75	Initiator

## Chapter 2

1-MP	 <b>1-Methylpiperazine</b>	100.16	-6	9.14	Initiator
TBD	 <b>1,5,7-Triazabicyclo[4.4.0]dec-5-ene</b>	139.20	125 - 130	14.5	Initiator

The epoxy/hardener formulation was optimized using an equimolar ratio between epoxide and acid, according to the Equation ESI 5:

$$R = \frac{\text{Epoxy group}}{\text{Acid group}} \quad (\text{ESI 5})$$

Where the acid group is monofunctional<sup>1</sup> and the epoxy group is also monofunctional in reaction with acids according with Dusek *et al.*<sup>1</sup>.

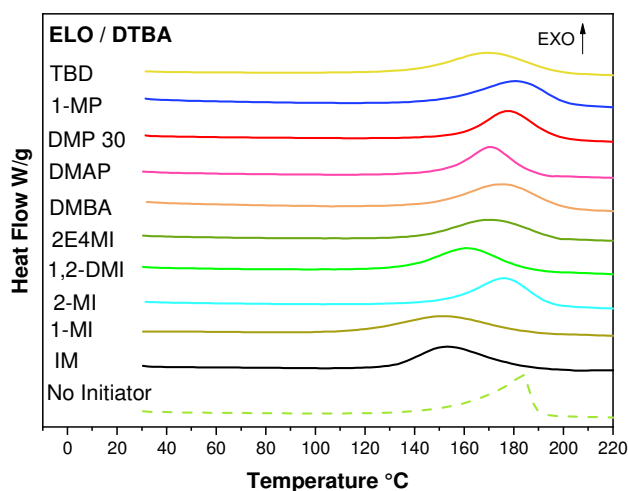


Figure ESI 1. Dynamic DSC scans of the reactions of ELO/DTBA with and without initiators

Table ESI 2. DSC results during ELO/DTBA curing: Enthalpy of reaction,  $T_{peak}$  and Reaction interval

ELO/DTBA	$\Delta H$ (J/g)	$T_{peak}$ (°C)	Reaction Interval	Curing	Post-curing
No Initiator	248	184	167 - 189	150 °C – 90 Min	180°C – 30 Min
IM	214	154	130 - 184	130°C – 60 Min	170°C – 30 Min
1-MI	206	152	117 - 184	120°C – 60 Min	170°C – 30 Min
2-MI	240	177	151 - 195	150°C – 60 Min	180°C – 30 Min
1,2-DMI	208	162	135 - 186	130°C – 60 Min	170°C – 30 Min
2E4MI	186	171	142 - 197	140°C – 60 Min	180°C – 30 Min
DMBA	260	176	145 - 200	140°C – 60 Min	180°C – 30 Min
DMAP	206	171	150 - 188	140°C – 60 Min	170°C – 30 Min
DMP30	220	178	158 - 197	150°C – 60 Min	180°C – 30 Min
1MP	244	181	152 - 202	150°C – 60 Min	180°C – 30 Min
TBD	189	170	141 - 198	140°C – 60 Min	180°C – 30 Min

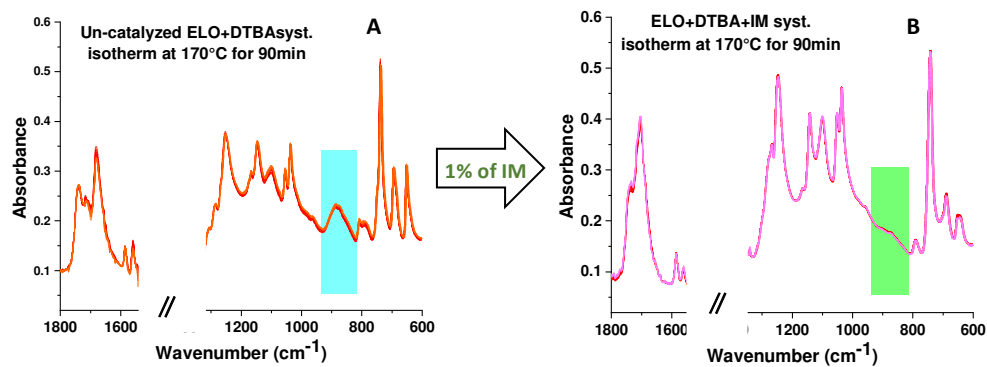


Figure ESI 2. Isothermal ATR-FTIR spectra, collected each 5 min during 90 min for the ELO/DTBA thermoset without initiator (A) and with 1wt.% of imidazole (B)

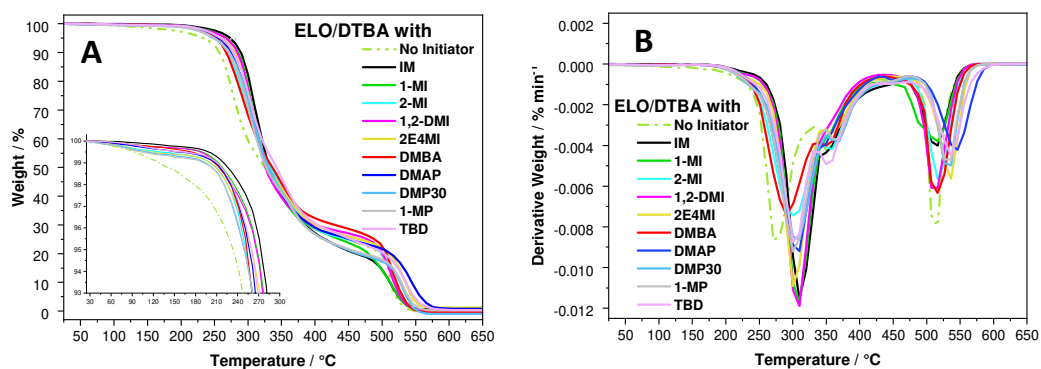


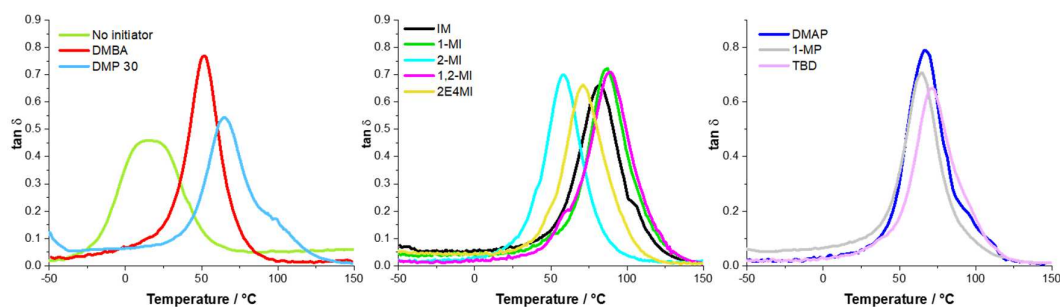
Figure ESI 3. TGA (A) and DTG (B) thermograms of ELO-DTBA curing mixtures

Table ESI 3. TGA results for ELO/DTBA curing mixtures

ELO/DTBA	$T_{5\%}$ (°C)	Residue 1 <sup>st</sup> (%)	1 <sup>st</sup> Degradation Peak (°C)	Final Residue (%)	2 <sup>nd</sup> Degradation Peak (°C)
No Initiator	230	25.2	271	0.39	510
IM	275	19.4	307	0.67	517
1MI	265	24.7	307	0.37	515
2MI	250	25.0	302	0.08	518
1,2DMI	265	27.8	307	0.39	512
2E4MI	260	25.4	302	1.22	535
DMBA	255	29.7	290	0.22	510
DMAP	245	22.2	305	0.77	540
DMP30	245	18.6	305	0.23	530
1MP	250	19.6	302	0.03	535
TBD	260	26.6	305	0.44	540



## Chapter 2



**Figure ESI 4.** DMA results:  $\tan \delta$  vs. temperature for ELO/DTBA thermosets prepared without and with initiators

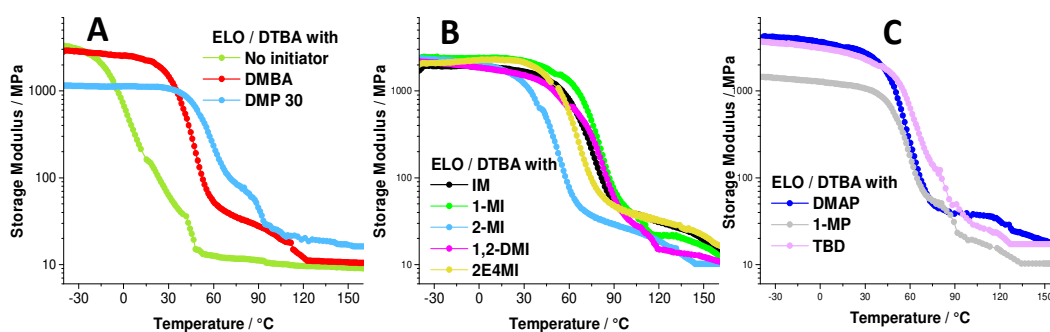


**Figure ESI 5.** DMA results: storage modulus vs. temperature for ELO/DTBA thermosets prepared without and with initiators

**Table ESI 4.** DMA data and networks properties for ELO/DTBA thermosets

	$\tan \delta$ (°C)	( $\tan \delta$ ) max	$E'$ at -50 °C (MPa)	$E'$ at 160°C (MPa)	Crosslinking density (mmol/cm <sup>3</sup> )	Density (g/cm <sup>3</sup> )	$M_c$ (g/mol)
<b>No Initiator</b>	15	0.45	3390	9.01	0.82	0.905	1104
<b>IM</b>	83	0.66	1560	15.7	1.25	1.025	820
<b>1-MI</b>	87	0.72	2030	11.2	1.03	0.988	876
<b>2-MI</b>	59	0.70	2100	6.1	1.14	0.788	691
<b>1,2-DMI</b>	89	0.71	1820	7.23	1.09	0.743	708
<b>2E4MI</b>	71	0.66	1900	15.6	1.84	0.935	508
<b>DMBA</b>	52	0.77	2660	7.2	0.98	0.896	914
<b>DMAP</b>	66	0.79	2380	8.2	1.18	0.913	774
<b>DMP30</b>	65	0.54	800	16.1	1.97	0.782	400
<b>1-MP</b>	65	0.70	1230	10.3	0.96	0.775	807
<b>TBD</b>	71	0.65	2560	17.17	1.62	0.837	517

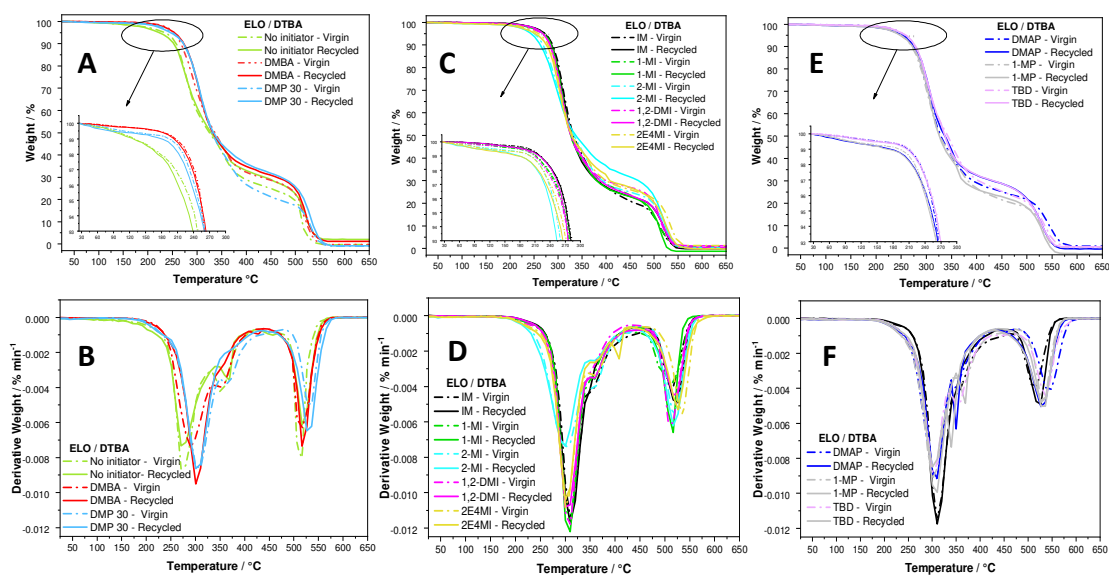


**Figure ESI 6.** TGA and DTG of the virgin and recycled thermosets: No initiator, DMBA and DMP30 (A and B), IM, 1-MI, 2-MI, 1,2-DMI and 2E4MI (C and D) and DMAP, 1-MP and TBD (E and F)

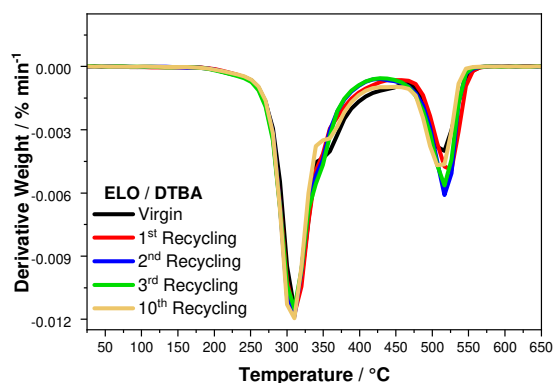


**Figure ESI 7.** DTG curves of the virgin and recycled ELO/DTBA/IM materials after several reprocessing steps

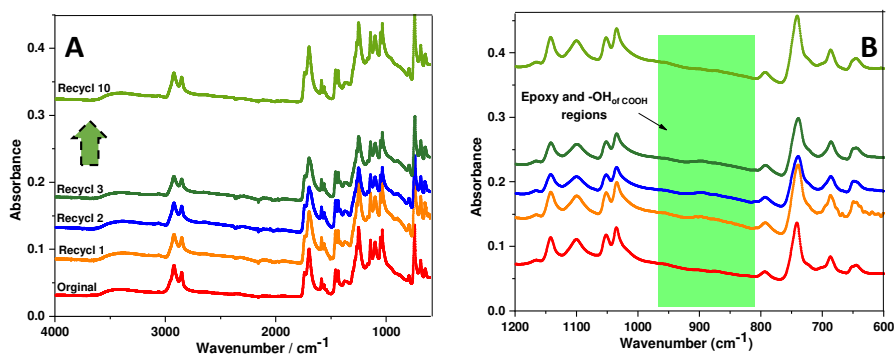


**Figure ESI 8.** ATR-FTIR spectra of the original and reprocessed thermosets (ten consecutive cycles were applied): (A): whole spectra from 4000-600  $\text{cm}^{-1}$ ; (B): zoom in the region of epoxy groups and -OH of carboxylic groups (DTBA) from 1200 to 600  $\text{cm}^{-1}$

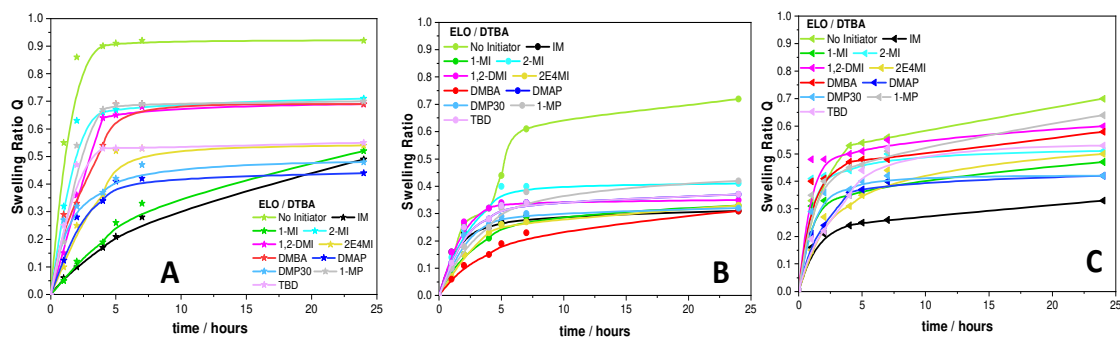


Figure ESI 9. Swelling ratio of the virgin ELO/DTBA thermosets prepared with and without initiator in Toluene (A), Methanol (B) and Acetone (C) for 24 hours

Table ESI 5. The reprocessing conditions (temperature and duration) performed at a pressure of 60 bars

	Temperature (°C)	Time (minutes)
<b>No Initiator</b>	170	10
<b>IM</b>	160	30
<b>1-MI</b>	150	20
<b>2-MI</b>	170	40
<b>1,2-DMI</b>	160	30
<b>2E4MI</b>	170	40
<b>DMBA</b>	170	30
<b>DMAP</b>	160	20
<b>DMP30</b>	170	30
<b>1-MP</b>	170	40
<b>TBD</b>	170	30

Table ESI 6. Properties of the virgin and recycled thermoset resins

		$T_g$ (°C) by DSC	$\tan \delta$ (°C)	Crosslink density (mmol/cm <sup>3</sup> )	$T_{5\%}$ (°C)
<b>No Initiator</b>	Virgin	13	15	0.82	230
	Recycled	12	13	0.30	220
<b>IM</b>	Virgin	76	83	1.25	275
	Recycled	74	97	0.81	275
<b>1-MI</b>	Virgin	74	87	1.03	265
	Recycled	72	95	0.38	265
<b>2-MI</b>	Virgin	46	59	1.14	250
	Recycled	42	63	0.34	250
<b>1,2-DMI</b>	Virgin	70	89	1.05	265
	Recycled	64	87	0.35	265
<b>2E4MI</b>	Virgin	64	71	1.84	260
	Recycled	59	77	0.38	252
<b>DMBA</b>	Virgin	37	52	0.98	255
	Recycled	36	58	0.21	252
<b>DMAP</b>	Virgin	55	66	1.18	255
	Recycled	50	63	0.79	245
<b>DMP30</b>	Virgin	65	65	1.97	245
	Recycled	56	69	0.58	245
<b>1-MP</b>	Virgin	64	65	0.96	250
	Recycled	57	73	0.23	245
<b>TBD</b>	Virgin	61	71	1.62	260
	Recycled	57	57	0.53	260

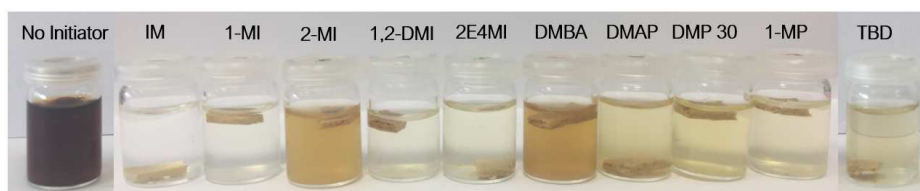


Figure ESI 10. Solvent test after 24 hours in 1N NaOH solution

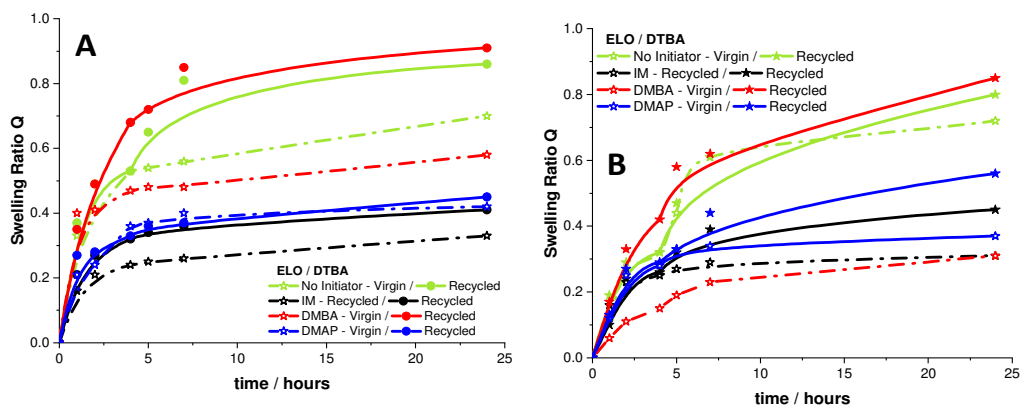


Figure ESI 11. Swelling test in Acetone (A) and Methanol (B) for the virgin and reprocessed thermoset resins

Table ESI 7. ELO/DTBA/IM thermoset resin after several reprocessing cycles

Virgin	1 <sup>st</sup> Recycling	2 <sup>nd</sup> Recycling	3 <sup>rd</sup> Recycling	10 <sup>th</sup> Recycling

- Matějka, L.; Pokorný, S.; Dušek, K. Acid curing of epoxy resins. A comparison between the polymerization of diepoxide-diacid and monoepoxide-cyclic anhydride systems. *Die Makromol. Chem.* **1985**, 186 (10), 2025–2036.

# Chapter 3

Building thermally and chemically reversible covalent bonds in vegetable oils-based epoxy thermosets.

Influence of epoxy-hardener ratio to promote recyclability



This chapter is based on Chiara Di Mauro, Aratz Genua , Alice Mija, Building thermally and chemically reversible covalent bonds in vegetable oils-based epoxy thermosets. Influence of epoxy-hardener ratio to promote recyclability. *Materials Advances*, 2020, 1 (6), 1788-1798.

DOI: 10.1039/D0MA00370K

### Abstract

Thermoset polymers with permanently cross-linked networks via thermally reversible covalent bonds have outstanding self-healing and adaptable properties, combined with very good mechanical properties and solvent resistance. This work reports in premiere the synthesis and characterization of such materials, derived from epoxidized linseed or soybean oils crosslinked with different ratios of 2, 2'- dithiodibenzoic acid. The epoxy/hardener ratio was studied as a key parameter influencing the overall process and moreover the networks recyclability. The synthesized thermosets showed excellent chemical recycling and mechanical reprocessing abilities. The elaborated networks were chemically recycled then the recuperated reprocessed material showed no or a small decrease in mechanical properties. These biobased thermosets open opportunities on the circular use of thermosets.

### 3.1 Introduction

The natural, biobased resources are opening myriad of possibilities offering in the last decade new ways for chemicals and materials development. For this reason, the development of polymers derived from vegetable oils are steadily increasing, by their low cost and lack of toxicity, in addition to the fact that they give access to processes minimizing the CO<sub>2</sub> emission, responsible for the global warming. To avoid continuous accumulation of materials in landfills we should find and propose solutions, as for example for the production of materials, especially thermosets, with recyclability properties.

Vegetable oils (VO) are an important family of renewable materials, mainly constituted by triglycerides formed between glycerol and fatty acids.<sup>1</sup> The most common vegetable oils contain fatty acid chains from 14 to 22 carbon atoms. Many scenarios of double bonds functionalization were proposed<sup>2</sup> and were much applied because allow mild conditions and green process as the oxidation of unsaturations producing epoxy derivatives.

Epoxidized vegetable oils (EVOs), mainly epoxidized linseed oil (ELO) and epoxidized soybean oil (ESO), are used in different applications as adhesives, additives in thermoplastics (to increase flexibility and stability), matrices for composite materials used in aerospace, structural, and sport applications.<sup>3-5</sup> ESO is known as plasticizer or stabilizer of thermoplastics such as poly(vinyl chloride).<sup>6</sup> The mechanical behaviour and chemical resistance of EVOs based thermosets are strongly dependent on the control of the crosslinking reactions, starting with the chemical aspects of the hardener until physical ones such the process parameters. There are scarce information regarding the EVOs curing with dicarboxylic acids.<sup>7-13</sup> However, an important aspect of epoxy / acid reaction is the formation of  $\beta$ -hydroxyesters that are responsible for the transesterification reactions, which allow the recyclability of the polymeric networks.<sup>14-15</sup> Another reaction favoring the network chains reorganization is the metathesis of disulfide covalent bonds by a dynamic exchange in the main or in side chains, usually triggered by external stimuli, such as pressure or temperature, known as disulfide exchange reaction.<sup>16-17</sup> Aromatic disulfide bridges are relatively often introduced into polymeric networks such as polyurethanes,<sup>18</sup> poly(urea-urethanes)<sup>19</sup> and epoxy resins.<sup>20</sup>

In this work we studied the influence of epoxy/hardener ratio as a key parameter influencing the reprocessing ability of the thermosets. Two kinds of EVOs were analysed and compared: ELO, ESO and their mixture (ELO+ESO). 2,2'-Dithiodibenzoic acid (DTBA) was used as dynamic hardener. Our team already studied, how the initiators influence the copolymerization of ELO/DTBA,<sup>13,21</sup> but to our knowledge, this study introduces for the first

time the chemical recyclability and the thermal reprocessing in function of the ratio of the thermoset systems. The epoxy/acid reactions were monitored via differential scanning calorimetry (DSC) and infrared spectroscopy (FT-IR) analyses. The obtained thermosets and the reprocessed resins were analysed and characterized by thermogravimetric analysis (TGA) and dynamic mechanical analysis (DMA). Finally, the swelling properties were exploited to chemical recycle the thermosets. By difference with Leibler *et al.*<sup>22</sup> that cured the ENR (Epoxidized Natural Rubber) with dithiodibutyric acid and performed the swelling in THF, we showed here the ability of the elaborated thermosets to swell until dissociation in THF. The obtained material was further filtered from THF, dried and was mechanically reprocessed and their properties compared with the virgin thermoset. The thermo-mechanical properties were evaluated to understand how the structural ratio between the comonomers influenced the chemical and mechanical recycling and moreover affected the materials performances.

## 3.2 Results and discussion

### 3.2.1 Influence of the EVO/DTBA ratio on the crosslinking by DSC investigation

To evaluate the effect of R ratio on the crosslinking reaction and also the effect of mixing ELO and ESO monomers on the reaction reactivity, the prepared formulations (displayed in Table ESI 2) were studied by dynamic DSC analyses.

The DSC thermograms obtained during the heating of elaborated formulations for curing are presented in Figure 1 and Figure ESI 1, where the exothermic events were associated to the crosslinking reactions. The formulation system in ratio R = 1 displays the highest reaction enthalpy (Table 1) in accord with Williams *et al.*<sup>14</sup> for ESO / citric acid (CA) curing, or with Leibler *et al.*<sup>15</sup> for DGEBA cured with a mixture of fatty dicarboxylic and tricarboxylic acids. Ma *et al.*<sup>23</sup> selected the equivalent ratio 1:1 for curing epoxidized sucrose soyate (ESS) with several natural acids: citric acid, D, L-malic acid, L-tartaric acid, malonic acid, oxalic acid, and glutaric acid.

ELO/DTBA-1 system is confirmed as the more reactive with reaction enthalpy of 197 J.g<sup>-1</sup>, followed by the system ELO/ESO/DTBA-1 with an enthalpy of 174 J.g<sup>-1</sup> while the formulation ESO/DTBA-1 gave a reaction enthalpy of 146 J.g<sup>-1</sup>. This result can be linked to the higher epoxy content in ELO, 5.61 meq.g<sup>-1</sup>, compared to ESO that has 4.66 meq.g<sup>-1</sup> of epoxy functions. This can explain why ELO/ESO blends show a higher reaction enthalpy compared to the ESO based system. The enthalpies and interval of reactions for ELO+ESO mixture display comparable trends with those of ELO based systems. Increasing the acids percentage in the curing



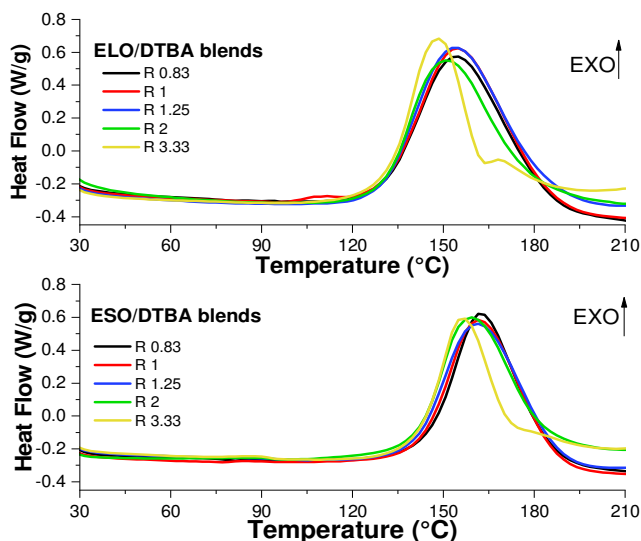


Figure 1. DSC thermograms of the curing process at  $10\text{ }^{\circ}\text{C}\cdot\text{min}^{-1}$  of ELO/DTBA (A) and ESO/DTBA (B) formulations

mixtures with ELO a decreasing of reaction enthalpy from  $197$  to  $184\text{ J}\cdot\text{g}^{-1}$  was measured (Table 1). Comparable results were obtained for ESO based systems, with enthalpies decrease from  $149$  to  $135\text{ J}\cdot\text{g}^{-1}$  while for ELO/ESO systems the reactions enthalpies vary from  $174$  to  $156\text{ J}\cdot\text{g}^{-1}$ . Matharu *et al.*<sup>8</sup> studied the excess of epoxy functionality (R of  $0.7$  for acid/epoxy groups) for the ELO crosslinked by different DCAs in presence DMAP.

Table 1. DSC results on the crosslinking reaction studies of selected systems

Formulations	Ratio e/a	$\Delta H$ (J/g)	$T_{\text{peak}}$ ( $^{\circ}\text{C}$ )	Reaction Interval
ELO/DTBA - 0.83	1:1.2	$182 \pm 3$	$151 \pm 1$	130 – 185
ELO/DTBA - 1	1:1	$197 \pm 3$	$151 \pm 1$	130 – 184
ELO/DTBA - 1.25	1:0.8	$184 \pm 3$	$151 \pm 1$	131 – 180
ELO/DTBA - 2	1:0.5	$158 \pm 3$	$148 \pm 1$	131 – 180
ELO/DTBA - 3.33	1:0.3	$125 \pm 3$	$146 \pm 1$	132 – 164
ESO/DTBA - 0.83	1:1.2	$139 \pm 3$	$160 \pm 1$	144 – 186
ESO/DTBA - 1	1:1	$149 \pm 3$	$159 \pm 1$	142 – 187
ESO/DTBA - 1.25	1:0.8	$146 \pm 3$	$158 \pm 1$	162 – 188
ESO/DTBA - 2	1:0.5	$135 \pm 3$	$156 \pm 1$	146 – 184
ESO/DTBA - 3.33	1:0.3	$106 \pm 3$	$154 \pm 1$	157 – 173
ELO/ESO/DTBA - 0.83	1:1.2	$156 \pm 3$	$159 \pm 1$	132 – 192
ELO/ESO/DTBA - 1	1:1	$174 \pm 3$	$155 \pm 1$	134 – 185

The authors reported the lowest reactivity when ELO was cured with aliphatic dicarboxylic acids with a high number of carbon atoms- $\text{C}_{36}$  ( $173\text{ J}\cdot\text{g}^{-1}$ ) and in contrast, an increasing of reaction enthalpy up to  $261\text{ J}\cdot\text{g}^{-1}$  in the presence of  $\alpha,\omega$ -DCA (from  $\text{C}_6$  to  $\text{C}_{18}$ ). From Figure 1 and Table 1, we can notice a reduction of reaction temperature interval for the systems in large excess of epoxy monomer in the mixtures. These results are in contrast with those of Zeng *et al.*<sup>9</sup> which reported for ESO/DCAs curing (adipic acid, sebacic acid and 1,2-dodecanedicarboxylic acid) an optimal ratio  $R = 0.7$ . The authors attributed the reaction enthalpy decreasing for  $R < 0.7$  to the insufficient amount of acids in the blend. In our systems, the decreasing of the reaction enthalpy for  $R < 1$  can be related to the fact that the systems are out of functional epoxy-acid copolymerization stoichiometry. For the systems with  $R > 2$

secondary reactions (homopolymerizations, etherifications) start to occur at high temperatures, as we can observe in the DSC thermograms by the presence of small exotherms at around 170, 180 °C in function of the system.

### 3.3.2 Influence of the epoxy/acid ratio analyzed by FT-IR studies

EVOs/DTBA mixtures and thermosets were prepared according with the protocol presented in the Experimental Section. Due to the insufficient hardener amount it wasn't possible to obtain cured thermosetting resins for the systems ESO/DTBA R = 2 and R = 3.33 and for ELO/DTBA R = 3.33. At the same time, due to the low epoxy content in ESO it was not possible to crosslink the ratio ESO/DTBA R = 2.

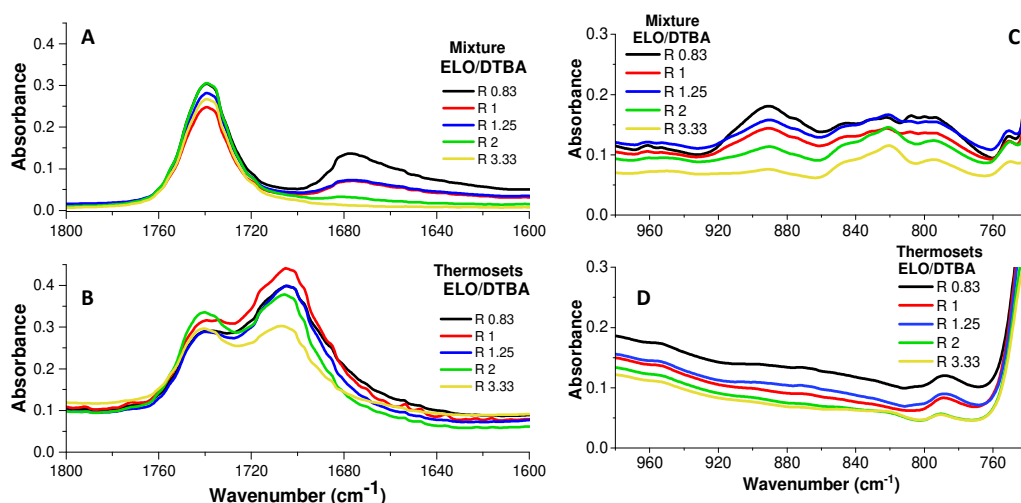


**Figure 2.** FTIR spectra for ELO/DTBA systems: ester + acid regions in the starting mixtures (A) and ester + new carbonyl regions in the cured resins (B); Epoxy 920–780  $\text{cm}^{-1}$  regions in the initial mixtures (C) in the final thermosets (D)

Figure 2 illustrates the FTIR spectra comparison of reactive mixtures and those of corresponding thermosets for ELO/DTBA systems at selected ratios. In Figure 2 A and B are presented the region from 1800 to 1600  $\text{cm}^{-1}$ . In this region, we can observe in Figure 2 A the presence of the references peaks, i.e. 1/ that of C=O from DTBA stretching at 1680  $\text{cm}^{-1}$ , peak that decreases continuously in intensity in the systems with excess of ELO, and 2/ that at 1740  $\text{cm}^{-1}$ , the stretching of the C=O of ELO triglyceride. As we can see in Figure 2 B, after the curing, the band at 1680  $\text{cm}^{-1}$  completely disappears while a new peak emerged at  $\sim 1700 \text{ cm}^{-1}$ , confirming the formation of ester by epoxy/acid polyaddition esterification reactions. From this figure we can notice that the intensity of this new ester peak is smaller in the systems with excess of epoxy. For the formulation R = 3.33 the two esters, of ELO triglyceride, and that of formed esters, have the same intensity. The characteristic absorption of the epoxy groups

## Chapter 3

can be observed in Figure 2 C, together with the homopolymerizations in the systems with excess of epoxy. Even if ELO/DTBA-3.33 system didn't conduct to a satisfactory hardening, the epoxy groups completely disappeared in the spectrum, indication that the ring opening reactions occurred via homopolymerization instead of copolymerization. This FTIR study highlights that the ratio  $R = 1$  is the optimal considering the higher copolymerization conversion percentage of epoxy, acid and ester functions, for all the studied systems (Table 2). From this study we can notice that an excess of epoxy functions conducts to a higher conversion than a system with excess of DTBA hardener. As example, for ELO/DTBA-1.25 system the conversion is around 96% versus 84% for ELO/DTBA-0.83. The copolymerization conversion decreases drastically from  $R = 1$  to  $R = 3.33$ , confirming that the secondary reactions took place in out of stoichiometry systems.

For ESO/DTBA (Figure ESI 3 A) and ELO/ESO/DTBA systems, the results show the same trend as the discussed systems with ELO.

*Table 2. Copolymerization conversion % for EVOs/DTBA systems*

Formulation	ELO/DTBA					ESO/DTBA					ESO/ELO/DTBA	
	Ratio	0.83	1	1.25	2	3.33	0.85	1	1.25	2	3.33	0.83
Conversion %	84	99	96	74	59	79	88	81	65	44	81	92

### 3.3.3 Thermo-mechanical analysis of virgin and recycled thermosets





The properties of the virgin and reprocessed materials were studied, in order to highlight firstly how the ratio  $R$  influences the recyclability and secondly to evaluate how the recycling affects the thermomechanical properties.

Table 3 and Table ESI 3 report the reprocessing conditions for the analysed systems. A fixed reprocessing temperature of 160 °C under 60 bars of pressure was applied to all the materials. Table 3 shows that for  $R > 1$  the reprocessing duration decreases, from 30 to 10 and 5 minutes, the recycled materials changing also its aspect, becoming more elastic and transparent aspect for  $R = 2$ . This result can be connected to the fact that the epoxy groups that are in excess promote homopolymerization and/or etherification, therefore the so created chains are more flexible compared to those formed by copolymerization with aromatic hardener. However, working in defect of hardener, the crosslinking density is low, therefore the chains have more freedom to rearrange. The elasticity and transparency diminish with the hardener percentage due to a higher crosslink density in copolymers network.

ESO recycled thermosets, in contrast with ELO resins, have higher elasticity also at  $R < 1$ , due to a lower epoxy content in ESO, guaranteeing high flexibility in the thermosetting resins and

consequently, in the reprocessed materials. Likewise, the mixture of ELO and ESO, produced rigid, hard or elastic materials following the behaviour of ELO based thermosets.

**Table 3.** Aspects of samples after reprocessing at 160 °C and 60 bars of ELO/DTBA thermosets. The durations of process are indicated

Ratio	0.83	1	1.25	2
ELO/DTBA M*- Reprocessed resins				
Time / min	30	30	10	5

### 3.3.3.1 Glass transition study

The virgin and reprocessed thermosets were analysed by DSC for the glass transition evaluation ( $T_g$ ), the results being displayed in Figure 3 A and summarized in Table 4. ELO/DTBA thermosets at different R ratios show the largest differences on  $T_g$  values, from 79 to 53 °C, *i. e.* from the system in excess of epoxy to that in excess of hardener. It's interesting to notice that both systems at ratios R = 1 and R = 1.25 are characterized by the same value of  $T_g$ , around 76 °C. Boquillon *et al.*<sup>24</sup> reported that the  $T_g$  values remain constant in the epoxy/acid ratio range from 1.66 to 1 in the thermoset resins of ELO cured with THPA (cis-1,2,3,6-tetrahydrophthalic anhydride) in presence of 2-methylimidazole. Wingard *et al.*<sup>25</sup> had analysed different ratios of DGEBA/methylene dianiline (MDA) and correlated the higher  $T_g$  value obtained in the case of stoichiometric ratio with a restricted molecular mobility in correlation with the highest degree of crosslinking. Galy *et al.*<sup>26</sup> by a thorough study of crosslinking of DGEBA with several diamines reported a decreasing of the  $T_g$  values in the systems with excess of epoxy, explained by the presence of unreacted epoxy functions as mobile pendant chain ends. As presented in Table 4, the ESO/DTBA thermosets are characterized by very close values of  $T_g$ , from 46 to 44 °C, for R = 0.83 and 1.25, respectively. The mixture of (ELO+ESO) systems have intermediate  $T_g$  values, ranging from 64 to 69 °C for ELO/ESO/DTBA in R = 0.83 and R = 1, respectively. Therefore, these thermosets are characterized by  $T_g$  closer to ELO based thermosets. After the mechanical reprocessing, a decreasing of the  $T_g$  with some degrees can be observed for ELO/DTBA off stoichiometry systems 0.83 and 2, more pronounced for the excess of hardener system. The other systems have a constant value of the  $T_g$  before and after the reprocessing.

**Table 4.** Glass transition values determined by DSC for virgin and reprocessed thermosets

	ELO/DTBA				ESO/DTBA			ESO/ELO/DTBA	
$T_g$ of Virgin	79	76	76	53	46	45	44	64	69
$T_g$ M*- Recycled	69	75	76	51	44	43	42	60	63

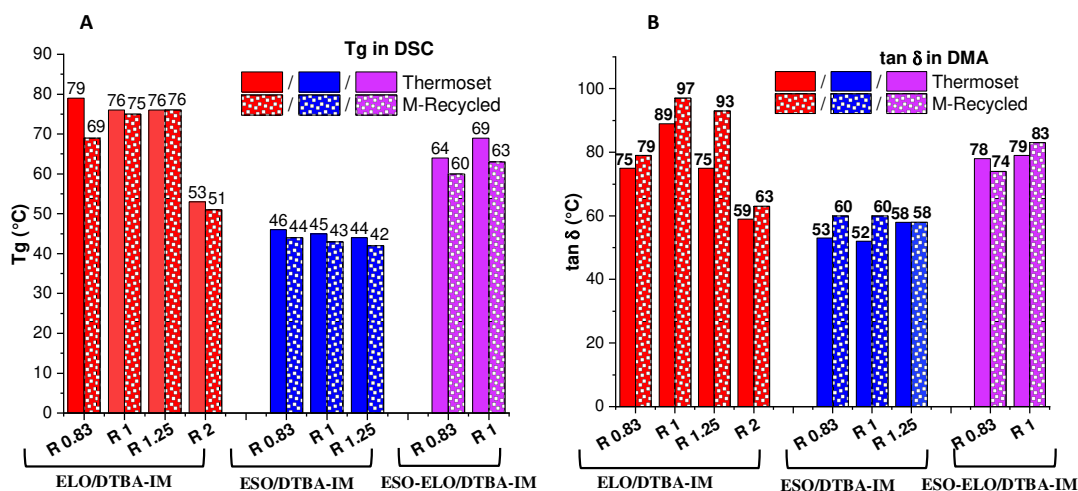


**Figure 3.** Comparison of virgin and mechanically reprocessed materials. Glass transition values evaluated by dynamic DSC analysis (A) and  $\tan \delta$  measured by DMA (B)

### 3.3.3.2 DMA analysis

In Figure 4 are illustrated the DMA results in form of  $\tan \delta = f(T)$  obtained during the thermomechanical analysis of virgin and reprocessed thermosets. Overall, for all the ratios, it is possible to observe that all materials, virgin or recycled, exhibit a single  $\tan \delta$  transition (Table 5, Table ESI 4 and ESI 5). Furthermore, we can constate also that these curves are symmetric. These results translate that the networks are structurally homogeneous, characterized by the same nature of the chains. This result is very important concerning the impact of the reprocessing on material structure and morphology. Moreover, the obtained  $\tan \delta$  values are in good correlation with that of  $T_g$  measured by DSC, with just small difference. As for example, the maximum value of  $\tan \delta$  was obtained for  $R = 1$  and not for 0.83 as for  $T_g$ s. The obtained results are in line with Boquillon *et al.*<sup>24</sup> that for  $R < 1$  observed a decreasing of the  $\tan \delta$ , this result being correlated with partly reacted hardener units that can freely move and increasing the interchain distance.

The mechanically reprocessed resins exhibit comparable  $\tan \delta$  trend as the virgin ones with a shift to higher damping factor transitions (Figure 4). This increasing of the  $\tan \delta$  amplitude observed in the reprocessed samples, is the proof of crosslinking density decrease. That means that during the reprocessing the chemical dynamic bonds rearranged in a different manner insight the network. However, the systems in excess of epoxy seem the less impacted by the reprocessing. Indeed, for ELO/DTBA-2 system, the  $(\tan \delta)_{\max}$  values before and after the recycling process are very close: 0.48 and 0.54.

Figure ESI 4 illustrates the dependence on the temperature of the storage modulus  $E'$ . The area above the  $\alpha$  relaxation and the value of the modulus in that area depend on many

factors, as the chemical structure, the ratio of the matrix components and the crosslink density of the network. The thermosets at  $R = 0.83$  exhibit the higher  $E'$  in the rubbery plateau. This result corroborates with that reported by Curtis *et al.*<sup>27</sup> for the epoxidized canola oil cured with phthalic anhydride (PA) thermoset in equimolar ratio and in excess of hardener. The authors explained that the higher  $E'$  modulus after the  $T_{gs}$  for the equimolar ratio can be associated with the presence of side chains able to move. An increase of hardener led to a greater cross-link density so fewer chains were available for relaxation and consequently the modulus was lower.

The calculations made by Equation 3 allowed to evaluate the crosslink densities of virgin and mechanically reprocessed materials, in the rubbery plateau. These results are summarized in Table 5 that displays the comparison of the crosslink densities for ELO/DTBA thermoset systems. The system with  $R = 1$  has the higher crosslink density, of around  $1.25 \text{ mmol.cm}^{-3}$ . This value decreasing in the system with excess of DTBA ( $R = 0.83$ ) at  $1.19 \text{ mmol.cm}^{-3}$ . For the systems in excess of epoxide,  $R = 1.25$  and  $2$ , the crosslink density decreases until  $0.61$  and  $0.28 \text{ mmol.cm}^{-3}$ . These results are in agreement with the data reported by Williams *et al.*<sup>14</sup> for DGEBA/citric acid thermosets which presents a sensible decrease of the crosslink density when the ratio  $R$  increases from 1 to 2.

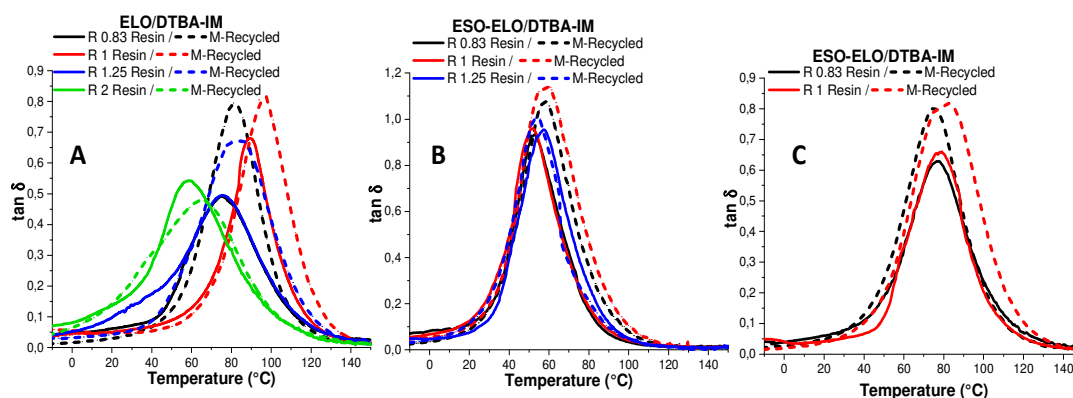


**Figure 4.** DMA results:  $\tan \delta$  vs. temperature analysis for virgin and recycled materials in function of composition: (A) ELO/DTBA, (B) ESO/DTBA (C) ELO-ESO/DTBA

Even if the  $E'$  values in the rubbery plateau are increased after the reprocessing, the crosslink density diminishes, excepting the system  $R = 2$  where the crosslink density augments after reprocessing from  $0.28$  to  $0.59 \text{ mmol.cm}^{-3}$ . In our previous work,<sup>21</sup> we explained that this increasing of the crosslink density can be attributed to the dual mechanism of networks internal rearrangement occurring during reprocessing. ESO/DTBA systems reveal similar trend as ELO based systems (Table ESI 4), with lower crosslink densities in systems with excess

## Chapter 3

of epoxide. But, ESO/DTBA R = 1 has the lowest network density compared with other ratios, while after reprocessing the value increases from 0.082 to 0.31 mmol.cm<sup>-3</sup>. Finally, the ELO/ESO/DTBA systems have intermediate properties (Table ESI 4), again the ELO/ESO/DTBA R=1 thermoset has the higher crosslinking and properties.

### 3.3.3.3 Thermal stability analysis

The thermal stabilities were tested to detect how the ratio R or the recycling process affect the materials stability. The TGA results obtained for ELO/DTBA systems are showed in Figure 5, displaying that the  $T_{5\%}$  values range from 271 °C for R = 0.83 to 291 °C for R = 2. The data concerning ESO/DTBA and those of ELO/ESO/DTBA systems are given in Figure ESI 5 and ESI

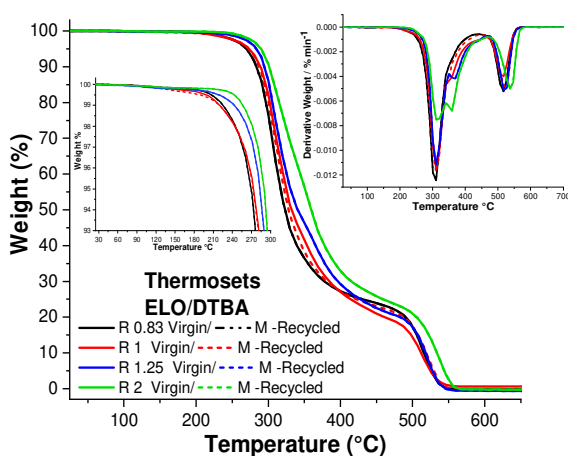


**Figure 5.** TGA, DTG and zoom in the region from 25 to 300 °C for ELO/DTBA systems during heating at 10 °C.min<sup>-1</sup> under air

6. The results show that the reprocessing didn't affect the thermal stability, with thermograms sometimes completely superposed between virgin and reprocessed materials (Figure 5, Table ESI 6). The lower thermal stability of the system in excess of DTBA can be associated to the degradation of the hardener ( $T_{5\%}$ , DTBA = 250 °C). In contrast, the systems with R > 1 have higher thermal stability, probably effect of the secondary reactions involving the excess of the epoxide, as the homopolymerization or etherification.

Comparable results were reported previously for ELO/diacid hardener (dipropylene glycol dimaleate) thermoset: the thermal stability ranged from  $T_{10\%}$  329 °C for R = 1.25 to 315 °C for R = 1.<sup>12</sup>

### 3.3.3.4 Chemical recycling and characterization of recycled materials

According to Leibler *et al.*<sup>15,22</sup> the vitrimers are crosslinked materials able to swell in adequate solvents, the swelling experiment giving information concerning the network. To study the swelling behaviour of virgin and recycled thermosets, all the selected ratios samples

were immersed in toluene at room temperature for 48 hours. Thereafter, the swelling ratio  $Q$  was calculated according with the Eq. ESI 4 and plotted in function of the time as illustrated in Figure 6 and Figure ESI 7. The systems at ratio  $R = 1$  given the lowest swelling together with

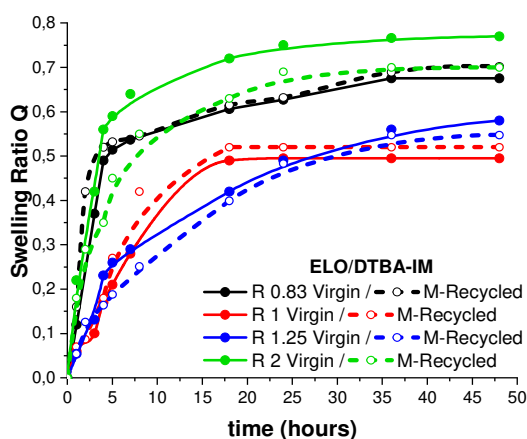


**Figure 6.** Swelling behaviour in toluene of the virgin and recycled ELO/DTBA thermosets

the ratio 1.25 that exhibits comparable behaviour. From all the virgin systems, that in large excess of epoxy,  $R = 2$ , shows the highest swelling, in good agreement with the previous results related to the lowest crosslinking density. A same trend can be observed for the system in excess of hardener,  $R = 0.83$ . Figure 6 shows that after 35 hours the swelling ratio reaches a plateau for most of the systems. The reprocessed resins show very similar swelling properties with the virgin ones.

Exception to this behaviour occurs in the systems with  $R > 1$  that exhibit lower swelling, in agreement with the increased crosslink densities and mechanical properties, compared to virgin samples, as evaluated by DMA analysis. For example, the reprocessed  $R = 2$  resin exhibits a decreasing of the swelling ratio compared with the virgin material, result corroborating with a three times higher crosslink density measured for the reprocessed material compared with the virgin one, as determined by DMA. Similar results were presented by Leibler *et al.*<sup>22</sup> for epoxidized natural rubber (ENR) cured by dithiodibutyric acid (DTDB), a disulphide diacid hardener.

According to vitrimers definition,<sup>15, 28</sup> the materials don't exhibit the loss in structural

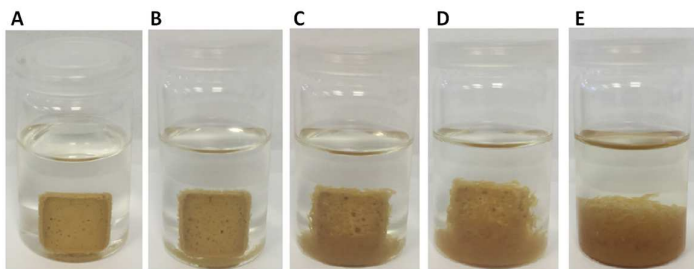


**Figure 7.** Evolution in time of ELO/DTBA  $R = 0.83$  thermoset immersed in THF at room temperature: initial time (A), 10 minutes (B), 20 minutes (C), 30 minutes (D) and 60 minutes (E)

integrity, even at elevated temperatures<sup>29</sup> in common solvents. For these reasons, we studied the solvent stability of prepared virgin samples in ethanol, methanol, acetone, water, DMF, DCM, DMSO and THF, at room temperature, for 48 hours. The solvent stability



tests are displayed in Figure ESI 8. All the thermosets exhibited good stability in ethanol, methanol, acetone and water. Swelling in toluene and dichloromethane was obtained for all the resins and a dissociative behaviour in THF, DMSO and DMF. At the end of the experiment in acetone, ESO/DTBA thermosets released a part into the solvent. Thereafter, the solid part was dried and the soluble percentage of resin determined (Table ESI 7).

In all cases, only a very small fraction ( $< 1\%$ ) of resin was released in the solvents, possible due to the unreacted molecules from out of stoichiometry systems. A different result was obtained in the experiments using the THF. Figure 7 shows the evolution of the immersed samples in THF. After 10 minutes the samples start to desegregate and after 60 minutes completely separated in small fragments. Therefore, these fragmented parts were dried in oven at  $80\text{ }^{\circ}\text{C}$  for 24 hours then weighted and analyzed. Table ESI 7 highlights that no mass loss occurred. At the end of the experiment the sample lost  $< 0.2\%$ .

To study the chemical stability of the thermosets in THF, the recuperated samples were dried and analysed in FTIR. Figure ESI 8 shows the FT-IR spectra of ELO/DTBA  $R = 0.83$  thermosets. By comparing the initial thermoset and that immersed in THF, in FTIR spectra no changes occurred, the spectra are identical. Moreover, the dried samples were mechanically reprocessed using the same protocol applied to the virgin thermosets ( $160\text{ }^{\circ}\text{C}$  and 60 bars) and surprisingly, the systems with  $R < 1$  required shorter time (10 minutes compared with 30 minutes) to reprocess satisfactory. Figure 8 shows the aspect of ELO/DTBA  $R = 0.83$  thermosets after the reprocessing and after chemical recycling in THF followed by reprocessing.

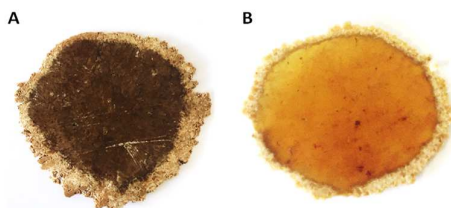


**Figure 8.** Aspect of ELO/DTBA  $R = 0.83$  thermosets after mechanical (M) (A) and chemical -mechanical (C-M) (B) recycling and reprocessing

The last one, associating the chemical-mechanical recycling (C-M), displays higher flexibility and transparency. This aspect was already observed after the reprocessing of the systems with  $R = 2$ , without chemical recycling in THF. The C-M recycled materials were studied by thermo-mechanical analysis to evaluate how the two combined recycling affected the materials properties and to compare them with that only mechanically reprocessed.

Figure 9 and Table ESI 8 report the results of TGA analysis of ELO/DTBA systems being mechanical and C-M recycled. The comparison of the obtained results shows that the systems with  $R \leq 1$  are the most affected by the C-M reprocessing with a decreasing of  $T_{5\%}$  from 273 to 250

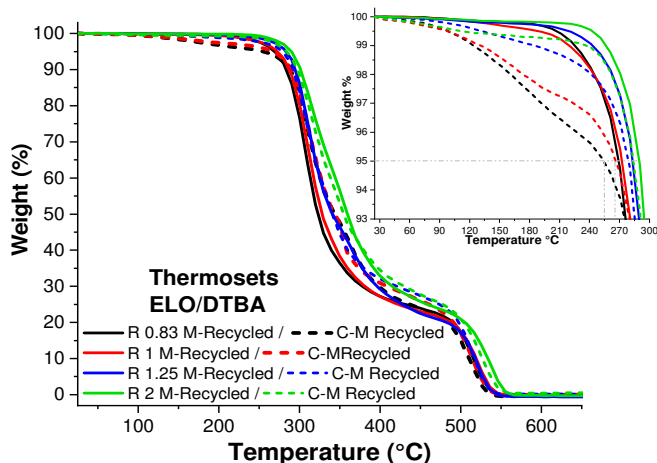


Figure 9. TGA and zoom of ELO/DTBA materials after the mechanical or C-M reprocessing

°C ( $R = 0.83$ ). For the other systems, the TGA results show that the  $T_{\text{onset}}$  decreased very few, all C-M reprocessed materials exhibiting similar thermal stability with the mechanical reprocessed materials.

In Figure 10 are illustrated the DMA results comparing ELO/DTBA virgin materials, those mechanical reprocessed (M) and those chemical-mechanical

reprocessed (C-M). The C-M reprocessed samples in  $R \leq 1$  exhibit a decreasing of the damping factor, compared with the mechanical reprocessed materials. Different behaviour can be observed for the systems with  $R > 1$ , comparable  $\tan \delta$  and peak amplitude can be observed. The ELO/DTBA  $R = 0.83$  material C-M reprocessed is the most affected, as displayed already by the TGA analysis, exhibiting a decreasing of the crosslink density from  $1.19 \text{ mmol.cm}^{-3}$  for the virgin thermoset to  $0.79 \text{ mmol.cm}^{-3}$ .

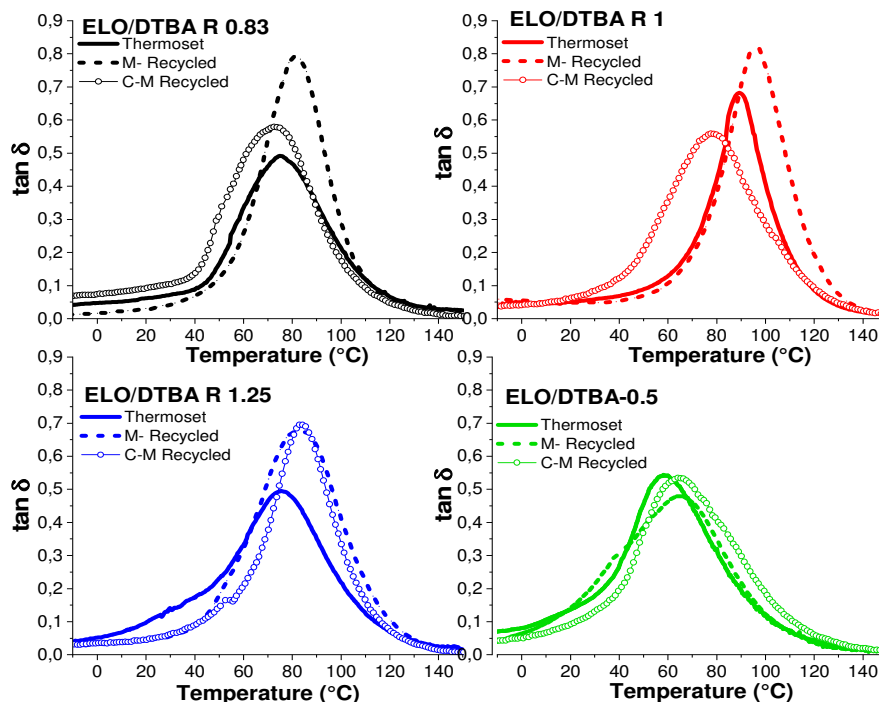


Figure 10. Comparison of  $\tan \delta$  vs. temperature curves for ELO/DTBA systems: virgin, M-reprocessed and C-M recycled and reprocessed materials

## Chapter 3

Anyhow, the combined C-M reprocessing seem to affect less the crosslink density, in comparison with single mechanical reprocessing where we have found for some systems an important decrease in network density. Moreover, some C-M reprocessed systems displayed even a higher modulus in the rubbery plateau (Figure ESI 9), exhibiting higher crosslink density. The ELO/DTBA R = 2 is the less impacted by the C-M recycling, showing almost the same crosslinking density after mechanical or C-M reprocessing.

**Table 1.** Thermomechanical properties of the virgin and reprocessed resins changing the ratio

ELO/DTBA		$\tan \delta$ (°C)	$(\tan \delta)_{\max}$	E'glassy plateau (MPa)	E'rubbery plateau (MPa)	Crosslink density (mmol.cm <sup>-3</sup> )
R = 0.83	V*	75	0.49	2000	4.48	1.19
	M-R*	79	0.77	2000	9.27	0.87
	C-M - R*	72	0.58	2000	8.37	0.79
R = 1	V*	89	0.68	1560	8.60	1.25
	M-R*	97	0.82	1720	8.90	0.81
	C-M - R*	78	0.56	1730	8.73	0.86
R = 1.25	V*	75	0.49	2800	4.42	0.61
	M-R*	93	0.60	1360	5.79	0.52
	C-M - R*	90	0.69	2240	10.59	0.99
R = 2	V*	59	0.54	1450	2.99	0.28
	M-R*	63	0.48	1900	6.54	0.59
	C-M - R*	65	0.53	2000	7.78	0.78

V\* virgin, M-R\* mechanical reprocessed, C-M\* chemical and mechanical recycled

### 3.3 Conclusions

Thermally and chemically reversible dynamic covalent networks were obtained by crosslinking ELO, ESO and (ELO+ESO) mixture of epoxidized vegetable oils with a disulfide-containing carboxylic diacids hardener. The dependence of the thermomechanical properties and the reprocessing ability and behaviour of elaborated thermosets from the ratio between epoxide monomer and aromatic diacid hardener was highlighted.

The FT-IR analysis confirmed that the higher copolymerization conversions were obtained for the systems in stoichiometric ratio. The thermomechanical analyses showed that the systems out of stoichiometry have lower values of  $\tan \delta$  and crosslink densities, in contrast with the thermal stability that increases with the lower crosslinker amount.

The synthesized thermosets showed excellent recycling and reprocessing abilities. The swelling abilities of these thermosets were studied before and after the reprocessing procedure showing that the reprocessed materials swell more than the virgin resins. Finally, due to the high swelling in THF until dissociation, the thermosets were chemically recycled, dried and reprocessed. The resulted materials were compared with those mechanical reprocessed, showing better properties when  $R < 1$ . Even if the stoichiometric ratio  $R = 1$

guarantee higher mechanical properties, the thermosets cured in defect of hardener showed better resistance and comparable reprocessing ability.

## Acknowledgments

This work was supported by ECOXY project funded by the Bio Based Industries Joint Undertaking under European Union Horizon 2020 research and innovation program (Grant agreement n° 744311).

## References

1. Karak, N., Vegetable oil-based polymers: properties, processing and applications. Cambridge, UK, Woodhead Publ. (Elsevier LTD); **2012**, 322 pp.
2. Petrović, Z., Polymers from biological oils. *Contemp Mater* **2010**, 1 (1), 39-50.
3. Gerbase, A. E.; Petzhold, C. L.; Costa, A. P. O., Dynamic mechanical and thermal behavior of epoxy resins based on soybean oil. *Journal of the American Oil Chemists' Society* **2002**, 79 (8), 797-802.
4. Altuna, F. I.; Espósito, L. H.; Ruseckaite, R. A.; Stefani, P. M., Thermal and mechanical properties of anhydride-cured epoxy resins with different contents of biobased epoxidized soybean oil. *Journal of Applied Polymer Science* **2011**, 120 (2), 789-798.
5. Shibata, M.; Teramoto, N.; Makino, K., Preparation and properties of biocomposites composed of epoxidized soybean oil, tannic acid, and microfibrillated cellulose. *Journal of Applied Polymer Science* **2011**, 120 (1), 273-278.
6. Benecke, H.P., Vijayendran, B.R., Elhard, J.D., **2004**. Plasticizers derived from vegetable oils. U.S. Patent 67 97753.
7. Jaillot, F.; Desroches, M.; Auvergne, R.; Boutevin, B.; Caillol, S., New biobased carboxylic acid hardeners for epoxy resins. *European Journal of Lipid Science and Technology* **2013**, 115 (6), 698-708.
8. Ding, C.; Shuttleworth, P. S.; Makin, S.; Clark, J. H.; Matharu, A. S., New insights into the curing of epoxidized linseed oil with dicarboxylic acids. *Green Chemistry* **2015**, 17 (7), 4000-4008.
9. Zeng, R.-T.; Wu, Y.; Li, Y.-D.; Wang, M.; Zeng, J.-B., Curing behavior of epoxidized soybean oil with biobased dicarboxylic acids. *Polymer Testing* **2017**, 57, 281-287.
10. Ma, S.; Kovash, C. S.; Webster, D. C., Effect of solvents on the curing and properties of fully bio-based thermosets for coatings. *Journal of Coatings Technology and Research* **2017**, 14 (2), 367-375.
11. Ding, C.; Tian, G.; Matharu, A., Adipic acid – glutaric anhydride – epoxidised linseed oil biobased thermosets with tunable properties. *Materials Today Communications* **2016**, 7, 51-58.
12. Falco, G.; Sbirrazzuoli, N.; Mija, A., Biomass derived epoxy systems: From reactivity to final properties. *Materials Today Communications* **2019**, 21, 100683.
13. Tran, T.-N.; Di Mauro, C.; Graillot, A.; Mija, A., Chemical Reactivity and the Influence of Initiators on the Epoxidized Vegetable Oil/Dicarboxylic Acid System. *Macromolecules* **2020**, 53 (7), 2526-2538.
14. Altuna, F. I.; Pettarin, V.; Williams, R. J. J., Self-healable polymer networks based on the cross-linking of epoxidised soybean oil by an aqueous citric acid solution. *Green Chemistry* **2013**, 15 (12), 3360-3366.
15. Montarnal, D.; Capelot, M.; Tournilhac, F.; Leibler, L., Silica-Like Malleable Materials from Permanent Organic Networks. *Science* **2011**, 334 (6058), 965.
16. Rekondo, A.; Martin, R.; Ruiz de Luzuriaga, A.; Cabañero, G.; J. Grande, H.; Odriozola, I., Catalyst-free room-temperature self-healing elastomers based on aromatic disulfide metathesis. *Materials Horizons* **2013**; Vol. 1, p 237.
17. Nevejans, S.; Ballard, N.; Miranda, J. I.; Reck, B.; Asua, J. M., The underlying mechanisms for self-healing of poly(disulfide)s. *Physical Chemistry Chemical Physics* **2016**, 18 (39), 27577-27583.
18. Jian, X.; Hu, Y.; Zhou, W.; Xiao, L., Self-healing polyurethane based on disulfide bond and hydrogen bond. **2017**; Vol. 29.

## Chapter 3

19. Martin, R.; Rekondo, A.; Ruiz de Luzuriaga, A.; Cabañero, G.; Grande, H. J.; Odriozola, I., The processability of a poly(urea-urethane) elastomer reversibly crosslinked with aromatic disulfide bridges. *Journal of Materials Chemistry A* **2014**, 2 (16), 5710-5715.
20. Ma, Z.; Wang, Y.; Zhu, J.; Yu, J.; Hu, Z., Bio-based epoxy vitrimers: Reprocessability, controllable shape memory, and degradability. *Journal of Polymer Science Part A: Polymer Chemistry* **2017**, 55 (10), 1790-1799.
21. Di Mauro, C.; Tran, T.-N.; Graillot, A.; Mija, A., Enhancing the Recyclability of a Vegetable Oil-Based Epoxy Thermoset through Initiator Influence. *ACS Sustainable Chemistry & Engineering* **2020**, 8 (20), 7690-7700.
22. Imbernon, L.; Oikonomou, E. K.; Norvez, S.; Leibler, L., Chemically crosslinked yet reprocessable epoxidized natural rubber via thermo-activated disulfide rearrangements. *Polymer Chemistry* **2015**, 6 (23), 4271-4278.
23. Ma, S.; Webster, D., Naturally Occurring Acids as Cross-Linkers To Yield VOC-Free, High-Performance, Fully Bio-Based, Degradable Thermosets. *Macromolecules* **2015**, 48, 7127-7137.
24. Boquillon, N.; Fringant, C., Polymer networks derived from curing of epoxidised linseed oil: influence of different catalysts and anhydride hardeners. *Polymer* **2000**, 41 (24), 8603-8613.
25. Wingard, C. D.; Beatty, C. L., Crosslinking of an epoxy with a mixed amine as a function of stoichiometry. II. Final properties via dynamic mechanical spectroscopy. *Journal of Applied Polymer Science* **1990**, 41 (11-12), 2539-2554.
26. Galy, J.; Sabra, A.; Pascault, J.-P., Characterization of epoxy thermosetting systems by differential scanning calorimetry. *Polymer Engineering & Science* **1986**, 26 (21), 1514-1523.
27. Omonov, T. S.; Curtis, J. M., Biobased epoxy resin from canola oil. *Journal of Applied Polymer Science* **2014**, 131 (8).
28. Jurowska, A.; Jurowski, K., Vitrimers - The miracle polymer materials combining the properties of glass and plastic? *CHEMIK nauka-technika-rynek* **2015**; Vol. 69, p 392-394.
29. Chen, M.; Zhou, L.; Wu, Y.; Zhao, X.; Zhang, Y., Rapid Stress Relaxation and Moderate Temperature of Malleability Enabled by the Synergy of Disulfide Metathesis and Carboxylate Transesterification in Epoxy Vitrimers. *ACS Macro Letters* **2019**, 8 (3), 255-260.

## Electronic Supplementary Information (ESI)

### Experimental Section

#### Materials

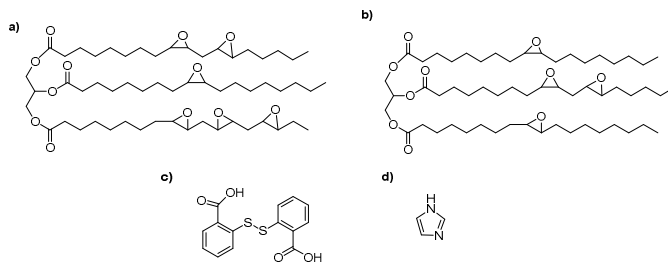


**Chart ESI 1.** Chemical structure of starting materials: ELO (a), ESO (b), DTBA (c), IM (d)

The structures of chemicals used in this study are illustrated in Chart ESI 1. The vegetable-based epoxy molecules, ELO (epoxidized linseed oil) (a), ESO (epoxidized soybean oil) (b) were obtained by Valtris Specialty Chemicals.

The hardener and initiator products are commercially available and used

as received without further purification. Were purchased from Sigma-Aldrich the 2,2'-dithiodibenzoic acid (DTBA) 95% (c) and the imidazole (IM) 99% (d). The reagents characteristics are summarized in Table ESI 1.

#### Samples preparation

To highlight the influence of epoxy/acid ratio (R) on recyclability, different formulations were prepared from ELO/DTBA; ESO/DTBA and (ELO+ESO)/DTBA. The epoxy/acid ratio, R, was considered in number of functional groups, so :

$$R = \frac{\text{epoxy groups}}{\text{acid groups}} \quad (\text{ESI 1})$$

where the acid and epoxy functions are considered both monofunctional in the reaction of epoxide versus acid.<sup>1</sup> Therefore, the following R ratios were studied: R = 0.83 (e/a = 1/1.2); 1 (e/a = 1/1); 1.25 (e/a = 1/0.8); 2 (e/a = 1/0.5) and 3.33 (e/a = 1/0.3). The initiator, imidazole, was used at optimal ratio of 1 wt.%, as previously determined.<sup>13</sup>

To prepare the reactive mixtures, the EVO was heated at 80 °C to decrease its viscosity and thereafter mixed with the initiator and the hardener. The obtained mixtures were placed into silicone moulds and cured in oven. The curing program was previously studied by DSC analyses of crosslinking reaction for each system. For all the systems, the curing was performed in temperatures range from 130 and 140 °C for 60 minutes, followed by a post-curing at 170 or 180 °C for 30 minutes for ELO and ESO resins, respectively. Two formulations were prepared by the combination of ELO and ESO. Starting from a molar mixture ELO/ESO of 2/1 the following epoxy/acid ratios were prepared R = 0.83 (e/a = 1/1.2) and 1 (e/a = 1/1). To prepare the thermosets we applied the same curing protocol as for ESO based systems (Table ESI 2).

#### Reprocessing protocol

For the mechanical recycling procedure, a piece of crosslinked thermoset was grounded. The obtained powder was compressed between two Kapton films in a CARVER heating press. The applied reprocessing conditions are reported in Table 2 and Table ESI 3.

### Analytical Methods

#### Differential Scanning Calorimetry (DSC)

DSC measurements were carried out on a Mettler-Toledo DSC 3 apparatus controlled by STAR<sup>®</sup> Software developed by Mettler-Toledo. The instrument heat flow and temperature were calibrated in 3 points using water, indium and zinc standards. Samples of 8 -12 mg were placed into 40  $\mu\text{L}$  aluminium crucibles. The DSC technique was used for the investigation of copolymerization reaction and for the identification of thermosets glass transition using a heating rate  $\beta$  of  $10\text{ }^\circ\text{C}\cdot\text{min}^{-1}$  over a temperature range from 25 to  $210\text{ }^\circ\text{C}$  for the copolymerization study and from  $-80$  to  $180\text{ }^\circ\text{C}$  for the  $T_g$  analysis.

#### Fourier-transformed infrared spectroscopy (FT-IR)

The FT-IR spectra of the samples were recorded using a Thermo Scientific Nicolet iS50 FT-IR spectrometer with a deuterated L-alanine doped triglycine sulfate (DLaTGS) detector in attenuated total reflectance (ATR) mode from  $500$  to  $4000\text{ cm}^{-1}$ , at a resolution of  $4\text{ cm}^{-1}$ . The decreasing of the epoxy and the acid intensities peaks were followed during the curing reactions, in order to evaluate their conversion. The obtained data were analysed using OMNIC software. The percentage of the copolymerization conversion, determined by this study, is defined by the Equation ESI 2:

$$\% = \frac{\left(\frac{A_{823}}{A_{1586}}\right)_0 - \left(\frac{A_{823}}{A_{1586}}\right)_t}{\left(\frac{A_{823}}{A_{1586}}\right)_0} * 100 \quad (\text{ESI } 2)$$

where the area of absorbance peaks was calculated considering the spectra of unreacted mixtures, at initial time ( $A_0$ ), and the spectra of crosslinked materials after the complete curing in oven ( $A_t$ ). The peak at  $823\text{ cm}^{-1}$  was followed, corresponding to the oxirane C-O groups. As reference band was used that at  $1586\text{ cm}^{-1}$ , belonging to the  $\delta_{\text{C-C}}$  of the aromatic signal from DTBA hardener.

#### Thermogravimetric Analysis (TGA)

TGA measurements were carried out on a Mettler-Toledo TGA 2. The microbalance has a precision of  $\pm 0.1\text{ }\mu\text{g}$ . Samples of about  $10\text{ mg}$  were placed into  $70\text{ }\mu\text{L}$  alumina pans. To characterize the thermal stability of the thermosets, the samples were heated at  $10\text{ }^\circ\text{C}\cdot\text{min}^{-1}$  from  $25$  to  $1000\text{ }^\circ\text{C}$  under  $50\text{ mL}\cdot\text{min}^{-1}$  air flow.

#### Dynamic Mechanical Analysis (DMA)

DMA were performed using a Mettler-Toledo DMA 1 instrument, equipped with STAR<sup>®</sup> software. The analysed samples had rectangular dimensions of  $30 \times 7 \times 2\text{ mm}^3$  (length x width x thickness). Each system was analysed 3 times and the values averaged. The DMA was operated in the temperature-scanning mode with a constant displacement amplitude and frequency using tension method for the analysis of virgin and recycled materials. Elastic modulus values ( $E'$ ) and damping factor ( $\tan \delta$ ) were collected at  $3\text{ }^\circ\text{C}\cdot\text{min}^{-1}$  heating rate from  $-20$  to  $150\text{ }^\circ\text{C}$  and  $1.0\text{ Hz}$  frequency. The glass transition temperature was assigned at the maximum of damping factor ( $\tan \delta = E''/E'$ ).

Crosslinking density was calculated by the Equation ESI 3:

$$\nu = \frac{E'}{3RT} \quad (\text{ESI } 3)$$

where  $E'$  is the storage modulus of the thermoset in the rubbery plateau region at  $T_g + 50$  °C,  $R$  is the gas constant and  $T$  is the absolute temperature in Kelvin.

### Solvent stability

Thermosets solvent stability was studied in ethanol, methanol, DMSO, acetone, toluene, water, DMF, DCM, THF and toluene for 48 hours at room temperature.

The toluene was selected as solvent for the swelling experiments. These experiments were performed for the virgin and reprocessed resins. The swelling ratio  $Q$  can be defined by Equation ESI 4:

$$Q = \frac{m_s - m_u}{m_u} \quad (\text{ESI 4})$$

here  $m_s$  and  $m_u$  are the swollen and unswollen mass of the sample, respectively. All the solvent tests were conducted on rectangular specimens of  $10 \times 10 \times 2$  mm<sup>3</sup> dimensions.

**Table ESI 1. Structures and characteristics of the selected reagents**

Acronym	Molecular weight [g.mol <sup>-1</sup> ]	Melting Point [°C]	Epoxy Content [meq.g <sup>-1</sup> ]
ELO	980	-	5,5
ESO	950	-	4,66
DTBA	306,35	287-290	/
IM	68,077	89 - 91	/

**Table ESI 2. Formulations composition of the curing systems**

Formulations	Ratio (e/a)	Epoxide (mol)	DTBA (mol)
ELO/DTBA-0.83	1:1.2	$2.5 \cdot 10^{-4}$	$8.4 \cdot 10^{-4}$
ELO/DTBA-1	1:1	$2.5 \cdot 10^{-4}$	$7 \cdot 10^{-4}$
ELO/DTBA- 1.25	1:0.8	$2.5 \cdot 10^{-4}$	$5.6 \cdot 10^{-4}$
ELO/DTBA- 2	1:0.5	$2.5 \cdot 10^{-4}$	$3.5 \cdot 10^{-4}$
ELO/DTBA-IM -3.33	1:0.3	$2.5 \cdot 10^{-4}$	$2.1 \cdot 10^{-4}$
ESO/ DTBA-IM -0.83	1:1.2	$2.6 \cdot 10^{-4}$	$6.9 \cdot 10^{-4}$
ESO/DTBA-IM -1	1:1	$2.6 \cdot 10^{-4}$	$5.8 \cdot 10^{-4}$
ESO/DTBA-IM-1.25	1:0.8	$2.6 \cdot 10^{-4}$	$4.6 \cdot 10^{-4}$
ESO/DTBA-IM-2	1:0.5	$2.6 \cdot 10^{-4}$	$2.9 \cdot 10^{-4}$
ESO/DTBA- IM-3.33	1:0.3	$2.6 \cdot 10^{-4}$	$1.7 \cdot 10^{-4}$
ESO/ELO/DTBA-IM-0.83	1:1.2	$7.7 \cdot 10^{-4}$	$2.4 \cdot 10^{-3}$
ESO/ELO/DTBA-IM-1	1:1	$7.7 \cdot 10^{-4}$	$2 \cdot 10^{-4}$

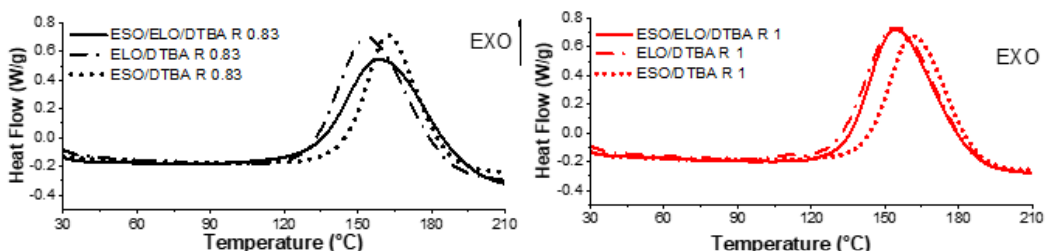


**Figure ESI 1. DSC thermograms during heating at 10 °C/min of the mixture ELO+ESO in comparison with the reference ELO and ESO, ratios 0.83 and 1**



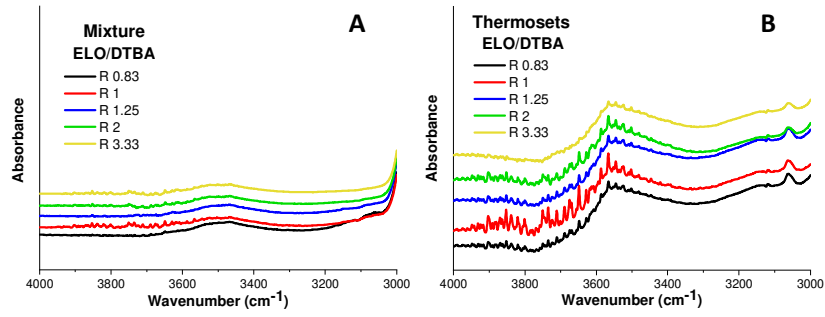


**Figure ESI 2.** FTIR spectra at -OH stretching regions ( $3700\text{--}3300\text{ cm}^{-1}$ ) for ELO/DTBA systems in function of the ratio at the beginning (A) and at the end of the curing (B)

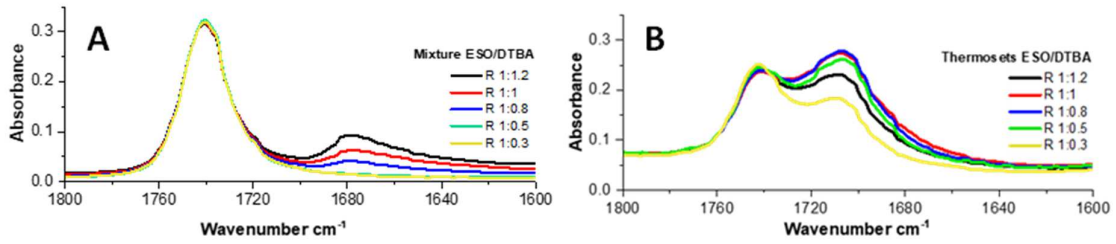


**Figure ESI 3.** FTIR spectra of ESO/DTBA systems at different ratios in ester-acid regions: the starting mixture (A) and the cured resins (B)

**Table ESI 3 .** Aspect and reprocessing duration at  $160\text{ }^{\circ}\text{C}$  and 60 bars for ESO/DTBA and ESO/ELO/DTBA resins

Ratio	0.83	1	1.25
<b>ESO/DTBA M-Reprocessed resins</b>			
Time / min	15	10	5
Ratio	0.83	1	
<b>ESO/ELO/DTBA M-Reprocessed resins</b>			
Time / min	15	10	

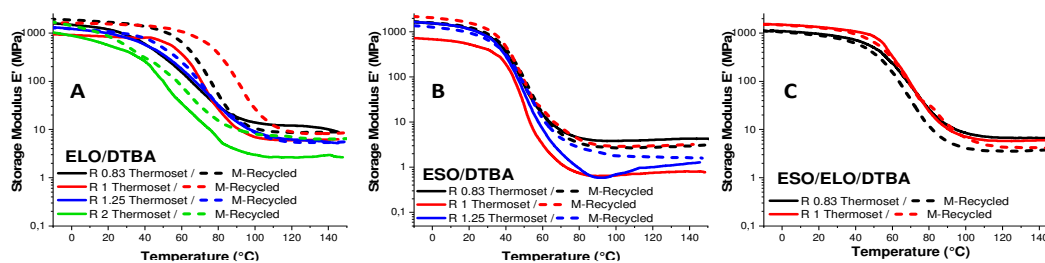


Figure ESI 4. Storage modulus  $E'$  vs. temperature for the virgin and mechanically reprocessed (M) thermosets

Table ESI 4. Thermomechanical properties of the virgin and reprocessed ESO/DTBA thermosets

Parameters	ESO/DTBA					
	Virgin/M-Recycled		V*	M-R*	V*	M-R*
Ratio	0.83		1		1.25	
$\tan \delta$	53	60	52	60	58	58
$\tan \delta_{\max}$	0.94	1.07	0.96	1.14	0.95	0.98
$E'_{\text{glassy state}}$ (MPa)	1900	1800	900	2330	2000	1450
$E'_{\text{rubbery state}}$ (MPa)	3.18	3.41	0.69	3.20	1.14	0.47
Crosslinking density (mmol/cm <sup>3</sup> )	0.41	0.28	0.082	0.31	0.12	0.18

Table ESI 5. Thermomechanical properties of the virgin and reprocessed ESO/ELO/DTBA thermosets

Parameters	ESO/ELO/DTBA			
	Virgin/M-Recycled		V*	M-R*
Ratio	0.83		1	
$\tan \delta$	78	74	79	83
$\tan \delta_{\max}$	0.56	0.82	0.66	0.82
$E'_{\text{glassy state}}$ (MPa)	1000	1170	1750	1580
$E'_{\text{rubbery state}}$ (MPa)	3.04	4.09	4.45	4.21
Crosslinking density (mmol/cm <sup>3</sup> )	0.45	0.36	0.58	0.42

Table ESI 2. TGA results for the resins and recycled materials during heating at 10 °C/min under air

EVOs/DTBA	Ratio		$T_{5\%}$ (°C)	1 <sup>st</sup> Residue (%)	1 <sup>st</sup> Degradation peak (°C)	2 <sup>nd</sup> Residue (%)	2 <sup>nd</sup> Degradation peak (°C)
ELO	0.83	V*	271	23.6	310	0.25	517
		M-R*	271	23.1	310	0.23	517
	1	V*	275	19.4	307	0.67	517
		M-R*	275	23.4	310	0.20	526
	1.25	V*	281	21.3	310	0.73	517
		M-R*	281	22.0	310	0.35	526
ESO	0.83	V*	271	19.9	310	0.29	526
		M-R*	271	18.4	310	0.99	517
	1	V*	271	18.4	310	0.42	526
		M-R*	271	19.9	310	0.53	517
	1.25	V*	281	24.1	310	0.22	507
		M-R*	281	24.1	310	0.46	517
ESO/ELO	0.83	V*	271	18.8	310	0.35	517
		M-R*	271	25.0	310	0.15	517
	1	V*	271	25.5	300	0.14	517
		M-R*	271	28.4	300	0.53	517

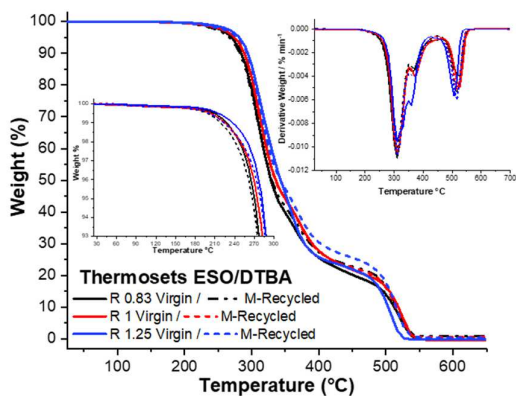


Figure ESI 5. TGA, DTG and zoom in the region from 25 to 300 °C for the systems ESO/DTBA (heating at 10 °C/min, under air)

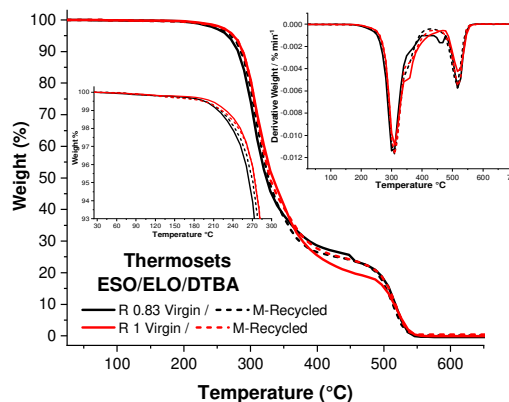


Figure ESI 6. TGA, DTG and zoom in the region from 25 to 300 °C for the systems ESO/ELO/DTBA (heating at 10 °C/min, under air)

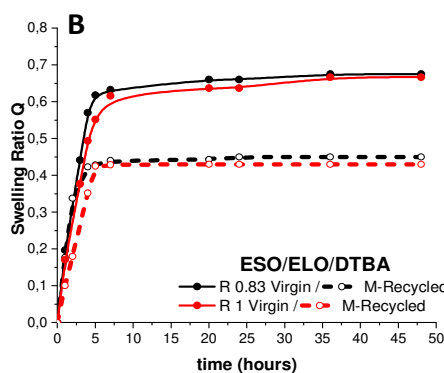
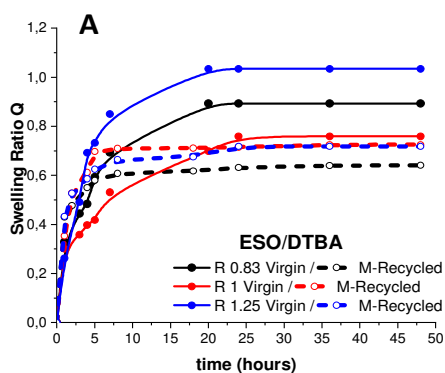
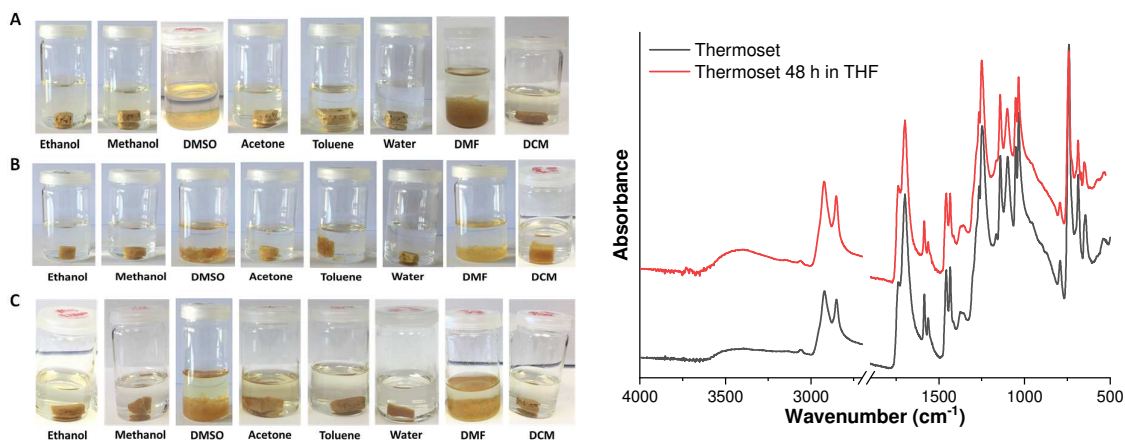


Figure ESI 7. Swelling ratio Q for the virgin and recycled ESO/DTBA (A) and ESO/ELO/DTBA (B) thermoset resins

Table ESI 7. Solvent solubility in acetone and THF after 48 hours

EVOs/DTBA	Ratio	Solubility % in acetone	Solubility % in THF
ELO/DTBA	0.83	0.70	0.095
	1	0.30	0.068
	1.25	0.15	0.057
	2	0.11	0.036
ESO/DTBA	0.83	0.87	0.12
	1	0.74	0.81
	1.25	0.55	0.055
ESO/ELO/DTBA	0.83	0.75	0.088
	1	0.51	0.064



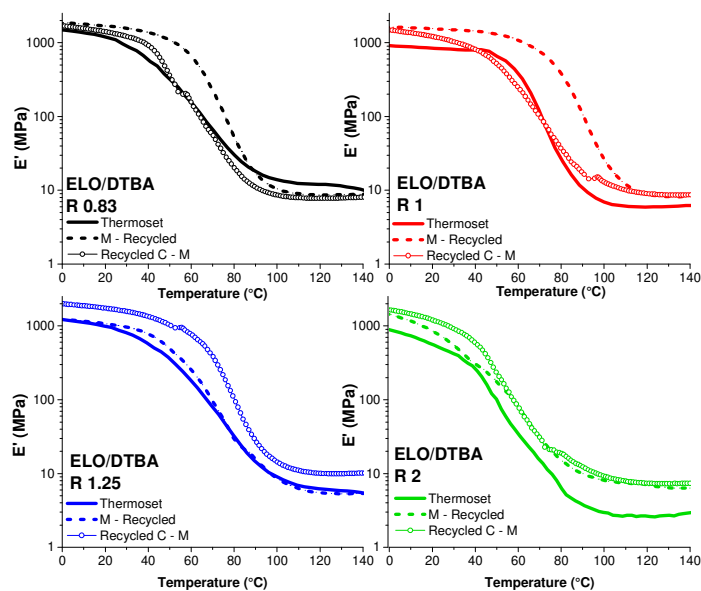
**Figure ESI 8.** Solvent stability test after 48 hours at room temperature for ELO/DTBA  $R = 0.83$  (A), ESO/DTBA  $R = 0.83$  (B) and ESO/ELO/DTBA  $R = 0.83$

**Figure ESI 9.** FT-IR of the crosslinked resin ELO/DTBA-IM  $R = 0.83$  before and after 48 hours in THF

**Table ESI 8.** TGA results for the ELO/DTBA recycled thermosets: mechanical (M) and chemical and mechanical recycling (C-M)

EVOs/DTBA	Ratio		$T_{5\%}$ (°C)	1 <sup>st</sup> Residue (%)	1 <sup>st</sup> Degradation peak (°C)	2 <sup>nd</sup> Residue (%)	2 <sup>nd</sup> Degradation peak (°C)
ELO	0.83	M-Recycled	271	23.1	310	0.23	517
		Recycled C-M	250	23.8	307	0.16	517
	1	M-Recycled	275	23.4	310	0.20	526
		Recycled C-M	265	28.3	308	0.13	513
	1.25	M-Recycled	281	22.0	310	0.35	526
		Recycled C-M	280	28.9	307	0.13	518
2	M-Recycled	291	27.9	310	0.20	526	
	Recycled C-M	290	20.9	310	0.09	520	

**Figure ESI 10.** Storage modulus  $E'$  vs. temperature curves for virgin resin ELO/DTBA compared with the resin recycled mechanically (M) and chemically-mechanically (C-M)

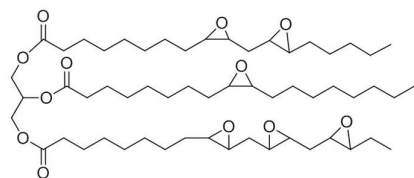


- Matějka, L.; Pokorný, S.; Dušek, K. Acid curing of epoxy resins. A comparison between the polymerization of diepoxide-diacid and monoepoxide-cyclic anhydride systems. *Die Makromol. Chem.* **1985**, 186 (10), 2025–2036.

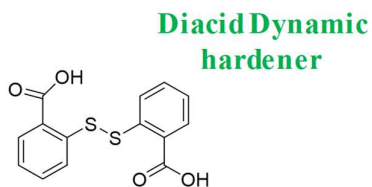
# Chapter 4

Sustainable access to bio-based epoxidized vegetable oil thermoset materials: from homopolymers to copolymers

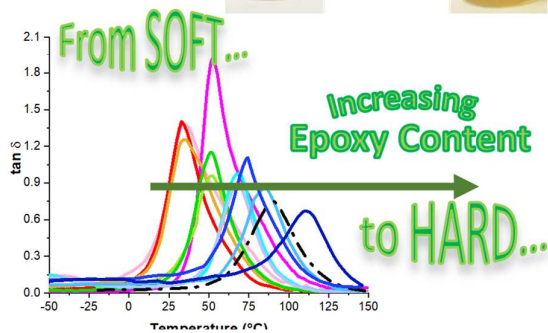
## Recyclable Bio-based Thermosets



Epoxidized Vegetable Oil



Diacid Dynamic hardener



This chapter is based on Malburet S., Di Mauro C., Noè C., Mazouane S., Mija A., Sangermano M. and Graillot A., Sustainable access to fully biobased epoxidized vegetable oil thermoset materials prepared by thermal or UV-cationic processes, 2020 (in peer review in *RSC Advanced*).

and

Di Mauro C., Malburet S., Genua A., Graillot A. and Mija A. Recyclable new epoxidized vegetable oils-based thermosets. *Biomacromolecules* 2020, 21 (9), 3923-3935.

DOI: 10.1021/acs.biomac.0c01059

## Abstract

This study focused in a first step on the conversion of mainly nonedible vegetable oils (VOs) into epoxy monomers, obtaining a series of EVOs with a range of epoxy index from 2.77 to 6.77 meq/g. The synthesized EVOs were used as starting monomers for (i) homopolymerization reaction, hardener-free thermo-curing and (ii) copolymerizations by reaction with a disulfide-based aromatic dicarboxylic acid (DCA) to produce thermoset materials with recyclability properties. Both processes enable the synthesis of bio-based EVOs thermoset materials whose reactivity, crosslinking density and final performances were proved to linearly increase with the EVOs epoxy content. The materials exhibited  $\tan \delta$  from -18 to 50 °C for the homopolymers and from 34 to 111 °C for the copolymers. The copolymers exhibited chemical recycling and high bio-based carbon content, from 58 to 79%, with potentially applications in coating or composite materials for automotive sector.

### 4.1 Introduction

Accumulation of plastic waste is becoming one of the major threats to our ecosystem. With a level of production around 140 million tons of synthetic polymers each year with less than 10% effectively recycled, the growing amount of plastic waste ending up in oceans or landfills raise several concerns. Developed countries, as the main consumers of energy, for a long time started planning and managing new renewable and alternative energy sources to solve the current problems related to air quality linked to ozone, carbon monoxide or particulate matters. The sustainable use of natural resources is one of the strategies to ensure the development of renewable materials and a sustainable economy. In the last decades, the use of biobased raw materials has led to the development of the green chemistry by integrating minor toxicity<sup>1</sup> and biodegradability,<sup>2-4</sup> offering a different scenario for coal as a basic feedstock.<sup>5</sup> However, most of these products still do not offer a competitive alternative compared with the products coming from the petrochemical industries. In the case of thermoset materials, this problematic is further duplicated since they cannot be recycled. Although relentless efforts are dedicated to reduce the use of petrobased resources, the ecological impact of thermosets at the end of the lifetime remains a crucial challenge that need to be addressed to limit the greenhouse emissions and the associated footprint. For this reason, important strategies are the replacing of petrobased raw materials and also the synthesis of recyclable, reusable and reshapable vitrimers-like thermoset materials based on reversible disulfide bond and carboxylate transesterification (vitrimers).<sup>6-8</sup>

Considering the growing amount of fibre-reinforced composite materials due to their outstanding properties in terms of light weight, high weight-to-strength ratio and long durability, next generation of biobased thermosetting resins need to be cost effective and based on non-depletable biobased resources. Within this scope, the vegetable oils' valorization through the synthesis of thermoset materials is supported by advantages like diversity, abundance and low price, promising to be a sustainable alternative for the chemical industry.<sup>9</sup>

Commonly, vegetable oils (VOs) are extracted from fruits or seeds by solvent extraction or by pressing process. More than 95% of the VOs are constitute of triglycerides,<sup>10</sup> containing three fatty acids branched to a glycerol unit. Nevertheless, VOs are a complex, variable and thus very interesting mixture. The diversity in VOs composition depends not only on the nature of the oil but also on geographical origin of the plants, maturity, species, as well as the method used for its extraction. As a matter of fact, length of main fatty acids is in a range of 4 to 28

carbons and unsaturated bonds or functional groups as hydroxyl (castor oil) or epoxy (vernolia oil) can be encountered alongside the alkyl chain.<sup>11</sup> According to the unsaturation degree of fatty acids, they can be generally classified into saturated, mono- and poly-unsaturated fatty acids, which may have different configurations, resulting in different physical and chemical properties. For instance, vegetable oils can be either liquid or waxy at room temperature. This property is mainly linked to 2 major criteria which can help to understand the composition of the oil. Firstly, the vegetable oil is certainly poor in unsaturated fatty acids which allow them to crystallize by self-organization, as in the case of coconut or palm oils for instance. Also, the fatty acids having long alkyl chain length will promote self-organization and crystallization. In fact, higher the melting point of the vegetable oil, higher is its content in saturated fatty acids with long alkyl chains. Finally, the unsaturation degree, also known as iodine value, has a major importance for the production of monomers and thermosetting resins. High iodine values indicate a high aptitude for functionalization and for polymerization.<sup>12</sup>

Usually, the industrial process to synthesize the commercial epoxy resins is based on epichlorohydrin as main reactant allowing to convert hydroxyl,<sup>13</sup> phenol<sup>14</sup> or acid<sup>15</sup> functions into epoxides. Vegetable oils have been used for long time as paints, lubricants,<sup>16</sup> and coatings but in the last decades, polymeric systems based on these raw materials have been developed using a variety of polymerization techniques.<sup>11</sup> One considerable advantage of the use of VOs as raw materials is their potential of double bonds functionalization, as for example into epoxies using oxidizing agents and thus avoiding the very hazardous epichlorohydrin, the usual reactant for diglycidyl ether of bisphenol A (DGEBA) synthesis.

Therefore, based on a big variety of VOs, we were able to develop and implement a robust, sustainable and harmless synthetic pathway giving access to fully biobased epoxidized vegetable oils exhibiting a wide range epoxy content from 2.77 to 6.77 meq.g<sup>-1</sup> and reaching an almost complete double bonds conversion with an epoxy selectivity above 94%. The details and the methodology implemented for new EVOs synthesis are reported elsewhere, using acetic acid, hydrogen peroxide and amberlite® IR-120 at 55 °C in toluene or cyclopentyl methyl ether (CMPE) as non-hazardous and green alternative solvents.<sup>17-18</sup> It has been then important to evaluate the potential of synthesized EVOs as precursors for thermoset materials and to highlight how the thermomechanical properties of the obtained materials can be influenced by their epoxy content. The latter is determined by the relative proportion of palmitic (saturated), stearic (saturated), oleic (mono-unsaturated), linoleic (di-unsaturated) and linolenic (tri-unsaturated) fatty acids in the composition of corresponding VOs (Table 1).



**Table 1.** Chemical composition of VO raw materials and corresponding EVOs

EVOs	Fatty acid				Epoxy index (meq.g <sup>-1</sup> )
	Saturated <sup>E</sup>	Mono-unsaturated <sup>f</sup>	Di-unsaturated <sup>g</sup>	Tri-unsaturated <sup>h</sup>	
Karanja <sup>a</sup>	22	56	21	1	2.77
Castor <sup>a</sup>	3	92 <sup>d</sup>	5	-	2.85
St John's Wort <sup>a</sup>	21	63	16	-	2.97
Peanut <sup>b</sup>	20	53	27	-	3.35
Rapeseed <sup>a</sup>	7	62	25	7	3.99
Soybean	11	24	54	8	4.54
Rose Hip Seed <sup>a</sup>	17	20	57	5	4.7
Safflower <sup>c</sup>	12	18	70	-	4.93
Grapeseed <sup>b</sup>	11	22	67	-	4.94
Camelina <sup>c</sup>	10	30	28	32	5.29
Linseed	6	22	16	52	5.61
Hemp <sup>c</sup>	10	12	65	13	6.09
Perilla <sup>c</sup>	3	21	18	58	6.77

<sup>a</sup>Non-edible oils. Rapeseed oil is the high erucic fatty acid compared to canola which have low erucic fatty acid. <sup>b</sup>Edible oils. <sup>c</sup>Edible but non-valuated. <sup>d</sup>Mono-unsaturated fatty acids of castor oil are comprised to 90% of ricinoleic acid. <sup>E</sup>mainly comprised of palmitic and stearic fatty acids. <sup>f</sup>Mainly comprised of oleic fatty acid. <sup>g</sup>Mostly linoleic fatty acid. <sup>h</sup>Mostly linolenic fatty acid

Moreover, considering the rising demand of vegetable oils notably due to the population growth, a careful selection of vegetable oil feedstocks has been carried out to avoid food competition.

For the first time in a preliminary work we showed the recycling properties of epoxidized linseed oil (ELO) based thermosets.<sup>19-21</sup> In the present work, we developed a new series of vegetable-based thermosetting resins, by thermo-curing of 12 newly synthesized EVOs (i) catalyst and hardener free and (ii) copolymerizing with 2,2'- dithiodibenzoic acid (DTBA). Through this study, the 12 new EVOs were synthesized with the objective to cover the larger domain of epoxy content, *i.e.* from 2.77 to 6.77 meq.g<sup>-1</sup>. In this manner, we will gain knowledge on EVOs potential to generate thermosets when reacted with DTBA, and on their properties. If the literature is rich on reporting studies dedicated to EVOs crosslinking with anhydrides, or aliphatic diacids, there are no many studies on EVOs curing using aromatic diacids, and with aromatic diacids containing disulfide linkage are not at all. Indeed, these S-S linkages allow the incorporation of dynamic crosslinks to form covalent adaptable networks (CANs)<sup>22</sup> that conducts to thermosets with reprocessable, recyclable and reshapable abilities. Disulfide dynamic bonds have attracted much attention in the design of a series of CANs, as displayed using 4-aminophenyl disulfide (AFD) as crosslinker for DGEBA by Odriozola *et al.*<sup>23</sup> or for the castor oil (CO) derived polyurethane by Chen *et al.*<sup>24</sup> To our knowledge, this paper investigates for the first time how the epoxy content characterizing the new EVOs impact on the homopolymerization reactivity and in parallel to the copolymerization reactivity with the

DCAs and therefore on the performances of corresponding epoxy / acid vitrimers-like thermosets. Indeed, the current work reports (i) the reactivity study of these new EVOs with and without crosslinker and (ii) how the use of DTBA dynamic hardener provides additional properties of chemical recyclability.

The reactivity study was achieved by differential scanning calorimetry analysis (DSC). The structural evolution of the thermosetting resins was studied by Fourier Transform Infrared Spectroscopy (ATR-FTIR). Thereafter, the thermo-mechanical properties of the thermosets were analyzed by DSC, thermogravimetric analysis (TGA), dynamic mechanical analysis (DMA) and tensile testing. Finally, their solvent stability and network degradability were investigated for the copolymerized thermosets, as a possible option of recycling mechanism. Therefore, this work gives an overview, a complete study, from thermosets synthesis to a detailed investigation of their properties, for a large series of newly epoxidized vegetable oils crosslinked with an aromatic diacid hardener.

## 4.2 Results and discussion

### 4.2.1 Study of EVOs homopolymerization

The homopolymerization were studied to characterize bio-based epoxy monomers and to verify how the properties of the obtained materials can be influenced in function of the epoxy content. As reference were choose the Epoxidized Linseed Oil (ELO) and the Epoxidized Soybean Oil (ESO). The evolution of the properties in function of the structure will be analysed considering the bio-based epoxidized vegetable monomers will be evaluated starting from the thermal stability of the EVOs, proceeding with the reactivity studies, until the analysis of the properties of the thermo-cured homopolymers.

#### 4.2.1.1 Thermal stability of EVOs

The thermal stability of the EVOs was studied by thermogravimetric analysis (TGA) in order to characterize the starting monomers. The obtained EVOs thermal stability ( $T_{5\%}$ ) was determined to be in the range from 271 °C for EHO to 305 °C for ESFO and EKRNO, which is similar to the value commonly obtained with other epoxy resins such as DGEBA.<sup>25</sup> (Figure ESI 1 and Table ESI 2). All the EVOs underwent a complex multistep thermal degradation in air atmosphere, with an onset temperature higher than 250 °C. The  $T_{30\%}$  it has allowed to find a correlation between the thermal-degradation temperature of the EVOs and the epoxy content: epoxy monomers with lower epoxidation showed a lower  $T_{30\%}$  temperature, showing less resistant at higher temperature, confirming also by the final residue at 1000 °C.

## 4.2.1.2 EVOs reactivity analysed by DSC and FT-IR

The EVOs reactivity in function of the temperature was thus analysed by dynamic DSC (Figure 1). All the data are collected in Table ESI 2. The DSC study shows that all the EVOs exhibit the

ability to homopolymerize under heating which is consistent with results already highlighted by Lee *et al.*<sup>26</sup> or by Levchik *et al.*<sup>25</sup>. Overall, the selected monomers show a decreasing of homopolymerization with the epoxy content (from 197 for EKRNO to 156 °C for ECMO or ELO), while the  $T_{\text{peak}}$  value is very close for all the monomers, around 220 °C. In a study

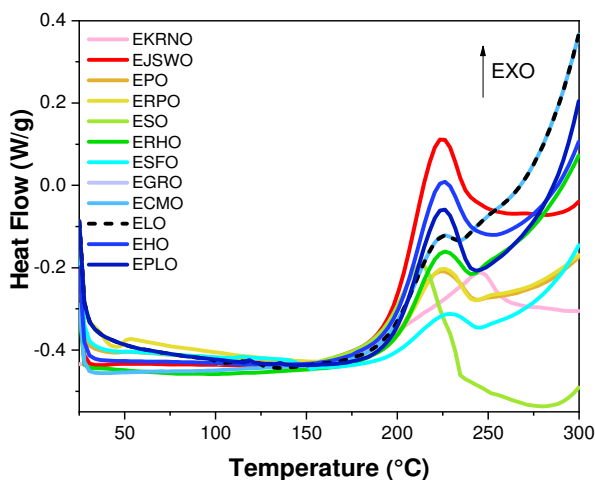


**Figure 1.** DSC dynamic analysis of EVOs homopolymerization reaction during heating from 25 to 300 °C at 10 °C.min<sup>-1</sup>

reported by La Scala *et al.*<sup>27</sup> it was put in evidence that epoxidation kinetic is notably dictated by 2 major parameters, the electronic and the steric effects. The electronic effect was determined by comparing fatty acid methyl ester from oleic, linoleic and linolenic acids. By increasing the degree of unsaturation and thus the electronic density, it was observed that the rate constant of epoxidation can be increased up to a factor 3. In the second case, reactivity of triglycerides

with high oleic, linoleic and linolenic fatty acids against epoxidation were compared. Although, reactivity of double bonds of oleic and linoleic acids are similar, that of linolenic acid was evaluated to be 2 times higher. Located at the end of the fatty acid chain, the double bond of linolenic acid is less sterically hindered.

Herein, we can assume that the difference on the crosslinking temperature onset could be assigned to the reactivity of the oxirane group alongside the alkyl chains which may be directly linked to their

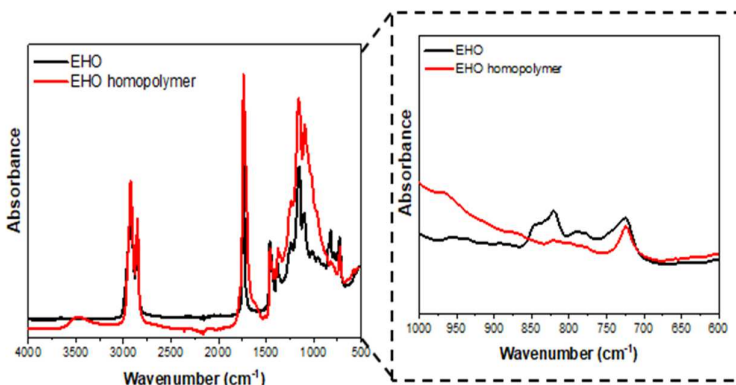


**Figure 2.** FT-IR spectrum of EHO before (dark line) and after (red line) thermal curing

difference of reactivity during epoxidation process. Indeed, results presented in Table ESI 2 clearly exhibit that the increase of the double bond and thus the epoxy content is, in most of the cases, correlated with the increase of linolenic chains for which the epoxy located at the chains' ends is more reactive. Thus, it can be assumed that the thermal initiated self-curing reaction starts on this position and then activates the polymerization of other, less reactive, epoxy groups.

Finally, based on the results obtained by TGA and DSC, all the EVOs were thermo-cured at 180 °C over 24 h.

Such curing temperature, above or very close to the crosslinking onset temperature, would allow the thermal self-curing of the EVOs. It was measured by FT-IR analysis (Figure ESI 2 and Table 2) that the conversion of oxirane rings was range between 85% for ELO and 99% in the case of EPO and ERPO. A representative FT-IR analysis corresponding to the cured EHO is displayed in Figure 2.

#### 4.2.1.3 Properties of thermo-cured EVOs thermoset

Several reactions could occur during the heating of the epoxy resins. The most probable ones are the epoxides isomerization to generate unsaturated alcohols<sup>26,28</sup> and the etherification reactions by intermolecular additions. An ionic mechanism was spotlighted to explain the curing of thermo-cured epoxy homopolymers.<sup>29</sup> It can moreover be assumed that, in parallel to this ring opening polymerization initiated by the heating, a competitive mechanism corresponding to the reaction in between epoxies with some hydroxyl functions can occurs. Finally, another conceivable mechanism is the transesterification reaction by

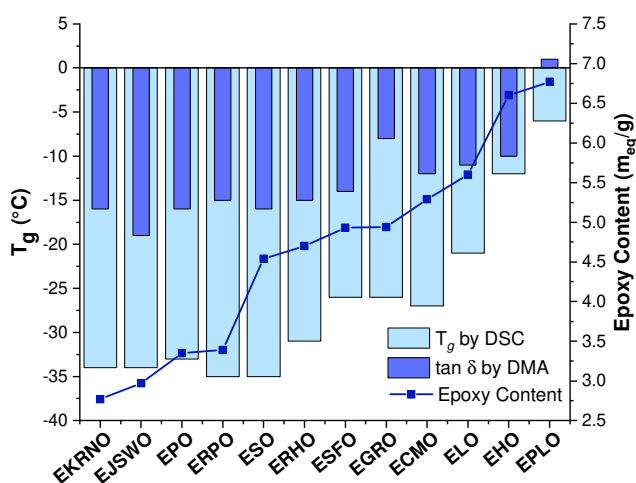


**Figure 3.** Correlation between  $T_g$  from DSC or  $\tan \delta$  from DMA and epoxy index for the EVOs thermoset materials

action of the forming hydroxyl on the ester bond of the triglyceride,<sup>30</sup> which is likely to have an impact on the structure of the thermo-cured crosslinked networks and finally on the thermomechanical performances.

The viscoelastic properties of the crosslinked materials were evaluated by DSC and DMA (Figure 3 and Figure ESI 3). All the data are gathered in Table 2. As expected, the materials obtained by thermal

## Chapter 4

homopolymerization have low curing densities, since the reactions are only thermally induced and are uncatalyzed. Even if the conversions are high, we can suppose that the obtained chains have more or less heterogeneous architecture, hypothesis supported by the presence, for some cured samples, of two  $T_g$  in DSC or by some shoulders in DMA analyses. Anyhow, the materials generated by triglyceride thermo-curing have low  $T_g$ , from -35 to -6 °C by DSC analysis and from -19 to 1 °C by DMA, due to the contribution of aliphatic segments.

Alike photocured EVO based thermoset, the  $T_g$  and the  $\tan \delta$  values are depending on the epoxy content on the EVO's building-blocks. It can be observed that an increase of the epoxy content lead to an increase of crosslinking density and therefore impacting the thermomechanical properties. The materials exhibit viscoelastic properties from 600 (ERHO) to 4000 MPa (ERPO). It must anyhow be noted that such performances collapse to 0.25 (ESFO) to 2.4 MPa (EPLO) at rubbery plateau. The homopolymers exhibit characteristics of low crosslinked elastomers and for the high epoxy content EVOs, similar with natural rubber.

*Table 2. Properties of homopolymerized EVOs thermoset materials*

EVOs label	FT-IR Conversion (%)	$T_g$ DSC (°C)	$\tan \delta$ DMA (°C)	$E'$ GLASSY STATE (MPa)	$E'$ RUBBERY STATE (MPa)	$\nu$ (mmol/cm <sup>3</sup> )
EKRNO	98	-34/-9	-16	2400	0.11	0.09
ESJWO	87	-34/-10	-19	1400	0.17	0.09
EPO	99	-33/-8	-16	1650	0.9	0.11
ERPO	99	-35/-9	-15	4000	0.52	0.07
ESO	83	-35/-12	-16	1100	0.55	0.07
ERHO	92	-32/-10	-15	600	0.38	0.06
ESFO	96	-26	-14	1200	0.25	0.05
EGRO	97	-26	-8	2050	1.97	0.27
ECMO	91	-27/-4	-12	1000	1.27	0.19
ELO	85	-12	-10	900	1.8	0.23
EHO	97	-21	-11	1700	1.7	0.24
EPLO	92	-6	1	1350	2.4	0.35

### 4.2.2 Study of EVOs copolymerization with DTBA

The copolymerization reactions of the EVOs with the DTBA hardener were studied using 3 different initiators, i.e. imidazole (IM), 1-methylimidazole (1-MI) and N, N-dimethylbenzylamine (DMBA) (respectively D, E and F in Figure ESI 1). The correlation of EVO's structure and their epoxy index vs. thermoset properties is part of the aim of this study. As references were chosen the epoxidized linseed oil (ELO) and the epoxidized soybean oil (ESO) because (i) these two EVOs have epoxy indexes in the middle point of the variation range of new synthesized and here studied EVOs and (ii) because both ELO and ESO are commercially available, produced and applied at industrial scale. Moreover, numerous studies highlighted the reactivity of these two epoxidized monomers with anhydride or acid hardeners.<sup>31-36</sup> The

evolution of the thermoset's properties in function of the EVOs structure will be analyzed considering EVO's monomers with comparable structure as the ELO and ESO references (i.e. same natures of fatty acids) but will also be compared with epoxidized castor oil (ECO) in order to gain knowledge on the influence of the additional hydroxyl groups present its structure on the thermoset material performances. For all aforementioned systems, we will discuss further the properties of the final thermoset materials as function of their epoxy content.

#### 4.2.2.1 Copolymerization reactions followed by DSC and FT-IR studies

The copolymerization reactions of the EVOs with DTBA catalyzed by IM, 1-MI and DMBA were investigated by DSC in order to analyze if the EVOs show comparable reactivity in function of the initiators, as the reference systems ELO/DTBA/initiator.

The dynamic DSC analyses were performed without initiator and also with three selected initiators: IM, 1-MI and DMBA. The DSC results are displayed in Figure ESI 4. Firstly, we can highlight the very good reactivity between the EVO's monomer and the DTBA hardener. Indeed, all the studied systems are characterized by high values of reaction enthalpies, even in the systems without initiators. Moreover, the uncatalyzed systems react with a higher reaction enthalpy than the systems with initiators (Table ESI 3). This result could be attributed to the occurring of concomitant main and secondary reactions, as homopolymerization or etherification. In comparison, the initiators introduce a selectivity through the EVOs/DTBA copolymerization, therefore it decreases the starting temperature and the enthalpy of reaction is given mainly by the main reaction. According with these results it appears clearly that IM, as demonstrated for ELO,<sup>19-20</sup> allows higher conversions during copolymerization, together with a lower interval of reaction for all the EVOs/DTBA systems.

According to our previous results,<sup>19-20</sup> the ELO/DTBA reaction in presence of 1-MI is characterized by a low reaction enthalpy and low onset temperatures,  $T_{on}$ , compared with those of system initiated by IM (Table ESI 3). Thus, 1-MI activates the conversion of epoxides at lower temperatures but with a lower selectivity of the copolymerization reaction. Thereafter, when DMBA is used as catalyst, an efficient activation of copolymerization reaction is produced, with high reaction enthalpy for EKRNO, ECO, ERPO and EHO monomers, but the reaction temperature range is shifted to higher temperature. This result, combined with the low copolymerization conversions obtained for ELO reference, made us discard also this initiator from the subsequent studies.

An exception to this trend is the ECO/DTBA formulation which has a particular behavior: a higher reactivity and a lower reaction temperature was obtained without using a catalyst. This

result can be attributed to the effect of the hydroxyl groups present in the ECO's structure.

In conclusion, IM was selected as the optimal initiator for the EVOs/ DTBA copolymerization studies. The copolymerization and reactivity of ELO/DTBA/IM system was then considered as the reference and therefore the reactivities of the new EVOs were compared with this formulation. In Table ESI 4 and Figure ESI 5 are reported the comparison of the DSC thermograms of EVOs/DTBA/IM copolymerization

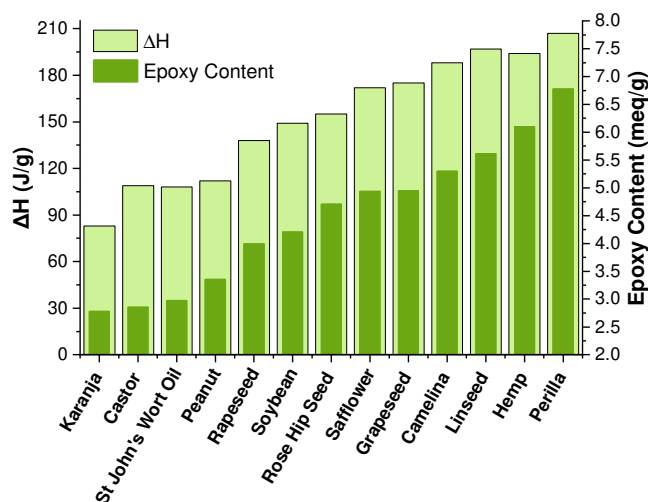


Figure 4. Correlation of EVOs/DTBA/IM copolymerization enthalpy and monomers' epoxy content

reactions. The DSC results display that the enthalpy of copolymerization reaction increases with the EVO's epoxy content (Table 3 and Figure 4). The EVOs with low epoxy content, as EKRNO or ESJWO with 2.77 and 2.97 meq.g<sup>-1</sup>, exhibit lower copolymerization enthalpy (84 and 108 J.g<sup>-1</sup>) compared with EPLO characterized by the highest epoxy content and thus the highest enthalpy of copolymerization (207 J.g<sup>-1</sup>).

Table 3. Reaction enthalpy, interval and temperature of the reaction peak ( $T_{peak}$ ) of EVOs/DTBA/IM systems during the copolymerization reaction

VOs feedstock	EVOs in copolymerization systems	Epoxy content (meq/g)	ΔH (J/g)	$T_{peak}$ (°C)	Reaction Interval
Karanja Oil	EKRNO	2.77	84 ± 3	164 ± 1	145 – 186
Castor Oil	ECO	2.85	109 ± 3	147 ± 1	130 – 170
St John's Wort Oil	ESJWO	2.97	108 ± 3	168 ± 1	154 – 186
Peanut Oil	EPO	3.35	112 ± 3	171 ± 1	151 – 192
Rapeseed Oil	ERPO	3.99	138 ± 3	164 ± 1	147 – 184
Soybean Oil	ESO	4.20	149 ± 3	159 ± 1	142 – 182
Rose Hip Seed Oil	ERHO	4.7	155 ± 3	161 ± 1	140 – 189
Safflower Oil	ESFO	4.93	172 ± 3	158 ± 1	142 – 180
Grapeseed Oil	EGRO	4.94	175 ± 3	162 ± 1	139 – 182
Camelina Oil	ECMO	5.29	188 ± 3	153 ± 1	136 – 176
Linseed Oil	ELO	5.61	197 ± 3	151 ± 1	131 – 180
Hemp Oil	EHO	6.09	194 ± 3	160 ± 1	135 – 190
Perilla Oil	EPLO	6.77	207 ± 3	152 ± 1	126 – 187

With the increase of the EVO's epoxy content we can notice an increase of the temperature interval of reaction. As we can observe in Figure ESI 4 the copolymerization exothermic peaks have comparable  $T_{endset}$  but the  $T_{onset}$  values appear at lower temperature for the EVOs with

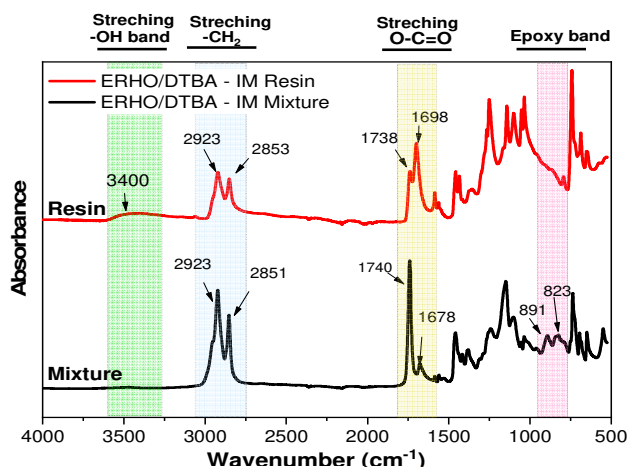


Figure 5. FT-IR comparison analysis of the reactive groups of ERHO/DTBA/IM mixture and of the thermoset resin

and the thermoset resin. In the FTIR spectrum of uncured mixture we can notice the oxirane characteristic bands at 823 and 891  $\text{cm}^{-1}$  that completely disappear in the spectrum of cured material. In the thermoset's spectrum we can notice the increased -OH peak at peak at 1678  $\text{cm}^{-1}$  in the mixture, disappears after curing, being  $\sim 3400 \text{ cm}^{-1}$ . Moreover, the formation of new ester peak, with the stretching of the carbonyl ( $\text{C}=\text{O}_{\text{ester}}$ ), appears in the resin spectrum at 1738  $\text{cm}^{-1}$ .

In compliance with the DSC analysis, ECO system gave different FTIR results for the epoxy monomers and for the thermosets, due to the presence of alcohol groups in their structure. The FTIR spectrum of ECO monomer (Figure 6), shows the presence of the typical bands of -OH, -CH<sub>2</sub> and O=C=O at respectively  $\sim 3400$ , 2925, 2855, and 1737  $\text{cm}^{-1}$ , while the absorption band of characteristic epoxide ring vibration appears at 844  $\text{cm}^{-1}$ . In the spectrum of the thermoset material new ester peak appears but we should notice the presence of few residual epoxy peaks at 865  $\text{cm}^{-1}$ . The presence of these residual groups can be explained by the fact that the DTBA can also react with the -OH functions from ECO structure.

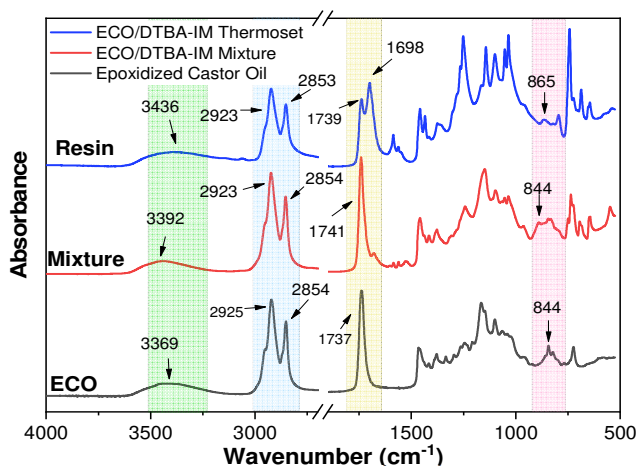


Figure 6. FTIR results and comparison between the ECO epoxy monomers, the mixture with DTBA/IM and the final thermoset



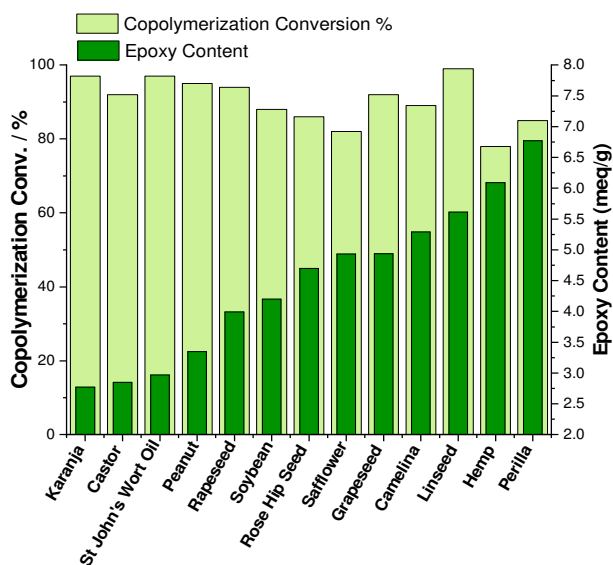


Figure 7. Conversion of epoxy functions for the EVOs thermosets correlated with the epoxy content

Therefore, the DTBA is in defect regarding the main copolymerization stoichiometry. The copolymerization conversions for the EVO thermosets were calculated by applying the Equation 1. The results are summarized in Figure 7 and Table ESI 5. EKRNO and ESJWO based thermosets display the highest conversion (97%) in the series of EVOs excepting the reference, ELO<sup>19,21</sup> (99%). Conversions superior to 90% were also obtained for EPO (95%), ERPO (94%), ECO (92%), and EGRO (92%). EHO shows the lowest conversion compared to EVOs having similar structure. This result has to be correlated to the larger copolymerization reaction range and predicts a lower  $T_g$  value for this thermoset. The same trend was observed for ESFO based thermoset.

#### 4.2.2.2 Thermomechanical properties of EVOs/DTBA/IM thermosets

Figure 8 shows the results of DMA analysis, i.e. the temperature dependence of loss factor ( $\tan \delta$ ) (Figure 8 A) and of the storage modulus ( $E'$ ) (Figure 8 B) for the prepared thermosets. The values of DMA data are listed in Table 4. We can notice that all the thermosets reveal a single  $\tan \delta$  peak, as in the case of  $T_g$  measurements performed by DSC, highlighting the existence of homogeneous networks. As shown in Figure 8 and Table 4 we can observe an increase of the  $\tan \delta$  values with the epoxy content in the copolymer's formulation. The  $\tan \delta$  value varies from 33 °C, for thermosets made with EVOs with low epoxy content, to 111 °C, for EPLO having the highest epoxy content (6.77 meq.g<sup>-1</sup>). To compare the viscoelastic results, both the evolution of the  $T_g$ , determined by DSC, and that of  $\tan \delta$ , measured by DMA, are plotted in Figure 9 showing that the data fit with a linear trend in function of the epoxide content. In line with these results, the evolution of storage modulus with the temperature (Figure 6 B) shows high  $E'$  values for the thermosets based on EVOs having high epoxy content. The calculation made by the Equation 3 allows to evaluate the crosslink density of the prepared network. Once again, the results show that increasing the epoxy content leads to increase the thermosets crosslink density from 0.025 (EKRNO thermoset) to 3.0 mmol.cm<sup>-3</sup>

(EPLO thermoset). We can notice that EPLO and the reference ELO thermosets are the resins with highest crosslinking (Table 4), while, thermosets with low epoxy content exhibit lowest crosslinking density (Figure 14).

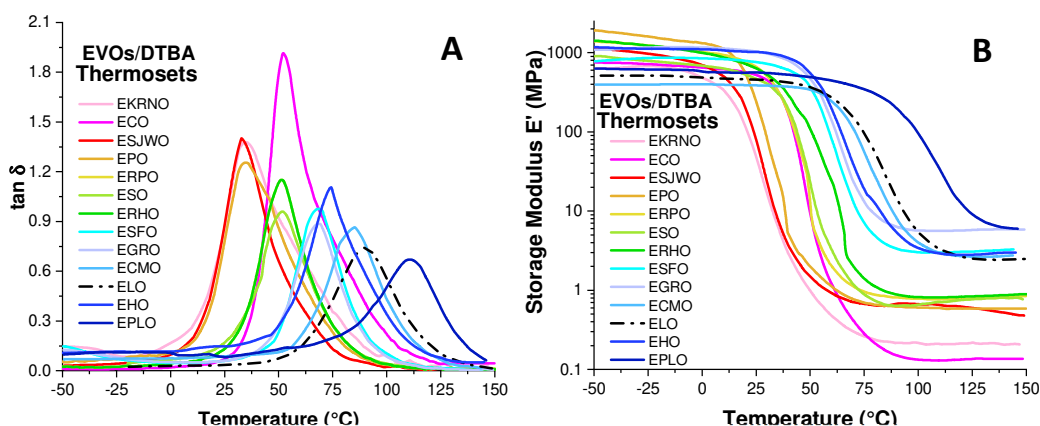


**Figure 8.** DMA results:  $\tan \delta$  (A) and storage modulus  $E'$  (B) vs temperature for the EVOs/DTBA/IM thermosets

ECO based thermoset material shows the  $\alpha$  transition at 52 °C and the lowest modulus in the rubbery plateau. Beside its low epoxy content, this low value of  $E'$  could be correlated with the lower reactivity with the DTBA hardener. However, considering all aforementioned outcomes obtained for this system, the main hypothesis explaining these results is the presence of the hydroxyl groups in the ECO structure and its possible reaction with DTBA leading to imbalanced stoichiometry and thus to incomplete epoxy/DTBA curing reactions. Moreover, secondary reactions as esterification or etherification implying the -OH reactions with -COOH or with epoxy functions could occur the copolymerization reaction, according with Hernandez *et al.*<sup>37</sup> A large range of  $T_g$  values was obtained in the series of prepared thermosets, from 17 °C for EKRNO based thermoset to 91 °C for EPLO based resin. Figure 9 (A) shows the evolution of this transition in function of the EVOs epoxy content. These results are presented also in function of  $\tan \delta$  values correlated with the epoxy content in Figure 9 (B).

Likewise, the study of copolymerization reactivity, we can highlight that the increase of epoxy content leads to an increase of the corresponding  $T_g$  values of thermosets. In the case of ECO thermosets, higher values of  $T_g$  were measured,  $\sim 27$  °C, again probably due to the presence of alcohol moieties in the structures participating to the crosslinking reactions, or to the hydrogen bonding, compared to the EVOs with similar epoxy content as ESJWO,  $T_g \sim 17$  °C. These results are consistent with those reported by Gerbase *et al.*<sup>38</sup> in which the lower  $T_g$  of ESO thermosets compared with that of ELO based resins were correlated with ESO lower

epoxy index. The low values of  $T_g$  obtained for EVOs with low epoxy content are also in agreement with the polymers derived from EVOs with low iodine content as presented in literature for ECO cured with citric acid.<sup>37</sup> Generally, the aliphatic and flexible structures usually lead to low  $T_g$  values, compared with aromatic thermosets. For instance, William *et al.*<sup>7</sup> prepared DGEBA/DCAs epoxy vitrimers with  $T_g$  values ranging from 50 to 70 °C. Wang *et al.*<sup>39</sup> reported synthesis of ESO/MHHPA resins with  $T_g \sim 40$  °C while an increasing of mechanical properties was obtained by adding DGEBA in the blends.

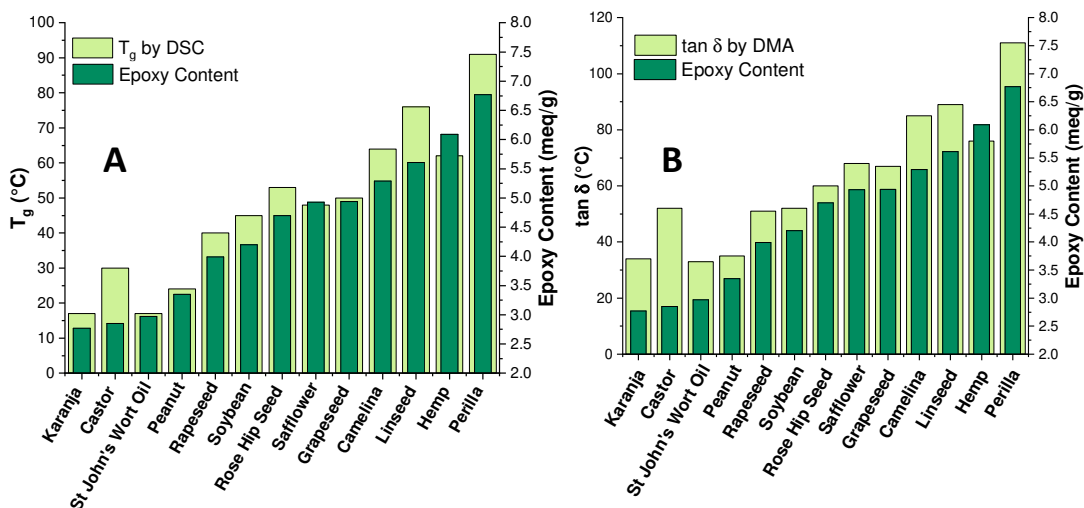


Figure 9. Glass transition evaluated by dynamic DSC analysis (A) and  $\tan \delta$  (B) measured by DMA analysis in function of the EVO's monomers epoxy content

Table 4. Summarized DSC and DMA data of EVOs/DTBA/IM thermosets

EVOs/DTBA/IM thermosets	$T_g$ (°C)	$\tan \delta$ (°C)	$(\tan \delta)_{\max}$	$E'_{\text{glassy plateau}}$ (MPa)	$E'_{\text{rubbery plateau}}$ (MPa)	Crosslink density (mmol/cm <sup>3</sup> )	$\rho$ (g.cm <sup>-3</sup> )
EKRNO	17	34	1.40	630	0.21	0.025	1.11
ECO	27	52	1.91	850	0.14	0.02	0.93
ESJWO	17	33	1.40	1145	0.48	0.072	1.06
EPO	24	35	1.36	1900	0.59	0.07	1.33
ERPO	40	51	1.11	1400	0.82	0.09	1.35
ESO	45	52	0.96	900	0.82	0.08	0.95
ERHO	53	60	0.86	1430	0.92	0.11	1.13
ESFO	48	68	0.99	780	3.13	0.31	1.12
EGRO	50	67	0.90	1090	5.84	0.58	1.11
ECMO	64	85	0.86	400	2.78	0.77	0.98
ELO	76	91	0.75	500	2.63	1.25	1.02
EHO	62	76	1.11	1200	3.03	0.75	1.15
EPLO	91	111	0.68	630	5.98	3.00	0.98

Kodam *et al.*<sup>4</sup> investigated the epoxidized karanja oil cured with citric and tartaric acid and measured higher  $T_g$  values ( $\sim 112$  °C) attributed to high acid functionalities of the hardeners and to the hydroxyl groups of the starting building blocks producing higher crosslinking density. Similarly, high  $T_g$  were obtained by curing ELO with methylhexahydrophthalic

anhydride (MHHPA) obtaining thermosets with  $\alpha$ -transition of 134 °C whereas ELO cured with 3,3,4,4-benzophenone-tetracarboxylic dianhydride (BTDA) lead to a crosslinked resins with  $\tan \delta$  around 245 °C.<sup>34</sup> In contrast, Zeng *et al.*<sup>31</sup> obtained materials with  $T_g$  values from - 16 to - 21 °C for ESO / aliphatic diacid crosslinkers.

Therefore, the  $T_g$  values are strongly dependent on the EVOs structure but also on the nature and structure of the hardener. A proper selection of the hardener contributes to the achievement of high performances even if the EVOs have aliphatic structures. Here, without changing the hardener structure, we succeeded to reach high  $T_g$  value, of 91 °C, by copolymerization of epoxidized perilla oil with DTBA.

The static mechanical properties of the samples were studied by tensile testing. Figure 8 shows the stress-strain curves of EVOs/DTBA thermosets and Table 5 summarizes the main tensile results. From Figure 10 we can notice that two kinds of stress-strain results were obtained, separating the synthesized thermosets into hard and brittle (Figure 8 A) and soft and plastic (Figure 8 B). The EVOs with in general low epoxy content and therefore low crosslinked network behave as soft and flexible, which is well consistent with the trend of their  $T_g$ . From Figure 8 B we can notice that these EVOs, based on ERPO, EPO, ESJWO and EKRNO, have low to very low Young modulus and tensile strength, the stress at break values ranging from 2.73 to 0.39 MPa. These resins exhibited high elongation at break, from 117 to 347%. These results are in good agreement with the results reported by Imbernon *et al.*<sup>40</sup> for elastomers synthesized from epoxidized natural rubber and dithiodibutyric acid crosslinker. In contrast, the thermosets obtained from EVOs with an epoxy content  $> 4.20 \text{ meq.g}^{-1}$  reveal higher tensile strength and Young modulus values. These thermosets have a strength at break at around 10-12 MPa while the elongation values are very low,  $< 2\%$ , characteristics for hard and brittle thermosets.

A peculiar trend shows the ECO-based thermoset that has a tensile behavior close to that of thermosets based on EVOs with high epoxy content, despite the fact that ECO is from the category of EVOs with low content,  $\sim 2.85 \text{ meq.g}^{-1}$ . This result can be again explained by the contribution of hydroxyl functions present in its structure to increase the network chemical connectivity, confirmed by its  $T_g$  and  $\tan \delta$  values, superior to those of thermosets from EVOs with comparable epoxy content.

All the EVOs thermosets exhibit better mechanical properties than some other EVO based polymer networks, which were cured by carboxylic acids<sup>4,31,35,41</sup> or EVOs / disulfide crosslinker<sup>42</sup> that showed lower  $\sigma$  and  $\epsilon$ . These results open the window for industrial applications.

## Chapter 4

The literature shows that starting from vegetable oils, a large diversity of derivatives can be synthesized, with very good properties. For example, Webster and Pan<sup>43</sup> developed high performance thermosets, by preparing epoxidized sucrose esters of fatty acids (ESEFAs) (soybean, linseed, safflower) crosslinked with 4-methyl hexahydrophthalic anhydride (MHHPA) using two ratios epoxy / anhydride of 1:0.5 and 1:0.75. Modulus and tensile strength of ESS (epoxidized sucrose soyate) were higher than those of the ESO control thermoset by factors of 7.6 and 2, respectively while, the properties of the ESL (epoxidized sucrose linseedate) thermoset were even higher with a modulus 21 times superior and a tensile strength 4.5 times greater than that of the ESO thermoset. The same authors reported increased properties<sup>44</sup> replacing ESO crosslinked with dodecenylsuccinic anhydride (DDSA) with dipentaerythritol (DPE), tripentaerythritol (TPE) or sucrose esters of soybean oil, synthesized using transesterification from soybean methyl ester and the corresponding polyols. The increased values in  $T_g$  and moduli were correlated to the presence of available hydroxyl groups which can facilitate the formation of polyester nets through rapid reaction between hydroxyl and anhydride.

Wang *et al.*<sup>45</sup> reported very good properties of epoxy polymers derivatives of soybean oil, synthesized by amidation of soybean oil with three amino alcohols (1-amino-2-propanol, 3-amino-1-propanol, and 1,3-diamino-2-propanol), followed by their (meth)acrylation, then by the free radical polymerization of unsaturated fatty side chains and finally the epoxidation of unsaturations.

The authors obtained an increasing of tensile strength and modulus replacing ESO / 4-methyl-1,2-cyclohexanedicarboxylic anhydride with these soybean oil epoxy polymers, obtaining values from 1.4 MPa (control, ESO based thermoset) to 37 MPa for the tensile strength and from 2.4 MPa (ESO based thermoset) to 561 MPa Young modulus.

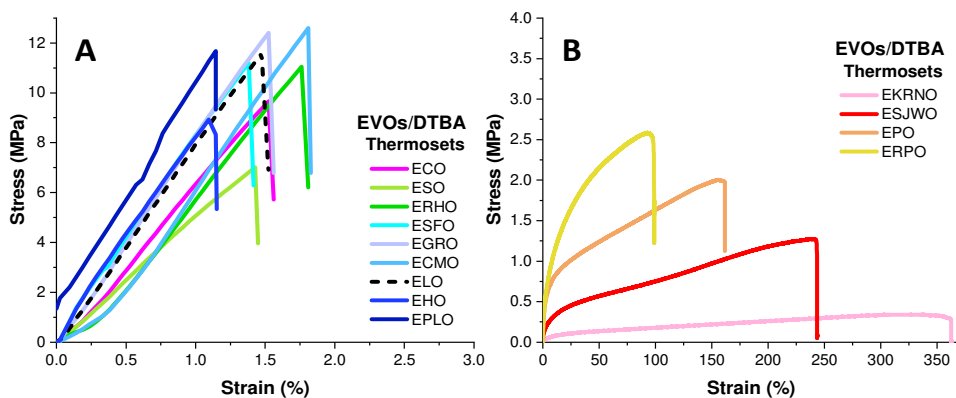


**Figure 10.** Stress–strain curves of EVOs/DTBA based thermosets (A) stiff and (B) ductile EVOs-based thermosets

Zhou *et al.*<sup>46</sup> observed that the mechanical strength, Young's modulus, and toughness improved with the increase of epoxy group density for sunflower oil-based epoxy copolymers EP(SFMA-co-VM) synthesized by sunflower oil-based monomer (SFMA) and vanillin-derived methacrylate (VM).

**Table 5.** Tensile properties for the EVOs/DTBA thermosetting resins

EVOs/DTBA/IM thermosets	Young Modulus (MPa)	Stress at break (MPa)	Elongation at break (%)
EKRNO	0.73 ± 0.08	0.39 ± 0.07	347.2 ± 54.7
ECO	731.6 ± 59.2	7.96 ± 1.85	1.21 ± 0.36
ESJWO	2.42 ± 0.77	1.21 ± 0.09	247.5 ± 11.0
EPO	21.1 ± 8.2	2.03 ± 0.21	167.4 ± 25.5
ERPO	476.2 ± 74.9	2.73 ± 0.42	117.4 ± 0.82
ESO	752.2 ± 20.2	10.3 ± 3.03	1.70 ± 0.15
ERHO	771.3 ± 39.2	10.1 ± 4.38	2.04 ± 0.55
ESFO	804.0 ± 32.54	11.5 ± 1.47	1.42 ± 0.20
EGRO	825.5 ± 31.93	12.7 ± 2.75	1.62 ± 0.38
ECMO	830.6 ± 37.3	12.1 ± 1.95	2.04 ± 0.29
ELO	811.0 ± 36.05	10.9 ± 1.10	1.36 ± 0.13
EHO	822.1 ± 96.6	9.82 ± 0.67	1.21 ± 0.18
EPLO	815.3 ± 10.1	11.5 ± 4.55	1.23 ± 0.68

The thermal stability profiles of the obtained thermosets are displayed in Figure 11, Figure ESI 6, Table 6 and Table ESI 6. All the EVOs thermosets show similar degradation behavior in air, with a good thermal stability, in the same range of ELO thermoset reference. The  $T_{5\%}$  values are ranging from 265 °C for EPLO thermosets to 290 °C for ESJWO. Resins of EVOs with low epoxy content exhibit higher thermal stability, while increasing the epoxy content the thermal stability decreases. The reason of these behavior could be connected to the amount of DTBA

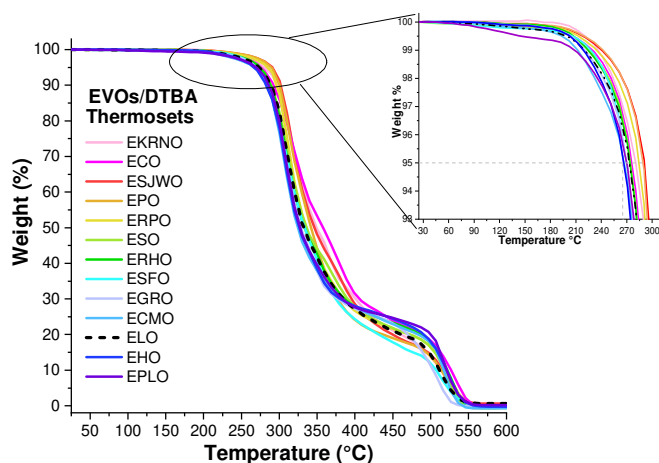


**Figure 11.** TGA thermograms during heating the EVOs thermosets at 10 °C.min<sup>-1</sup> under air; zoom in the region 25-320 °C

in the network, and consequently to the S-S bonds in the resins. Ma *et al.*<sup>47</sup> reported that the presence of S-S bonds provokes a decrease of thermoset's thermal stability due to their lower dissociation energy compared with that of C-C bonds. Moreover, higher the oxirane rings content, more ester and hydroxyl groups are created through the curing. These functions can also promote the

## Chapter 4

thermal scissions of the networks. The thermal stability of the EVOs thermosets are similar with those of epoxy resins containing disulphide dynamic bonds,<sup>48</sup> but lower if we compare it with ELO/adipic acid or glutaric anhydride systems<sup>35</sup> or with ESO/DCA thermosets with different carbon chain-lengths.<sup>31</sup> Figure ESI 6 displays the DTG curves highlighting the main degradation steps.

The statistic heat-resistant index temperature values ( $T_5$ ) (Table 6) have similar trend as the  $T_{5\%}$ . For the thermosets based on EVOs with low epoxy content, ESJWO and EKRNO thermosets, the  $T_5$  values are higher compared to the reported values for epoxidized sucrose soyate cured with citric or malic acids<sup>49</sup> (148–154 °C). Supanchaiyamat *et al.*<sup>50</sup> correlated the first thermal degradation stage with the breaking of the ester linkages, while the second one with the cleavage of the products formed during the first degradative step.

**Table 6.**  $T_{5\%}$  and  $T_5$  determined by TGA analysis for thermosets

EVOs/DTBA/IM thermosets	$T_{5\%}$ (°C)	$T_5$ (°C)	EVOs/DTBA/IM thermosets	$T_{5\%}$ (°C)	$T_5$ (°C)
EKRNO	285	171	ESFO	271	162
ECO	275	169	EGRO	265	161
ESJWO	290	170	ECMO	265	162
EPO	285	164	ELO	275	167
ERPO	285	172	EHO	265	164
ESO	271	167	EPLO	265	159
ERHO	275	165			

### 4.2.2.3 Solvent and chemical stabilities

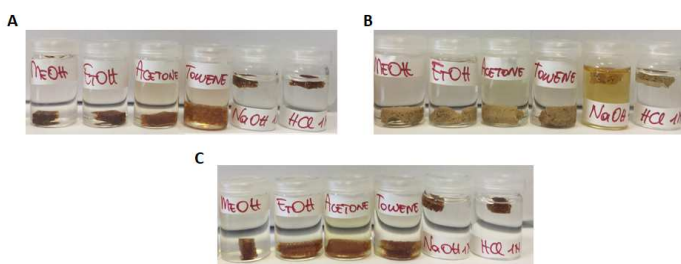


**Figure 12.** Solvent stability study for selected thermosets: ESJWO (A), EPLO (B), and ECO (C) after 72 hours in methanol, ethanol, acetone, toluene, 1 N NaOH and HCl

To evaluate the solvent stability of the EVOs thermosets, weighted and measured samples were immersed for 72 hours in: methanol, ethanol, acetone, toluene, 1 N NaOH and 1N HCl. Three thermosets were selected

to analyze how the low or high epoxy content impact on solvent stability: ESJWO, ECO and EPLO thermosets. Their behavior after immersion in mentioned solvents were compared (Figure 12 A, B and C). After 72 hours these resins were generally stable in all solvents and no changes was observed in 1N HCl solution. ECO resin (Figure 12 C) shows similar behavior as ESJWO and EPLO resins. Gerbase *et al.*<sup>38</sup> reported higher chemical resistance for ESO cured

with cyclic anhydrides in polar organic solvents (acetone, ethanol) than in toluene where was observed an interaction polymer-solvent by network's swelling. Ruiz de Luzuriaga *et al.*<sup>51</sup> showed for DGEBA cured with 4-aminophenyl disulfide that the materials were not affected after immersion at room temperature for 72 hours in 1N NaOH and HCl, THF, toluene, acetone and ethanol.

We already proved the ELO/DTBA thermosets disintegration in 1N NaOH at 80 °C or at room temperature after 3 days.<sup>20</sup> This behavior could be attributed to a synergic of effect: the disulfide metathesis<sup>52-53</sup> and also the cleavage of the ester bonds. As example, Ma *et al.*<sup>47</sup> reported that the isosorbide-derived epoxy crosslinked with 4-aminophenyl disulfide exhibits a complete degradation after 3 h in alkaline solution, attributing this result to S-S cleavage and to the water-soluble nature of isosorbide.

From Figure 12 B we can observe that EPLO resin presents a faster auto-degradation in alkaline solution compared to ESJWO thermoset, due to its higher epoxy content and consequently due to a higher content on ester connections formed during crosslinking.

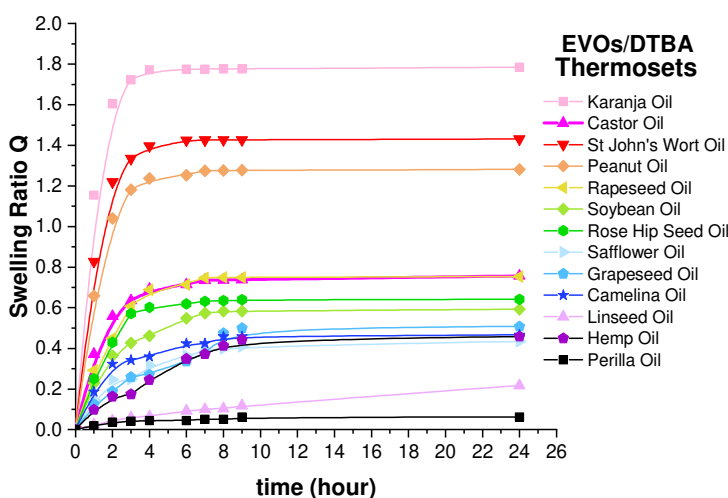


Figure 13. Swelling test performed in toluene for 24 hours

Regarding the swelling tests, the toluene was selected as solvent for this test for 24 hours at room temperature. The results are traced and plotted in Figure 13.

Vitrimers are known for “swell, but do not dissolve, in good solvents” as reported by Leibler *et al.*<sup>54</sup> and the

swelling equilibrium of the thermosets in given solvents is an indicator of the crosslinking.<sup>55</sup> The degree of swelling is known to be dependent upon the crosslink density of thermoset networks. Higher the crosslink density, lower is the degree of swelling: EPLO has the lowest swelling ability.

EKRNO and ESJWO thermosets show the highest swelling, confirming the lowest network crosslink density. The swelling ratio of the EVOs is lower than that of AESBO/maleic anhydride thermosets<sup>55</sup> or of other bio-based thermosets.<sup>56</sup>



The swelling testing results were used further to determine the crosslink density of the networks, as described by Flory-Rehner theory.<sup>57-58</sup>

Applying this method, the network density values were evaluated by measuring their swelling in toluene at room temperature for 48 hours.

Previously we determined by DMA data (Figure 14) that the crosslinking significantly increased with the epoxy content, as confirmed by the rubbery-elasticity theory. The results are reported and compared in Table ESI 8. The corroborated data by the two

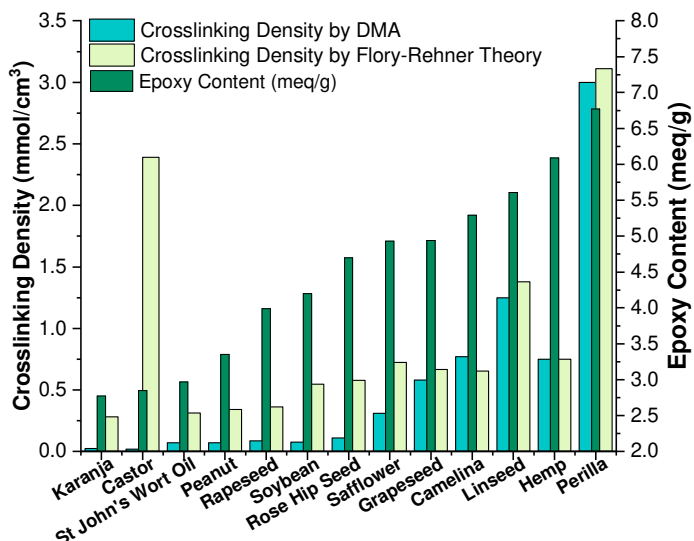


Figure 14. Crosslinking density by the rubber elasticity and Flory-Rehner theory in function of the EVOs epoxy content

analyses demonstrate the same trend but with higher values for the results extracted by the swelling tests. For the thermosets based on EVOs with high epoxy content the results are close, especially for EPLO and EHO materials. A contradictory result has been observed for ECO thermoset with one of the highest crosslinking densities measured by Flory-Rehner theory.

Finally, the reduction of the disulphide bonds to thiols was performed using a DMF solution with 5 wt.% of dithiothreitol, according with Zhou *et al.*<sup>48</sup>, at 50 °C for 24 hours. Similar results were obtained by Ruiz de Luzuriaga *et al.*<sup>51</sup> who showed a complete dissolution of DGEBA/4-aminophenyl disulfide thermosets in 2-mercaptoethanol in DMF solution immersed at room

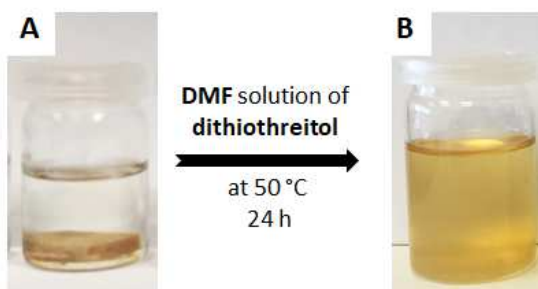


Figure 15. ERHO thermoset (A) Before and (B) after in immersion in DMF solution with dithiothreitol

temperature for 24 hours. Figure 15 displays this reduction for ERHO thermoset resin. The thiols groups present in the solvent solution react with the crosslinked dynamic disulphide networks, producing a complete debonding of the S-S connections. This complete thermosets' dissolution opens important windows to

chemical recyclability for thermoset materials.

#### 4.2.2.4 Bio-based content

Finally, the bio-based content of the EVOs/DTBA/IM thermosets was evaluated as “the amount of bio-based carbon in the material or product as a percent of the weight (mass) of the total organic carbon in the product”.<sup>59</sup>

All the starting EVOs monomers were obtained from renewable materials, as seeds of vegetables, while the hardener and the initiator aren't bio-based products. Considering ELO thermoset formulation, the carbon content in the starting materials is: in ELO ~ 70.5%, in DTBA ~ 47% and in IM ~ 53%, respectively. So, for the ratio EVO / hardener = 1/1 : 2.5 g of ELO reacts with 2.149 g of DTBA and 0.046 g of IM, consequently the bio-based content according with Pan *et al.*<sup>43</sup> is:

$$\text{Bio-based content \%} = \frac{(2.5 \text{ g} \cdot 70.5\%)}{(2.5 \text{ g} \cdot 70.5\%) + (2.149 \text{ g} \cdot 47\%) + (0.046 \text{ g} \cdot 53\%)} = 63.0 \%$$

$$\text{Carbon bio content \%} = \frac{\text{Bio-based carbon}}{\text{Bio-based carbon} + \text{petro-based carbon}}$$

$$\text{carbon bio content \%} = \frac{57 * 0.532}{57 * 0.532 + 14 * 0.458 + 3 * 0.01} = 82.5\%$$

The bio-based content determined for all the thermosets (Table ESI 8) is in the range from 79% for EKRNO to 58% for EPLO, while the carbon bio-content varies from 91% for EKRNO to 80% for EPLO. Increasing the epoxy content, the bio-based content and the carbon bio-content decrease due to a higher amount of needed hardener in the formulation.

### 4.2.3 Conclusions

A series of novel bio-based epoxy thermosets were developed using a broad range of epoxidized vegetable oils. These EVOs monomers were copolymerized with a disulfide aromatic dicarboxylic acid (DCA) and therefore the reactivity of these systems was compared. The new EVOs allow to obtain materials with wide range of thermomechanical properties thanks to their variation in chemical structures and concomitant reactivities with acid hardener. By an appropriate choice of epoxy content in the EVOs structure the final properties could be predicted. Indeed, the copolymerization of EVOs with DTBA produced materials exhibiting either high  $T_g \sim 91$  °C,  $\tan \delta$  values of 111 °C and crosslink density of 3 mmol.cm<sup>-3</sup> as in the case of EPLO or low  $T_g$  values ( $\sim 17$  °C) as in the case of EKRNO based thermoset, characterized by a low epoxy content. The large range of tensile properties, from soft and plastic (for thermosets based on EVOs with an epoxy content < 4 meq.g<sup>-1</sup>) to hard and rigid

## Chapter 4

could be used to develop novel sustainable thermosetting materials with modulated properties and thus of interest for very different application fields. The obtained materials, with a high biobased carbon content > 80% can find applications in protective coatings, structural matrix, and composites. The chemical recyclability results are opening windows for a future work that will be dedicated to the investigation of 3R ability (recyclability, repairability and reshapability) of these new EVOs thermosets.

## Acknowledgments

This work was supported by ECOXY project. ECOXY is a project funded by the European Commission. This project has received funding from the Bio Based Industries Joint Undertaking under the European Union's Horizon 2020 research and innovation program (Grant agreement n° 744311).

## References

1. Parada Hernandez, N. L.; Bonon, A. J.; Bahú, J. O.; Barbosa, M. I. R.; Wolf Maciel, M. R.; Filho, R. M., Epoxy monomers obtained from castor oil using a toxicity-free catalytic system. *Journal of Molecular Catalysis A: Chemical* **2017**, 426, 550-556.
2. Lathi, P. S.; Mattiasson, B., Green approach for the preparation of biodegradable lubricant base stock from epoxidized vegetable oil. *Applied Catalysis B: Environmental* **2007**, 69 (3), 207-212.
3. Wu, X.; Zhang, X.; Yang, S.; Chen, H.; Wang, D., The study of epoxidized rapeseed oil used as a potential biodegradable lubricant. *Journal of the American Oil Chemists' Society* **2000**, 77 (5), 561-563.
4. Kadam, A.; Pawar, M.; Yemul, O.; Thamke, V.; Kodam, K., Biodegradable biobased epoxy resin from karanja oil. *Polymer* **2015**, 72, 82-92.
5. Eissen, M.; Metzger, J. O.; Schmidt, E.; Schneidewind, U., 10 Years after Rio—Concepts on the Contribution of Chemistry to a Sustainable Development. *Angewandte Chemie International Edition* **2002**, 41 (3), 414-436.
6. Capelot, M.; Unterlass, M. M.; Tournilhac, F.; Leibler, L., Catalytic Control of the Vitrimer Glass Transition. *ACS Macro Letters* **2012**, 1 (7), 789-792.
7. Altuna, F. I.; Casado, U.; dell'Erba, I. E.; Luna, L.; Hoppe, C. E.; Williams, R. J. J., Epoxy vitrimers incorporating physical crosslinks produced by self-association of alkyl chains. *Polymer Chemistry* **2020**, 11(7), 1337-1347.
8. García, F.; Smulders, M. M. J., Dynamic covalent polymers. *J Polym Sci A Polym Chem* **2016**, 54 (22), 3551-3577.
9. Biermann, U.; Friedt, W.; Lang, S.; Lühs, W.; Machmüller, G.; Metzger, J. O.; Rüschen, Klaas, M.; Schäfer, H. J.; Schneider, M. P., New Syntheses with Oils and Fats as Renewable Raw Materials for the Chemical Industry. *Angewandte Chemie International Edition* **2000**, 39 (13), 2206-2224.
10. Hammond, E. W., VEGETABLE OILS | Types and Properties. In *Encyclopedia of Food Sciences and Nutrition* (Second Edition), Caballero, B., Ed. Academic Press: Oxford, **2003**; pp 5899-5904.
11. Xia, Y.; Larock, R. C., Vegetable oil-based polymeric materials: synthesis, properties, and applications. *Green Chemistry* **2010**, 12 (11), 1893-1909.
12. Kim, J. R.; Sharma, S., The development and comparison of bio-thermoset plastics from epoxidized plant oils. *Industrial Crops and Products* **2012**, 36 (1), 485-499.
13. Hong, J.; Radojčić, D.; Ionescu, M.; Petrović, Z. S.; Eastwood, E., Advanced materials from corn: isosorbide-based epoxy resins. *Polymer Chemistry* **2014**, 5 (18), 5360-5368.
14. Noè, C.; Malburet, S.; Bouvet-Marchand, A.; Graillot, A.; Loubat, C.; Sangermano, M., Cationic photopolymerization of bio-renewable epoxidized monomers. *Progress in Organic Coatings* **2019**, 133, 131-138.

15. Ma, S.; Liu, X.; Jiang, Y.; Tang, Z.; Zhang, C.; Zhu, J., Bio-based epoxy resin from itaconic acid and its thermosets cured with anhydride and comonomers. *Green Chemistry* **2013**, 15 (1), 245-254.
16. Czub, P., Synthesis of high-molecular-weight epoxy resins from modified natural oils and Bisphenol A or Bisphenol A-based epoxy resins. *Polym. Adv. Technol.* **2009**, 20 (3), 194.
17. Sinadinović-Fišer, S.; Janković, M.; Petrović, Z. S., Kinetics of in situ epoxidation of soybean oil in bulk catalyzed by ion exchange resin. *Journal of the American Oil Chemists' Society* **2001**, 78 (7), 725-731.
18. Danov, S. M.; Kazantsev, O. A.; Esipovich, A. L.; Belousov, A. S.; Rogozhin, A. E.; Kanakov, E. A., Recent advances in the field of selective epoxidation of vegetable oils and their derivatives: a review and perspective. *Catalysis Science & Technology* **2017**, 7 (17), 3659-3675.
19. Tran, T.-N.; Di Mauro, C.; Graillot, A.; Mija, A., Chemical Reactivity and the Influence of Initiators on the Epoxidized Vegetable Oil/Dicarboxylic Acid System. *Macromolecules* **2020**, 53 (7), 2526-2538.
20. Di Mauro, C.; Tran, T.-N.; Graillot, A.; Mija, A., Enhancing the Recyclability of a Vegetable Oil-Based Epoxy Thermoset through Initiator Influence. *ACS Sustainable Chemistry & Engineering* **2020**, 8 (20), 7690-7700.
21. Di Mauro, C.; Genua, A.; Mija, A., Building thermally and chemically reversible covalent bonds in vegetable oils-based epoxy thermosets. Influence of epoxy-hardener ratio to promote recyclability. *Materials Advances* **2020**, 1 (6), 1788-1798.
22. Bowman, C. N.; Kloxin, C. J., Covalent Adaptable Networks: Reversible Bond Structures Incorporated in Polymer Networks. *Angewandte Chemie International Edition* **2012**, 51 (18), 4272-4274.
23. Azcune, I.; Odriozola, I., Aromatic disulfide crosslinks in polymer systems: Self-healing, reprocessability, recyclability and more. *European Polymer Journal* **2016**, 84, 147-160.
24. Chen, J.-H.; Hu, D.-D.; Li, Y.-D.; Meng, F.; Zhu, J.; Zeng, J.-B., Castor oil derived poly(urethane urea) networks with reprocessability and enhanced mechanical properties. *Polymer* **2018**, 143, 79-86.
25. Ng, F.; Bonnet, L.; David, G.; Caillol, S., Novel biobased and food contact epoxy coatings for glass toughening applications. *Progress in Organic Coatings* **2017**, 109, 1-8.
26. Lee, H.; Neville, K., Handbook of epoxy resins. McGraw-Hill Inc., New York, **1967**.
27. La Scala, J.; Wool, R. P., Effect of FA composition on epoxidation kinetics of TAG. *Journal of the American Oil Chemists' Society* **2002**, 79 (4), 373-378.
28. Morgan, R. J. In Structure-property relations of epoxies used as composite matrices, Epoxy Resins and Composites I, Berlin, Heidelberg, 1985//; Springer Berlin Heidelberg: Berlin, Heidelberg, **1985**; pp 1-43.
29. Jenkins, A. D., Photoinitiators for free radical cationic and anionic photopolymerisation, 2<sup>nd</sup> edition J V Crivello and K Dietliker Edited by G Bradley John Wiley & Sons, Chichester **1998**. *Polymer International* **2000**, 49 (12), 1729-1729.
30. Caillol, S.; Desroches, M.; Boutevin, G.; Loubat, C.; Auvergne, R.; Boutevin, B., Synthesis of new polyester polyols from epoxidized vegetable oils and biobased acids. *Eur. J. Lipid Sci. Technol.* **2012**, 114 (12), 1447.
31. Zeng, R.-T.; Wu, Y.; Li, Y.-D.; Wang, M.; Zeng, J.-B., Curing behavior of epoxidized soybean oil with biobased dicarboxylic acids. *Polymer Testing* **2017**, 57, 281-287.
32. Falco, G.; Sbirrazzuoli, N.; Mija, A., Biomass derived epoxy systems: From reactivity to final properties. *Materials Today Communications* **2019**, 21, 100683.
33. Gobin, M.; Loulergue, P.; Audic, J.-L.; Lemiègre, L., Synthesis and characterisation of bio-based polyester materials from vegetable oil and short to long chain dicarboxylic acids. *Industrial Crops and Products* **2015**, 70, 213-220.
34. Pin, J. M.; Sbirrazzuoli, N.; Mija, A., From epoxidized linseed oil to bioresin: An overall approach of epoxy/anhydride cross-linking. *ChemSusChem* **2015**, 8, 1232.
35. Ding, C.; Tian, G.; Matharu, A., Adipic acid – glutaric anhydride – epoxidised linseed oil biobased thermosets with tunable properties. *Materials Today Communications* **2016**, 7, 51-58.
36. Pin, J.-M.; Guigo, N.; Vincent, L.; Sbirrazzuoli, N.; Mija, A., Copolymerization as a Strategy to Combine Epoxidized Linseed Oil and Furfuryl Alcohol: The Design of a Fully Bio-Based Thermoset. *ChemSusChem* **2015**, 8 (24), 4149-4161.
37. Parada Hernandez, N. L.; Bahú, J. O.; Schiavon, M. I. R. B.; Bonon, A. J.; Benites, C. I.; Jardini, A. L.; Maciel Filho, R.; Wolf Maciel, M. R., (Epoxidized castor oil – citric acid) copolyester as a candidate polymer for biomedical applications. *Journal of Polymer Research* **2019**, 26 (6), 149.
38. Gerbase, A. E.; Petzhold, C. L.; Costa, A. P. O., Dynamic mechanical and thermal behavior of epoxy resins based on soybean oil. *Journal of the American Oil Chemists' Society* **2002**, 79 (8), 797-802.

## Chapter 4

39. Wang, R.; Schuman, T. P., Vegetable oil-derived epoxy monomers and polymer blends: A comparative study with review. *eXPRESS Polymer Letters* **2013**, Vol.7, No.3, 272–292.
40. Imbernon, L.; Oikonomou, E. K.; Norvez, S.; Leibler, L., Chemically crosslinked yet reprocessable epoxidized natural rubber via thermo-activated disulfide rearrangements. *Polymer Chemistry* **2015**, 6 (23), 4271-4278.
41. Supanchaiyamat, N.; Shuttleworth, P. S.; Hunt, A. J.; Clark, J. H.; Matharu, A. S., Thermosetting resin based on epoxidised linseed oil and bio-derived crosslinker. *Green Chemistry* **2012**, 14 (6), 1759-1765.
42. Liu, W.; Xie, T.; Qiu, R., Biobased Thermosets Prepared from Rigid Isosorbide and Flexible Soybean Oil Derivatives. *ACS Sustainable Chemistry & Engineering* **2017**, 5 (1), 774-783.
43. Pan, X.; Sengupta, P.; Webster, D. C., High Biobased Content Epoxy–Anhydride Thermosets from Epoxidized Sucrose Esters of Fatty Acids. *Biomacromolecules* **2011**, 12 (6), 2416-2428.
44. Pan, X.; Webster, D. C., Impact of Structure and Functionality of Core Polyol in Highly Functional Biobased Epoxy Resins. *Macromolecular Rapid Communications* **2011**, 32 (17), 1324-1330.
45. Wang, Z.; Yuan, L.; Ganewatta, M. S.; Lamm, M. E.; Rahman, M. A.; Wang, J.; Liu, S.; Tang, C., Plant Oil-Derived Epoxy Polymers toward Sustainable Biobased Thermosets. *Macromolecular Rapid Communications* **2017**, 38 (11), 1700009.
46. Zhou, J.; Xu, K.; Xie, M.; Wu, H.; Hua, Z.; Wang, Z., Two Strategies to precisely tune the mechanical properties of plant oil-derived epoxy resins. *Composites Part B: Engineering* **2019**, 173, 106885.
47. Ma, Z.; Wang, Y.; Zhu, J.; Yu, J.; Hu, Z., Bio-based epoxy vitrimers: Reprocessability, controllable shape memory, and degradability. *Journal of Polymer Science Part A: Polymer Chemistry* **2017**, 55 (10), 1790-1799.
48. Zhou, F.; Guo, Z.; Wang, W.; Lei, X.; Zhang, B.; Zhang, H.; Zhang, Q., Preparation of self-healing, recyclable epoxy resins and low-electrical resistance composites based on double-disulfide bond exchange. *Composites Science and Technology* **2018**, 167, 79-85.
49. Ma, S.; Kovash, C. S.; Webster, D. C., Effect of solvents on the curing and properties of fully bio-based thermosets for coatings. *Journal of Coatings Technology and Research* **2017**, 14 (2), 367-375.
50. Supanchaiyamat, N.; Hunt, A. J.; Shuttleworth, P. S.; Ding, C.; Clark, J. H.; Matharu, A. S., Bio-based thermoset composites from epoxidised linseed oil and expanded starch. *RSC Advances* **2014**, 4 (44), 23304-23313.
51. Ruiz de Luzuriaga, A.; Martin, R.; Markaide, N.; Rekondo, A.; Cabañero, G.; Rodríguez, J.; Odriozola, I., Epoxy resin with exchangeable disulfide crosslinks to obtain reprocessable, repairable and recyclable fiber-reinforced thermoset composites. *Materials Horizons* **2016**, 3 (3), 241-247.
52. Takahashi, A.; Ohishi, T.; Goseki, R.; Otsuka, H., Degradable epoxy resins prepared from diepoxide monomer with dynamic covalent disulfide linkage. *Polymer* **2016**, 82, 319-326.
53. Lei, Z. Q.; Xiang, H. P.; Yuan, Y. J.; Rong, M. Z.; Zhang, M. Q., Room-Temperature Self-Healable and Remoldable Cross-linked Polymer Based on the Dynamic Exchange of Disulfide Bonds. *Chemistry of Materials* **2014**, 26 (6), 2038-2046.
54. Montarnal, D.; Capelot, M.; Tournilhac, F.; Leibler, L., Silica-like malleable materials from permanent organic networks. *Science* **2011**, 334 (6058), 965.
55. Luo, Q.; Liu, M.; Xu, Y.; Ionescu, M.; Petrović, Z. S., Thermosetting Allyl Resins Derived from Soybean Oil. *Macromolecules* **2011**, 44 (18), 7149-7157.
56. Faye, I.; Decostanzi, M.; Ecochard, Y.; Caillol, S., Eugenol bio-based epoxy thermosets: from cloves to applied materials. *Green Chemistry* **2017**, 19 (21), 5236-5242.
57. Flory, P. J., Principles of polymer chemistry. Cornell University Press: **1953**.
58. Treloar, L. R. G., The physics of rubber elasticity. Oxford University Press, USA: **1975**.
59. Norton, G. A.; Devlin, S. L., Determining the modern carbon content of biobased products using radiocarbon analysis. *Bioresource Technology* **2006**, 97 (16), 2084-2090.
60. Matějka, L.; Pokorný, S.; Dušek, K., Acid curing of epoxy resins. A comparison between the polymerization of diepoxide-diacid and monoepoxide-cyclic anhydride systems. *Die Makromolekulare Chemie* **1985**, 186 (10), 2025-2036.
61. Onn, M.; Nor, H.; Khairuddin, W. A., Development of Solid Rocket Propellant based on Isophorone Diisocyanate – Hydroxyl Terminated Natural Rubber Binder. *Jurnal Teknologi* **2014**, 69.

## Electronic Supplementary Information (ESI)

### Experimental Section

#### Materials

The general material structures used in this - study are shown in Chart 1. The new bio-renewable epoxidized monomers are classified based on the epoxy content tabulated in Table 1. Chart 1 (A) exhibits the general structure of the EVOs and epoxidized castor oil (ECO) (B).

ELO and ESO were obtained by Valtris Chemicals - Specialty Chemicals (England) while the new EVOs (SP-3S-30-005 and SP-3S-30-006) were provided by SPECIFIC POLYMERS (France). Their chemical characteristics are reported in Table S1.

The hardener and the initiators are commercially

available and were purchased from Sigma-Aldrich and used as received without further purification: DTBA (2,2'-dithiodibenzoic acid, 95%) (C), IM (imidazole, 99%) (D), 1-MI (1-methylimidazole, 99 %) (E) and DMBA (N, N-dimethylbenzylamine, 99%) (F).

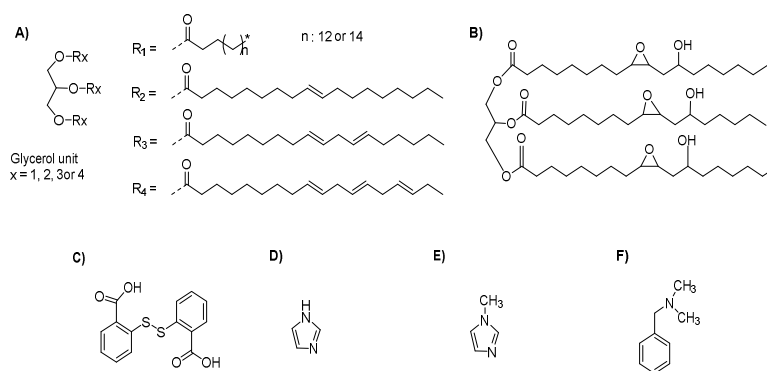


**Chart 1.** Structures of selected reagents

**Table ESI 1.** Characteristics of the selected reagents

EVOs	EVOs Acronym	Epoxy Index (meq.g <sup>-1</sup> )	Mw EVO (g.mol <sup>-1</sup> )
Karanja	EKRNO	2.77	892.5
St John's Wort Oil	ESJWO	2.97	932.3
Peanut	EPO	3.35	937.7
Rapeseed	ERPO	3.99	948.8
Soybean	ESO	4.20	949.8
Rose Hip Seed	ERHO	4.7	956.9
Safflower	ESFO	4.93	960.2
Grapeseed	EGRO	4.94	960.3
Camelina	ECMO	5.29	965.3
Linseed	ELO	5.61	969.9
Hemp	EHO	6.09	976.7
Perilla	EPLO	6.77	986.4
Castor	ECO	2.85	980.8
Hardener/Initiator	Hardener/Initiator Acronym	Melting Point (°C)	Mw (g.mol <sup>-1</sup> )
2,2'-Dithiodibenzoic acid	DTBA	287 – 290	306.35
Imidazole	IM	81 – 91	68.07
1-Methylimidazole	1-MI	- 60	82.10
N, N-Dimethylbenzylamine	DMBA	43 – 45	149.19

#### Samples preparation

The homopolymerization reactions were carried out using the optimized curing program determined by the help of DSC studies. The EVOs thermosets were obtained by isothermal curing in an oven, at 180 °C for

## Chapter 4

24 hours. The copolymerization formulations were carried out by mixing the EVO monomer with the DTBA at a 1:1 molar ratio between epoxy and acid groups, according with Dusek *et al.*<sup>1</sup> The selected initiator was added at 1 wt.% and mixed at 80 °C with the previous mixture. The curing and post-curing protocols for the preparation of the EVOs thermosets were determined based on DSC study of reactivity and are given in Table ESI 4.

### Characterization techniques

#### Differential Scanning Calorimetry (DSC)

The EVOs homopolyzation and copolymerization reactions were carried out on a Mettler-Toledo DSC 3 instrument equipped with STAR<sup>®</sup> software. The samples (about 10 - 15 mg) were placed in 100 µL aluminium crucibles. The heating rate for all of scanning runs was 10 °C.min<sup>-1</sup>. The DSC technique was used also to study the glass transition of the obtained thermosets using the same heating rate, under air (100 mL.min<sup>-1</sup>), over a temperature range from - 80 to 180 °C.

#### Fourier-transformed infrared spectroscopy (FT-IR)

FTIR analyses were performed using a Thermo Scientific Nicolet iS50 FT-IR spectrometer with a deuterated L-aniline doped triglycine sulfate (DLaTGS) detector in attenuated total reflectance (ART) mode. The absorption bands were recorded in the range of 4000-525 cm<sup>-1</sup> and 4 cm<sup>-1</sup> resolution. The data were analysed using the OMNIC software. The percentage of the functional group conversion is defined by the Equation ESI 1:

$$\% = \frac{\left(\frac{A_{823}}{A_{1586}}\right)_0 - \left(\frac{A_{823}}{A_{1586}}\right)_t}{\left(\frac{A_{823}}{A_{1586}}\right)_0} * 100 \quad (\text{ESI 1})$$

where area absorbance peaks were calculated at the initial time ( $A_0$ ) and at the end of the curing protocol ( $A_t$ ). The peak at 823 cm<sup>-1</sup> corresponds to oxirane C-O groups and that at 1586 cm<sup>-1</sup> is the reference band which belongs to the  $\delta_{C-C}$  of the aromatic signal.

#### Thermogravimetric Analysis (TGA)

TGA measurements were carried out on a Mettler-Toledo TGA 2. The microbalance has a precision of ± 0.1 mg. Samples of about 10 mg were placed into 70 µL alumina pans. To characterize the thermal stability of the thermosets, the samples were heated under air flow, 50 ml.min<sup>-1</sup> at 10 °C.min<sup>-1</sup> from 25 to 1000 °C.

The statistic heat-resistant index temperature ( $T_S$ ) is characteristic of the thermal stability of the cured resins was calculated according with the Equation ESI 2:

$$T_S = 0.49 \cdot [T_{5\%} + 0.6 \cdot (T_{30\%} - T_{5\%})] \quad (\text{ESI 2})$$

where  $T_{5\%}$  and  $T_{30\%}$  are the temperatures at respectively 5 and 30 % weight loss.

#### Dynamic Mechanical Analysis (DMA)

DMA were carried out on Mettler-Toledo DMA 1 instrument, equipped with STAR<sup>®</sup> software for curve analysis. The analysed samples prepared according with the curing protocol in Table ESI 4 had rectangular dimensions of 30 x 7 x 2 mm<sup>3</sup> (length x width x thickness). Elastic modulus values ( $E'$ ) and damping factors ( $\tan \delta$ ) were collected at 3 °C.min<sup>-1</sup> heating rate from -80 to 170 °C for the copolymers and from - 80 to 80 °C for the homolymers, at 1 Hz frequency. The DMA was operated using tension method. The glass transition was assigned at the maximum of damping factor ( $\tan \delta = E''/E'$ ).

Crosslink density for the EVOs-based thermosets were calculated by the Equation ESI 3, according to Flory theory<sup>2</sup> of the rubber-elasticity:

$$\nu = \frac{E'}{3RT} \quad (\text{ESI 3})$$

where  $E'$  is the storage modulus of the thermoset in the rubbery plateau region at  $T_g + 50$  °C,  $R$  is the gas constant and  $T$  is the absolute temperature in Kelvin.

### Tensile Test

The tensile strength and the Young's modulus of the EVOs / DTBA thermosets were determined by tensile tests according to standard ISO 527-141 and ASTM D638-0842 on a mechanical universal testing machine Instron, model 3365, controlled by BlueHill Lite software developed by Instron (Norwood, MA, USA). The analysis were performed using a crosshead speed of 10 mm min<sup>-1</sup> on samples of dimensions 75 × 10 × 2 mm<sup>3</sup> (length × width × thickness). For each formulation, five samples were tested to evaluate the average calculations of mechanical properties (Young's modulus, tensile strength and elongation at break).

### Density calculation

Density was done by measuring the volume of each EVOs copolymer samples and its weight using a Mettler Toledo ML 3002T precision balance (± 0.0001 g).

### Solvent Stability

The stability in solvent of EVOs copolymers was studied in methanol, ethanol, acetone, toluene and solutions of 1 N NaOH and HCl for 72 hours at room temperature in order to confirm the complete crosslinking and to evaluate the samples resistance in these solvents. Toluene was chosen as a good solvent for the swelling test for 24 hours, the swelling factor ( $Q_m$ ) being calculated according to the Equation ESI 6. Swelling measurements are often used to measure the crosslink density of the cured materials.

Toluene was used to determine the materials crosslink density by using Flory-Rehner theory<sup>2-3</sup> according with the Equation ESI 4:

$$\nu = \frac{\ln(1-\nu_{2,s}) + \nu_{2,s} + \chi_1 \nu_{2,s}^2}{\nu_1 \left( \frac{\nu_{2,s}}{2} - \frac{1}{3} \sqrt{\nu_{2,s}} \right)} \quad (\text{ESI 4})$$

where  $\nu_1$  is the molar volume of the solvent (for toluene  $\nu_1 = 106.27$  cm<sup>3</sup>.mol<sup>-1</sup>, calculated as ratio between the molecular weight and the density of the solvent),  $\chi_1$  is the Flory Huggins polymer - solvent interaction parameter that for toluene is ~ 0.391<sup>4</sup> and  $\nu_{2,s}$  is calculated by Equation ESI 5:

$$\nu_{2,s} = \frac{\frac{1}{\rho_{polymer}}}{\frac{Q_m}{\rho_{solvent}} + \frac{1}{\rho_{polymer}}} \quad (\text{ESI 5})$$

where  $\rho_{polymer}$  and  $\rho_{solvent}$  are the densities of the polymer and of the solvent. The swelling factor  $Q_m$  is given by the ratio:

$$Q_m = \frac{w_s - w_d}{w_s} \quad (\text{ESI 6})$$

with  $w_s$  and  $w_d$  respectively the swelled mass and the swelled dry mass at the equilibrium. The test was performed at room temperature, keeping the rectangular specimens in toluene for 2 days. The complete dissolution of the thermosets was tested in DMF solution of 5 wt.% of 1-4 dithiothreitol for 24 hours at 50 °C. All the solvent tests were conducted on small rectangular 10 x 10 x 2 mm<sup>3</sup> specimens.



Figure ESI 1. TGA analyses of the EVO monomers in air at 10 °C min<sup>-1</sup> heating

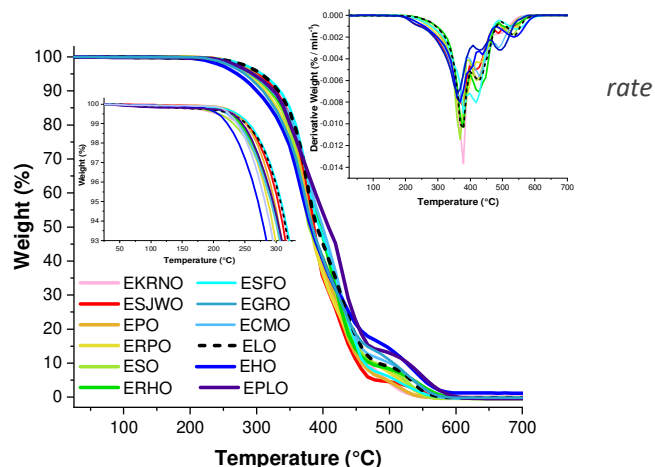
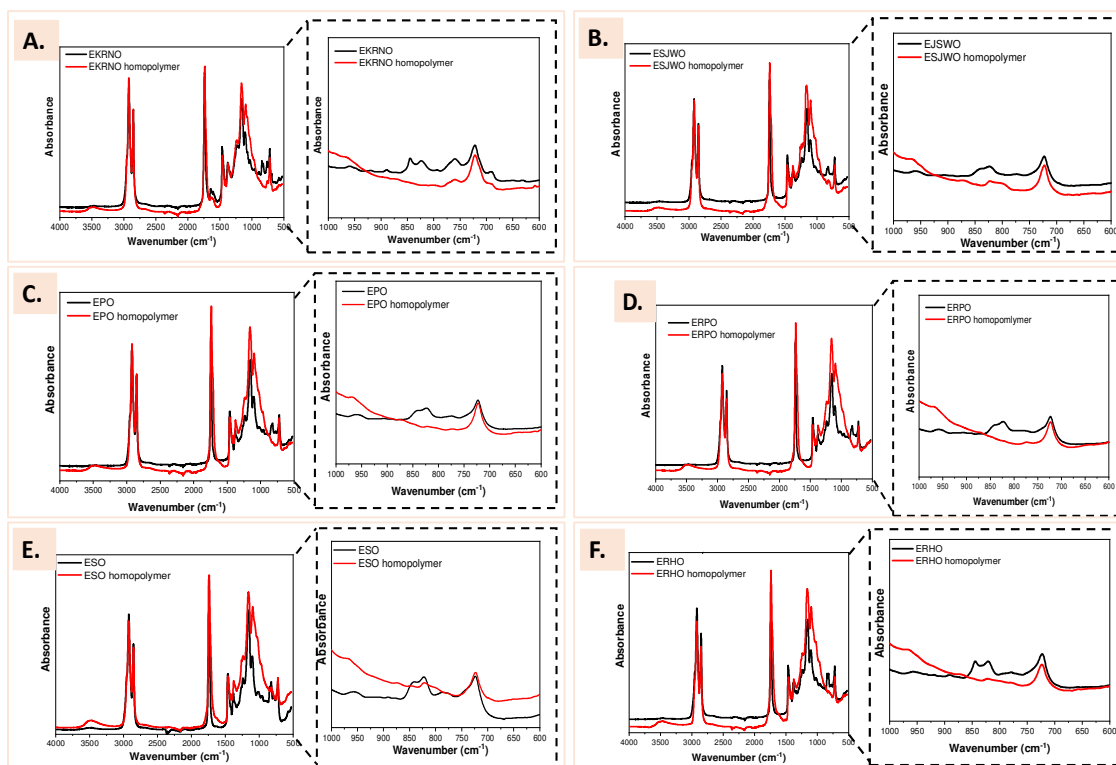


Table ESI 2.  $T_{5\%}$  and  $T_{30\%}$  determined by TGA analysis for the starting EVO monomers. Determination of the reaction interval and temperature of the reaction peak ( $T_{peak}$ ) by DSC

EVOs label	TGA $T_{5\%}$ (°C)	TGA $T_{30\%}$ (°C)	DSC $T_{peak}$ (°C)	DSC Reaction interval (°C)	$\Delta H$ (J/g)
EKRNO	305 ± 1	415 ± 1	245 ± 2	197 – 270	14
ESJWO	300 ± 1	410 ± 1	217 ± 1	176 – 247	12
EPO	300 ± 1	415 ± 1	219 ± 1	170 – 250	12
ERPO	291 ± 1	415 ± 1	223 ± 2	174 – 246	21
ESO	300 ± 1	425 ± 1	213 ± 2	169 – 239	43
ERHO	295 ± 1	415 ± 1	223 ± 1	172 – 244	19
ESFO	305 ± 1	425 ± 1	225 ± 1	179 – 248	12
EGRO	285 ± 1	425 ± 1	212 ± 1	160 – 231	26
ECMO	295 ± 1	430 ± 1	221 ± 1	175 – 261	17
ELO	300 ± 1	428 ± 1	221 ± 2	156 – 234	54
EHO	271 ± 1	425 ± 1	221 ± 1	156 – 245	16
EPLO	295 ± 1	430 ± 1	223 ± 1	161 – 236	29



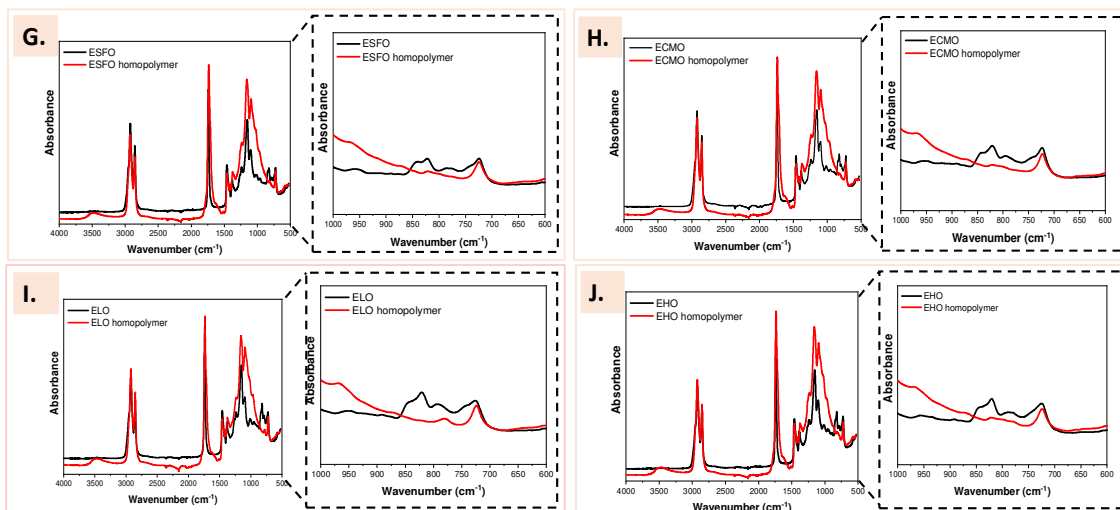


Figure ESI 2. FT-IR analysis of (A) EKRNO, (B) ESJWO, (C) EPO, (D) ERPO, (E) ESO, (F) ERHO, (G) ESFO, (H) ECMO, (I) ELO and (J) EPLO monomers and thermoset materials

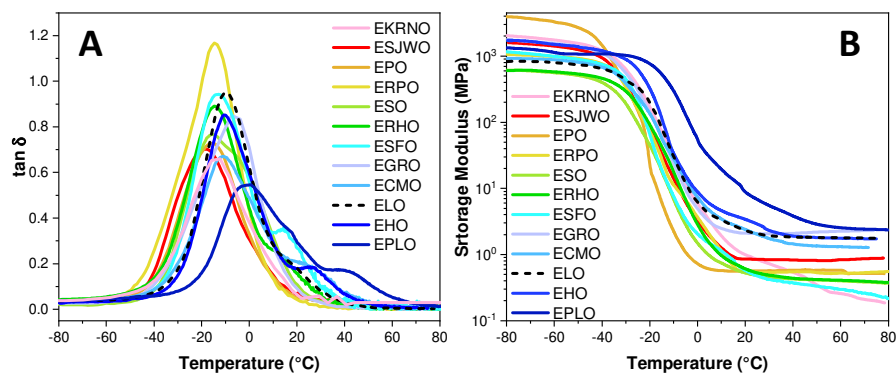
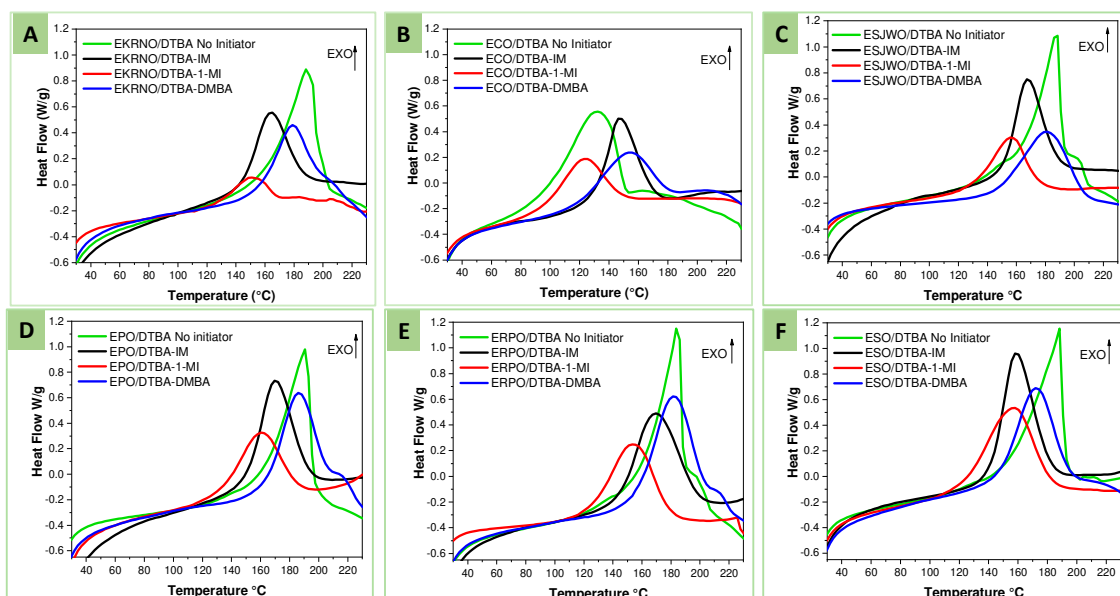
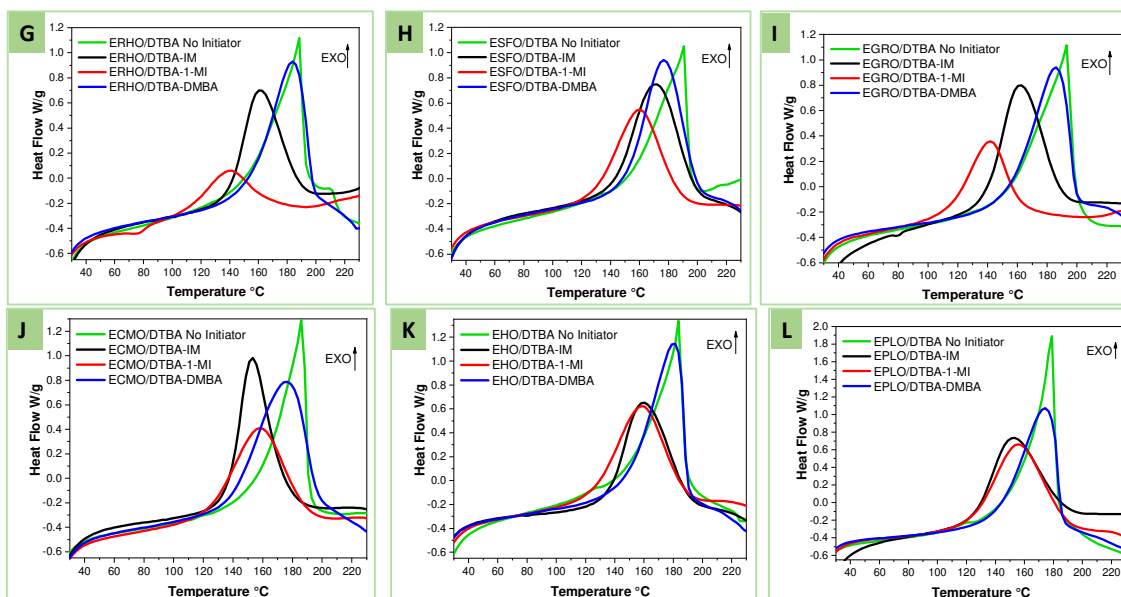


Figure ESI 3.  $\tan \delta$  and Storage Modulus vs. temperature of EVOs materials determined by DMA





**Figure ESI 4.** DSC thermograms of the thermo-curing of EVOs/DTBA systems without initiator or and catalysed by IM, 1-MI and DMBA: (A) EKRNO, (B) ECO, (C) EJSWO, (D) EPO, (E) ERPO, (F) ESO, (G) ERHO, (H) ESFO, (I) EGRO, (J) ECMO, (K) EHO, (L) EPLO

**Table ESI 3.** DSC results of EVOs/DTBA copolymerization with or without initiator: reaction enthalpy, interval and temperature of the reaction peak ( $T_{peak}$ ) EVOs

EVOs/DTBA	Initiator	$\Delta H$ (J/g)	$T_{peak}$ (°C)	Reaction Interval (°C)	EVOs/DTBA	Initiator	$\Delta H$ (J/g)	$T_{peak}$ (°C)	Reaction Interval (°C)
EKRNO	No Initiator	134	188	166 – 198	ERHO	No Initiator	177	188	168 – 193
	IM	84	164	145 – 186		IM	155	161	140 – 189
	1-MI	42	150	130 – 166		1-MI	127	153	118 – 176
	DMBA	74	179	157 – 199		DMBA	168	175	150 – 207
ECO	No Initiator	146	131	75 – 151	ESFO	No Initiator	151	191	158 – 194
	IM	109	147	130 – 170		IM	172	158	142 – 180
	1-MI	70	123	95 – 148		1-MI	169	156	122 – 179
	DMBA	80	154	120 – 180		DMBA	185	179	143 – 193
ESJWO	No Initiator	144	188	166 – 191	EGRO	No Initiator	225	193	165 – 198
	IM	108	168	154 – 186		IM	175	162	139 – 182
	1-MI	86	159	131 – 182		1-MI	90	142	115 – 161
	DMBA	125	187	138 – 213		DMBA	181	186	155 – 199
EPO	No Initiator	160	192	162 – 196	ECMO	No Initiator	201	187	168 – 191
	IM	112	171	151 – 192		IM	188	153	136 – 176
	1-MI	120	156	131 – 182		1-MI	180	149	113 – 175
	DMBA	145	184	158 – 209		DMBA	219	177	151 – 203
ERPO	No Initiator	177	185	162 – 189	EHO	No Initiator	195	184	169 – 188
	IM	138	164	147 – 184		IM	194	160	135 – 190
	1-MI	116	150	122 – 179		1-MI	191	160	125 – 189
	DMBA	125	178	157 – 207		DMBA	189	171	143 – 196
ESO	No Initiator	177	188	166 – 192	EPLO	No Initiator	217	179	167 – 183
	IM	149	159	142 – 182		IM	207	152	126 – 187
	1-MI	135	155	115 – 195		1-MI	201	148	112 – 184
	DMBA	155	168	164 – 190		DMBA	227	173	141 – 209

Table ESI 4. Curing and post-curing conditions for EVOs/DTBA/IM systems

EVOs/DTBA/IM systems	Curing Condition	Post-Curing Condition	EVOs/DTBA/IM systems	Curing Condition	Post-Curing Condition
EKRNO	150°C – 120 min	180 °C – 120 min	ESFO	140°C – 60 min	180°C – 30 min
ECO	130°C – 60 min	170°C – 30 min	EGRO	140°C – 60 min	180°C – 30 min
ESJWO	150°C – 60 min	180°C – 60 min	ECMO	130°C – 60 min	170°C – 30 min
EPO	140°C – 60 min	180 °C – 60 min	ELO	130°C – 60 min	170°C – 30 min
ERPO	140°C – 60 min	180 °C – 30 min	EHO	130°C – 60 min	170°C – 30 min
ESO	140 °C – 60 min	180 °C – 30 min	EPLO	130°C – 60 min	170°C – 30 min
ERHO	140 °C – 60 min	180 °C – 30 min			

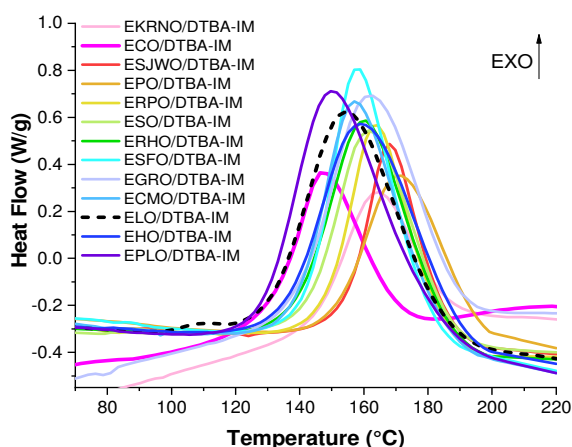
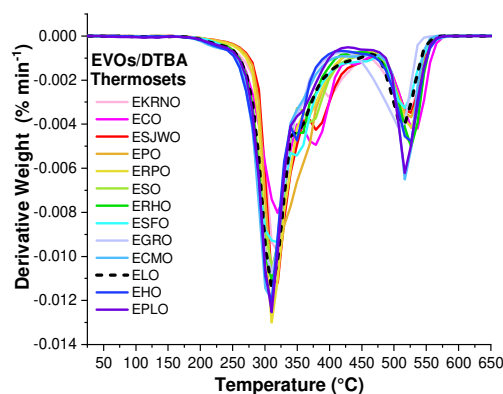
Figure ESI 5. DSC thermograms of EVOs/DTBA/IM copolymerizations during heating at 10 °C.min<sup>-1</sup>Figure ESI 6. DTG of EVOs/DTBA/IM thermosets during heating at 10 °C.min<sup>-1</sup> under air flow

Table ESI 5. Copolymerization conversion in % for EVOs/DTBA/IM systems

EVOs/DTBA/IM systems	Copolymerization Conversion %	EVOs/DTBA/IM systems	Copolymerization Conversion %
EKRNO	97	ESFO	82
ECO	92	EGRO	92
ESJWO	97	ECMO	89
EPO	95	ELO	99
ERPO	94	EHO	78
ESO	88	EPLO	85
ERHO	86		

Table ESI 6. TGA results obtained for EVOs/DTBA/IM thermosets during analysing under air at 10 °C.min<sup>-1</sup> heating rate: T<sub>5%</sub>, T<sub>30%</sub> and residual mass %

EVOs/DTBA/IM Thermosets	T <sub>5%</sub> (°C)	T <sub>30%</sub> (°C)	1 <sup>st</sup> Degradation Interval	1 <sup>st</sup> Degradation Peak (°C)	1 <sup>st</sup> Residue (%)	2 <sup>nd</sup> Degradation Interval	2 <sup>nd</sup> Degradation Peak (°C)	Final Residue (%)
EKRNO	285 ±1	400	220 – 470	315	19.4	470 – 650	530	0.54
ECO	275 ±1	400	210 – 500	318/350	20.8	500 – 650	538	0.24
ESJWO	290 ±1	393	220 – 480	315	17.1	480 – 650	525	0.85
EPO	285 ±1	375	230 – 470	312	17.9	470 – 650	530	0.42
ERPO	285 ±1	382	220 – 480	310	20.0	480 – 650	525	0.21
ESO	271 ±1	389	230 – 480	310	18.4	480 – 650	526	0.42
ERHO	275 ±1	382	210 – 470	307	22.9	470 – 650	523	0.29
ESFO	271 ±1	372	230 – 480	318	14.9	480 – 650	518	0.29
EGRO	265 ±1	375	210 – 470	310	25.5	470 – 650	520	0.17
ECMO	265 ±1	365	200 – 430	307	25.4	430 – 650	530	0.34
ELO	275 ±1	385	210 – 470	310	19.4	470 – 650	515	0.67
EHO	265 ±1	380	220 – 450	310	23.9	450 – 650	520	1.14
EPLO	265 ±1	382	200 – 450	308	24.9	450 – 650	530	0.92

Table ESI 7. Crosslinking density comparison

EVOs/DTBA/IM Thermosets	Epoxy content (meq.g <sup>-1</sup> )	Crosslink Density by rubber-elasticity Theory (DMA) (mmol.cm <sup>-3</sup> )	Crosslink Density by Flory-Rehner Theory (mmol.cm <sup>-3</sup> )
EKRNO	2.77	0.025	0.282
ECO	2.85	0.02	2.39
ESJWO	2.97	0.072	0.313
EPO	3.35	0.072	0.342
ERPO	3.99	0.087	0.362
ESO	4.20	0.075	0.547
ERHO	4.7	0.11	0.577
ESFO	4.93	0.31	0.723
EGRO	4.94	0.58	0.667
ECMO	5.29	0.43	0.652
ELO	5.61	1.25	1.38
EHO	6.09	0.75	0.75
EPLO	6.77	3.0	3.11

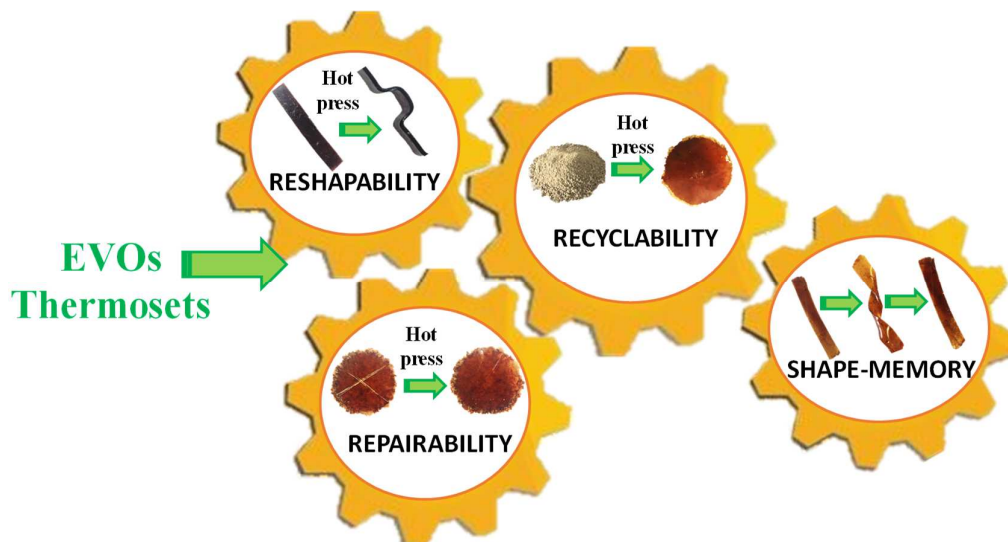
Table ESI 8. Bio-based content and carbon bio content % for EVOs/DTBA/IM thermosets in function of the epoxy content

EVOs/DTBA/IM Thermosets	Epoxy content (meq.g <sup>-1</sup> )	Bio-based Content (%)	Carbon bio-content (%)
EKRNO	2.77	79	91
ECO	2.85	76	90
ESJWO	2.97	77	90
EPO	3.35	75	89
ERPO	3.99	71	87
ESO	4.20	68	86
ERHO	4.7	67	85
ESFO	4.93	66	84
EGRO	4.94	66	84
ECMO	5.29	65	84
ELO	5.61	63	83
EHO	6.09	61	81
EPLO	6.77	58	80

1. Matějka, L.; Pokorný, S.; Dušek, K., Acid curing of epoxy resins. A comparison between the polymerization of diepoxide-diacid and monoepoxide-cyclic anhydride systems. *Die Makromolekulare Chemie* **1985**, 186 (10), 2025-2036.
2. Flory, P. J., *Principles of polymer chemistry*. Cornell University Press: **1953**.
3. Treloar, L. R. G., *The physics of rubber elasticity*. Oxford University Press, USA: **1975**.
4. Onn, M.; Nor, H.; Khairuddin, W. A., Development of Solid Rocket Propellant based on Isophorone Diisocyanate – Hydroxyl Terminated Natural Rubber Binder. *Jurnal Teknologi* **2014**, 69.

# Chapter 5

Recyclable, Repairable and Reshapable (3R) Thermoset materials with shape memory properties from bio-based epoxidized vegetable oils



## Chapter 5

This chapter is based on Di Mauro C., Malburet S., Graillot A. and Mija A. Recyclable, Repairable and Reshapable (3R) Thermoset Materials with Shape Memory Properties from Bio-based Epoxidized Vegetable Oils, 2020 (in peer review in *ACS Applied Bio Materials*).

### Abstract

The preparation of thermosets based on epoxidized vegetable oils (EVOs) has attracted great attention in recent years, however, most of them cannot be reprocessed once crosslinked. In the present work, epoxy thermosetting resins like-vitrimer with dynamic disulfide covalent bonds were prepared by copolymerizing twelve EVOs with 2,2'-dithiodibenzoic acid (DTBA), as hardener. Here, we show for the first time the reprocessability, reparability and recyclability properties of EVOs thermosets. The 3R abilities were evaluated in correlation with the EVOs epoxy contents, which influence the final thermo-mechanical properties of the recycled material. The virgin vs. recycled materials' comparison was studied by FT-IR, DSC, TGA and DMA, also comparing their swelling ability and high gel content. The study investigates, in addition, the excellent shape memory properties of the reprocessed EVOs / disulfide materials.

## 5.1 Introduction

Global plastics production was around 335 million tons in 2016, of which over 8.4 million tons of plastic waste was collected for recycling, and only 2% of total plastic waste was worldwide recycled, whereas in Europe around 31%.<sup>1-2</sup> Among the European Union countries the waste management strategies vary significantly,<sup>3</sup> unfortunately conducting to large landfill accumulations with harmful effects on water, land and all living species. To deal with these problems, in 2018, the European Commission communicated a strategy for plastics in a circular economy use, promoting the design and production of plastics with repairability and recycling skills and by limiting the production of plastic from fossils resources.<sup>4</sup>

A new class of thermoset networks incorporating dynamic covalent bonds have attracted a special attention in recent years. These thermoset materials renamed "covalent adaptive network polymers (CAN) by Bowman's group<sup>5-6</sup> combine the excellent mechanical properties of thermosets with the reprocessability of thermoplastics. This type of bonds undergoes splitting/reforming exchanges under external stimuli such as heat, light or pressure and thus impart repairability and recyclability to the thermoset materials. There are a variety of dynamic covalent reactions allowing the CANs: transesterification,<sup>7-10</sup> Michael reactions,<sup>11</sup> disulfides exchange,<sup>12-13</sup> Diels-Alder reactions<sup>14</sup> or even physical bonds exchange as the hydrogen-bonds exchange.<sup>15-16</sup> Based on transesterification reactions, Leibler *et al.*<sup>8</sup> defined the "vitrimers" as materials remaining crosslinked at high temperatures, showing a gradual change in viscosity<sup>17-18</sup> but concomitantly demonstrating a certain type of malleability or fluidity.<sup>17,19</sup> These materials showed a unique combination of solvent resistance, repairability and reprocessability. The first vitrimers were synthesized through the reaction between diglycidyl ether of bisphenol A (DGEBA) and a mixture of fatty dicarboxylic and tricarboxylic acids in presence of transesterification catalysts.<sup>19</sup> Following this idea, several researches introduced a series of vitrimer systems formed by the incorporation of different exchangeable bonds, such as disulfides linkage.<sup>13,20-21</sup> Odriozola *et al.*<sup>22</sup> synthesized a reinforced polymeric composite made with an epoxy resin based on DGEBA and 4-AFD (4-aminophenyl disulfide). The obtained material showed excellent mechanical properties and also 3R functionality, *i.e.* recyclability, repairability and reshapability. The relentless need for the use of sustainable materials has led to the development of bio-based vitrimers consisting of isosorbide-derived epoxy (IS-EPO) and aromatic diamines containing disulfide bonds. This resin, devised by Ma *et al.*<sup>23</sup> showed shape memory properties and high degradability in alkaline solutions. Zhan *et al.*<sup>24</sup> reacted a multifunctional epoxy monomer, based on bis (4-glycidylphenoxy) disulfide



## Chapter 5

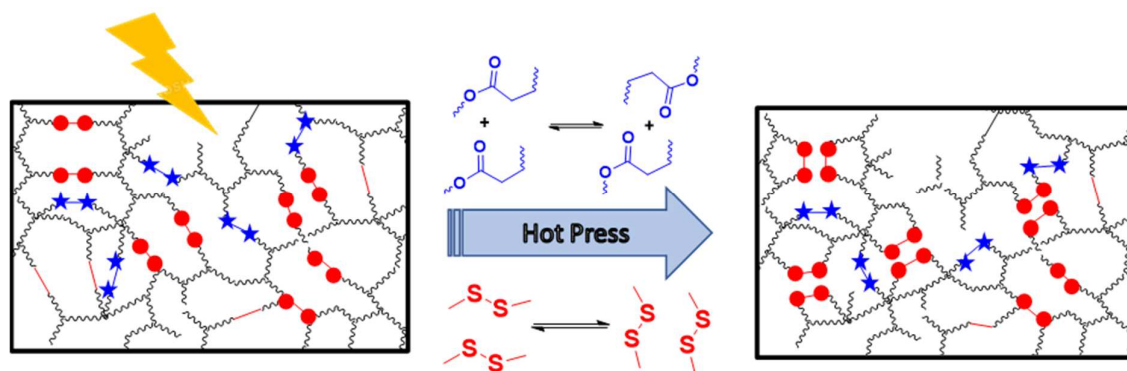
with 4-AFD, without catalyst, producing a thermoset with short relaxation times (9 s) and  $T_g$  above 130 °C. The obtained thermosets were reprocessed and the authors showed that the chemical and thermomechanical properties didn't dropped after 3 recycling cycles. Furthermore, the development of vitrimers focused on creating networks based on a double recycling synergy: the disulfides metathesis and the carboxylate transesterifications. Imbernon *et al.*<sup>25</sup> crosslinked the ENR (epoxidized natural rubber) with an aliphatic dicarboxylic acid containing disulfides (dithiodibutyric acid) showing how the resin is able to reorganize at temperatures above 150 °C, recovering most of its mechanical properties after reprocessing. Similarly, Chen *et al.*<sup>26</sup> prepared an epoxy vitrimer through the crosslinking of the same hardener and DGEBA.

Our team reported the crosslinking study of reference epoxidized linseed oil (ELO) and epoxidized soybean oil (ESO) with an aromatic carboxylic acid with disulfide bonds, by a high selective copolymerization reaction.<sup>27-28</sup> The 10 times reprocessed thermosets maintained almost unchanged their thermo-mechanical properties and retained a  $T_g$  value around 80 °C.<sup>29</sup> In another study, 12 cross-linked bio-based networks were prepared by reacting 12 EVOs with 2,2'-dithiodibenzoic acid (DTBA)<sup>30</sup>. In this work we investigate their 3R ability (recyclability, repairability and reshapability) and shape memory behavior. Even if several studies have been conducted on polymers with 3R ability,<sup>22,31-32</sup> to our knowledge, this is the first work on a large series of vegetable oils-based materials. The comparison between these EVOs, also between virgin and reprocessed materials were investigated by FTIR, DSC, TGA and DMA. A correlation was done between the swelling ability, the gel content and the epoxy content of the EVOs monomers. Furthermore, the properties of the recycled thermosets and also the shape memory properties, were explored.

### 5.2 Results and discussions

The thermoset resins once crosslinked cannot be recycled. Vitrimers, due to the intrinsic nature of the network, can undergo reversible crosslinks through bonds cleavage and reformation / exchange, guaranteeing a future benefit from economic and environmental point of view. Leibler *et al.*<sup>33</sup> displayed this behavior in DGEBA epoxy / acid and epoxy / anhydride thermoset networks in presence of transesterification catalysts, as zinc acetate ( $Zn(OAc)_2$ ), triazabicyclodecene (TBD) or a less efficient catalyst of transesterification, the triphenylphosphine ( $PPh_3$ ). Other authors, as Odriozola *et al.*<sup>13,22,31</sup> revealed the possibility to obtain reprocessed thermoset and elastomer materials made with disulfide crosslinkers.

Apart their work, few studies were dedicated on the properties of the recycled materials, especially those of EVOs thermosets. As previously shown,<sup>27-28</sup> the bio-based thermosets prepared with ELO or ESO and a dicarboxylic acid, as dynamic disulfide crosslinker, can be used to produce innovative networks with recycling abilities due to the synergy of two recycling mechanisms: disulfides exchange and transesterification reactions (Figure 1). Several authors<sup>17,19,22</sup> proved that the recyclability requires temperatures above the  $T_g$ , usually elevated temperature beyond the topology freezing transition temperature ( $T_v$ ), to allow the network to flow and to guarantee a successful reprocessing.



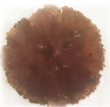











**Figure 1.** Network rearrangement mechanisms by dual exchange reactions: disulfide metathesis and carboxylate transesterification

The processing conditions for the synthesis of thermosetting resins are in strong relationship with their epoxy content as shown in Table 1 and schematized in Figure 2 for the series of 12 EVOs resins. As presented in Table 1, thermosets from the category 1 are needing milder recycling conditions due to a lower number of crosslinking nodes, that are spaced, correlated to lower  $T_g$ , so favoring an easier rearrangement during the reprocessing protocol. In contrast, increasing the EVOs epoxy content, so the thermosets glass transition, as for the thermosets from category 3, the high crosslink density required stronger conditions to recombine the network. The temperature, pressure and time necessary to obtain recycled thermosets were compared with those applied for DGEBA dynamic networks. Odriozola *et al.*<sup>22</sup> used for the DGEBA / 4-AFD vitrimer a reprocessing at 200 °C, 100 bars for 5 minutes. The same crosslinker, 4-AFD, was used by Ma *et al.*<sup>23</sup> to test the recyclability of IS-EPO (isosorbide-derived epoxy) by heating the samples at 100 °C for 1 hour (no pressure specification). Zhang *et al.*<sup>24</sup> reprocessed the bis(4-glycidioxyphenyl) disulfide / 4-AFD thermoset at 180 °C for 20 minutes and 200 bars. Chen *et al.*<sup>26</sup> showed that the system DGEBA/DTDA (4,4'-dithiodibutyric acid) catalysed by TBD (1,5,7-triazabicyclo[4.4.0]dec-5-ene) produced a vitrimer that can be efficiently reprocessed at 100 °C for 1 hour with full recovery of

## Chapter 5

mechanical properties at the end of the four cycles. The aliphatic chains of DTDA and the presence of DGEBA were reported as responsible for the milder recycling conditions compared to those used by Leibler *et al.*<sup>25</sup> for the recycling of ENR (Epoxidized Natural Rubber) / DTDA vitrimer at 180 °C for 40 minutes and 8 tons of pressure.

**Table 1.** Reprocessing conditions and visual aspect of EVOs/DTBA thermosets

EVOs in EVO/DTBA Thermosets	Epoxy Content (meq.g <sup>-1</sup> )	Recycling Conditions	Aspect	EVOs in EVO/DTBA Thermosets	Epoxy Content (meq.g <sup>-1</sup> )	Recycling Conditions	Aspect
	T <sub>g</sub> of thermoset (°C)				T <sub>g</sub> of thermoset (°C)		
EKRNO	2.77	120 °C 10 min 9 bars		ERHO	4.7	160 °C 10 min 60 bars	
	17 ± 1	53 ± 1					
ECO	2.85	140 °C 10 min 30 bars		ESFO	4.93	170 °C 10 min 60 bars	
	30 ± 1	48 ± 1					
ESJWO	2.97	140 °C 10 min 30 bars		EGRO	4.94	170 °C 10 min 60 bars	
	17 ± 1	50 ± 1					
EPO	3.35	150 °C 10 min 30 bars		ECMO	5.29	170 °C 10 min 60 bars	
	24 ± 1	64 ± 1					
ERPO	3.99	160 °C 10 min 30 bars		EHO	6.09	170 °C 10 min 60 bars	
	40 ± 1	62 ± 1					
ESO	4.42	160 °C 10 min 30 bars		EPLO	6.77	170 °C 10 min 60 bars	
	45 ± 1	91 ± 1					



**Figure 2.** Mechanical reprocessing of ESFO/DTBA thermoset by hot pressing

### 5.2.1 Mechanical recycling

#### 5.2.1.1 Investigation of the recycled thermosets

To investigate how the recycling affected the structure of thermosets network, FTIR comparative studies were performed on uncured thermosetting resins, on the virgin

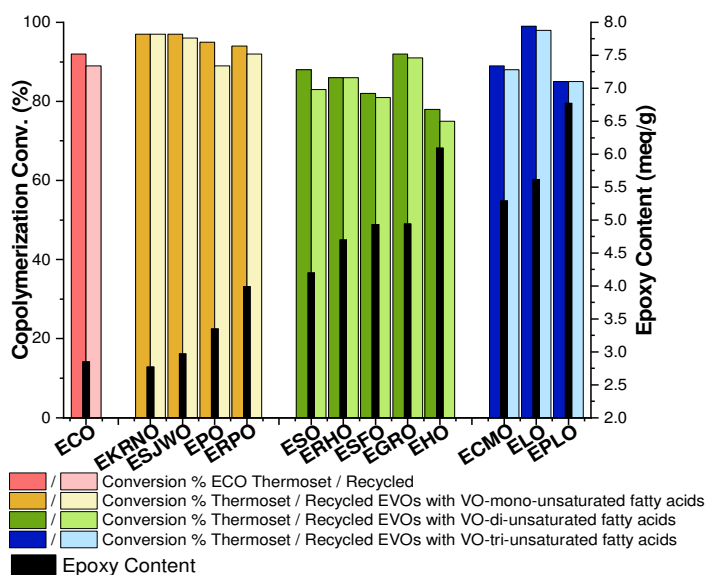


**Figure 3.** Epoxy conversion % for the virgin and recycled materials, determined by FTIR, correlated with the epoxy content of the EVOs

thermoset materials and the recycled one. Starting with the FTIR results, the copolymerization conversions were calculated according with Equation ESI 1. Figure ESI 1 and Table ESI 3 present and summarize the comparison for all the studied materials. The results presented in Figure ESI 1 highlight that the absorption of epoxy functions located at 823 and 847  $\text{cm}^{-1}$  disappeared in both virgin and recycled thermosets. The FTIR spectra do not show sensible difference between the virgin and recycled thermosets.

Moreover, as shown in Figure 3, ELO thermosets display high copolymerization conversion for both the virgin and the recycled materials (with 99 and 98% of conversion). Thereafter, the virgin and recycled EKRNO and EPLO thermosets show a constant conversion (before and after the reprocessing) while the EHO thermosets present the lowest copolymerization percentage, decreasing after the recycling from 78 to 75%. The other reprocessed thermosets show conversions superior to 90 %, with a small drop after recycling: EJSWO (from 97 to 96%), ERPO (from 94 to 92%), and EGRO (from 92 to 91%). Figure 3 summarizes the results of calculated epoxy conversions in function of the kind of EVOs and their epoxy content.

The reprocessed thermosets were analyzed also by dynamic DSC studies to determine the glass transition before and after recycling so to evaluate how the recycling affected the materials properties. Figure 4 (A) and Table ESI 4 display the obtained and compared results. We can notice a small decrease of  $T_g$  values after the recycling process in the majority of EVOs thermosets, excepting ERPO/DTBA system that kept the same glass transition value after the reprocessing. The most affected is the system with perilla oil, EPLO/DTBA resin and the thermosets of category 3, showing a decreasing of  $T_g$  from 91 to 84 °C. Hu *et al.*<sup>23</sup> reported also a decrease of the  $T_g$  for the isosorbide-derived epoxy systems cured with 4,4'-disulfanediyldianiline attributed to some loss in disulfide linkages. In our case, the decrease

of  $T_g$  can be associated to a higher amount of DTBA (so in disulfide linkages and ester linkages) in the formulation with EPLO that has the higher epoxy content. In consequence, it is possible that not all the dynamic bonds were reformed during the reprocessing, due to the high crosslink density of this category of EVOs. The other reprocessed resins present a reduction with only 1- 2 °C, as EKRNO and ESJWO (from 17 to 16 °C), ESO (from 45 to 43 °C), EGRO (from 50 to 48 °C) or ECO (from 30 to 29 °C). This result can be attributed to the lower network reticulation facilitating the bond reorganization and therefore the maintain of mechanical properties after recycling. Similar results were obtained by Zeng *et al.*<sup>34</sup> for castor oil/4-aminophenyl disulfide polyurethane networks.

The analysis of thermomechanical behaviour, performed by DMA, shows that each recycled sample (Figure ESI 3) displays an unique and clear  $\alpha$  transition. In Figure ESI 2 are illustrated the comparison of the  $\tan \delta$  and storage moduli,  $E'$ , for virgin and recycled resins. Figure 4 (B) confronts the values of  $\tan \delta$  correlated also with the epoxy content. From this figure we can notice that the  $\tan \delta$  values of recycled samples do not follow the same trend with the corresponding  $T_g$  results presented in Figure 4 (A). As example we can observe an increase of the  $\tan \delta$  after recycling for ESJWO, EPO, ERPO, ESO and ESFO thermosets, consistent with the results obtained for the ELO reference system.<sup>29</sup> In contrast, surprisingly, the other reprocessed resins exhibit a drop of  $\tan \delta$  values, the more evident decrease being measured the case of EPLO recycled vs. virgin resin. Moreover, the amplitudes of the damping factor show a sensible increasing after the recycling, especially for reprocessed resins with higher epoxy content. Also, all the reprocessed resins exhibited higher  $E'$  in the glassy state than the virgin thermosets. Higher moduli in both glassy state and at room temperature, were observed by Memon *et al.*<sup>35</sup> for the recycled vitrimers obtained by bio-based vanillin diglycidyl ether and petroleum-based counterpart (DGEBA) crosslinked with isophorone diamine (IPDA) in presence of ethylene glycol diglycidyl ether as reactive diluent. The authors explained that the degree of hardening of the two epoxy networks would increase slightly after heat press treatment. Recycled EVOs thermosets of the category 3 exhibited, in general, higher moduli than the virgin resins. The analysis of the crosslinking density applied using Flory's theory,<sup>36</sup> shows that after the reprocessing procedure, the crosslink densities of EVOs with higher epoxy content suffer a reduction, in contrast with EVOs with low epoxy content that have a constant or even increased crosslinking. As example, EPLO virgin resin has the higher crosslinking and performance properties, showing after recycling a loss of properties, and a decrease in crosslinking from 3.0 to 0.82 mmol.cm<sup>-3</sup>, according with the previous considerations regarding the difficulty of recycling high reticulated thermosets. In contrast,

some recycled EVOs thermosets, as ECO, ESJWO, EPO, ESO and ERHO, exhibited higher values compared with the virgin materials. This result can be explained probably by the initial lower crosslinking favoring an easier rearrangement of the network during the reprocessing.

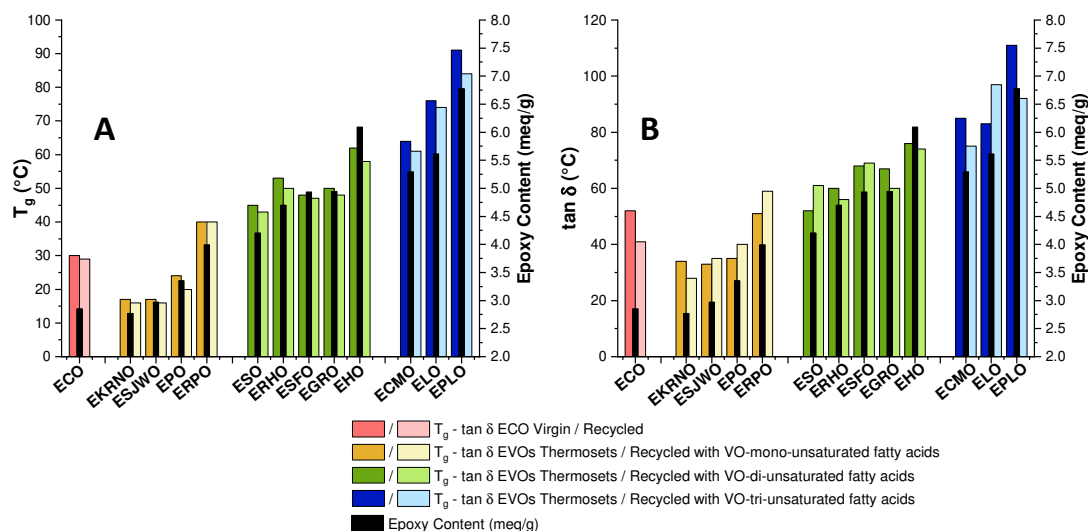


**Figure 4.** Glass transition values evaluated by dynamic DSC (A) and  $\tan \delta$  (B) measured by DMA for the virgin and the reprocessed thermosets. Correlation with the EVOs epoxy content

**Table 2.** DMA results obtained for virgin (V) and reprocessed (R) thermosets

EVO/DTBA	$\tan \delta$ (°C)		$*E'_G$ (MPa)		$**E'_R$ (MPa)		$***\nu$ mmol.cm <sup>-3</sup>	
	V	R	V	R	V	R	V	R
EKRNO	34 ± 1	28 ± 1	630	1950	0.21	0.14	0.025	0.017
ECO	52 ± 1	41 ± 1	850	1500	0.14	0.05	0.02	0.05
ESJWO	34 ± 1	35 ± 1	1145	1700	0.48	0.27	0.072	0.094
EPO	35 ± 1	40 ± 1	1900	1080	0.59	0.55	0.07	0.158
ERPO	51 ± 1	59 ± 1	1400	1080	0.82	1.24	0.09	0.158
ESO	52 ± 1	61 ± 1	900	2100	0.85	4.34	0.08	0.41
ERHO	60 ± 1	56 ± 1	1430	2100	0.92	2.71	0.11	0.26
ESFO	68 ± 1	69 ± 1	780	1920	3.13	0.32	0.31	0.27
EGRO	67 ± 1	60 ± 1	1090	1550	5.84	2.46	0.58	0.21
ECMO	85 ± 1	75 ± 1	400	2290	2.78	0.83	0.71	0.24
ELO	83 ± 1	97 ± 1	2550	2660	9.0	8.0	1.25	0.81
EHO	76 ± 1	74 ± 1	1200	2370	3.3	2.15	0.75	0.39
EPLO	111 ± 1	92 ± 1	630	2400	5.95	9.15	3.0	0.82

\* $E'_G$  - Storage modulus in glassy state; \*\* $E'_R$  - Storage modulus in rubbery state; \*\*\* Crosslinking density

The thermal stabilities of the virgin and recycled EVOs resins were investigated by thermogravimetric analysis under air atmosphere. The obtained results as the temperature at 5% weight-loss ( $T_{5\%}$ ) were displayed in Figure 5 and summarized in Table ESI 4. These results indicate that the recycling do not affect the thermal stabilities of the thermosets, as also presented in Figures ESI 3 where the thermograms of virgin and recycled resins are almost

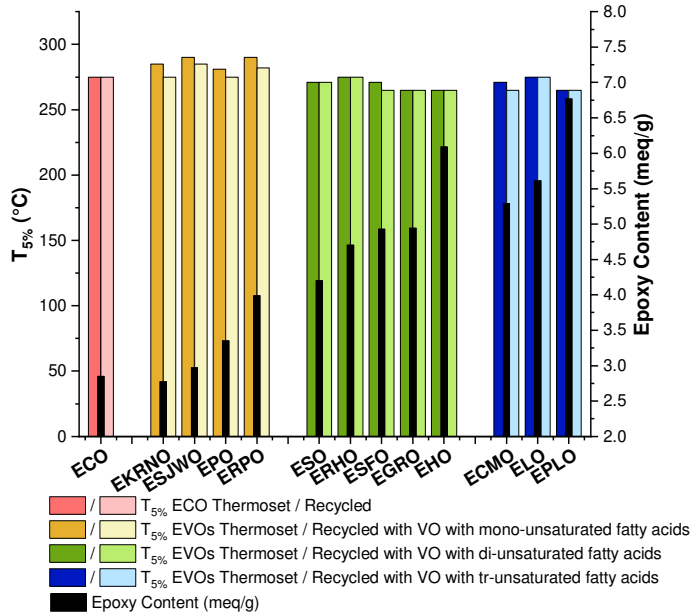


**Figure 5.** TGA analysis: comparison of thermal stabilities,  $T_{5\%}$ , of virgin and recycled EVOs thermosets. The EVOs epoxy content is indicated

similar. For the ELO reference, no degradation was observed after the recycling protocol, a  $T_{5\%} = 275\text{ }^{\circ}\text{C}$  being measured for the virgin and reprocessed thermosets.<sup>29</sup> Similar results were obtained for other EVOs<sup>30</sup> after reprocessing: ECO and ERHO ( $275\text{ }^{\circ}\text{C}$ ), ESO ( $271\text{ }^{\circ}\text{C}$ ), EGRO, ECMO, EHO and EPLO ( $265\text{ }^{\circ}\text{C}$ ). The thermal properties reported by Ma *et al.*<sup>23</sup> for the isosorbide-derived epoxy/4-AFD thermoset shown a

decreasing of the  $T_{5\%}$  from  $269\text{ }^{\circ}\text{C}$  for the virgin to  $263\text{ }^{\circ}\text{C}$  for the 1<sup>st</sup> recycled until to reach  $250\text{ }^{\circ}\text{C}$  at the end of the third recycling. The authors explained the obtained  $T_{5\%}$  decreasing due to the increasing of dangling chains induced by the loss of S-S or C-C bonds.

**Table 3.**  $T_{5\%}$  values determined by TGA analysis for virgin (V) and recycled (R) materials

EVOs/DTBA	$T_{5\%}$ , (°C) V	$T_{5\%}$ , (°C) R	EVOs/DTBA	$T_{5\%}$ , (°C) V	$T_{5\%}$ , (°C) R
EKRNO	$285 \pm 1$	$275 \pm 1$	ERHO	$275 \pm 1$	$275 \pm 1$
ECO	$275 \pm 1$	$275 \pm 1$	ESFO	$271 \pm 1$	$265 \pm 1$
ESJWO	$290 \pm 1$	$285 \pm 1$	EGRO	$265 \pm 1$	$265 \pm 1$
EPO	$285 \pm 1$	$275 \pm 1$	ECMO	$265 \pm 1$	$265 \pm 1$
ERPO	$285 \pm 1$	$282 \pm 1$	EHO	$265 \pm 1$	$265 \pm 1$
ESO	$271 \pm 1$	$271 \pm 1$	EPLO	$265 \pm 1$	$265 \pm 1$

### 5.2.1.2 Repairability and reshapability

Figure 6 (A) displays the aspect of a damage in the surface of the recycled EKRNO/DTBA/IM resin and that it is possible to repair the scratch caused in the material by applying the temperature used for the recycling, for 5 minutes, to obtain a fully recovered surface. Odriozola *et al.*<sup>22</sup> repaired completely the scratch performed in a specimen based on DGEBA/4-AFD applying  $200\text{ }^{\circ}\text{C}$  heating and pressure and demonstrating that the DGEBA network prepared using a diamine crosslinker without disulfide bonds

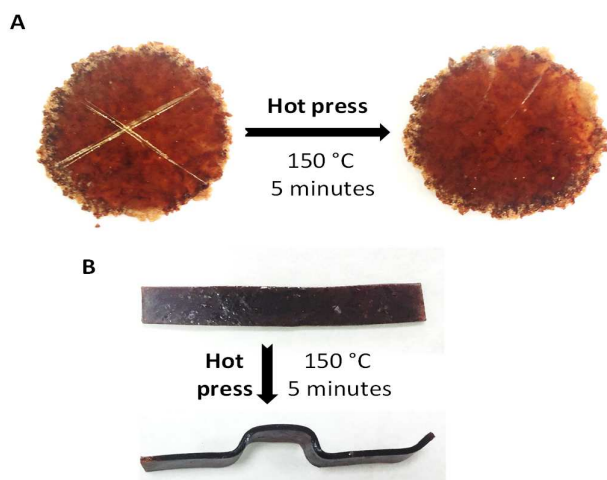


**Figure 6.** (A) Repairability experiments of the EKRNO/DTBA and (B) Reshapability of ESJWO/DTBA recycled thermosets

recycled ESJWO/DTBA is shown in Figure 6 (B). A CARVER manual press using zig-zag shaped mold was used, applying a heating to 150 °C that was kept for 5 minutes. Reshapability appears occur easier in recycled thermosets of the categories 1 and 2, while the repairability gave excellent results for all recycled EVOs.

### 5.2.1.3 Shape memory

Finally, the shape memory properties were tested for prepared recycled thermosets. In Figure 7 are presented the results obtained with EPO recycled thermoset. To test the materials shape memory, the sample was deformed to a temporary shape and recovered to their original shape by applying a stimulus. Figure 7 (a) shows the initial, permanent strip shape n° 1. This specimen was twisted manually after heating at 90 °C for 10 s and immediately giving the helix shape (b), then the strip was allowed to reach the room temperature to fix the temporary shape. Afterwards, immersing the strip in hot water (~ 90 °C) the original flat permanent shape n° 1 was recovered (c). Consequently, to reach the permanent shape n° 2, the strip was twisted and maintained with a clamp to keep constant the shape and located in oven at 150 °C for 20 minutes (d), then was cooled to room temperature. After a heating at 90 °C for 10s a new temporary shape was given to the specimen by manually applying a stress (e). At the end, a new immersion in hot water led to reach the helix permanent shape n° 2 again (f).

However, all the recycled thermoset materials exhibited shape memory ability. Due to the high  $T_g$  of the recycled EVOs resins from category 3, higher temperature are necessary to reach the temporary and consequently the permanent shape n° 1. It was found that are

(diethyltoluenediamine) was unsuccessful to be repaired. The dynamic disulfide networks allow the reprocessing, giving to the chains the ability to relax at elevated temperature and moreover to modify their shape.

The reshaping of some thermosets was reported for disulfide based materials<sup>22,24,31</sup> as for transesterification mechanisms<sup>8,33</sup> or for imine<sup>37</sup> networks. The results of thermoforming applied for the



required temperatures with  $\sim 30\text{ }^{\circ}\text{C}$  above the  $T_g$  of the material to obtain satisfactory shape memory results.

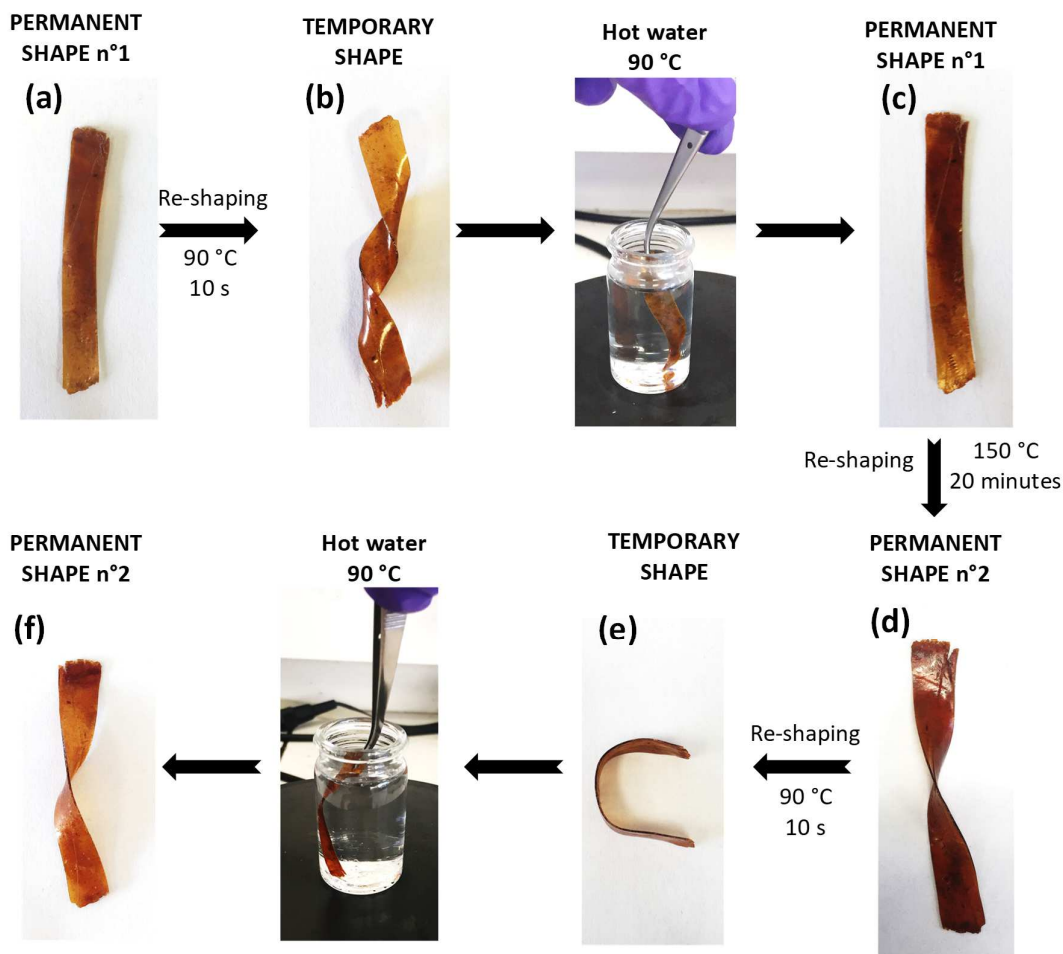


**Figure 7.** Shape memory and permanent shape for EPO/DTBA recycled thermosetting resin: (a) permanent shape n° 1, (b) temporary shape after heating and twisting, (c) permanent shape n° 1 after recovering, (d) permanent shape n° 2, (e) temporary shape after heating, and (f) recovered permanent shape n° 2

Some thermosetting polymers exhibited shape memory properties. Williams *et al.*<sup>38</sup> reported shape memory properties of DGEBA crosslinked with citric acid/ sebacic acid thermosets demonstrating that, when  $T > T_g$ , the sample went back to the permanent shape. Zhang *et al.*<sup>39</sup> made an epoxy vitrimer based on eugenol epoxide crosslinked with succinic anhydride, explaining that the shape changing is reversible and can be repeated several times due to the thermally induced dynamic exchange reactions. Also, dynamic epoxy resins with shape-memory effect were presented by Hu *et al.*<sup>23</sup> for isosorbide-derived epoxy / 4-AFD or by Irusta *et al.*<sup>40</sup> for DGEBA/Polycaprolactone blends cured with 4-AFD crosslinker. Recently, Mu *et al.*<sup>41,42</sup> prepared a recyclable, mechanically robust epoxy resins with programmable shape

memory properties converting palm oil-based methyl methacrylate monomers into epoxy monomers cured with citric acid without using any catalyst. The prepared epoxy resins showed both thermo- and chemo-responsive shape memory, using solvents that disrupted the H-bonding, such as water and methanol, or by using THF vapors that can easily penetrate the polymer matrix causing a rapid return to the original form in 6 minutes.

### 5.2.2 Chemical stability

Our team<sup>30</sup> demonstrated that the EVOs-based thermosets can be chemically recycled selecting appropriate solvents and conditions. However, both virgin and reprocessed EVO-thermosets exhibited excellent solvent resistance. To study the solvent stability of the recycled EVOs materials, the toluene was selected as solvent test. The experiment was performed immersing the specimens for 48 hours at room temperature, the results being displayed in Figure 8.

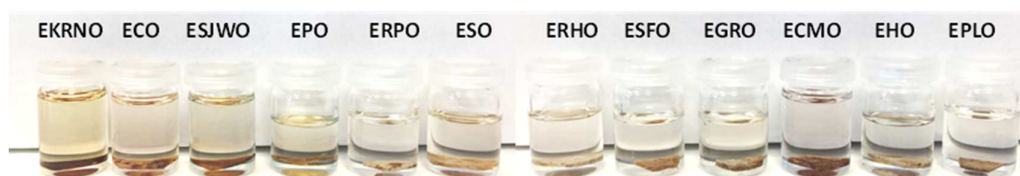


**Figure 8.** Solvent stability in toluene after 48 hours at room temperature for the EVOs recycled thermosets

At the end of the 48 hours, the recycled thermosets were weighted and, accordingly with the Equation ESI 4, the determined swelling ratio,  $Q$ , do not showed a mass loss. The results are plotted in Figure 9 (A), displaying that the recycled thermosets provided by EVOs with low epoxy content have lower swelling ratio compared to the virgin ones, while moving from category 1 to 3 and increasing the epoxy content, the reprocessed specimens showed an increased swelling ratio compared with the virgin resins. The recycled ERHO resin is the single case of category 2, which shows a decrease in swelling ability. These results can be explained by evolution of crosslinking decreases after recycling. As previously shown, the EVOs with low epoxy content had increased values of crosslinking density after recycling. Therefore, in this case the swelling ratio is lower in the recycled resins. For EVOs with high epoxy content, the network density decreases after recycling, so the ratio  $Q$  is increased.

The gel content (GC) is a crucial parameter related with the performance of thermosetting materials and has a direct relationship with crosslink density: a high gel content indicates a high density of crosslinks.<sup>43</sup>

Figure 9 (B) displays the GC % of the thermosets and recycled materials, analyzed at the end of 48 hours in toluene. All the EVOs thermosets have high gel content % from 95.8 to 99.8% for the virgin and from 95.3 to 99.9 % for the reprocessed, which indicates that EVOs are well-cured by DTBA, even after reprocessing. Higher GC % values were observed for the thermosets from category 3: the results are in good agreement with fully bio-based thermosets based on epoxidized sucrose soyate (ESS) and citric or malic acids in different solvents (ethanol, 2-propanol, 1-propanol and 1,4-dioxane).<sup>44</sup> The authors showed a gel content range from 97.3 to 99.6% using acetone and performing the experiment at room temperature for 24 hours. The same authors reported GC between 94.4 and 99.7% for ESS crosslinked with several natural acids in presence of water to assist the reaction and to solubilize the acids (citric, DL-malic, L-tartaric, malonic, oxalic, and glutaric acid) using extra catalyst or toxic compounds.<sup>45</sup>

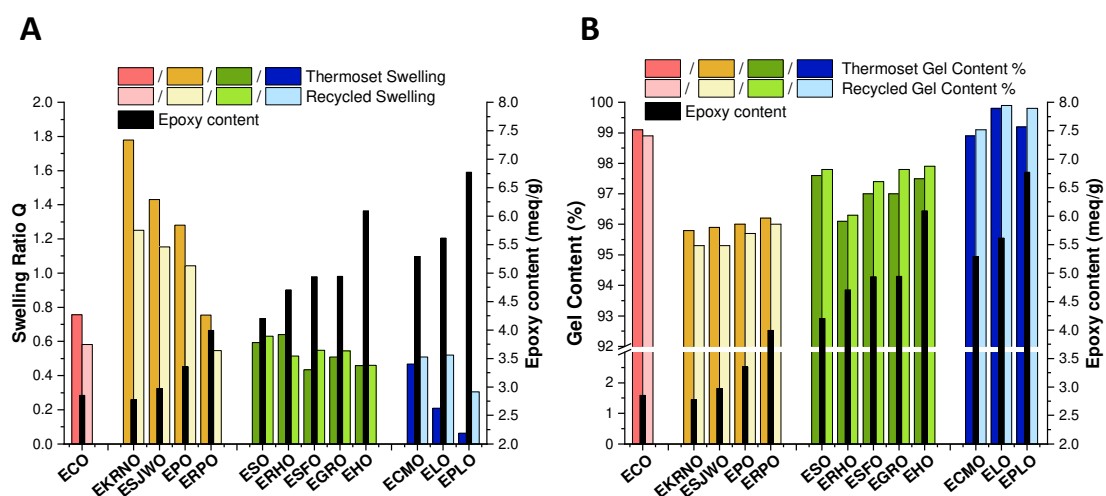


**Figure 9.** (A) Swelling ratio  $Q$  and (B) Gel Content % at the end of the 48 hours of immersion in toluene in function of the epoxy content for the virgin and recycled materials

GC % higher than 99 % were obtained applying the same conditions by Ozawa *et al.*<sup>46</sup> for the reprocessable disulfide-containing bismaleimide-amine thermosets prepared by Michael addition reaction of 4,4'-bismaleimidodiphenylmethane, 4-aminophenyl disulfide (APDS) and Jeffamine® ED-600. Yu *et al.*<sup>47</sup> reported vanillin-based epoxy vitrimers prepared by reacting mono-glycidyl structure of vanillin with isophorone diamine hardener.

The authors found GC ratios up to 91.3% and after the 1<sup>st</sup> reprocessing the GC increased to 94.5% to reach 96.2% for the 3<sup>rd</sup> times reprocessed vitrimers. Tan *et al.*<sup>48-49</sup> reported for ESO/methylhexahydrophthalic anhydride vitrimer obtained using 2-ethyl-4-methylimidazole as catalyst GC values between 87 and 95.9%, in function of the catalyst percentage and the

authors compared the values with ESO / DGEBA blends obtaining 98% for 50:50 mixture. As shown in Figure 9, for the virgin EVOs thermosets from category 1 lower GC % were obtained. After reprocessing, these values decreased, according with the crosslinking density decreasing. The low swelling ratio value and high gel content % obtained for ECO-virgin thermoset were confirmed even after recycling.<sup>30</sup>

### 5.3 Conclusions

In this work, 12 thermosets based on EVOs cured with a disulfide containing diacid hardener have been recycled and the properties compared with those of virgin resins. The synergy of the mechanisms, disulfide exchange and transesterification reaction, guaranteed complete mechanical recycling for all materials. Thermosets from category 1, with low epoxy content shown greater facility of reprocessing. Also, these materials showed a lower decreasing of crosslinking, mechanical properties and a better solvents resistance compared with the thermosets from the 3<sup>rd</sup> category, made using VOs with tri-unsaturated fatty acids. The 3R skills have been confirmed following repairability and reshaping tests. Finally, excellent shape memory properties have been observed for the recycled materials, as vitrimers, opening to a category of renewable and sustainable materials.

### Acknowledgments

This work was supported by ECOXY project funded by the Bio Based Industries Joint Undertaking under European Union Horizon 2020 research and innovation program (Grant agreement n° 744311).

### References

1. AISBL, PlasticsEurope, Plastics—the Facts 2018, <http://www.-plasticseurope.org/application>. **2019**.
2. Rahimi, A.; García, J. M., Chemical recycling of waste plastics for new materials production. *Nature Reviews Chemistry* **2017**, 1 (6), 1-11.
3. Okan, M.; Aydin, H. M.; Barsbay, M., Current approaches to waste polymer utilization and minimization: a review. *Journal of Chemical Technology & Biotechnology* **2019**, 94 (1), 8-21.
4. Strategy, P., A European strategy for plastics in a circular economy. Communication from the Commission to the European Parliament, the Council, the European Economic and Social Committee and the Committee of the Regions. Brussels **2018**.
5. Bowman, C. N.; Kloxin, C. J., Covalent Adaptable Networks: Reversible Bond Structures Incorporated in Polymer Networks. *Angewandte Chemie International Edition* **2012**, 51 (18), 4272-4274.
6. Kloxin, C. J.; Scott, T. F.; Adzima, B. J.; Bowman, C. N., Covalent Adaptable Networks (CANs): A Unique Paradigm in Crosslinked Polymers. *Macromolecules* **2010**, 43 (6), 2643-2653.
7. Rowan, S. J.; Cantrill, S. J.; Cousins, G. R. L.; Sanders, J. K. M.; Stoddart, J. F., Dynamic Covalent Chemistry. *Angewandte Chemie International Edition* **2002**, 41 (6), 898-952.

## Chapter 5

8. Montarnal, D.; Capelot, M.; Tournilhac, F.; Leibler, L., Silica-like malleable materials from permanent organic networks. *Science* **2011**, 334 (6058), 965.
9. Corbett, P. T.; Leclaire, J.; Vial, L.; West, K. R.; Wietor, J.-L.; Sanders, J. K. M.; Otto, S., Dynamic Combinatorial Chemistry. *Chemical Reviews* **2006**, 106 (9), 3652-3711.
10. Altuna, F. I.; Hoppe, C. E.; Williams, R. J. J., Epoxy Vitrimers: The Effect of Transesterification Reactions on the Network Structure. *Polymers* **2018**, 10 (1), 43.
11. Shi, B.; Greaney, M. F., Reversible Michael addition of thiols as a new tool for dynamic combinatorial chemistry. *Chemical Communications* **2005**, (7), 886-888.
12. Jin, Y.; Yu, C.; Denman, R. J.; Zhang, W., Recent advances in dynamic covalent chemistry. *Chemical Society Reviews* **2013**, 42 (16), 6634-6654.
13. Rekondo, A.; Martin, R.; Ruiz de Luzuriaga, A.; Cabañero, G.; Grande, H. J.; Odriozola, I., Catalyst-free room-temperature self-healing elastomers based on aromatic disulfide metathesis. *Materials Horizons* **2014**, 1 (2), 237-240.
14. Sanyal, A., Diels–Alder Cycloaddition-Cycloreversion: A Powerful Combo in Materials Design. *Macromolecular Chemistry and Physics* **2010**, 211 (13), 1417-1425.
15. Kolomiets, E.; Lehn, J.-M., Double dynamers: molecular and supramolecular double dynamic polymers. *Chemical Communications* **2005**, (12), 1519-1521.
16. Crego Calama, M.; Timmerman, P.; N. Reinhoudt, D.; Crego Calama, M.; Hulst, R.; Timmerman, P.; Fokkens, R.; M. M. Nibbering, N., Libraries of non-covalent hydrogen-bonded assemblies; combinatorial synthesis of supramolecular systems. *Chemical Communications* **1998**, (9), 1021-1022.
17. Denissen, W.; Winne, J. M.; Du Prez, F. E., Vitrimers: permanent organic networks with glass-like fluidity. *Chemical Science* **2016**, 7 (1), 30-38.
18. Jurowska, A.; Jurowski, K., Vitrimers-the miracle polymer materials combining the properties of glass and plastic? *Chemik* **2015**, 69 (7), 392-394.
19. Capelot, M.; Unterlass, M. M.; Tournilhac, F.; Leibler, L., Catalytic Control of the Vitrimer Glass Transition. *ACS Macro Letters* **2012**, 1 (7), 789-792.
20. Lei, Z. Q.; Xiang, H. P.; Yuan, Y. J.; Rong, M. Z.; Zhang, M. Q., Room-Temperature Self-Healable and Remoldable Cross-linked Polymer Based on the Dynamic Exchange of Disulfide Bonds. *Chemistry of Materials* **2014**, 26 (6), 2038-2046.
21. Tsuruoka, A.; Takahashi, A.; Aoki, D.; Otsuka, H., Fusion of Different Crosslinked Polymers Based on Dynamic Disulfide Exchange. *Angewandte Chemie International Edition* **2020**, 59 (11), 4294-4298.
22. Ruiz de Luzuriaga, A.; Martin, R.; Markaide, N.; Rekondo, A.; Cabañero, G.; Rodríguez, J.; Odriozola, I., Epoxy resin with exchangeable disulfide crosslinks to obtain reprocessable, repairable and recyclable fiber-reinforced thermoset composites. *Materials Horizons* **2016**, 3 (3), 241-247.
23. Ma, Z.; Wang, Y.; Zhu, J.; Yu, J.; Hu, Z., Bio-based epoxy vitrimers: Reprocessability, controllable shape memory, and degradability. *Journal of Polymer Science Part A: Polymer Chemistry* **2017**, 55 (10), 1790-1799.
24. Zhou, F.; Guo, Z.; Wang, W.; Lei, X.; Zhang, B.; Zhang, H.; Zhang, Q., Preparation of self-healing, recyclable epoxy resins and low-electrical resistance composites based on double-disulfide bond exchange. *Composites Science and Technology* **2018**, 167, 79-85.
25. Imbernon, L.; Oikonomou, E. K.; Norvez, S.; Leibler, L., Chemically crosslinked yet reprocessable epoxidized natural rubber via thermo-activated disulfide rearrangements. *Polymer Chemistry* **2015**, 6 (23), 4271-4278.
26. Chen, M.; Zhou, L.; Wu, Y.; Zhao, X.; Zhang, Y., Rapid Stress Relaxation and Moderate Temperature of Malleability Enabled by the Synergy of Disulfide Metathesis and Carboxylate Transesterification in Epoxy Vitrimers. *ACS Macro Letters* **2019**, 8 (3), 255-260.
27. Tran, T.-N.; Di Mauro, C.; Graillot, A.; Mija, A., Chemical Reactivity and the Influence of Initiators on the Epoxidized Vegetable Oil/Dicarboxylic Acid System. *Macromolecules* **2020**, 53 (7), 2526-2538.
28. Di Mauro, C.; Genua, A.; Mija, A., Building thermally and chemically reversible covalent bonds in vegetable oils based epoxy thermosets. Influence of epoxy-hardener ratio to promote recyclability. *Materials Advances* **2020**, 1 (6), 1788-1798.
29. Di Mauro, C.; Tran, T.-N.; Graillot, A.; Mija, A., Enhancing the Recyclability of a Vegetable Oil-Based Epoxy Thermoset through Initiator Influence. *ACS Sustainable Chemistry & Engineering* **2020**, 8 (20), 7690-7700.
30. Di Mauro, C.; Malburet, S.; Genua, A.; Graillot, A.; Mija, A., Sustainable series of new epoxidized vegetable oils-based thermosets with chemical recycling properties. *Biomacromolecules* **2020**, 21 (9), 3923-3935.

31. Azcune, I.; Odriozola, I., Aromatic disulfide crosslinks in polymer systems: Self-healing, reprocessability, recyclability and more. *European Polymer Journal* **2016**, *84*, 147-160.
32. Casatorre, E.; Luzuriaga, A. R. D.; Rekondo, A.; Genua, A.; Azcune, I.; Grande, H.-J.; Martinx, M. F. S.; Aparicio, X. Reworkable crosslinked polythiourethanes with intrinsic injectability, repairability and recyclability. **2019**, Patent No. WO 2019/063787.
33. Capelot, M.; Montarnal, D.; Tournilhac, F.; Leibler, L., Metal-Catalyzed Transesterification for Healing and Assembling of Thermosets. *Journal of the American Chemical Society* **2012**, *134* (18), 7664-7667.
34. Chen, J.-H.; Hu, D.-D.; Li, Y.-D.; Meng, F.; Zhu, J.; Zeng, J.-B., Castor oil derived poly(urethane urea) networks with reprocessability and enhanced mechanical properties. *Polymer* **2018**, *143*, 79-86.
35. Memon, H.; Liu, H.; Rashid, M. A.; Chen, L.; Jiang, Q.; Zhang, L.; Wei, Y.; Liu, W.; Qiu, Y., Vanillin-Based Epoxy Vitrimer with High Performance and Closed-Loop Recyclability. *Macromolecules* **2020**, *2* (53), 621-630.
36. Flory, P. J., Principles of polymer chemistry. Cornell University Press: **1953**.
37. Zhao, S.; Abu-Omar, M. M., Recyclable and Malleable Epoxy Thermoset Bearing Aromatic Imine Bonds. *Macromolecules* **2018**, *51* (23), 9816-9824.
38. Altuna, F. I.; Hoppe, C. E.; Williams, R. J. J., Shape memory epoxy vitrimers based on DGEBA crosslinked with dicarboxylic acids and their blends with citric acid. *RSC Advances* **2016**, *6* (91), 88647-88655.
39. Liu, T.; Hao, C.; Wang, L.; Li, Y.; Liu, W.; Xin, J.; Zhang, J., Eugenol-Derived Biobased Epoxy: Shape Memory, Repairing, and Recyclability. *Macromolecules* **2017**, *50* (21), 8588-8597.
40. Razquin, I.; Iregui, A.; Orduna, L.; Martin, L.; González, A.; Irusta, L., Reprogrammable Permanent Shape Memory Materials Based on Reversibly Crosslinked Epoxy/PCL Blends. *Molecules* **2020**, *25* (7), 1568.
41. Mu, S.; Zhang, Y.; Zhou, J.; Wang, B.; Wang, Z., Recyclable and Mechanically Robust Palm Oil-Derived Epoxy Resins with Reconfigurable Shape-Memory Properties. *ACS Sustainable Chemistry & Engineering* **2020**, *8* (13), 5296-5304.
42. Lamm, M. E.; Wang, Z.; Zhou, J.; Yuan, L.; Zhang, X.; Tang, C., Sustainable epoxy resins derived from plant oils with thermo- and chemo-responsive shape memory behavior. *Polymer* **2018**, *144*, 121-127.
43. Saithai, P.; Lecomte, J.; Dubreucq, E.; Tanrattanakul, V., Effects of different epoxidation methods of soybean oil on the characteristics of acrylated epoxidized soybean oil-co-poly(methyl methacrylate) copolymer. *Express Polymer Letters* **2013**, *7* (11), 910-924.
44. Ma, S.; Kovash, C. S.; Webster, D. C., Effect of solvents on the curing and properties of fully bio-based thermosets for coatings. *Journal of Coatings Technology and Research* **2017**, *14* (2), 367-375.
45. Ma, S.; Webster, D., Naturally Occurring Acids as Cross-Linkers To Yield VOC-Free, High-Performance, Fully Bio-Based, Degradable Thermosets. *Macromolecules* **2015**, *48*, 7127-7137.
46. Ozawa, M.; Shibata, M., Reprocessable bismaleimide-diamine thermosets based on disulfide bonds. *Reactive and Functional Polymers* **2020**, *146*, 104404.
47. Yu, Q.; Peng, X.; Wang, Y.; Geng, H.; Xu, A.; Zhang, X.; Xu, W.; Ye, D., Vanillin-based degradable epoxy vitrimers: Reprocessability and mechanical properties study. *European Polymer Journal* **2019**, *117*, 55-63.
48. Tan, S. G.; Ahmad, Z.; Chow, W. S., Interpenetrating polymer network structured thermosets prepared from epoxidized soybean oil/diglycidyl ether of bisphenol A. *Polymer international* **2014**, *63* (2), 273-279.
49. Tan, S. G.; Chow, W. S., Curing Characteristics and Thermal Properties of Epoxidized Soybean Oil Based Thermosetting Resin. *Journal of the American Oil Chemists' Society* **2011**, *88* (7), 915-923.
50. Matějka, L.; Pokorný, S.; Dušek, K., Acid curing of epoxy resins. A comparison between the polymerization of diepoxide-diacid and monoepoxide-cyclic anhydride systems. *Die Makromolekulare Chemie* **1985**, *186* (10), 2025-2036.

# Electronic Supplementary Information (ESI)

## Experimental Section

### Materials

The epoxidized linseed and soybean oils, ELO (A) and ESO (B), were provided by Valtris Chemicals (England). The 11 new EVOs (epoxidized karanja oil - EKRNO, epoxidized castor oil - ECO, epoxidized St John's Wort oil - EJSWO, epoxidized peanut oil - EPO, epoxidized rapeseed oil - ERPO, epoxidized rose hip seed oil - ERHO, epoxidized safflower oil - ESFO, epoxidized grapeseed oil - EGRO, epoxidized camelina oil - ECMO, epoxidized hemp oil - EHO and epoxidized perilla oil - EPLO) were provided by SPECIFIC POLYMERS (France) as references SP-3S-30-006.

These EVOs can be classified in three categories, in function of their nature and content in unsaturated fatty acids: *i/* category 1: EVOs from VO containing mainly mono-unsaturated fatty acids: EKRNO, ECO, EJSWO, EPO and ERPO; *ii/* category 2: EVOs from VO containing mainly di-unsaturated fatty acids: ESO, ERHO, ESFO, EGRO and EHO; *iii/* category 3: EVOs from VO containing mainly tri-unsaturated fatty acids ECMO, ELO and EPLO.

The 2,2'-dithiodibenzoic acid (DTBA) 95% hardener (E) and the imidazole (IM) initiator (99%) (F) were purchased from Sigma-Aldrich and were used as received. The physico-chemical characteristics of all these materials are given in Table ESI 1.

### Samples preparation

The epoxy / hardener ratio was fixed at 1:1 according with Dusek *et al.*<sup>1</sup>. The initiator was added at 1 wt.% and mixed at 80 °C in the epoxy monomer. Subsequently, the hardener was added in the previous mixture, stirred at the same temperature for 10 minutes and placed into a silicone mold. The curing and post-curing protocols for the preparation of the EVOs thermosets were determined based on DSC study of reactivity presented in Table ESI 2.<sup>2</sup>

### Recycling, repairing and reshaping procedures

A piece of crosslinked thermoset was grounded and the obtained powder heated between two Kapton films using a CARVER manual press. The reprocessing conditions, temperature, pressure and duration were optimized and adapted to each resin: starting from 120 °C and 0.3 tons until 170 °C and 2 tons for high epoxy content (Table 1). Recycled specimens with rectangular dimensions of 30 x 7 x 2mm<sup>3</sup> were prepared for the thermo-mechanical characterizations. For the repairing and reshaping tests, the recycled EVOs specimens obtained using the parameters given in Table 1, were prepared with dimensions 50 x 10 x 1 mm<sup>3</sup>.

To prove the thermosets repairing ability, on their surface were produced scratches. The so injured specimens were heated according with the recycling protocol (Table 1) for 5 minutes between the plates of the CARVER manual press, without applying any pressure.

The reshaping process was performed in a zig-zag shaped mold following the same conditions as for the repairing.

## Analytical Methods

### Differential Scanning Calorimetry (DSC)

The thermosets glass transition evaluations were carried out on a Mettler-Toledo DSC 3 instrument equipped with STAR software. The DSC studies were performed using 2 cycles of heating-cooling from -80 to 180 °C at 10 °C/min heating rate. The samples (around 5 - 7 mg) were placed into 40 µL aluminum crucibles.

### Fourier-Transformed Infrared Spectroscopy (FT-IR)

FT-IR analyses were performed using a Thermo Scientific Nicolet iS50 FT-IR spectrometer with a deuterated L-aniline doped triglycine sulfate (DLATGS) detector in attenuated total reflectance (ATR) mode. The absorption bands were recorded in the range of 4000-500 cm<sup>-1</sup> at 32 scans and 4 cm<sup>-1</sup> resolution. The data were analysed using OMNIC software. The percentage of the functional group conversion is defined by the Equation (ESI 1):

$$\% = \frac{\left(\frac{A_{823}}{A_{1586}}\right)_0 - \left(\frac{A_{823}}{A_{1586}}\right)_t}{\left(\frac{A_{823}}{A_{1586}}\right)_0} * 100 \quad (\text{ESI 1})$$

where the area of absorbance peaks was calculated at the initial time ( $A_0$ ) and at the end of the curing protocol ( $A_t$ ). The peak at 823 cm<sup>-1</sup> corresponds to the oxirane C-O groups and that at 1586 cm<sup>-1</sup> is the reference band which belongs to the  $\delta_{C-C}$  of the aromatic signal from DTBA hardener.

### Thermogravimetric Analyses (TGA)

TGA measurements were carried out on a Mettler-Toledo TGA 2, with a microbalance having a precision of  $\pm 0.1$  µg. Samples of about 10 mg were placed into 70 µL alumina pans. To characterize the thermal stability of the thermosets, the samples were heated under air flow, 50 ml.min<sup>-1</sup> at 10 °C.min<sup>-1</sup> from 25 to 1000 °C.

The statistic heat-resistant index temperature ( $T_s$ ) is characteristic of the thermal stability of materials and can be calculated according with the Equation ESI 2:

$$T_s = 0.49 \cdot [T_{5\%} + 0.6 \cdot (T_{30\%} - T_{5\%})] \quad (\text{ESI 2})$$

where  $T_{5\%}$  and  $T_{30\%}$  are the temperatures at 5, respectively 30% weight loss.

### Dynamic Mechanical Analyses (DMA)

DMA were carried out on Mettler-Toledo DMA 1 instrument, equipped with STAR<sup>®</sup> software for curve analysis. The analysed samples prepared according with the curing protocol (Table ESI 2) had rectangular dimensions of 30 x 7 x 2 mm<sup>3</sup> (length x width x thickness). Elastic modulus values ( $E'$ ) and damping factors ( $\tan \delta$ ) were collected at 3 °C.min<sup>-1</sup> heating rate from - 80 to 170 °C and 1.0 Hz frequency. The DMA was operated using tension method. The  $\alpha$ relaxation, associated to the glass transition, was assigned at the maximum of damping factor ( $\tan \delta = E''/E'$ ).

### Crosslinking density

Crosslinking density of virgin and recycled thermosets was calculated by the Equation ESI 3, according to Flory's theory<sup>3</sup> of rubber-elasticity:



## Chapter 5

$$\nu = \frac{E'}{3RT} \quad (\text{ESI 3})$$

where  $E'$  is the storage modulus of the thermoset in the rubbery plateau region at  $T_g + 50$  °C,  $R$  is the gas constant and  $T$  is the absolute temperature in Kelvin.

### Shape-memory

Shape memory properties were studied by visual methods and performed using rectangular specimens of recycled resin ( $10 \times 5 \times 1$  mm<sup>3</sup>). The specimen was heated at 90 °C for about 10 s, then twisted manually and kept at room temperature to fix the temporary shape. Then the twisted sample was immersed in hot water (~ 90 °C) to observe the shape recovery. To apply a second permanent shape, the sample was heated to 150 °C for 20 minutes, and by the help of a clamp a helix shape was formed (second permanent shape). At the end the protocol, the sample was cooled at room temperature to fix the shape. Consequently, the specimen was heated at 90 °C for 10 s and deformed to “C” shape (temporary shape) then cooled to room temperature. Finally, the specimen was immersed in hot water to recover the second permanent shape.

### Solvent stability and swelling ratio (Q)

The tests were studied in toluene for 48 hours at room temperature in order to confirm the complete crosslinking and to evaluate the samples resistance in the solvent. The tests were conducted on small rectangular  $10 \times 10 \times 2$  mm<sup>3</sup> specimens. The swelling ratio was determined according with Eq. ESI 4:

$$Q_m = \frac{w_s - w_d}{w_s} \quad (\text{ESI 4})$$

where  $w_s$  and  $w_d$  are the swelled mass and the swelled dry mass at the equilibrium.

### Gel Content (GC %)

Gel content % values of the thermosets were determined by keeping the thermoset samples ( $10 \times 10 \times 2$  mm<sup>3</sup>) in toluene until equilibrium was achieved. After 48 hours, the insoluble fraction was removed from solvent and dried under vacuum at 50 °C. The gel content value was calculated as follows:

$$\text{GC \%} = \frac{w}{w_0} \quad (\text{ESI 5})$$

where  $w$  is the mass of the material after drying and  $w_0$  is the initial mass of the material.

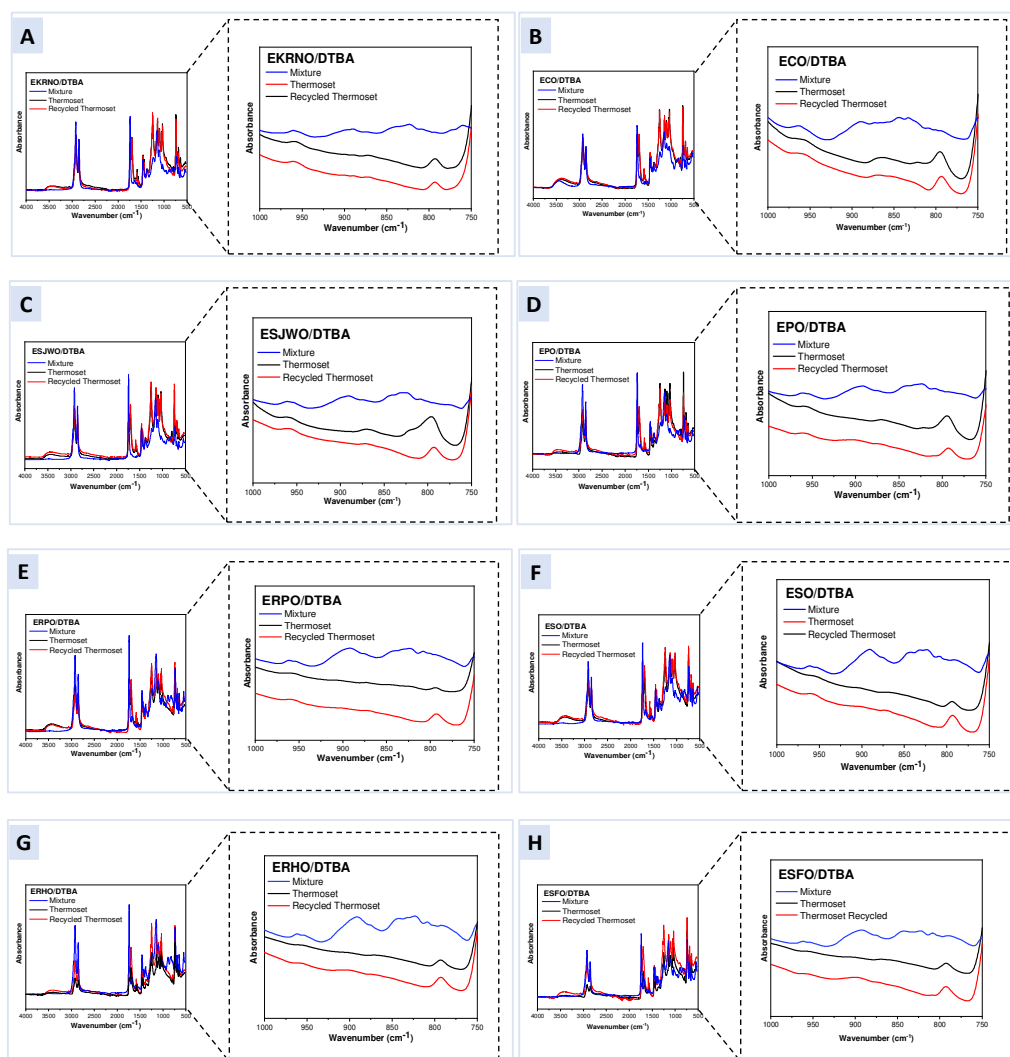
*Table ESI 1. Characteristics of the selected reagents*

EVOs	EVO Acronym	Epoxy index (m <sub>eq</sub> .g <sup>-1</sup> )	Mw EVO (g.mol <sup>-1</sup> )
Karanja	EKRNO	2.77	892.5
St John's Wort	ESJWO	2.97	932.3
Peanut	EPO	3.35	937.7
Rapeseed	ERPO	3.99	946.8
Soybean	ESO	4.20	949.8
Rose Hip Seed	ERHO	4.7	956.9
Safflower	ESFO	4.93	960.2
Grapeseed	EGRO	4.94	960.3
Camelina	ECMO	5.29	965.3
Linseed	ELO	5.61	969.9
Hemp	EHO	6.09	976.7
Perilla	EPLO	6.77	986.4
Castor	ECO	2.85	980.8

Hardener/Initiator	Acronym	Melting temp. (°C)	Mw (g/mol)
2,2'-Dithiodibenzoic acid	DTBA	287 - 290	306.35
Imidazole	IM	89 - 91	68.07

Table ESI 2. Curing and post-curing conditions for the selected EVOs

EVOs/DTBA Thermosets	Curing Condition	Post-Curing Condition	EVOs/DTBA Thermosets	Curing Condition	Post-Curing Condition
EKRNO	150 °C – 120 min	180 °C – 120 min	ESFO	140 °C – 60 min	180 °C – 30 min
ECO	130 °C – 60 min	170 °C – 30 min	EGRO	140 °C – 60 min	180 °C – 30 min
ESJWO	150 °C – 60 min	180 °C – 60 min	ECMO	130 °C – 60 min	170 °C – 30 min
EPO	140 °C – 60 min	180 °C – 60 min	ELO	130 °C – 60 min	170 °C – 30 min
ERPO	140 °C – 60 min	180 °C – 30 min	EHO	130 °C – 60 min	170 °C – 30 min
ESO	140 °C – 60 min	180 °C – 30 min	EPLO	130 °C – 60 min	170 °C – 30 min
ERHO	140 °C – 60 min	180 °C – 30 min			



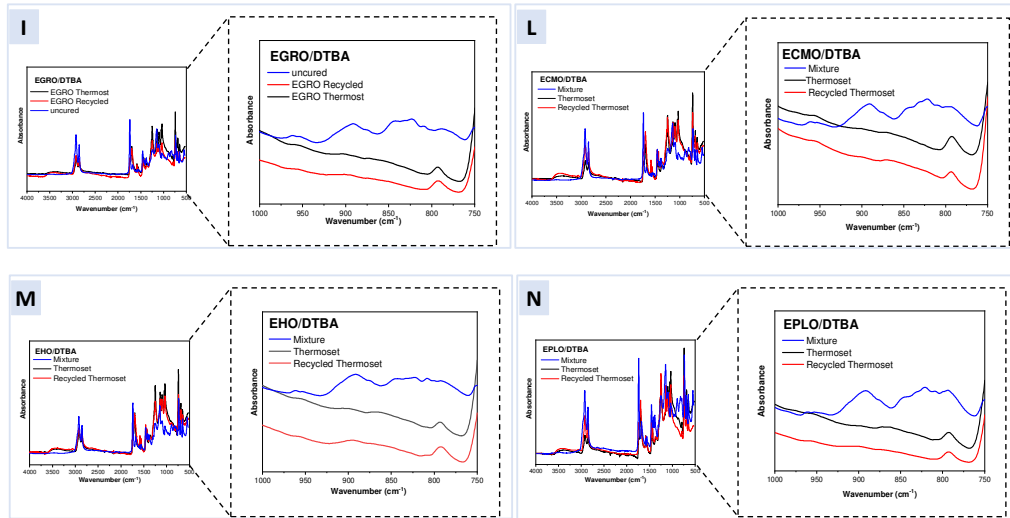


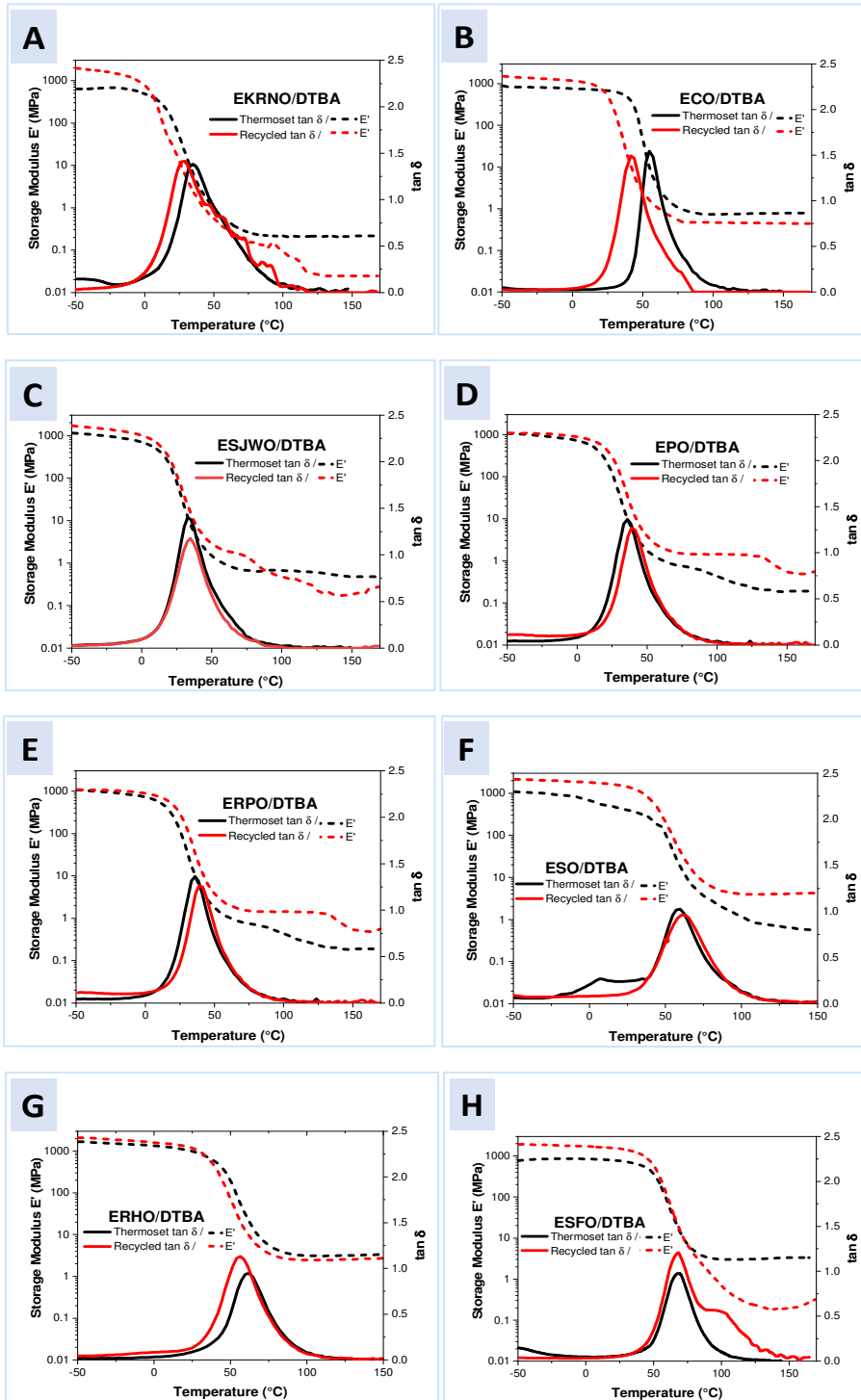
Figure ESI 1. FT-IR analysis comparison of (A) EKRNO, (B) ECO, (C) ESJWO, (D) EPO, (E) ERPO, (F) ESO, (G) ERHO, (H) ESFO, (I) EGRO, (L) ECMO, (M) EHO, (N) EPLO mixture with DTBA and 1 wt.% IM, thermosetting resins and recycled thermosetting materials

Table ESI 3. Copolymerization Conversion in % for the EVOs thermosetting resins

EVOs Thermoset Blends	Copolymerization Conversion % Virgin	Copolymerization Conversion % Recycled	EVOs Thermoset Blends	Copolymerization Conversion % Virgin	Copolymerization Conversion % Recycled
EKRNO	97	97	ESFO	82	81
ECO	92	89	EGRO	92	91
ESJWO	97	96	ECMO	89	88
EPO	95	89	ELO	99	98
ERPO	94	92	EHO	78	75
ESO	88	83	EPLO	85	85
ERHO	86	86			

Table ESI 4. Glass transition values obtained by DSC for virgin (V) and reprocessed (R) resins

EVOs Thermoset Blends	T <sub>g</sub> (°C) Virgin	T <sub>g</sub> (°C) Recycled	EVOs Thermoset Blends	T <sub>g</sub> (°C) Virgin	T <sub>g</sub> (°C) Recycled
EKRNO	17 ± 1	16 ± 1	ESFO	48 ± 1	47 ± 1
ECO	30 ± 1	29 ± 1	EGRO	50 ± 1	48 ± 1
ESJWO	17 ± 1	16 ± 1	ECMO	64 ± 1	61 ± 1
EPO	24 ± 1	20 ± 1	ELO	76 ± 1	74 ± 1
ERPO	40 ± 1	40 ± 1	EHO	62 ± 1	58 ± 1
ESO	45 ± 1	43 ± 1	EPLO	91 ± 1	84 ± 1
ERHO	53 ± 1	50 ± 1			



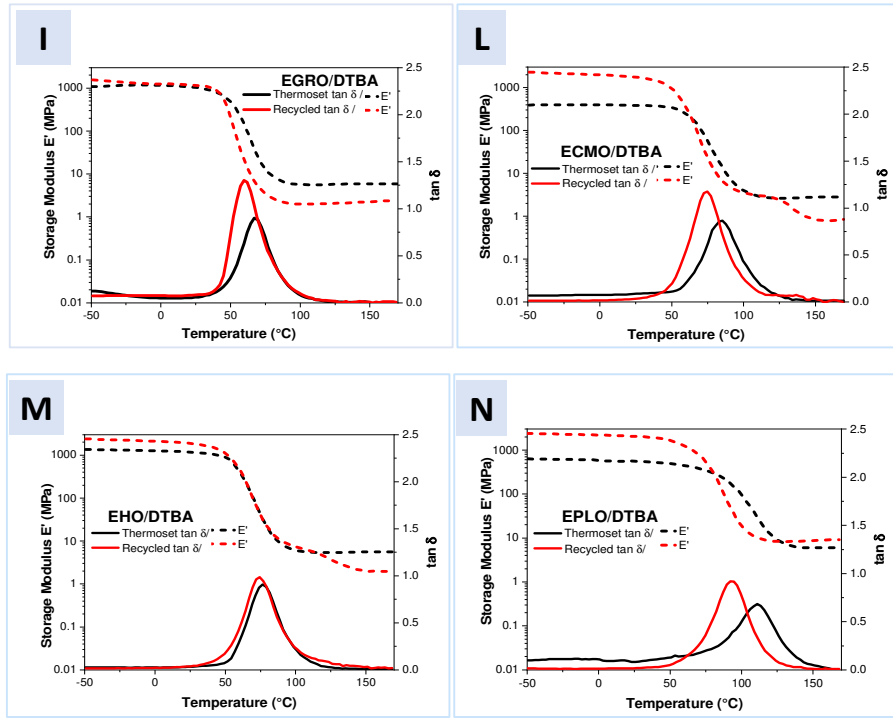
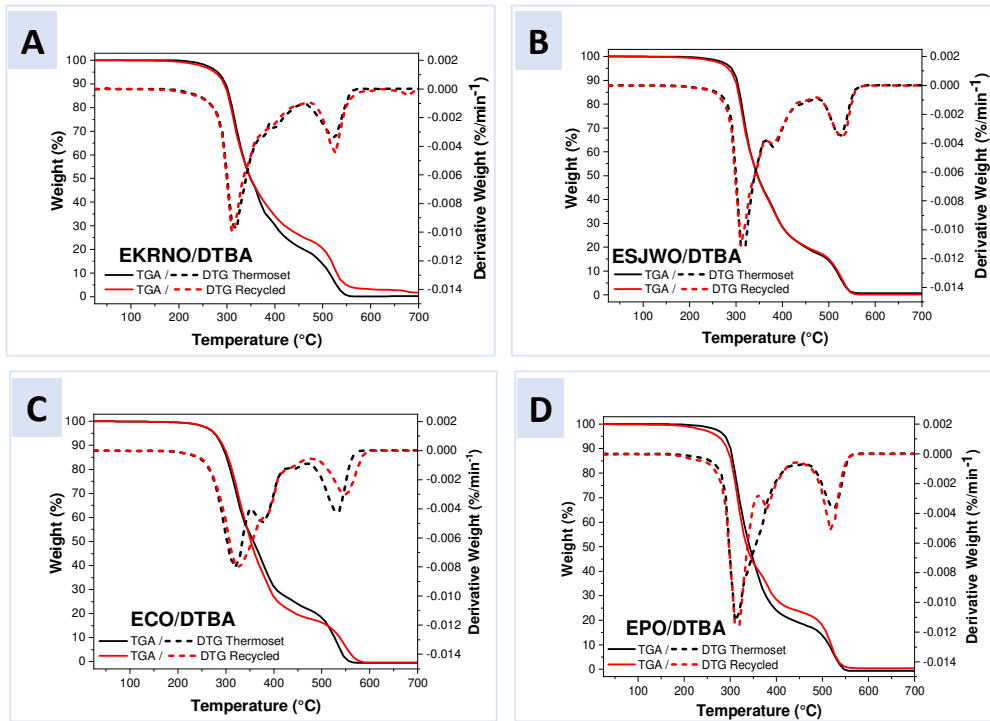
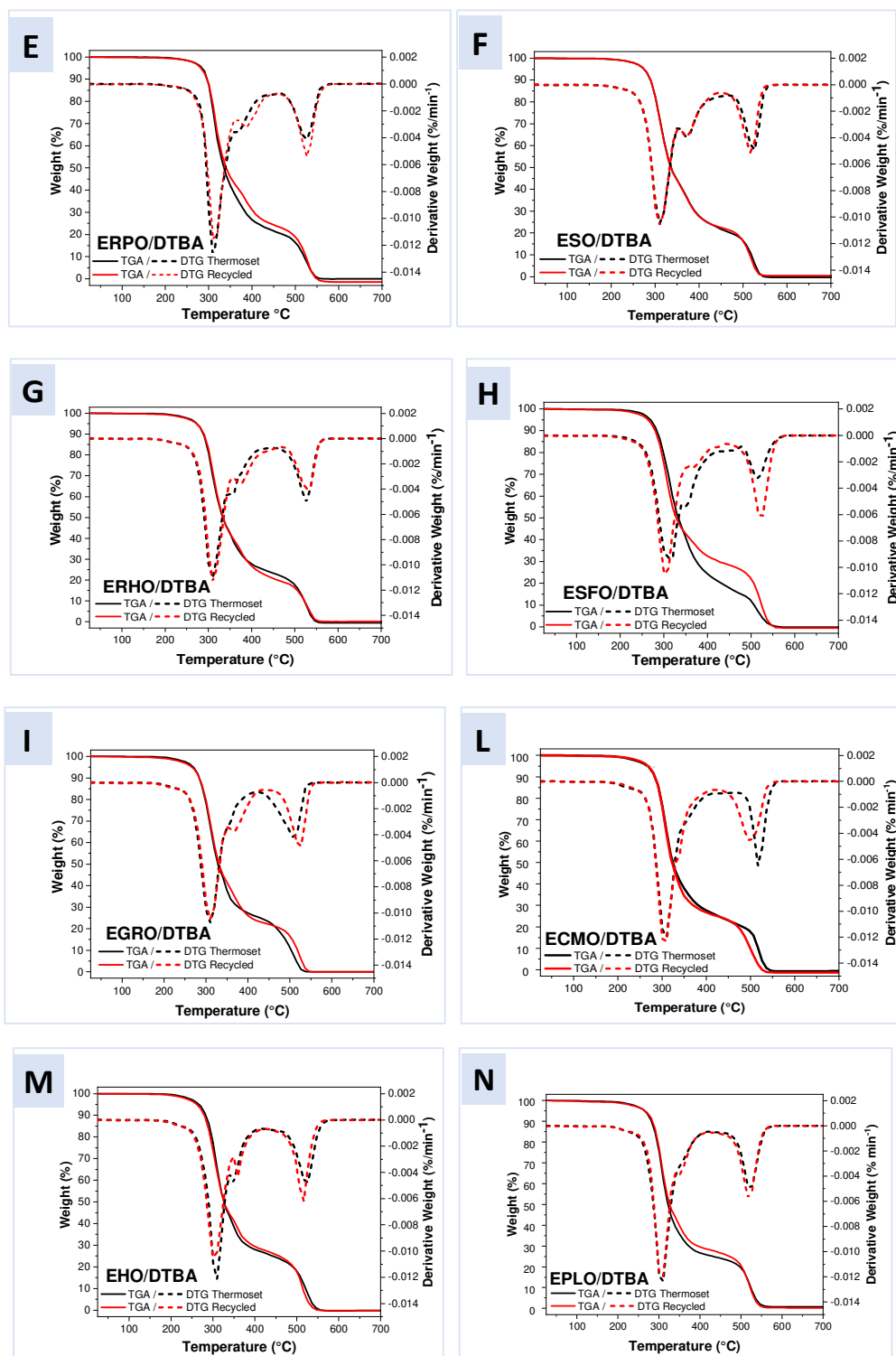


Figure ESI 2.  $\tan \delta$  and storage modulus  $E'$  vs. temperature dependence of: (A) EKRNO, (B) ECO, (C) ESJWO, (D) EPO, (E) ERPO, (F) ESO, (G) ERHO, (H) ESFO, (I) EGRO, (L) ECMO, (M) EHO, (N) EPLO virgin and recycled materials





**Figure 3.** TGA and DTG analysis of (A) EKRNO, (B) ECO, (C) ESJWO, (D) EPO, (E) ERPO, (F) ESO, (G) ERHO, (H) ESFO, (I) EGRO, (L) ECMO, (M) EHO, (N) EPLO virgin and recycled materials

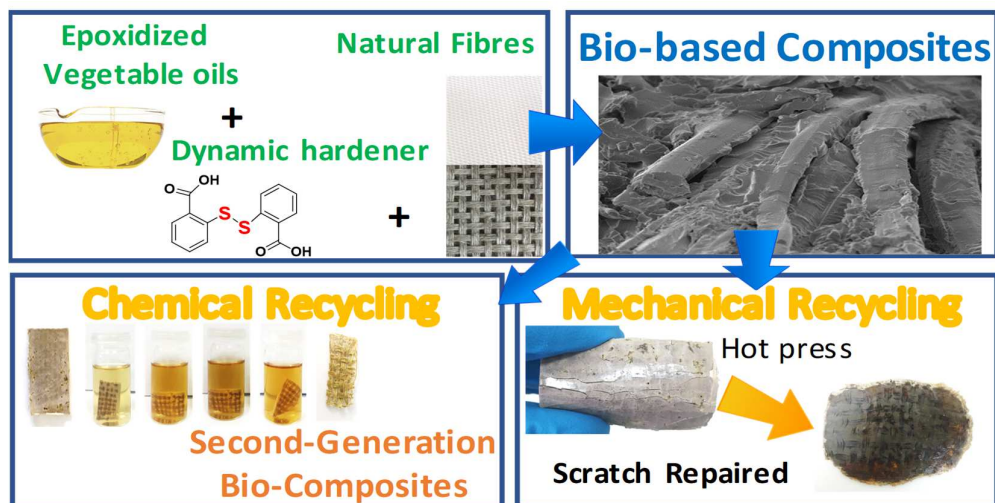
Table ESI 5.  $T_{5\%}$  and  $T_s$  determined by TGA analysis of virgin and recycled materials

EVOs Thermoset Blends	$T_{5\%}$ Virgin (°C)	$T_{5\%}$ Recycled (°C)	$T_s$ Virgin (°C)	$T_s$ Recycled (°C)
EKRNO	285 ±1	275 ±1	171	169
ECO	275 ±1	275 ±1	169	164
ESJWO	290 ±1	285 ±1	170	168
EPO	285 ±1	275 ±1	164	168
ERPO	285 ±1	282 ±1	172	173
ESO	271 ±1	271 ±1	167	167
ERHO	275 ±1	275 ±1	165	161
ESFO	271 ±1	265 ±1	162	174
EGRO	265 ±1	265 ±1	161	160
ECMO	265 ±1	265 ±1	162	160
ELO	275 ±1	275 ±1	167	165
EHO	265 ±1	265 ±1	164	166
EPLO	265 ±1	265 ±1	159	159

1. Matějka, L.; Pokorný, S.; Dušek, K. Acid curing of epoxy resins. A comparison between the polymerization of diepoxide-diacid and monoepoxide-cyclic anhydride systems. *Die Makromol. Chem.* **1985**, 186 (10), 2025–2036.
2. Di Mauro, C.; Malburet, S.; Genua, A.; Graillet, A.; Mija, A., Sustainable series of new epoxidized vegetable oils-based thermosets with chemical recycling properties. *Biomacromolecules* **2020**, 21 (9), 3923-3935.
3. Flory, P. J., *Principles of polymer chemistry*. Cornell University Press: **1953**.

# Chapter 6

Chemical and mechanical reprocessed resins and bio-composites based on five epoxidized vegetable oils thermosets reinforced with flax fibers or PLA woven





## Chapter 6

This chapter is based on Chiara Di Mauro, Aratz Genua, Monica Rymarczyk, Caroline Dobbels, Samuel Malburet, Alain Graillet and Alice Mija, Chemical and mechanical reprocessed resins and bio-composites based on five epoxidized vegetable oils thermosets reinforced with flax fibers or PLA woven, 2020 (in peer review in *Composites Science and Technology*).

### Abstract

Bio-epoxy resins based on five epoxidized vegetable oils were formulated with an aromatic disulfide crosslinker with diacid functionality, 2,2'-dithiodibenzoic acid (DTBA), to obtain recyclable epoxy thermosets. Flax fibres (FF) and PLA woven were used as bio-based reinforcements for these matrices. Different percentages of reinforcement were tested and the effect of the natural fibres on the matrix's crosslinking reaction was studied by DSC analysis. Then, the obtained materials were analyzed by DSC, TGA, DMA, water absorption and SEM. The reinforcements improved the thermal and mechanical properties of the neat resins, with  $\tan \delta$  values varying from 91 to 148 °C showing a good compatibility matrix-FF but a reduced one in case of matrix-PLA woven. The dynamic nature of the networks crosslinking allowed the chemical and mechanical recycling of both resins and bio-composites. Moreover, the obtained results show the possibility to recuperate the natural FF filler for the preparation of second-life generation bio-composites.

## 6.1 Introduction

The use of natural reinforcements in the composites area has grown rapidly since the early 90s as a response to the growing demand for a sustainable development in the production chain. The strategy of using natural reinforcements in the automotive industry started in 1940 when Henry Ford produced external body panels car from hemp fibres and a resin based on soybean oil.<sup>1</sup> The great worldwide availability, the low cost and biodegradability have made the natural fibres generally suitable for reinforcing plastic (thermoplastic and thermosetting), thanks to their relative strength and rigidity.<sup>2-3</sup> Bledzki *et al.*<sup>4</sup> compared different vegetable fibres such as flax, jute, cotton, underlining the low density of these fibres (1.3 - 1.5 g.cm<sup>-3</sup>) compared to those of traditional fibres used as reinforcements such as glass and carbon, making them attractive for the automotive market and ensuring weight savings and cheaper transportation.<sup>5</sup> The study of the environmental impact of these materials revealed that the replacement of glass fibres with flax fibres (FF) guaranteed a 12% reduction in primary energy consumption.<sup>6-7</sup>

The poly(lactic acid) (PLA) is a biopolymer, obtained from renewable and natural raw materials such as corn, known for its biodegradability and biocompatibility.<sup>8</sup> Its fibres find applications in the medical field or automotive interiors.<sup>9</sup> Composites based on PLA, modified PLA and woven FF textiles, with an increasing in impact resistance compared with that of unmodified PLA, therefore guaranteeing an ecological alternative to natural reinforced composites, were reported.<sup>10</sup>

Green bio-composites, made with natural fibres and bio-resins, are offering a sustainable alternative to traditional composites. Epoxidized vegetable oils (EVO) have received attention in composites application, especially in the past two decades to produce bio-based reinforced materials. Liu *et al.*<sup>11-13</sup> explored composites from epoxidized soybean oil (ESO) reinforced with glass, carbon, mineral and natural fibres. Scanning electron microscopy (SEM) results reported by the authors confirmed the excellent adhesion fibres-polymer matrix, resulting in a composition with good flexural properties. High mechanical strength has been obtained in the case of the bio-composites based on ESO / maleic anhydride reinforced with FFs.<sup>14</sup> Shibata *et al.*<sup>15</sup> showed that the tensile strength and modulus are increased when a natural reinforcement based on micro fibrillated cellulose are added into the ESO and tannic acid matrix. Fejos *et al.*<sup>16</sup> studied the compounds prepared with epoxidized linseed oil (ELO) crosslinked with anhydrides or amines and reinforced with FFs. Although ELO allowed the

## Chapter 6

formation of dense crosslinks, their composites have limited mechanical properties compared to similar petrochemical resins.<sup>17-18</sup>

The bio-composites produced in this work were obtained using five EVOs with different epoxy contents crosslinked with a dynamic covalent hardener, the 2,2'-dithiodibenzoic acid (DTBA). ELO-based resin was used as reference. The synthesis and properties of EVOs / DTBA resins were reported previously,<sup>19-22</sup> showing good thermo-mechanical properties of bio-based resins and recycled materials. As natural reinforcements, flax and PLA woven were used for the preparation of bio-composites. The details and the methodology implemented for the PLA woven production are reported elsewhere.<sup>23-24</sup>

The influence of the fiber on resins curing was studied by DSC. The thermo-mechanical characterization of composites was done by TGA and DMA, and the obtained results discussed in correlation with the percentage of reinforcement. The morphological analysis of the interaction fibers-matrices were conducted by SEM analysis. The water absorption of the composites was investigated in order to evaluate their use in outdoor applications and the data were correlated with the network crosslink density. Finally, the recycling and repairing ability of the prepared composites were analysed. The properties of the bio-composites were tested after mechanical recycling.

## 6.2. Results and discussion

### 6.2.1 Reactivity study of the EVOs-based resins in presence of FF or PLA fillers

The DSC analysis was used to analyse the effect of fillers' presence during the chemical curing reaction. Figures ESI 3 - ESI 4(c), Table 1 and Table ESI 4 show the thermograms and the corresponding data obtained during crosslinking reactions of ELO reference with DTBA in presence of FF and PLA woven. These DSC results show a decrease in the reaction enthalpy as the percentage of fibres in the mixture increases. The normalized reaction enthalpy decreases from 174 J.g<sup>-1</sup> for the neat resin to 97 J.g<sup>-1</sup> and to 106 J.g<sup>-1</sup> for the blend with 20% of FF and PLA, respectively. In contrast, no sensible change in the T<sub>peak</sub> was observed. Analysing the thermograms shape and the  $\Delta H$  for the formulations with PLA, the blend with 5% is the least affected, with only 10% reduction in the reaction enthalpy. For this reason, the formulation EVOs/DTBA/5% PLA was chosen for the further analysis, since at this filler percentage their steric hindrance do not affect too much the chemical crosslinking. In Figure ESI 3 we can notice that the formulations with 10 or 20% PLA are accompanied during dynamic DSC curing by a small endothermic peak of PLA melting at around 168 °C. Fiore *et al.*<sup>25</sup> and

Du *et al.*<sup>26</sup> explained that this PLA melting can be due to several aspects as the formation of a disordered phases in the PLA, or to a crystalline reorganization.

Figure ESI 4 and Table 1 display the influence of the two fillers on the thermal crosslinking of the EVOs based resins, compared with the reference ELO. By adding 5% FF, the normalized reaction enthalpies decreased from 10%, in ESFO/DTBA, to 28% in EHO/DTBA. EPLO/DTBA formulation recorded the smaller decrease in enthalpy, in both the cases, with 5 and 20% fibers. It can be observed that increasing the fibre percentage, also the interval of reaction,  $\Delta T$ , increases, even if the reaction starts at comparable temperatures. Similar results were obtained for the reference ELO/DTBA systems (Figure ESI 4 (c)). A decreasing in the exothermic reaction enthalpies was observed, as reported by Boquillon *et al.*<sup>27</sup> for ELO/methyl tetrahydrophthalic anhydride resin reinforced with 20% of hemp fibre. The EVOs/DTBA-PLA formulations have a similar trend as ELO/DTBA-PLA reference. As previously demonstrated by our team,<sup>28</sup> higher reactivity was obtained for higher epoxy content of the starting monomer (EPLO), even in the composite's formulations.

**Table 1.** EVOs reactivity vs. DTBA in presence of FF or PLA fibers. Temperatures of reaction onset, maximum, endset, total ( $\Delta H_{tot}$ ) and normalized ( $\Delta H_{normalized}$ ) enthalpy of curing; values calculated from DSC experiments

EVOs in EVOs/DTBA	Fibres (%)	$T_{on}$ (°C)	$T_{peak}$ (°C)	$T_{end}$ (°C)	$\Delta H_{tot}$ (J/g)	$\Delta H_{normalized}$ (J/g)	
ESFO	-	142	158	184	172 ± 1	-	
	FF	5	141	157	189	162 ± 1	154
		20	138	162	193	143 ± 1	114
	PLA	5	121	158	195	124 ± 1	118
ECMO	-	136	153	176	188 ± 1	-	
	FF	5	138	153	178	162 ± 1	154
		20	136	156	188	135 ± 1	108
	PLA	5	136	153	187	135 ± 1	128
ELO	-	133	149	185	174 ± 1	-	
	FF	5	132	150	186	164 ± 1	156
		20	132	150	171	121 ± 1	97
	PLA	5	134	150	175	164 ± 1	156
EHO	-	135	160	190	194 ± 1	-	
	FF	5	129	155	196	167 ± 1	159
		20	155	161	192	148 ± 1	118
	PLA	5	136	155	193	155 ± 1	147
EPLO	-	126	152	187	207 ± 1	-	
	FF	5	127	150	192	206 ± 1	195
		20	128	150	191	205 ± 1	164
	PLA	5	128	148	189	196 ± 1	186

## 6.2.2 Thermo-mechanical characterization of bio-composites

## 6.2.2.1 Glass transition analysis

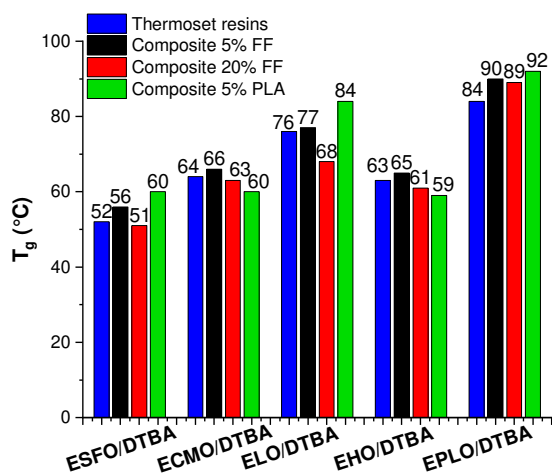


Figure 1.  $T_g$  values of the resins and composites with 5 and 20% FF and 5% of PLA

The glass transitions of the reinforced blends were determined using dynamic DSC measurements. Taking the ESFO/DTBA composites as example, the  $T_g$  shifts from 52 °C for the neat resin to 56 °C in the composition with 5% of FF, but in presence of 20% of FF the  $T_g$  decreases to 51 °C. In general, we can observe that the incorporation of 20% FF produces a small decrease of the  $T_g$  values for all the composites, excepting the EPLO/DTBA composites (Figure 1).

The results obtained with the ELO reference display intermediate glass transition values between ECMO and EPLO-based composites.

In the case of epoxide composites reinforced with 23% - 34% of FF, Muralidhar<sup>29</sup> explained that the shift of the  $T_g$  to higher temperatures in the reinforced composites, can be associated with the decrease in the mobility of the matrix, due to the incorporation of fibres. Boquillon *et al.*<sup>27</sup> observed a decrease of the  $T_g$  for thermosetting ELO resins reinforced with hemp fibres, explaining that the functional groups of the crosslinker might react with the hydroxyl groups of the fibres, to form covalent bonding.

A different trend can be observed for the composites made with PLA: ESFO, ELO and EPLO resins reinforced with PLA exhibit an increasing of  $T_g$  from 9 to 15% by adding the bio-filler, while the composites of ECMO and EHO resins with PLA show a decreasing of the glass transition compared with the corresponding neat resins. Figure ESI 5-6 display the DSC thermograms of PLA and bio-composites. The decrease of  $T_g$  can be attributed to the contribution of PLA (Figure ESI 5) that exhibits close values to the bio-composites transitions (57 – 60 °C). Yan *et al.*<sup>30</sup> reported for the PLA glass transition values in the range from 56 – 65 °C. The DSC data related to the biocomposites'  $T_g$ , or neat PLA related contribution on thermal events like cold crystallization temperature ( $T_{cc}$ ) and enthalpy ( $\Delta H_{cc}$ ) melting enthalpy ( $\Delta H_m$ ) and melting temperature ( $T_m$ ) are summarized in Table 2. As illustrated in Figure ESI 7 a small

endothermic peak of cold crystallization can be observed for the neat PLA and for the all the composites, during the first heating. Several authors,<sup>25-26,31</sup> correlated this peak to the physical aging of the PLA. More in detail, the  $T_{cc}$  seems not to be influenced by the type of EVOs, with a peak between 110 and 112 °C. Neat PLA and bio-composites show double melting peaks ( $T_{m1}$  and  $T_{m2}$ ). Du *et al.*<sup>26</sup> manufactured composites with PLA and natural cellulosic and reported these double melting peaks in the range between 150 and 170 °C. The same authors explained that the double melting peaks can be attributed to less regular PLA crystals formed during composites fabrication.

The degree of crystallinity ( $\mathcal{X}_{\text{sample}}\%$ ) of the PLA neat or in composites are reported in Table 2. This value has an impact on the physical and mechanical properties, such as the stiffness, strength, and degradation rate. The low values obtained for the composites can be due to the fact that the matrix disrupt the crystallization and also due to the rapid cooling at the end of the post-curing to 25 °C (during the composite fabrication). The maximum degree of crystallinity ( $\mathcal{X}_{\text{max}}\%$ ) for the neat PLA shows comparable value as Du *et al.*<sup>26</sup>, with 40.5%.

*Table 2. DSC results of neat PLA and EVOs-bio composites with PLA*

	PLA %	$T_{cc}$ (°C)	$T_{m1}$ (°C)	$T_{m2}$ (°C)	$\Delta H_{cc}$ (J/g)	$\Delta H_m$ (J/g)	$\mathcal{X}_{\text{sample}}$ %	$\mathcal{X}_{\text{max}}$ %
PLA	100	110	162.8	167.8	30.6	37.99	7.83	40.5
EPLO/DTBA/PLA	5	111	163.7	169.7	27.4	6.91	4.45	7.37
EHO/DTBA/PLA	5	112	163.1	169.7	6.98	7.39	0.44	7.89
ELO/DTBA/PLA	5	110	162.0	168.6	2.78	3.24	0.49	3.46
ECMO/DTBA/PLA	5	112	163.7	170.3	8.13	8.85	0.77	9.44
ESFO/DTBA/PLA	5	112	163.9	170.3	11.5	12.44	1.03	13.3

### 6.2.2.2 Dynamic mechanical analysis

The thermomechanical properties of EVOs-based resins and their bio-composites in presence of FF and PLA were analysed. The results concerning the  $\tan \delta$  and storage moduli ( $E'$ ) vs. temperature are given in Figure 2 and Table 3. We can notice that in general the composites exhibit higher storage moduli compared to those of neat resins, in the glassy plateau. Before the  $\alpha$  transition,  $E'$  values are in the following order: Resins < Composites 5% FF < Composites 20% FF. For the Composites 5% PLA the moduli are in all cases lower than those of Composites 20% FF, excepting the case of EPLO-composites. The higher values of moduli in the composites show the reinforcement of the resin matrix by the FF or PLA fibers. Muralidhar<sup>29</sup> reported for epoxy-FF reinforced composites higher moduli in glassy plateau for the composites than for the epoxy resin. The authors explained this result by the stress transfer from the matrix to the fibres. Similar results were obtained by Liu *et al.*<sup>32</sup> for ESO

resins reinforced with FF and by Manthey *et al.*<sup>33</sup> for ESO and EHO resins and their mixture with a commercial epoxy resin reinforced by jute fibres.

As summarized in Table 3 and according with previous results,<sup>28</sup> the crosslinking density in the EVOs thermosets increases linearly with the epoxy content of the starting EVOs monomer. The values are ranging from 0.34 mmol.cm<sup>-3</sup> for ESFO/DTBA to 0.68 mmol.cm<sup>-3</sup> for EPLO/DTBA. Therefore, the network density obtained for bio-composites varies in the same trend, with superior values compared to the neat resins. Adding 5% of FF a significant increase can be observed, from 12 to 380%, with for example for EPLO system an increasing from 0.68 to 3.26 mmol.cm<sup>-3</sup>. For the same system, the composite with 20%FF reached an increasing with 7260% of the crosslink density (from 0.68 to 5.62 mmol.cm<sup>-3</sup>). The composites with PLA reached similarly an increase of crosslinking densities, at higher values compared with the FF at the same ratio (50%). The addition of PLA produced a decrease of the damping factor in the case of ESFO and ELO bio-composites. However, PLA allows to obtain higher modulus values in the rubbery state for all reinforced materials, compared with the neat resins. The composites based on EVOs with high epoxy content reached approximately double the modulus value of neat resins. Nonetheless, a more significant increase in crosslinking density was achieved by using 5% PLA fibers compared to same amount of FF. The composites network density are strongly affecting their thermomechanical properties, as for example illustrated by the amplitude of the loss factor ( $\tan \delta_{max}$ ). Indeed, in Figure 2 we can observe

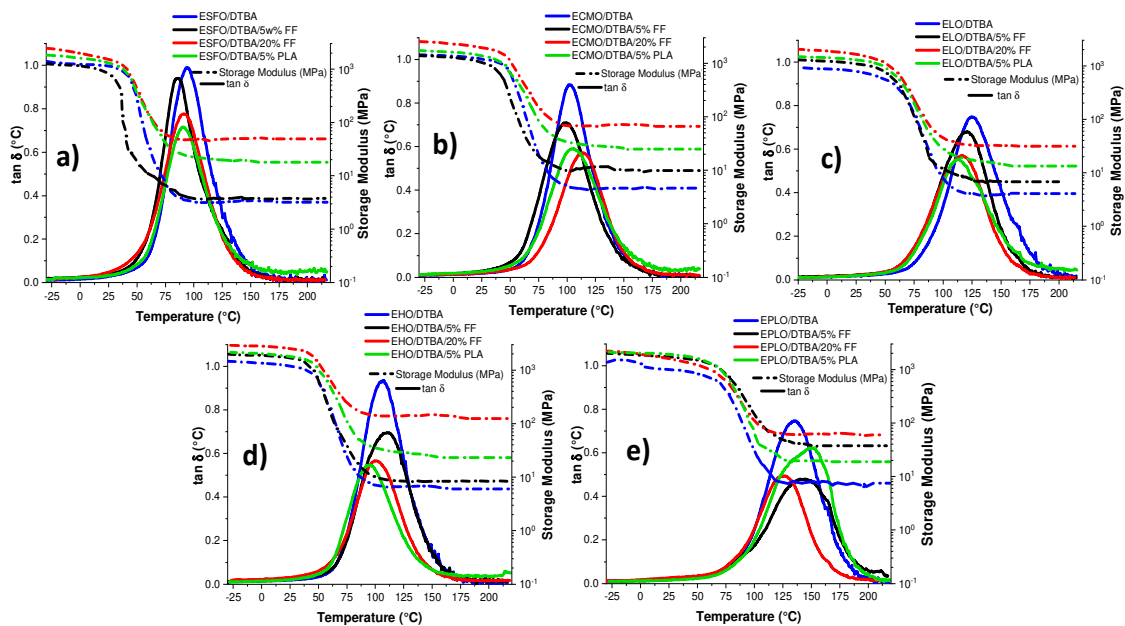


**Figure 2.** Evolution of storage and  $\tan \delta$  vs. temperature for the EVOs-based resins (blue line) and their composites with 5% FF (black line), 20% (red line) and 5% PLA (green line)

that the  $\tan \delta$  amplitude is decreasing in the composites systems, this decreasing being more pronounced for the systems with higher epoxy content so crosslink density.

Concerning the damping factor, in the case of reference system the maximum value of  $\tan \delta$  is shifted to lower temperatures for the bio-composites, which means that both FF and PLA fibres act as plasticizers for the matrix. The same behaviour was obtained for ESFO-based resin and composites. For the other systems, we can emphasize the high values of the  $\tan \delta$ ,  $> 100^\circ\text{C}$ , especially in the case of EPLO system. An increasing of the  $\tan \delta$  values can be observed for this system, from  $135^\circ\text{C}$  (neat resin) to  $142^\circ\text{C}$  (EPLO/DTBA/5% FF) and  $148^\circ\text{C}$  (EPLO/DTBA/5% PLA).

**Table 3.** Thermomechanical properties of resins and composites with FF and PLA fibres

EVOs in EVOs/DTBA	Fibres (wt.%)	$\tan \delta$ ( $^\circ\text{C}$ )	$(\tan \delta)_{\max}$	$E'$ in glassy state (MPa)	$E'$ in rubbery state (MPa)	Crosslink density ( $\text{mmol.cm}^{-3}$ )	
ESFO	-	$95 \pm 1$	0.99	1385	3.14	0.34	
	FF	5	$85 \pm 1$	0.94	1264	3.8	0.38
		20	$91 \pm 1$	0.77	2460	49.5	4.79
	PLA	5	$91 \pm 1$	0.71	1836	17.9	1.73
ECMO	-	$102 \pm 1$	0.88	1440	4.8	0.43	
	FF	5	$100 \pm 1$	0.71	1380	9.8	0.93
		20	$113 \pm 1$	0.57	2550	70.0	6.43
	PLA	5	$105 \pm 1$	0.60	1720	24.8	2.32
ELO	-	$124 \pm 1$	0.75	920	4.0	0.55	
	FF	5	$120 \pm 1$	0.68	1290	6.8	0.62
		20	$116 \pm 1$	0.57	2050	31.4	2.86
	PLA	5	$113 \pm 1$	0.55	1500	13.4	1.23
EHO	-	$106 \pm 1$	0.94	1460	6.0	0.60	
	FF	5	$111 \pm 1$	0.70	1970	8.3	0.77
		20	$101 \pm 1$	0.57	2900	134	2.83
	PLA	5	$95 \pm 1$	0.55	2170	23.3	2.22
EPLO	-	$135 \pm 1$	0.75	1370	7.8	0.68	
	FF	5	$142 \pm 1$	0.48	2000	37.8	3.26
		20	$127 \pm 1$	0.49	2200	63.1	5.62
	PLA	5	$148 \pm 1$	0.63	2120	18.8	1.60

### 6.2.2.3 Thermal stability

Figure ESI 9 and Table 4 show the thermogravimetric analyses results for the prepared resins and reinforced composites. Comparing all the results, no significative difference was obtained between all the materials that have similar behaviour as the reference system in Figure ESI 9 (c). As general observation, we should notice that the PLA produces an increasing of the  $T_{5\%}$  values, with the higher increasing obtained for EHO/DTBA composite, with  $T_{5\%}$  from 265 (neat resin) to  $275^\circ\text{C}$ . The improved thermal stability of the composites is associated with the good thermal stability of the PLA fibres. Chieng *et al.*<sup>34</sup> reported higher thermal stabilities



## Chapter 6

for the composites compared to the neat PLA (at 313 °C and 330 °C) when 5% of EPO (epoxidized palm oil) and ESO, respectively, are incorporated into PLA. The corresponding DTG (Figure ESI 10) curves display the thermal decomposition peaks according to the major constituents of the natural fibres. In contrast with the PLA, by adding FF the thermal stability decreases, the lower values  $T_{5\%}$  being obtained with 20% of FF (Table 4). These results were predictable since the FF have lower thermal stability ( $T_{5\%} \sim 231$  °C, Figure ESI 2 and Table ESI 3).

**Table 4.** Thermal characterization results for bio-based resins and the FF-PLA reinforced composites

EVOs in EVOs/DTBA	Fibres (wt.%)	$T_{5\%}$ (°C)	1 <sup>st</sup> Degradation peak (°C)	2 <sup>nd</sup> Degradation peak (°C)
ESFO	-	270	318	518
	FF	5	270	318
		20	265	317
	PLA	5	275	318
ECMO	-	265	312	517
	FF	5	265	310
		20	265	310
	PLA	5	272	320
ELO	-	275	310	515
	FF	5	265	310
		20	260	310
	PLA	5	260	310
EHO	-	265	309	520
	FF	5	268	309
		20	260	302
	PLA	5	275	318
EPLO	-	265	305	518
	FF	5	265	315
		20	270	315
	PLA	5	275	320

### 6.2.2.4 Fibre-resin interaction: SEM investigation

The wetting and compatibility between the fibres and the matrix are parameters determining the adhesion fibre–matrix and the composites' properties. In Figure ESI 11 are presented the SEM results for the composites of ELO/DTBA reference system. It can be observed that the compatibility between resins and the FF is good, with few gaps and voids in both analyzed fibre percentages and that the matrix remains attached to the fibres. Comparable results were obtained by Manthey *et al.*<sup>33</sup> for the bio-composites from EHO mixed with a synthetic epoxy resin and jute fibre reinforcement. The authors justified the result by the absence of a chemical treatment of the fibers prior to the reinforcement. In contrast, a poorer interaction between matrix and the PLA fibres (Figure ESI 11 (c)) can be observed. The PLA yarns seem to be easily separated from the epoxy matrix, leaving voids close to the matrix. The composites based on the EVOs-based resins show comparable results as the reference. Figure 3 show the micrographs of EHO/DTBA composites. Increasing the FF

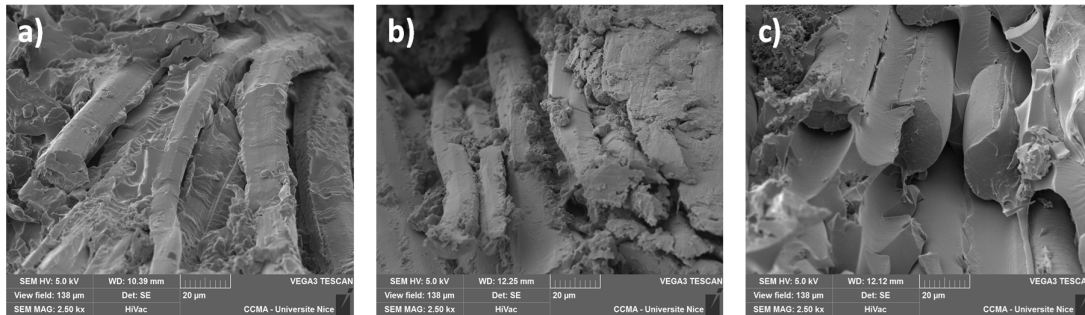


**Figure 3.** SEM micrographs at magnifications of 20  $\mu\text{m}$  for the cross-section of EHO/DTBA composites with (a) 5% FF (b) 20% FF and (c) 5% PLA

from 5 and 20% no sensible changes were observed, showing in both cases a good adhesion FF-matrix. As in the case of the reference, a reduced compatibility can be observed for the composites with PLA (Figure 3 (c)). All the analysed composites presented in Figure ESI 12 - ESI 14 show comparable results, whatever the type of the EVO in the matrix constitution. The interaction between ESFO or ECMO systems with PLA show a better interaction and compatibility, probably due to the fact that a soft matrix is better impregnated. In general, for EVOs, Chieng *et al.*<sup>34</sup> explained that a possible interaction between the hydroxyl group of PLA and the epoxy group of epoxidized palm or soybean oils through hydrogen bonding could occurred.

### 6.2.3 Water absorption analysis

Figure ESI 15 illustrates the water absorption (WA) results for FF and PLA-epoxy composites performed at 25 and 50  $^{\circ}\text{C}$  in function of time. The introduction of FF produces an increasing in the absorption percentage, higher for the composites made with EVOs with low epoxy content (Figure ESI 15 (a)). This result is correlated to the lower crosslinking density: poorly crosslinked resins and bio-composites shows a higher WA or a higher swelling capacity.<sup>20,28</sup> The amount of WA increases linearly at the beginning of the test, to reach a plateau after 12-25 hours. Higher values are observed for the 20% FF reinforcement. ESFO/DTBA systems present an increasing of the WA from 0.83, for the neat resin, to 4.9% at 25 $^{\circ}\text{C}$  and  $\sim$  9% at 50  $^{\circ}\text{C}$  for the composite with 20% FF. The reference ELO composites show an intermediate behavior between ECMO and EHO-based composites (Figure ESI 15 (c)). The low WA values for the FF composites, show comparable results as reported by Manthey *et al.*<sup>33</sup> for the bio-composites based on mixture of EHO-ESO reinforced with jute fibres.

## 6.2.4 Recycling and repairing

The recycling of fiber-reinforced composites has been growing in recent years, as for example investigating the effect of mechanical recycling.<sup>35-36</sup> Cicala *et al.*<sup>37</sup> recycled composites panels based on bio-based epoxy monomer (SuperSap) and the cure inhibitor INH by Entropy Resins mixed with cleavable amine (Recyclamine® 301) with hybrid flax / carbon fibers. The authors recycled chemically the cured laminated composites in mild acetic acid aqueous solutions, obtaining clean fibers and obtaining from the epoxy matrix a reusable thermoplastic. The presence of dynamic covalent bonds allows, as already demonstrated,<sup>20</sup> to reach the recyclability of the EVOs-based thermosets. Depending on the nature of the disulphide bonds, the recycling can be achieved both chemically<sup>38-40</sup> and mechanically.<sup>38</sup>

### 6.2.4.1 Mechanical reprocessing



**Figure 4.** Mechanical recycling of ELO/DTBA/20% FF: virgin (a), damaged (b), repaired (c)

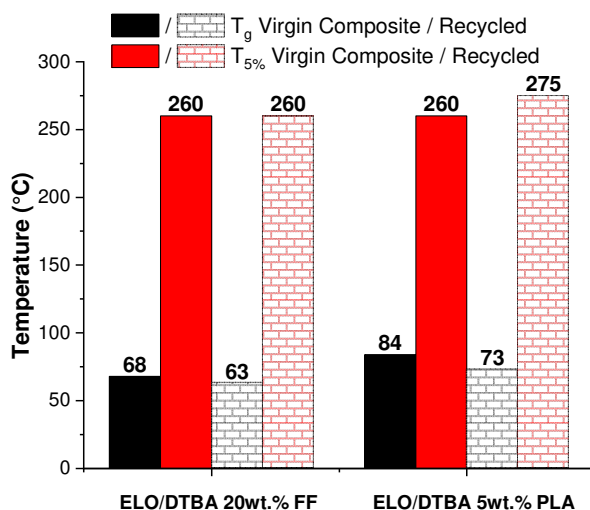


**Figure 5.**  $T_g$  and  $T_{5\%g}$  comparison between virgin and mechanically reprocessed composites based on ELO/DTBA with 20% FF and 5% PLA fibres

For the mechanical recycling, damages in composites samples of ELO/DTBA/20% FF and 5% PLA were caused. The scratches were fully repaired in hot press at 170 °C for 30 minutes under 60 bars as illustrated in Figure 4. For the ELO-based resin reinforced with PLA, due to the possible melt of the reinforcement, the repairing was done for 15 minutes under the same temperature and 30 bars (Figure ESI 16).

Thereafter, the recycled and repaired composites were characterized to

verify the effect of the reprocessing on materials' properties. For both tested composites the

$T_g$  was analysed by DSC, after the mechanical reprocessing. It was observed a decreasing from 68 °C for the virgin ELO/DTBA/20% FF, to 65 °C after the recycling, while for the ELO/DTBA/5% PLA composite from 84 °C to 73 °C (Figure 5). The thermal stability of the virgin and reprocessed composites was investigated by TGA and the results are summarized in Figure 5 and displayed in Figure ESI 17. The reprocessed FF composites present equivalent thermal stability as the virgin ones,  $T_{5\%} = 260$  °C, while the reinforced/recycled composite with PLA display an increase of the  $T_{5\%}$  from 260 °C to 275 °C.

#### 6.2.4.2 Chemical

Concerning the chemical recycling and according with the dissociative nature of disulphide bonds in alkaline conditions<sup>20,40-41</sup>, the reference ELO-based composites reinforced with 20% FF and 5% of PLA, were immersed for different time in 1 N NaOH solution at 80 °C. After 18 hours the matrixes were completely dissolved. At the end of 24 hours, PLA fibers from composites presents significant damages and the woven is partially dissolved, not allowing subsequent uses (Figure ESI 18). Different behaviour was obtained for FF that at the end of the test were dried at 50 °C for 12 hours in oven (Figure 6), and a tested to verify if the alkaline solution affected the thermal stability of the fibre.

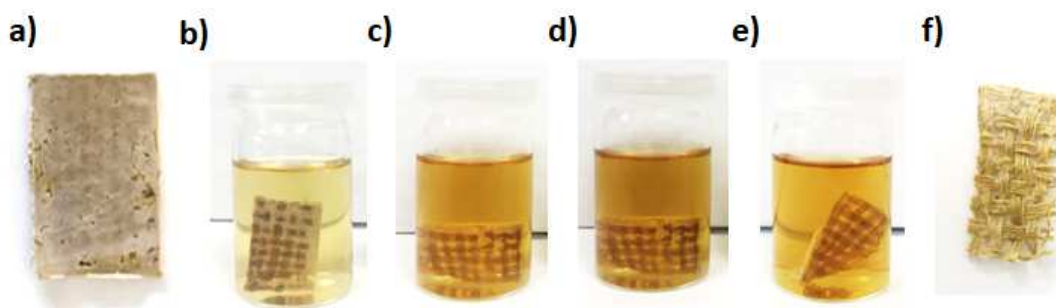


**Figure 6.** Chemical recycling in 1 N NaOH at 80 °C of the composite ELO/DTBA with 20% FF: initial composite (a), after 3h (b), 9h (c), 18h (d), 24 h (e) end dried fibre (f)

Thermogravimetric analysis (Figure ESI 19 and Table ESI 5) highlights that the chemical recycling affected thermally the FF, with a decreasing of the  $T_{5\%}$  from 231 °C for the virgin natural fibre to 165 °C after the chemical reprocessing test. However, the chemically recycled FF were combined for a second life with the ELO resin for a new composite preparation. The obtained composite, cured according with the procedure displayed in Table ESI 2, was tested again in DSC and TGA to evaluate the final properties of the second-generation composite. The obtained  $T_g$  value shift from 68 °C, for the virgin ELO/DTBA/20% FF, to ~ 73 °C for the bio-composite based on recycled FF. The second-generation composite exhibited  $T_{5\%} \sim 260$  °C, as the virgin one. These results show that the thermal properties of the “second life” composite

## Chapter 6

are similar with the first ones, even if the FF fibre presented a decreasing in thermal properties after the chemical recycling (Figure ESI 20 and Table ESI 5). This explains that the thermal degradation of the bio-composite is strongly influenced by the thermal stability of the resin. The shifting at higher  $T_g$ , could be associated to the better interaction between matrix-fibre after the alkaline treatment. These results combined with composites chemical recycling can open a new scenario for the multi uses of the fibre, guarantying several applications minimizing the lost properties.

### 6.3 Conclusions

The effects of the quantity and types of FF and PLA fibre woven were studied when used as reinforcement in matrix based on five different EVOs having different epoxy contents. ELO-based resin and composites were used as reference. The increase in fibre percentage has led to a decrease in the  $T_g$  of FF-based composites with a sensible increasing of the storage modulus in the rubbery state than the EVOs-based resins. For PLA-reinforced composites the  $T_g$  of resins and composites are in the same range as the neat resins. All the composites exhibited comparable thermal stability as the respective resins with very low water absorption even at 50 °C, especially for PLA-based composites made with EVOs with high epoxy content as starting matrix monomers. SEM detection highlights good interaction FF-matrix with few gaps even and sensible reduced compatibility between matrix-PLA. Due to the dynamic nature of the disulfide hardener excellent mechanical recycling capabilities were achieved after causing damage to the composites, with comparable  $T_g$  and thermal stability. Chemical recycling, in a green solvent, made possible to use a second time the FF and recover them for next uses. These results open a scenario for the multi uses of the fibres, guaranteeing several applications without losing the final composite properties, opening to application in construction or automotive sectors.

### Acknowledgments

This work was supported by ECOXY project funded by the Bio Based Industries Joint Undertaking under European Union Horizon 2020 research and innovation program (Grant agreement n° 744311).

### References

1. Smits, J., Fiber-Reinforced Polymer Bridge Design in the Netherlands: Architectural Challenges toward Innovative, Sustainable, and Durable Bridges. *Engineering* **2016**, 2 (4), 518-527.

2. Bledzki, A. K.; Gassan, J., Composites reinforced with cellulose based fibres. *Progress in Polymer Science* **1999**, 24 (2), 221-274.
3. Satyanarayana, K. G.; Guimarães, J. L.; Wypych, F., Studies on lignocellulosic fibers of Brazil. Part I: Source, production, morphology, properties and applications. *Composites Part A: Applied Science and Manufacturing* **2007**, 38, 1694-1709.
4. Bledzki, A. K.; Reihmane, S.; Gassan, J., Properties and modification methods for vegetable fibers for natural fiber composites. *Journal of Applied Polymer Science* **1996**, 59 (8), 1329-1336.
5. Wambua, P.; Ivens, J.; Verpoest, I., Natural fibres: Can they replace glass in fibre reinforced plastics? *Composites Science and Technology* **2003**, 63, 1259-1264.
6. Bachmann, J.; Hidalgo, C.; Bricout, S., Environmental analysis of innovative sustainable composites with potential use in aviation sector—A life cycle assessment review. *Science China Technological Sciences* **2017**, 60 (9), 1301-1317.
7. Duigou, A.; Baley, C., Coupled micromechanical analysis and life cycle assessment as an integrated tool for natural fibre composites development. *Journal of Cleaner Production* **2014**, 83, 61–69.
8. Tokiwa, Y.; Calabia, B., Biodegradability and biodegradation of poly(lactide). *Applied microbiology and biotechnology* **2006**, 72, 244-51.
9. Babu, R. P.; O'Connor, K.; Seeram, R., Current progress on bio-based polymers and their future trends. *Progress in Biomaterials* **2013**, 2 (1), 8.
10. Siengchin, S.; Dangtungee, R., Effect of woven flax structures on morphology and properties of reinforced modified polylactide composites. *Journal of Thermoplastic Composite Materials* **2013**, 26, 1424-1440.
11. Liu, Z.; Erhan, S. Z.; Akin, D. E.; Barton, F. E., "Green" Composites from Renewable Resources: Preparation of Epoxidized Soybean Oil and Flax Fiber Composites. *Journal of Agricultural and Food Chemistry* **2006**, 54 (6), 2134-2137.
12. Liu, Z. S.; Erhan, S. Z.; Xu, J.; Calvert, P. D., Development of soybean oil-based composites by solid freeform fabrication method: Epoxidized soybean oil with bis or polyalkyleneamine curing agents system. *Journal of Applied Polymer Science* **2002**, 85 (10), 2100-2107.
13. Liu, Z.; Erhan, S. Z.; Calvert, P. D., Solid freeform fabrication of soybean oil-based composites reinforced with clay and fibers. *Journal of the American Oil Chemists' Society* 2004, 81 (6), 605-610.
14. Tran, P.; Graiver, D.; Narayan, R., Biocomposites synthesized from chemically modified soy oil and biofibers. *Journal of Applied Polymer Science* **2006**, 102 (1), 69-75.
15. Shibata, M.; Teramoto, N.; Makino, K., Preparation and properties of biocomposites composed of epoxidized soybean oil, tannic acid, and microfibrillated cellulose. *Journal of Applied Polymer Science* **2011**, 120 (1), 273-278.
16. M. Fejós, J. K.-K. a. S. G., Effects of fibre content and textile structure on dynamic-mechanical and shape-memory properties of ELO/flax biocomposites. *Journal of Reinforced Plastics and Composites* **2014**, 32(24) 1879–1886.
17. Pfister, D. P.; Larock, R. C., Cationically cured natural oil-based green composites: Effect of the natural oil and the agricultural fiber. *Journal of Applied Polymer Science* **2012**, 123 (3), 1392-1400.
18. Bertomeu, D.; García-Sanoguera, D.; Fenollar, O.; Boronat, T.; Balart, R., Use of eco-friendly epoxy resins from renewable resources as potential substitutes of petrochemical epoxy resins for ambient cured composites with flax reinforcements. *Polymer Composites* **2012**, 33 (5), 683-692.
19. Tran, T.-N.; Di Mauro, C.; Graillot, A.; Mija, A., Chemical Reactivity and the Influence of Initiators on the Epoxidized Vegetable Oil/Dicarboxylic Acid System. *Macromolecules* **2020**, 53 (7), 2526-2538.
20. Di Mauro, C.; Tran, T.-N.; Graillot, A.; Mija, A., Enhancing the Recyclability of a Vegetable Oil-Based Epoxy Thermoset through Initiator Influence. *ACS Sustainable Chemistry & Engineering* **2020**, 8 (20), 7690-7700.
21. Tran, T.-N.; Di Mauro, C.; Graillot, A.; Mija, A., Monitoring the structure–reactivity relationship in epoxidized perilla and safflower oil thermosetting resins. *Polymer Chemistry* **2020**, 11 (31), 5088-5097.
22. Di Mauro, C.; Genua, A.; Mija, A., Building thermally and chemically reversible covalent bonds in vegetable oils-based epoxy thermosets. Influence of epoxy-hardener ratio to promote recyclability. *Materials Advances* **2020**, 1 (6), 1788-1798.
23. Kleščik, M.; Bizubová, B.; Zatroch, T.; Balogová, A.; Pedraza, L. A. R.; Skalková, P.; Krmelová, V.; Krmela, J.; Muks, E.; der Scheuren, L. V., Research and application of PLA fibres. *IOP Conference Series: Materials Science and Engineering* **2020**, 776, 012091.

## Chapter 6

24. Reichert, C. L.; Bugnicourt, E.; Coltelli, M.-B.; Cinelli, P.; Lazzeri, A.; Canesi, I.; Braca, F.; Martínez, B. M.; Alonso, R.; Agostinis, L.; Verstichel, S.; Six, L.; Mets, S. D.; Gómez, E. C.; Ißbrücker, C.; Geerinck, R.; Nettleton, D. F.; Campos, I.; Sauter, E.; Pieczyk, P.; Schmid, M., Bio-Based Packaging: Materials, Modifications, Industrial Applications and Sustainability. *Polymers* **2020**, 12 (7), 1558.
25. Fiore, V.; Botta, L.; Scaffaro, R.; Valenza, A.; Pirrotta, A., PLA based biocomposites reinforced with *Arundo donax* fillers. *Composites Science and Technology* **2014**, 105, 110-117.
26. Du, Y.; Wu, T.; Yan, N.; Kortschot, M.; Farnood, R., Fabrication and characterization of fully biodegradable natural fiber-reinforced poly(lactic acid) composites. *Composites Part B Engineering* **2014**, 56, 717-723.
27. Boquillon, N., Use of an epoxidized oil-based resin as matrix in vegetable fibers-reinforced composites. *Journal of Applied Polymer Science* **2006**, 101 (6), 4037-4043.
28. Di Mauro, C.; Malburet, S.; Genua, A.; Grailot, A.; Mija, A., Sustainable series of new epoxidized vegetable oils-based thermosets with chemical recycling properties. *Biomacromolecules* **2020**, 21 (9), 3923-3935.
29. Muralidhar, B. A., Study of flax hybrid preforms reinforced epoxy composites. *Materials & Design (1980-2015)* **2013**, 52, 835-840.
30. Yan, L.; Chouw, N.; Jayaraman, K., Flax fibre and its composites – A review. *Composites Part B: Engineering* **2014**, 56, 296-317.
31. Struik, L. C. E., Physical aging in amorphous polymers and other materials Elsevier, New York: **1978**.
32. Liu, Z.; Erhan, S. Z., “Green” composites and nanocomposites from soybean oil. *Materials Science and Engineering: A* **2008**, 483-484, 708-711.
33. Manthey, N. W.; Cardona, F.; Francucci, G.; Aravinthan, T., Thermo-mechanical properties of epoxidized hemp oil-based bioresins and biocomposites. *Journal of Reinforced Plastics and Composites* **2013**, 32 (19), 1444-1456.
34. Chieng, B. W.; Ibrahim, N. A.; Then, Y. Y.; Loo, Y. Y., Epoxidized Vegetable Oils Plasticized Poly(lactic acid) Biocomposites: Mechanical, Thermal and Morphology Properties. *Molecules* **2014**, 19 (10), 16024-16038.
35. Pietrolungo, M.; Padovano, E.; Frache, A.; Badini, C., Mechanical recycling of an end-of-life automotive composite component. *Sustainable Materials and Technologies* **2020**, 23, e00143.
36. Feraboli, P.; Kawakami, H.; Wade, B.; Gasco, F.; DeOto, L.; Masini, A., Recyclability and reutilization of carbon fiber fabric/epoxy composites. *J. Compos. Mater.* **2012**, 46 (12), 1459-1473.
37. Cicala, G.; Pergolizzi, E.; Piscopo, F.; Carbone, D.; Recca, G., Hybrid composites manufactured by resin infusion with a fully recyclable bioepoxy resin. *Composites Part B: Engineering* **2018**, 132, 69-76.
38. Ruiz de Luzuriaga, A.; Martin, R.; Markaide, N.; Rekondo, A.; Cabañero, G.; Rodríguez, J.; Odriozola, I., Epoxy resin with exchangeable disulfide crosslinks to obtain reprocessable, repairable and recyclable fiber-reinforced thermoset composites. *Materials Horizons* **2016**, 3 (3), 241-247.
39. Zhou, F.; Guo, Z.; Wang, W.; Lei, X.; Zhang, B.; Zhang, H.; Zhang, Q., Preparation of self-healing, recyclable epoxy resins and low-electrical resistance composites based on double-disulfide bond exchange. *Composites Science and Technology* **2018**, 167, 79-85.
40. Ma, Z.; Wang, Y.; Zhu, J.; Yu, J.; Hu, Z., Bio-based epoxy vitrimers: Reprocessability, controllable shape memory, and degradability. *Journal of Polymer Science Part A: Polymer Chemistry* **2017**, 55 (10), 1790-1799.
41. Lei, Z. Q.; Xiang, H. P.; Yuan, Y. J.; Rong, M. Z.; Zhang, M. Q., Room-Temperature Self-Healable and Remoldable Cross-linked Polymer Based on the Dynamic Exchange of Disulfide Bonds. *Chemistry of Materials* **2014**, 26 (6), 2038-2046.

## Electronic Supplementary Information (ESI)

### Experimental

#### Materials

##### Bio-based epoxy resins, hardeners and initiator

ELO was obtained by Valtris Specialty Chemicals. The epoxidized perilla oil (EPLO), the epoxidized hemp oil (EHO), the epoxidized camelina oil (ECMO) and the epoxidized safflower oil (ESFO) were provided by *SPECIFIC POLYMERS*.

The resin formulations were made using 2,2'-dithiodibenzoic acid (DTBA), 95%, as hardener and imidazole (IM), 99%, as initiator, both commercially available and purchased from Sigma-Aldrich. All reagents were used without further purification. The characteristics of the selected reagents are given in Table ESI 1.

##### Natural fibers

As reinforcement, the 100% FFs Basket 4/4 woven (Figure ESI 1 (a)) was provided by *Flipts & Dobbels*. The weave is essentially a plain weave with warp fibres interlaced with four fill fibres, based on long fibres (long brin), and a surface mass of 270 g.m<sup>-2</sup>.

The plain-woven PLA (Figure ESI 1 (b)) was supplied by *Centexbel*. The PLA fibers are characterized by a tenacity of 4.6 - 5.0 cN/dtex, elongation at break 25%, modulus between 9.4 - 9.94 GPa and hot air shrinkage 3.8 - 4.3% at 100°C. For the woven preparation, two yarns were twisted in one, with 60 turns / meter, the warp and weft density were 18 yarns.cm<sup>-1</sup> and a surface mass of 190 g.m<sup>-2</sup>. Both FF and PLA fibres were dried in oven at 90 °C for 2 hours and used as received without further purification.

##### Formulation and curing of bio-based thermosets

The five EVOs thermosetting resins were formulated for composite preparation according to our previous work.<sup>1-2</sup> The formulations were prepared at a 1:1 ratio between epoxy and acid groups, according with Dusek *et al.*<sup>3</sup>. The EVOs were heated to around 80 °C to decrease their viscosity. Thereafter, the selected initiator was added at 1wt.% and mixed until homogenization. At this mixture was introduced the hardener. Each formulation was stirred at 80 °C for 10 minutes, then placed into a silicone mold and cured in oven, according to the curing protocol presented in our previous work and displayed in Table ESI 2. The curing protocols were determined after a reactivity study by DSC and by TGA to confirm the completion of reaction and that no thermal degradation occurred during the curing process. ELO-based resin was considered as reference. According to this procedure, the samples for DMA analysis were prepared in special rectangular molds (48 × 8 × 4 mm<sup>3</sup>).

##### Bio-composites preparation

The composites were prepared by adding different percentages of FF and PLA to the uncured resins. The optimization of the fibre's percentage was performed using the ELO reference. The results are given in Figure ESI 3 and ESI 4 (c). The optimal PLA woven percentage was chosen at 5 wt.%, while for the FF two percentages were selected 5 and 20 wt.%, respectively. The resin-coated fibre-mats were stacked in a



## Chapter 6

silicon mold. Consequently, the mold was hot-pressed at 120 °C for 1 hour under a pressure of 5 bars. Thereafter, the so prepared composites were post cured at parameters given with Table ESI 2 . To test the thermal stability of the mixtures resin-fibre, thermogravimetric analyses were performed to verify that the samples are stable during the curing and post curing protocols.

### Composites recyclability

**Mechanical:** To test the bio-composites repairability, a damage (scratch) was performed on the surface of the samples. Thereafter, the repairability test was performed in a hot press (at 170 °C for 30 minutes for FF composites and for 15 minutes for PLA composites, respectively), until the scratch was completely repaired. The properties of the reprocessed composites were analyzed and compared with those of the virgin ones.

**Chemical:** The dissociative ability of the S-S bonds in alkaline solutions was used to disintegrate the prepared composites and to recuperate the fibers for a second use. The composites were kept for 24 hours in 1 N NaOH solution at 80 °C. At the end of the matrix dissociation, the fibres were dried at 50 °C for 12 hours and used for a new composite preparation.

*Table ESI 1. Structures and characteristics of the selected reagents*

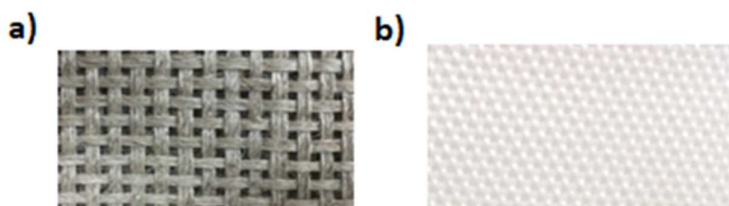
EVOs	EVO Acronym	Epoxy index (meq/g)	Mw EVO (g/mol)
Safflower	ESFO	4.93	960.2
Camelina	ECMO	5.29	965.3
Linseed	ELO	5.61	980.0
Hemp	EHO	6.09	976.7
Perilla	EPLO	6.77	986.4

Hardener/Initiator	Acronym	Melting Point (°C)	Mw (g/mol)
2,2'-Dithiodibenzoic acid	DTBA	287 - 290	306.35
Imidazole	IM	89 - 91	68.07

*Table ESI 2. Curing and post-curing conditions for EVOs/DTBA systems*

EVOs/DTBA/IM resins and composites	Curing Condition	Post-Curing Condition
ESFO	140 °C – 60 min	180 °C – 30 min
ECMO	130 °C – 60 min	170 °C – 30 min
ELO	130 °C – 60 min	170 °C – 30 min
EHO	130 °C – 60 min	170 °C – 30 min
EPLO	130 °C – 60 min	170 °C – 30 min



*Figure ESI 1.a) Flax fibres basket 4/4 woven (FF) and b) PLA weaves*

## Fibres thermal stability

TGA measurements were carried out under air atmosphere in order to determine the thermo-oxidative stability of the fibres. The  $T_{5\%}$  obtained values are ranging from 231 °C, for the FF, to 330 °C for the PLA fabrics, (Figure ESI 2 and Table ESI 3). For the FF the weight loss from 35 to 140 °C can be assigned to loss of water.<sup>4</sup> The thermal degradation involves two steps: thermal depolymerisation of the hemicellulose and the cleavage of glycosidic linkages of cellulose and the second one due to decomposition of the  $\alpha$ -cellulose.<sup>5-6</sup> The lower percentage of lignin in these fibres, guarantee high stability compared with jute and sisal.<sup>7</sup>

As natural fibres, the FF are composed primarily of cellulose, hemicellulose, lignin, etc. The last one starts the decomposition at 160 °C that continues at around 400 °C.<sup>8-9</sup> According with Van De Velde *et al.*<sup>10</sup>, the low value for the FF thermal degradation at temperature < 300 °C can be attributed to the presence of water and also to an autocatalytic mechanism due to the CO<sub>2</sub> formed.

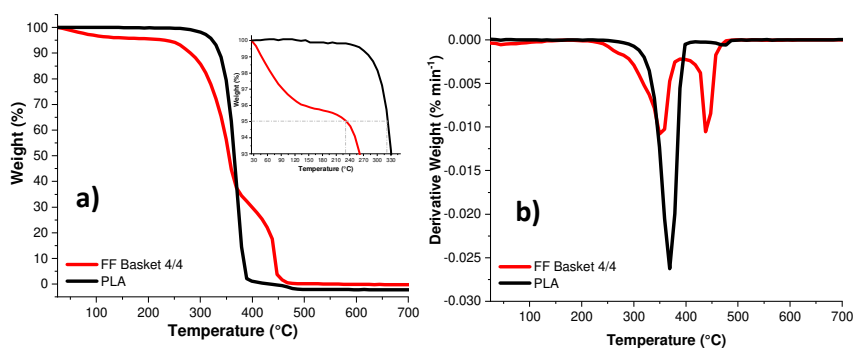


Figure ESI 2. TGA, zoom from 25-330 °C and DTG curves of the FF and PLA fibres

Table ESI 3. Thermogravimetric data for the different fibres

	$T_{5\%}$ (°C)	1 <sup>st</sup> $T_{onset}$ (°C)	1 <sup>st</sup> $T_{endset}$ (°C)	1 <sup>st</sup> Degradation peak (°C)	1 <sup>st</sup> Residue %	2 <sup>nd</sup> $T_{onset}$ (°C)	2 <sup>nd</sup> $T_{endset}$ (°C)	2 <sup>nd</sup> Degradation peak (°C)	Final Residue %
FF Basket 4/4	231	50	400	355	31.0	400	650	445	0.39
PLA woven	330	250	600	375	0.34				

Table 5. ELO/DTBA with 1 wt.% IM thermal data and comparison increasing the flax and PLA fibres percentage

ELO/DTBA	Resin	PLA wt.%		
	/	5	10	20
$T_{on}$ (°C)	133	134	133	132
$T_{peak}$ (°C)	149	150	148	147
$T_{end}$ (°C)	185	175	167	167
$\Delta H$ (J/g)	174	164	158	132
$\Delta H_{normalized}$ (J/g)	/	156	142	106

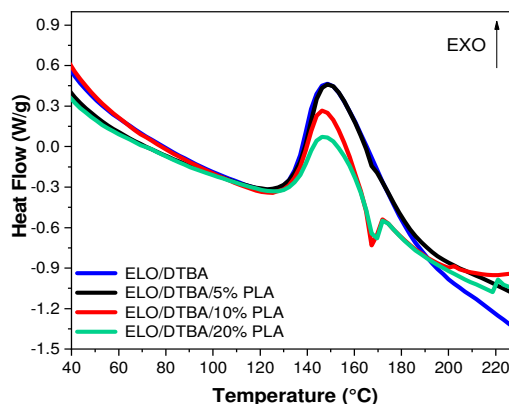
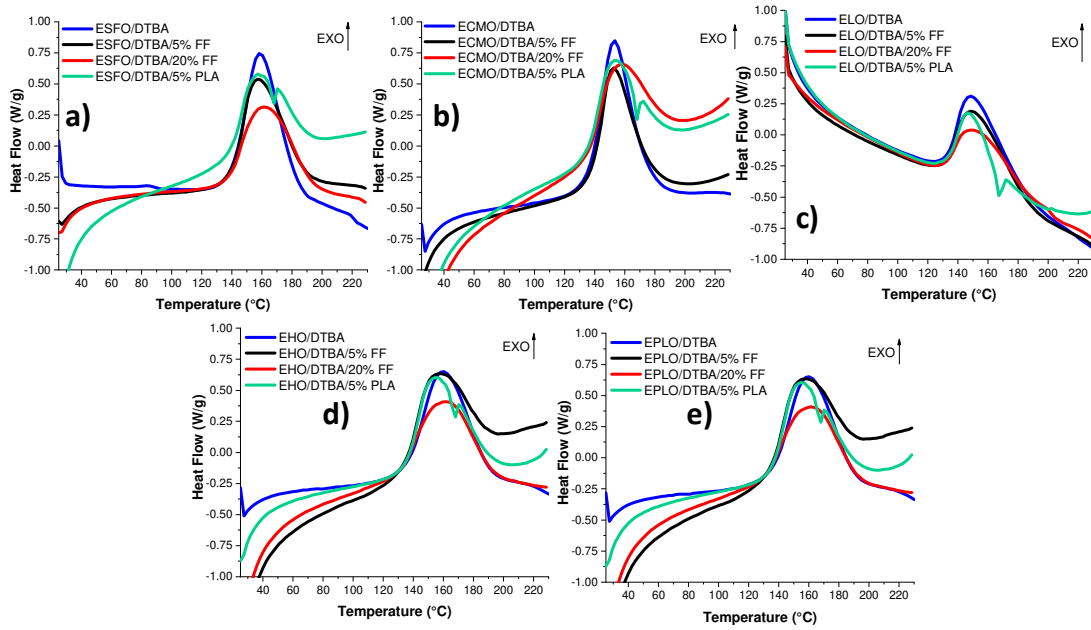
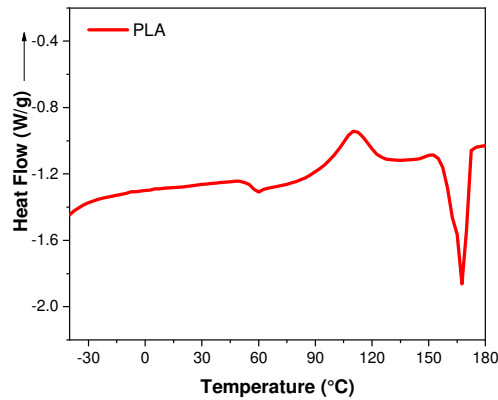


Figure ESI 3. DSC thermograms of ELO/DTBA reference reactivity with PLA



**Figure ESI 4.** Dynamic DSC thermograms obtained during crosslinking of EVOs/DTBA. ESFO (a), ECMO (b), ELO (c), EHO (d) and EPLO (e). Reactivities of neat resins (blue line) and composites formulations with 5% FF (black line), 20% (red line) and 5% PLA (green line)



**Figure ESI 5.** DSC thermogram for the PLA fibre

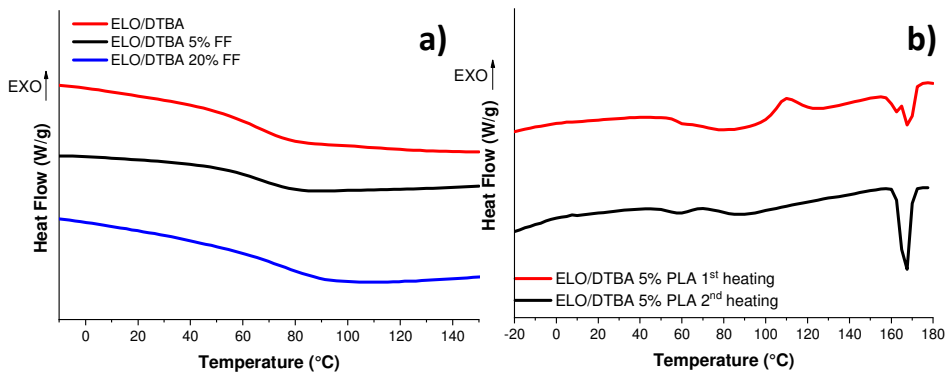


**Figure ESI 6.** DSC thermograms of the  $T_g$  of the ELO/DTBA composites with the FF (a) and PLA (b) fibres

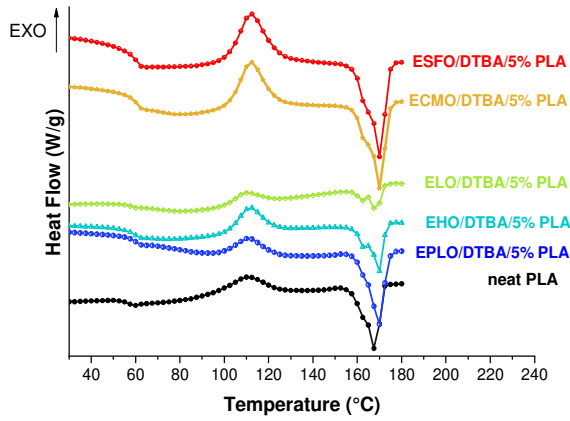


Figure ESI 7. First DSC heating thermograms of PLA and PLA composites, 10 °C.min<sup>-1</sup>

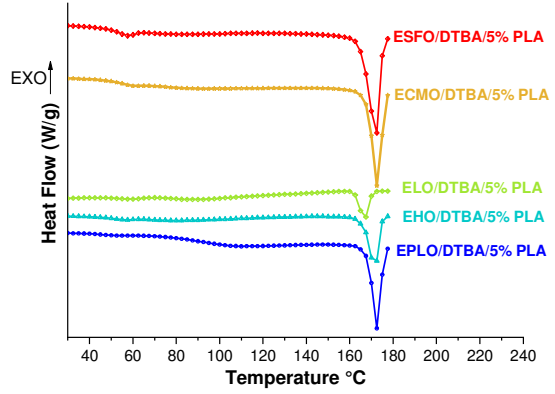


Figure ESI 8. Second heating DSC thermograms of the EVO-based resins reinforced with 5% PLA

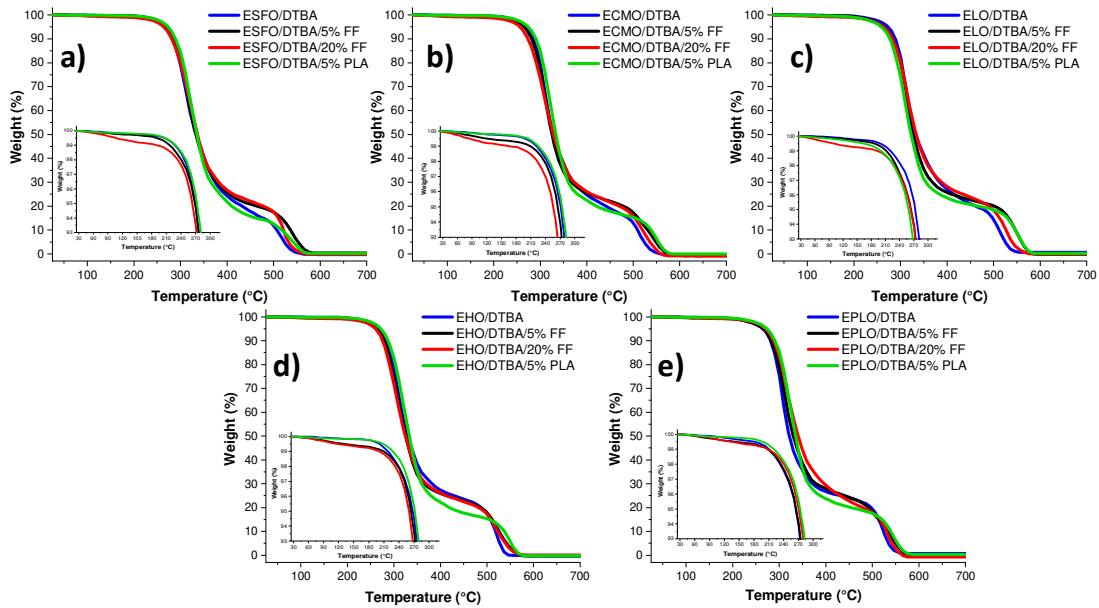
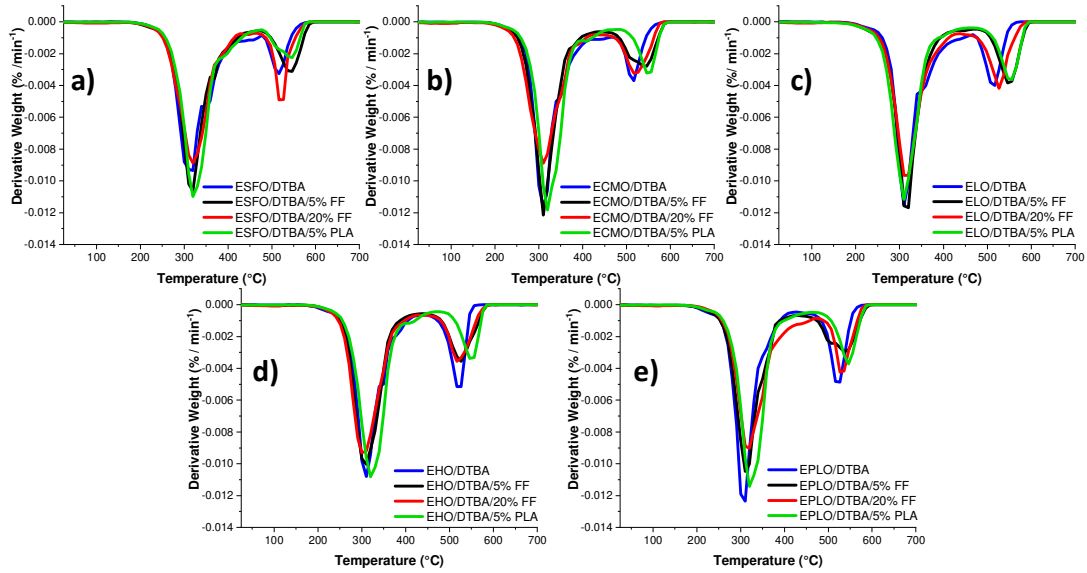
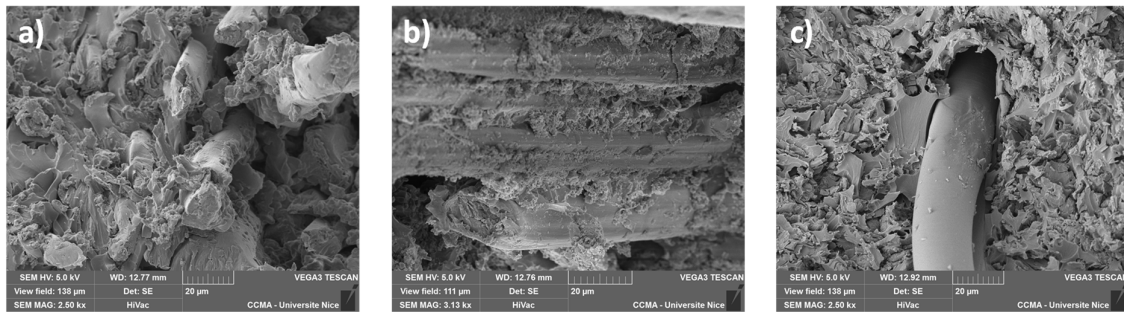


Figure ESI 9. TGA comparison between bio-based resins with ESFO (a), ECMO (b), ELO (c), EHO (d) and EPLO (e) (blue lines) and reinforced with 5 (black lines) and 20% FF (red lines) and 5% PLA (green lines)



**Figure ESI 10.** DTG comparison between bio-based resin and composites with ESFO (a), ECMO (b), ELO (c), EHO (d) and EPLO (e) reinforced with 5 and 20% of FF and 5% PLA fibre



**Figure ESI 11.** SEM micrographs of the cross-sections for ELO composite at 20 µm (a) with 5 wt.% FF (b) 20 wt.% FF and (c) with 5 wt.% PLA

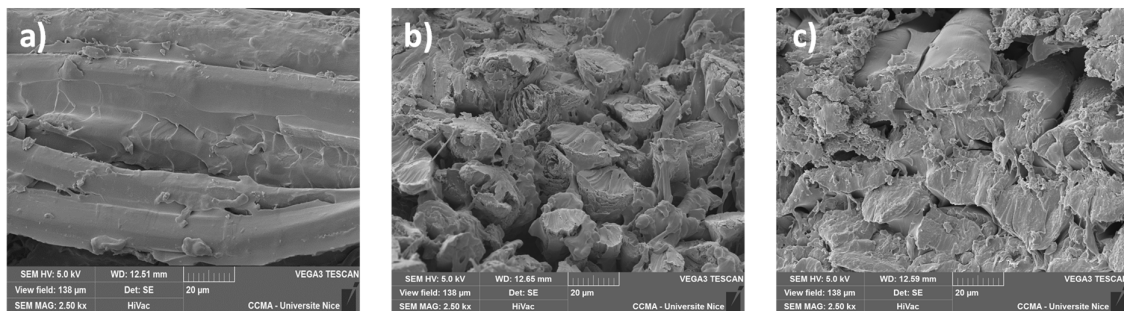


**Figure ESI 12.** SEM micrographs of the cross-sections for ESFO composite at 20 µm (a) with 5 wt.% FF (b) 20 wt.% FF and (c) with 5 wt.% PLA

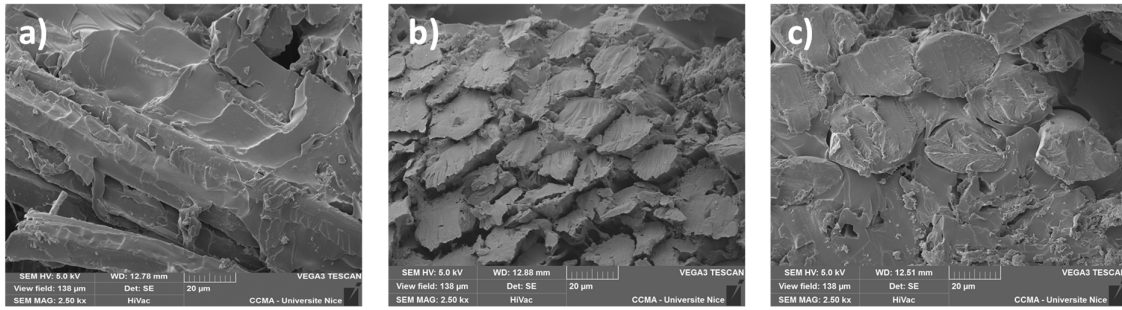


Figure ESI 13. SEM micrographs of the cross-sections for ECMO composite at 20  $\mu\text{m}$  (a) with 5 wt.% FF (b) 20 wt.% FF and (c) with 5 wt.% PLA

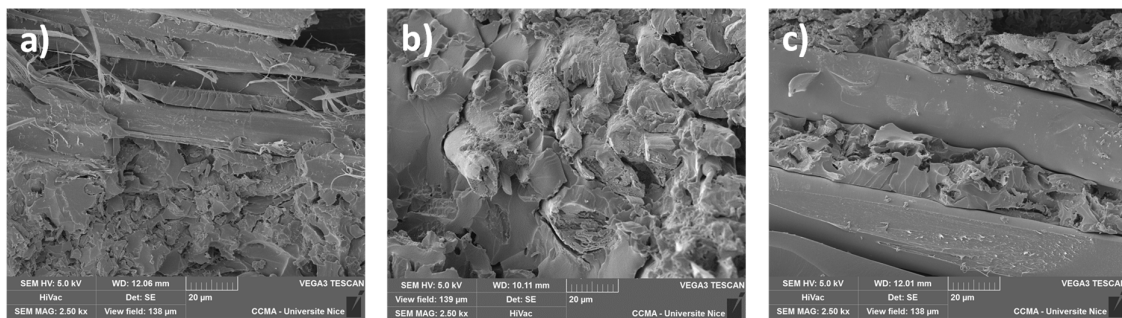


Figure ESI 14. SEM micrographs of the cross-sections for EPLO composite at 20  $\mu\text{m}$  (a) with 5 wt.% FF (b) 20 wt.% FF and (c) with 5 wt.% PLA

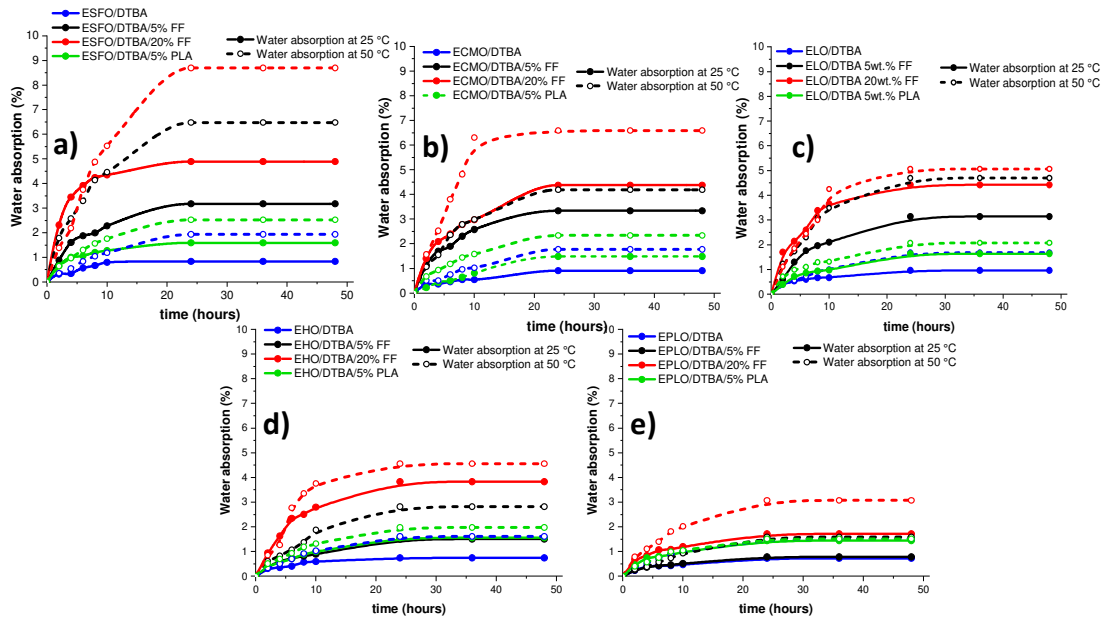


Figure ESI 15. Water absorption results in function of time for EVOs/DTBA resins and reinforced bio-composites with FF and PLA at 25 °C and 50 °C



Figure ESI 16. Mechanical recycling of ELO/DTBA with 5wt.% PLA: virgin (a), damaged (b), repaired (c)

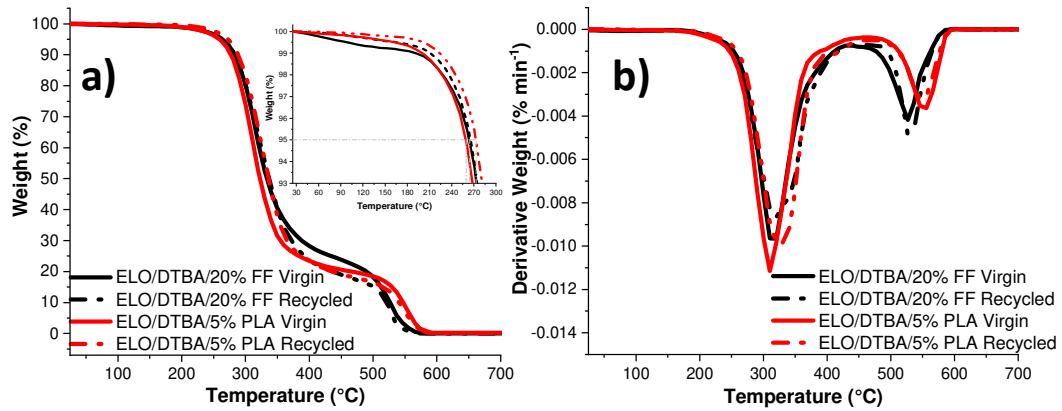


Figure ESI 17. TGA and zoom from 25 - 300 °C (a) and DTG (b) of the virgin and reprocessed ELO/DTBA reinforced composites with 20% FF and 5% PLA

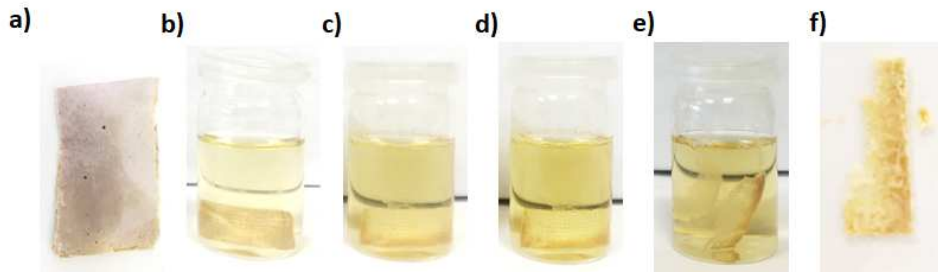
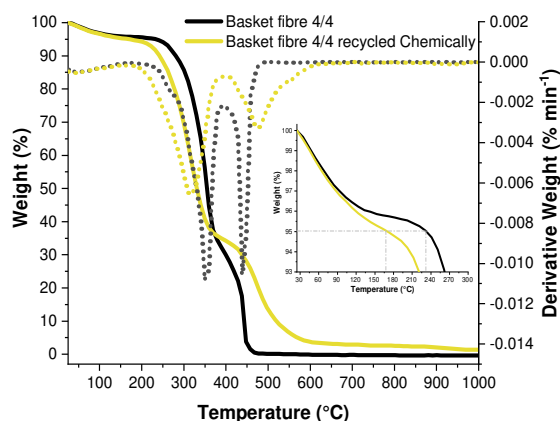


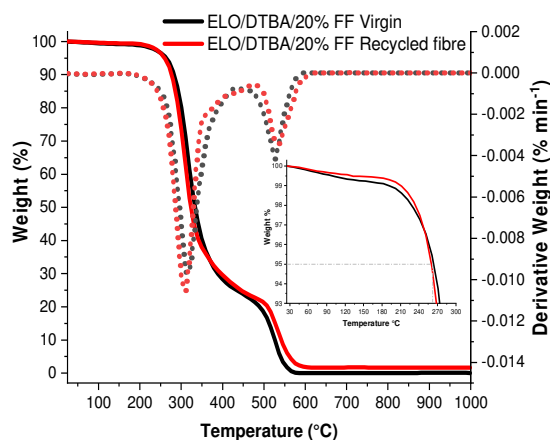
Figure ESI 18. Chemical recycling in NaOH 1 N at 80 °C of the ELO/DTBA reinforced with 5 % PLA: initial composite (a), after 3h (b), 9h (c), 18h (d), 24 h (e) end dried fibre (f)

Table ESI 5. Thermal characterization results for FF compared with the chemically recycled in 1 N NaOH

	$T_{5\%}$ (°C)	1 <sup>st</sup> $T_{onset}$ (°C)	1 <sup>st</sup> $T_{endset}$ (°C)	1 <sup>st</sup> Degradation peak (°C)	1 <sup>st</sup> Residue %	2 <sup>nd</sup> $T_{onset}$ (°C)	2 <sup>nd</sup> $T_{endset}$ (°C)	2 <sup>nd</sup> Degradation peak (°C)	Final Residue %
FF Virgin	231	50	400	355	31.0	400	650	445	0.39
FF Recycled Chemically	165	50	400	315	34.3	400	650	470	1.39



**Figure ESI 19.** TGA, DTG curves and zoom for chemically recycled FF and compared with the virgin



**Figure ESI 20.** TGA, DTG curves and zoom for virgin composite made with the reference matrix and with the chemically recycled flax fibres

**Table ESI 6.** Thermal characterization results for flax fibre composite compared with the one reinforced with fibre recycled in NaOH

	$T_{5\%}$ (°C)	1 <sup>st</sup> $T_{onset}$ (°C)	1 <sup>st</sup> $T_{endset}$ (°C)	1 <sup>st</sup> Degradation peak (°C)	1 <sup>st</sup> Residue %	2 <sup>nd</sup> $T_{onset}$ (°C)	2 <sup>nd</sup> $T_{endset}$ (°C)	2 <sup>nd</sup> Degradation peak (°C)	Final Residue %
<b>ELO/DTBA 20% FF</b>	260	210	450	310	22.0	450	650	520	0.19
<b>ELO/DTBA20% FF RECYCLED</b>	260	210	480	307	22.8	480	650	535	1.65

- Tran, T.-N.; Di Mauro, C.; Graillot, A.; Mija, A., Chemical Reactivity and the Influence of Initiators on the Epoxidized Vegetable Oil/Dicarboxylic Acid System. *Macromolecules* **2020**, 53 (7), 2526-2538.
- Di Mauro, C.; Tran, T.-N.; Graillot, A.; Mija, A., Enhancing the Recyclability of a Vegetable Oil-Based Epoxy Thermoset through Initiator Influence. *ACS Sustainable Chemistry & Engineering* **2020**, 8 (20), 7690-7700.
- Matějka, L.; Pokorný, S.; Dušek, K., Acid curing of epoxy resins. A comparison between the polymerization of diepoxide-diacid and monoepoxide-cyclic anhydride systems. *Die Makromolekulare Chemie* **1985**, 186 (10), 2025-2036.
- George, J.; Verpoest, J. I., I., Mechanical properties of flax fibre reinforced epoxy composites. *Die Angewandte Makromolekulare Chemie* **1999**, 272 (1), 41-45.
- Poletto, M.; Zattera, A. J., Mechanical and dynamic mechanical properties of polystyrene composites reinforced with cellulose fibers: Coupling agent effect. *Journal of Thermoplastic Composite Materials* **2015**, 30 (9), 1242-1254.
- Manthey, N.; Cardona, F.; Aravinthan, T.; Wang, H.; Cooney, T. In Natural fibre composites with epoxidized vegetable oil (EVO) resins: a review, *Proceedings of the Southern Region Engineering Conference (SREC 2010)*, Engineers Australia: **2010**; pp 100-106.
- Manfredi, L. B.; Rodríguez, E. S.; Wladyka-Przybylak, M.; Vázquez, A., Thermal degradation and fire resistance of unsaturated polyester, modified acrylic resins and their composites with natural fibres. *Polymer Degradation and Stability* **2006**, 91 (2), 255-261.
- Ahmad, F.; Choi, H. S.; Park, M. K., A Review: Natural Fiber Composites Selection in View of Mechanical, Light Weight, and Economic Properties. *Macromolecular Materials and Engineering* **2015**, 300 (1), 10-24.
- Manfredi, L. B.; Rodríguez, E.; Wladyka-Przybylak, M.; Vázquez, A., Thermal Properties and Fire Resistance of Jute-Reinforced Composites. *Composite Interfaces* **2010**, 17 (5-7), 663-675.
- Van De Velde, K.; Kiekens, P., Thermal degradation of flax: The determination of kinetic parameters with thermogravimetric analysis. *Journal of Applied Polymer Science* **2002**, 83 (12), 2634-2643.



### Conclusions and Perspectives

The main objective of this thesis was the synthesis of new series of sustainable bio-based epoxy resins, based on epoxidized vegetable oil, reinforced by flax fibres and PLA woven, to produce composites with recycling ability, with possible applications in automotive or construction sectors. The modulation of the key parameters involved in the creation of the 3D polymer networks have been studied to understand its impact on the final properties of the resins or reprocessed materials.

To ensure the synthesis of reprocessable materials, a dynamic hardener with disulfide bonds and acid functionality was selected. The hardener combination with a reference epoxidized vegetable oil (ELO) was studied focusing in a first step on the role of the initiator. Its nature and ratio were analysed, to evaluate its impact on polymer crosslinking conversion, and also on the physico-chemical and mechanical properties of the virgin or reprocessed resins. Thereafter, the optimal initiator was used to test how many times the resin can be reprocessed without losing its thermo-mechanical properties. Furthermore, in order to ensure a green disposal, avoiding the use of toxic solvents, all the prepared resins were tested and shown the ability to be completely degraded into NaOH solution, modulating time and temperature.

The initiator found as optimal was used in the second study to analyse the effect of the second parameter: the epoxy / hardener ratio ( $R$ ). The appropriate selection of  $R$  allowed the preparation of both virgin and recycled thermosets with high crosslinking density, thermal stability and high  $T_g$ . These thermosets presented marked similarities with vitrimers materials, showing also the ability to swell until fragmentation in a suitable solvent. The resins recovered from the solvent immersion exhibited the ability to be mechanically reprocessed. The so reshaped resins were characterized, showing a lower loss on physico-mechanical properties when the epoxy / hardener ratio was in defect of crosslinker.

The results obtained for the reference monomers (ELO, ESO) were compared with a series of thermosets based on twelve new epoxidized vegetable oils. The EVO's epoxy content, from 2.77 to 6.77 meq.g<sup>-1</sup>, represented the third parameter analysed for the formation and optimization of EVO's thermosets. Using hardener-free thermo-curing process applied to the new EVOs, fully bio-based homopolymers materials were obtained, with a large scale of properties with potential applications in polymeric coatings. The homopolymers exhibited high percentage conversions, ~ 98%, of epoxy groups, and  $\tan \delta$  from -19 to 1 °C. Thereafter, the copolymerization reactions of series of EVOs with the dynamic diacid hardener were studied. The EVOs with high epoxy content displayed higher reactivity reflected also on the final properties of the thermoset materials. The obtained thermosets varied from soft to hard, with a variation of  $\tan \delta$  and elongation at break from 34 ° C and ~ 350%, in case of EVOs with

low epoxy content, up to highly crosslinked materials with  $\tan \delta \sim 111$  °C and elongation at break  $\sim 1.2\%$ , in the case of EVOs with high epoxy content. These thermosets exhibited high biobased carbon content, from 58 to 79 %.

The networks created with the dynamic diacid hardener showed recyclability, repairability and reshapability (3R) abilities. The two mechanisms involved in the recycling process, disulfide metathesis and transesterification reactions, allowed to reprocess entirely the thermosets. Reduced time and lower temperatures were needed to reprocess the thermosets with low crosslink density, in contrast with the high crosslinked thermosets that required stronger conditions of recycling. The reprocessed EVOs thermosets kept their thermo-mechanical properties almost unaffected. Like many vitrimers, they showed shape memory ability. By applying external stimuli, the recycled thermosets were also able to change their shape, from a permanent one reconfigured to a temporary profile. The subsequent application of temperature allowed to the tested samples to be reconfigured for to 2 cycles. In order to guarantee a second life to some components, the last objective of this thesis research was to reinforce some of the obtained polymer matrices with vegetable or PLA fibers by continuing to achieve the composite recyclability despite the presence of the reinforcement. The bio-composites were developed using 5 and 20% by weight flax natural fibers and 5% by weight of PLA woven. Both the natural fibres led to a significant improvement in the properties of the composites. The morphological analysis performed by SEM proved the good interaction flax fiber-matrix and a lower one in the case of PLA woven. Nevertheless, both reinforcements allowed obtaining composites with good thermo-mechanical properties, that remained almost unaffected by the mechanical recycling. Finally, the ability of these resins to degrade in NaOH was exploited to chemically recycle the matrix and to possible reuse the flax fibers for the preparation of a second-generation composites. In conclusion, this thesis proposes the study of synthesis of bioderived resins based on vegetable oils, the polymerization optimization and the elaboration of bio-composites. The developed resins and composites were studied from the point of view of its recycling. The considerations made in this thesis presented how EVOs combined with dynamic disulfide hardeners and natural fibers can have a great potential for the development and production on an industrial scale thanks to their simplicity of synthesis and repairability. However, these goals represent only a first step towards a tangible path to use these materials for daily application on large-scale.

In future studies, rheology stress-relaxation experiments and determination of the topology freezing transition temperature ( $T_v$ ) will be performed to confirm the vitrimers properties of EVOs-based reprocessed thermosets. Also, the recycling ability obtained through the transesterification and disulfide exchange mechanisms will be emphasized and deepened, with the synthesis of a dynamic hardener with acidic functionality starting from renewable and green resources. As a last study in perspective, fully bio-based thermosetting

## Conclusions and Perspectives

like-vitrimer materials, with the transesterification reaction as the only reprocessability mechanism, will be developed. The use of bio-based raw materials and renewable derivatives will be used for the manufacture of this dynamic polymers. The use of sustainable raw materials, low-priced and with an expected green and environmentally friendly recycling mechanism will be used as a parameter for the choice of starting monomers and to ensure future uses in edible and biomedical applications.

## Scientific contributions

### Publications

**Di Mauro, C.;** Tran, T.-N.; Graillet, A.; Mija, A., Enhancing the Recyclability of a Vegetable Oil-Based Epoxy Thermoset through Initiator Influence. *ACS Sustainable Chemistry & Engineering* **2020**, 8 (20), 7690-7700.

DOI: 10.1021/acssuschemeng.0c01419

**Di Mauro, C.;** Genua, A.; A.; Mija, Building thermally and chemically reversible covalent bonds in vegetable oils based epoxy thermosets. Influence of epoxy-hardener ratio to promote recyclability. *Materials Advances*, **2020**, 1 (6), 1788-1798.

DOI: 10.1039/D0MA00370K

**Di Mauro, C.;** Malburet, S.; Genua, A.; Graillet, A.; Mija, Sustainable series of new epoxidized vegetable oils-based thermosets with chemical recycling properties. *Biomacromolecules*, **2020**, 21 (9), 3923-3935.

DOI: 10.1021/acs.biomac.0c01059

Tran, T.-N.; **Di Mauro, C.;** Graillet, A.; Mija, A., Chemical Reactivity and the Influence of Initiators on the Epoxidized Vegetable Oil/Dicarboxylic Acid System. *Macromolecules* **2020**, 53 (7), 2526-2538.

DOI:10.1021/acs.macromol.9b02700

Tran, T.-N.; **Di Mauro, C.;** Graillet, A.; Mija, A., Monitoring the Structure - Reactivity Relationship on Epoxidized Perilla and Safflower Oils Thermosetting Resins. *Polymer Chemistry*, **2020**, 11 (31), 5088-5097.

DOI: 10.1039/d0py00688b

Tran, T.-N.; **Di Mauro, C.;** Malburet, S.; Graillet, A.; Mija, A., Dual crosslinking of epoxidized linseed oil with combined aliphatic/aromatic diacids containing dynamic S-S bonds generating recyclable thermosets. *ACS Applied Bio Materials* **2020**.

Accepted Manuscript

### In peer review:

**Di Mauro, C.;** Malburet, S.; Graillet, A.; Mija, Recyclable, Repairable and Reshapable (3R) Thermoset Materials with Shape Memory Properties from Bio-based Epoxidized Vegetable Oils, submitted to *ACS Applied Bio Materials*.

**Di Mauro, C.;** Genua, A.; Rymarczyk, M.; Dobbels, C.; Graillet, A.; Malburet, S.; Mija, A.; Chemical and mechanical reprocessed resins and bio-composites based on five epoxidized

## Scientific contributions

vegetable oils thermosets reinforced with flax fibers or PLA woven, submitted to *Composites Science and Technology*.

Malburet, S.; **Di Mauro, C.**; Noè, C.; Mazouane, S.; Mija, A.; Sangermano, M.; Graillot, A., Sustainable access to fully biobased epoxidized vegetable oil thermoset materials prepared by thermal or UV-cationic processes, submitted to *RSC Advanced*.

## Cover pages

**Di Mauro, C.**; Tran, T.-N.; Graillot, A.; Mija, A., Enhancing the Recyclability of a Vegetable Oil-Based Epoxy Thermoset through Initiator Influence. *ACS Sustainable Chemistry & Engineering* **2020**, *8* (20).

Tran, T.-N.; **Di Mauro, C.**; Graillot, A.; Mija, A., Chemical Reactivity and the Influence of Initiators on the Epoxidized Vegetable Oil/Dicarboxylic Acid System. *Macromolecules* **2020**, *53* (7), 2526-2538.

## Oral presentations

**Di Mauro C.**, Graillot A., Malburet S., Genua A., Montes S., Mija A., “Bio-based recyclable, reshapable and repairable (3R) fibre-reinforced epoxy composites”, *3<sup>rd</sup> International Conference on Biobased Textiles and Plastics*, October 16, **2018**, Gent, Belgium.

Malburet S., Graillot A., Genua A., Montes S., Mija A., **Di Mauro C.**, Loubat C., “Bio-based Building-Blocks for Thermosets Epoxy Resins”, *International conference on Bioinspired and Biobased Chemistry & Materials, N.I.C.E.*, October **2018**, Nice, France.

**Di Mauro C.**, Graillot A., Genua A., Malburet S., Montes S., Mija A., “Bio-based recyclable, reshapable and repairable (3R) fibre-reinforced epoxy composites for automotive and construction sector” *257<sup>th</sup> ACS National Meeting & Exposition*, Orlando, FL, United States, Mar. 31-Apr. 4, **2019**.

Malburet S., **Di Mauro C.**, Graillot A., Mija A., Loubat C., “Epoxidized Vegetable Oils for Biobased Thermoset Epoxy Resins”, *ISGC, 2019 – 5<sup>th</sup> International Symposium on Green Chemistry*, La Rochelle, France.

**Di Mauro C.**, Graillot A., Malburet S., Mija A., “Recyclable and reprocessable epoxy resins based on vegetable oils”, *EUROMAT 2019*, September 1-5, **2019**, Stockholm, Sweden.

Tran, T.-N., **Di Mauro C.**, Graillot A., Mija A., “Bio-based, recyclable, reshapable & repairable (3R) fiber reinforced thermoset composites”, *EUROMAT 2019*, September 1-5, **2019**, Stockholm, Sweden.

## Posters

**Di Mauro C.**, Graillot A., Malburet S., Genua A., Montes S., Mija A., “Bio-based recyclable, reshapable and repairable (3R) fibre-reinforced epoxy composites”, *International Conference on Circular Economy for Textiles and Plastics*, November 13<sup>th</sup> -14<sup>th</sup>, **2018**, Bruges, Belgium.  
(1<sup>st</sup> Prize Poster Award)

Malburet S., Graillot A., Genua A., Montes S., Mija A., **Di Mauro C.**, Loubat C., “Bio-based, recyclable, reshapable & repairable (3R) fibre reinforced thermoset composites”, *ISGC 5<sup>th</sup> International Symposium on Green Chemistry*, La Rochelle, France, June **2019**.

Malburet S., Noe C., Graillot A., **Di Mauro C.**, Mija A., Sangermano M., Loubat C., “Epoxidized Vegetable Oils (EVOs) for Biobased Thermoset Epoxy Resins”, *ISGC 5<sup>th</sup> International Symposium on Green Chemistry*, La Rochelle, France, June **2019**.